The impact of metabolic disease, feeding and exercise training on autophagy

by

María Gabriela Morales Scholz

MD, MSc

Submitted in fulfilment of the requirements for the degree of

Doctor of Philosophy

Deakin University

December, 2019

DEAKIN UNIVERSITY
ACCESS TO THESIS - A

I am the author of the thesis entitled

The effects of insulin resistance and exercise on muscle autophagy

submitted for the degree of Doctor of Philosophy

This thesis may be made available for consultation, loan and limited copying in accordance with the Copyright Act 1968.

'I certify that I am the student named below and that the information provided in the form is correct'

Full Name: Maria Gabriela Morales Scholz

Signed: 

Date: 06.12.2019

DEAKIN UNIVERSITY
CANDIDATE DECLATARION

I certify the following about the thesis entitled

The effects of insulin resistance and exercise on muscle autophagy

submitted for the degree of Doctor of Philosophy

I am the creator of all or part of the whole work(s) (including content and layout) and that where reference is made to the work of others, due acknowledgment is given.

The work(s) are not in any way a violation or infringement of any copyright, trademark, patent, or other rights whatsoever of any person.

That if the work(s) have been commissioned, sponsored or supported by any organisation, I have fulfilled all of the obligations required by such contract or agreement.

That any material in the thesis which has been accepted for a degree or diploma by any university or institution is identified in the text.

All research integrity requirements have been complied with.

'I certify that I am the student named below and that the information provided in the form is correct'

Full Name: María Gabriela Morales Scholz

Signed: 

Date: 06.12.2019

Acknowledgments

Many people have been present, either overseas or in Australia, throughout my time as a PhD student and have certainly made this journey pleasant and easier. First, I would like to thank my exceptional supervisory team, Dr Chris Shaw and Dr Kirsten Howlett for accepting me within their research group. Your incredible patience, guidance, support, dedication and trust have been fundamental for me, not only to grow as a person, but also to learn and develop the necessary skills and resilience in a friendly atmosphere.

I would also like to thank Professor Robyn Murphy who allowed me to visit her lab and learn all about the quantitative immunoblotting technique, but also provided me with incredible support while I was troubleshooting with immunoblotting of pooled single fibres. I was able to meet great people there, such as Heidy, who I am thankful for teaching me the methods step by step making this an amazing training experience. Also, Stefan and Barny, who always had time to answer my questions, regardless of their busy schedule. Moreover, a few more people provided me with invaluable feedback throughout this time: Sean, Lee, Clinton and Greg, thank you for always answering my queries and helping me to develop a broader knowledge and new ways to analyse data results. Additionally, special thanks to Dr Alex Addinsall for helping me settle in the MRU lab, as well as Jacob, Liam and Kevin for always making lab work enjoyable despite the setbacks. I would also like to thank Courtney for being a constant help in the lab, teaching me countless ways to be more efficient, but also lifting the mood in the lab with her sparky personality.

I am also incredibly thankful for my vast support network, including my biological family and my friends both in Costa Rica and in Australia, who I like to call my chosen family. Nela, Adel, Fofo, Hells, Hanne and Bobby thanks for all the moral support and for always be willing to listen to me. A special thanks to my brother Erick for his incredible help illustrating parts of this document. Thanks to Fanny for organising the writing group in the library, which was key to boost my productivity. I would also like to thank the “Cliffe” members for bearing with my long nights and my endless Radiohead playlist.

Finally, but not less important, I would like to thank Ryan Pane, Bianca, Rors, Sanshu, Jess, Nima for all the help and support throughout the human study, as well as all the study participants, for their exceptional commitment and incredible attitude throughout the study.

General abstract

Autophagy is a well conserved and highly dynamic cellular recycling process that is important in maintaining cell homeostasis. Autophagy impairments have been linked with insulin resistance and autophagy may be modulated by feeding and exercise. This thesis explores the autophagy responses in important metabolic tissues in scenarios relating to metabolic disease, modulation of nutrient availability and in response to exercise training. Chapter 2 describes the autophagy responses in liver and muscle in response to high fat diet-induced obesity. A differential response in autophagy markers was observed between the liver and skeletal muscle. Autophagy in the liver was impaired, likely due to autophagosome clearance defects, while no changes were found in skeletal muscle. Chapter 3 illustrates the influence of overt type 2 diabetes mellitus on autophagy markers in mice in a fed and a fasted state. Diabetic mice also displayed marked divergent changes in autophagy markers in the liver and skeletal muscle, with increases in autophagy activity in skeletal muscle, along with a reduction in autophagy capacity in the liver, regardless of feeding status. Chapter 4 describes the impact of mixed meal ingestion on muscle fibre-type specific autophagy markers in human skeletal muscle. Autophagy in the fasted state was higher in type I muscle fibres, while the ingestion of a mixed meal induced a decline in autophagosome content in type I and type II fibres. Chapter 5 investigated the impact of a six-week aerobic exercise intervention in overweight males on muscle fibre-type specific autophagy responses. The exercise training intervention did not have an impact on macroautophagy marker protein abundance when assessed in whole muscle. However, when analysed in pooled single muscle fibres, the exercise intervention decreased the autophagosome content in type I fibres, but not in type IIa fibres. In conclusion, autophagy is responsive to both acute feeding and exercise training in human skeletal muscle and tissue specific autophagy dysfunction is present in animal models of metabolic disease. Finally, muscle fibre-type specific analysis provides novel insight on the autophagy responses in human skeletal muscle.

Table of contents

List of abbreviations

AMPK	AMP-activated protein kinase
ANOVA	analysis of variance
Atg	autophagy-related protein
BMI	body mass index
Bcl-2	B-cell lymphoma-2
BNIP3	BCL2/adenovirus E1B 119 kDa interacting protein 3
CMA	chaperone mediated autophagy
DAG	diacylglycerol
DFCP1/FZYVE1	double FYVE domain-containing protein1
ELISA	enzyme-linked immunoabsorbant assay
ER	endoplasmic reticulum
FoxO	Forkhead box protein class O
GABARAP	GABA receptor-associated protein
IFG	impaired fasting glucose
IGT	impaired glucose tolerance
IRS-1	insulin receptor substrate-1
LAMP	lysosome associated membrane protein
LC3B	microtubule-associated-protein 1 light chain 3
LIR	LC3B-interacting region
MHC	myosin heavy chain
mTOR	mammalian/mechanistic target of rapamycin
mTORC1	mammalian/mechanistic target of rapamycin complex 1
NAFLD	non-alcoholic fatty liver disease
OGTT	oral glucose tolerance test
p53	tumour suppressor protein 53
p70S6K	ribosomal protein S6 kinase of 70 kDa
PE	phosphatidylethanolamine
PI3K	phosphatidylinositol 3-kinase

PI3P	phosphatidylinositol-3 phosphate
PINK	PTEN-induced putative kinase 1
PLIN	perilipin
PVDF	polyvinylidene fluoride
SDS	sodium dodecyl sulfate
T2DM	type 2 diabetes mellitus
TBST	tris-buffered saline Tween 20
TFEB	transcription factor EB
TP53INP2	tumor protein 53 induced nuclear protein 2
TSC	tuberous sclerosis complex
ULK-1	unc-51-like kinase 1

List of figures

List of tables

Publications

The following paper has been submitted from the data collected in this thesis:

- **Morales-Scholz MG,** Swinton C, Murphy RM, Kowalski GM, Bruce CR, Howlett KF, Shaw CS. Differential hepatic and skeletal muscle autophagy responses in mice fed a high fat, high sucrose diet.

In addition, data from the current thesis resulted in the following conference communications:

- **Morales-Scholz MG**, Swinton C , Howlett KF, Murphy RM , Kowalski GM, Bruce CR, Shaw CS. Impaired autophagy in the liver, but not skeletal muscle of mice following a high fat diet intervention. 23rd Annual Congress of the European College of Sports Science (ECSS) in Dublin, July, 2018.
- **Morales-Scholz MG**, Tepper BT, Dwyer KM, Swinton C, Wette SG, Howlett KF, Murphy RM, Shaw CS. Human muscle fibre-type specific autophagy responses to a mixed meal tolerance test. Australian Physiological Society Annual Meeting, Canberra, December, 2019

During the period of postgraduate study at Deakin University, the following papers have been published or submitted:

- Hamley S, Kloosterman D, Dalla Man C, Visentin R, Mason SA, Ang T, Selathurai A, Kaur G, **Morales-Scholz MG**, Howlett KF, Kowalski GM, Shaw CS, Bruce CR. Mechanisms of hyperinsulinaemia in apparently healthy non-obese young adults: role of insulin secretion, clearance and action and associations with plasma amino acids. Diabetologia. 2019 Dec;62(12):2310-2324. PMID: 31489455
- Beyene HB, Hamley S, Giles C, Huynh K, Smith A, Cinel M, Mellet NA, **Morales-Scholz MG**, Kloosterman D, Howlett KF, Kowalski GM, Shaw CS, Magliano DJ, Bruce CR, Meikle PJ. Mapping the Associations of the Plasma Lipidome With Insulin Resistance and Response to an Oral Glucose Tolerance Test. J Clin Endocrinol Metab. 2020 Mar 1;105(3). PMID: 32016362
- Shaw CS, Swinton C, **Morales-Scholz MG**, McRae N, Erftemeyer T, Aldous A, Murphy RM, Howlett KF. Impact of exercise training status on the fiber type-

specific abundance of proteins regulating intramuscular lipid metabolism. J Appl Physiol. (1985). 2020 Feb 1;128(2):379-389. PMID: 31917629

- Hamley S, Kloosterman D, Dalla Man C, Visentin R, Mason SA, Ang T, Selathurai A, **Morales-Scholz MG**, Howlett KF, Shaw CS, Kowalski GM, Bruce CR. Reduced insulin clearance rather than increased insulin secretion as a major determinant of hyperinsulinemia in non-obese young adults (submitted)

Chapter 1

General introduction

1.1 Introduction

Insulin resistance is a pathological condition that is present in a variety of metabolic diseases, which constitute a growing financial and economic burden. The exact pathophysiology underlying insulin resistance still remains elusive (1, 2), but recent evidence suggests that a failure of cellular quality control mechanisms, namely autophagy, might contribute in the development and progression of this condition (3). Autophagy is a bulk process which degrades modified intracellular material and releases the end products to the cytosol where they can be used as metabolic substrates (4). Autophagy is acutely regulated by nutrient sensitive signalling pathways, such as the insulin/Akt, AMP-activated protein kinase (AMPK) and mammalian target of rapamycin (mTOR) pathways (5-7). This permits autophagy activation during periods of nutrient deprivation and increased energy expenditure but autophagy inhibition upon increased nutrient availability. The targeted removal of cellular components appears to be crucial for the removal of modified proteins and contributes to long-term cellular homeostasis. Since there is a clear overlap between autophagy regulation and nutrient sensing signalling pathways, structural and cell signalling modifications present in insulin resistant conditions could result in the cells' inability to appropriately modulate autophagy. This might contribute to the development and/or progression of insulin resistance through the accumulation of dysfunctional proteins/organelles (8-10). Furthermore, the autophagy responses to exercise training in this context could provide potential therapeutic insight into optimal treatments for metabolic diseases associated with insulin resistance (11, 12). This chapter will give an overview of the role of autophagy in maintaining cellular homeostasis, the mechanisms regulating its activity in the context of insulin sensitive and insulin resistance and also the potential adaptations in the autophagy machinery in response to exercise training.

1.2 Metabolic homeostasis in the context of insulin sensitive and insulin resistant conditions

Insulin resistance is central to the development of prediabetes, which itself constitutes one of the earliest metabolic abnormalities in people with a high risk of developing T2DM (13) and can be present 13 years before T2DM is diagnosed (14). In 2015, according to the International Diabetes Federation (IDF) (15), 318 million people worldwide were

estimated to have prediabetes and by 2040 this number is projected to increase to 482 million.

Around 70% of the population with prediabetes will eventually progress to T2DM (16) where insulin resistance combined with β-cell failure will result in chronic hyperglycaemia. T2DM accounts for 85% of all diagnosed diabetes cases (17). In 2015, it was estimated that around 374 million had T2DM and it is expected that by 2040, this number will increase up to 578 million (18). Diabetes in general, constitutes a considerable social and economic burden worldwide. Around 12% of the global health expenditure is spent on diabetes, and 75% of the diabetic population lives in a low or middle income country (18). In Australia, by year 2018, over 1 million people had T2DM and, according to a survey conducted in 2015-16, 9.9% of all hospitalisations in the country were due to this disease (19). Therefore, understanding the progression of insulin resistance and identifying optimal therapeutic interventions is of key importance.

From an evolutionary perspective, humans have adapted to cope with alternating periods of energy abundance and also prolonged periods of energy deficiency. During periods of energy abundance, anabolic processes permit synthesis of new proteins and storage of excess energy in the form of glycogen in the liver and skeletal muscle and triacylglycerol in adipose tissue and, to a lesser extent, in other tissues (20, 21). This anabolic phase is independently orchestrated by the hormone insulin (20, 21) and amino acids (22). However, during periods of nutrient deficiency, catabolic processes dominate, which liberate metabolic substrates to allow sufficient energy production for survival (2, 23, 24). In modern society, a combination of continued nutrient excess and a lack of physical activity has led to chronic periods of excess energy availability. The resultant storage of excess energy, primarily in the form of lipid storage in adipose tissue (2), has resulted in rising rates of obesity, along with the associated diseases, such as metabolic syndrome, non-alcoholic fatty liver disease (NAFLD), prediabetes, type 2 diabetes mellitus (T2DM) and atherosclerotic cardiovascular disease (17). Insulin resistance is a unifying factor among the previously mentioned diseases and can be defined as the inability of the tissues, like skeletal muscle, liver and white adipose tissue, to respond adequately to insulin (2, 25). Obesity and T2DM have been considered to be part of a continuum. Excess body fat accumulation, especially around the viscera is lipotoxic and has been linked to low insulin sensitivity (26). Hyperinsulinemia can initially overcome the presence of insulin resistance to maintain blood glucose homeostasis. However, a

combination of continued hyperinsulinemia and increasing plasma glucose levels, in conjunction with already existing lipotoxicity, lead to β-cell deficiency (27, 28). The resultant failure of adequate insulin secretion results in chronic elevations in blood glucose and the onset of overt T2DM (26)

The exact underlying mechanisms linking obesity to the development and progression of insulin resistance and type 2 diabetes remain unclear. Much of the research has focused on the accumulation of lipids and the development of mitochondrial dysfunction in non-adipose tissue, which has been proposed to impair insulin action in skeletal muscle and liver (2). There is increasing evidence that cell degradation systems can have profound effects on cellular metabolism by specifically targeting metabolic substrates and by regulating quality control of cell organelles, such as the mitochondria (29-31). More recently, these degradation processes have been linked with metabolic impairments observed in insulin resistant conditions (3, 29, 32-36). These studies have highlighted the potential importance of intracellular turnover mechanisms in maintaining cell homeostasis and optimal metabolic function.

1.3 Cell degrading systems

Cellular homeostatic mechanisms are vital for the survival and adequate function of cells and tissues. It is now well accepted that this homeostasis is achieved through a fine balance between synthesis and degradation pathways (23). Therefore, the integrity of degrading pathways is considered fundamental for the maintenance of normal cellular function. Catabolic pathways constantly occur and can include degradation of aged organelles, dysfunctional or aggregated proteins, due to endoplasmic reticulum (ER) stress, improper folding or mutations, as well as the breakdown of cellular energy stores, such as glycogen and intracellular lipids (23). Therefore, defects in catabolic processes could lead to accumulation of non-degraded cell components (e.g. lipids) and dysfunctional organelles (e.g. mitochondria) that can cause disturbances in metabolism and cell signalling that are involved in the pathogenesis of insulin resistance and metabolic disease (23). In eukaryotic cells, there are two main degradation systems: the ubiquitin-proteasome and the autophagy-lysosome. Both systems share common features, such as substrate ubiquitination, their subsequent transport to the catabolic site

and the recognition of the degradation signal by the respective catalytic arm in each case (23).

1.3.1 Ubiquitin-proteasome system

The ubiquitin-proteasome system constitutes a series of events that involve substrate marking by ubiquitin, followed by its delivery to the proteasome, where degradation takes place (37). The targeted proteins are ubiquitinated by a process involving three enzymes: E1, that activates ubiquitin, E2, a ubiquitin-carrier enzyme and E3, a ubiquitin ligase. After the first ubiquitin has been added to the target protein, additional ones can be added to a specific lysine (38) or methionine residue through the same reaction and create a ubiquitin chain (39). Once marked for degradation, the proteins are transported to the proteasome 26S, which consists of a core particle (20S) with one or two regulatory caps (19S) (40). The latter are responsible for recognizing the marked substrates which are then deubiquitinated and unfolded to undergo translocation to the proteolytic chamber (40). It is important to mention that under physiological conditions, the majority of the degrading activity in mitotic cells is undertaken by the ubiquitin-proteasome system and defects in this system activate compensatory mechanisms that are able to cope with the functional deficiency (41). However, in long-lived post-mitotic cells, like skeletal muscle, autophagy-lysosome system activity is more prominent and accounts for almost half of the degrading activity (42-44).

1.3.2 Autophagy-lysosome system

Autophagy derives from the Greek word *autóphagos*, which means “self-eating”. It is a highly dynamic, well-conserved process, in which cytoplasmic components are degraded by the lysosomes (45). Depending on the substrate selection and the delivery mechanisms, autophagy can be classified into three types: (a) microautophagy, (b) chaperone-mediated autophagy (CMA) and (c) macroautophagy (46) (Figure 1.1).

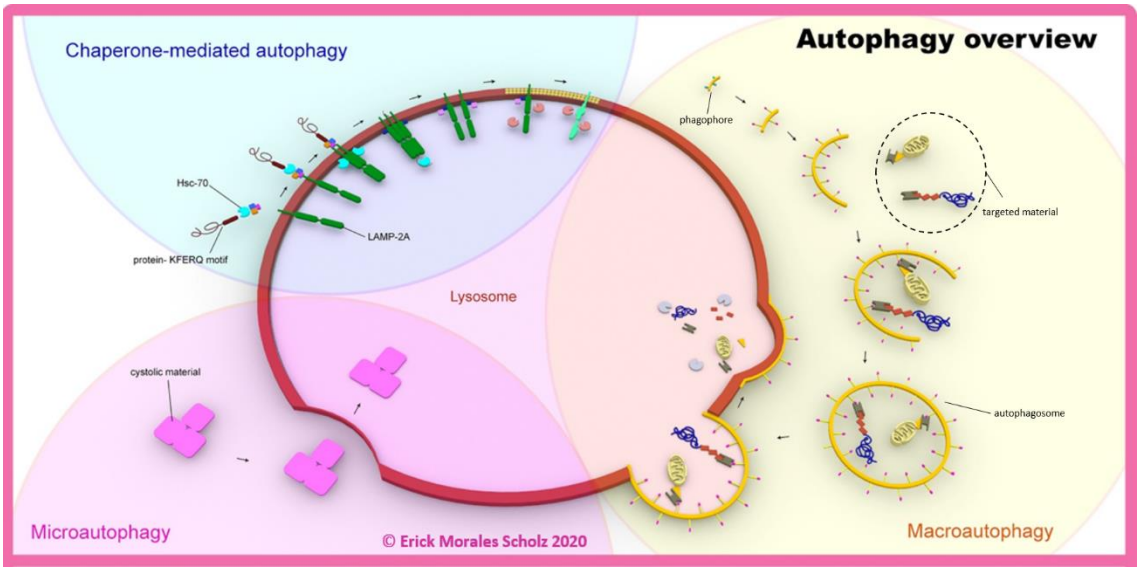

Figure 1.1. Overview of autophagy pathways. a) Chaperone-mediated autophagy: cytosolic targets are recognized through the presence of a KFERQ motif by an Hsc-70 chaperone complex that is directed to the lysosome and internalized for further degradation by the lysosomal receptor LAMP2A. b) Microautophagy: small portions of the cytosol are directly engulfed by the lysosome and degraded afterwards. c) Macroautophagy: cytosolic targeted material is engulfed by a double-membrane structure, called the phagophore, which forms the autophagosome and then fuses with the lysosome. Adapted from (5, 47-52). Graphic design by Erick Morales Scholz.

In microautophagy, the lysosome directly engulfs small portions of the cytosol, but little is known about this type of autophagy, its regulation and its role in the context of disease states (24). In CMA, the chaperone Hsc-70 directly target specific cytosolic proteins for delivery to the lysosome, by recognizing a common exposed KFERQ motif. The targeted proteins are delivered and enter the lysosome via a multimeric complex comprised of lysosome associated membrane protein-2A (LAMP-2A) (53-55). Macroautophagy is a process, in which a double membrane structure, named a phagophore, expands to form a vesicle-like structure called the autophagosome. The expanding phagophore engulfs targeted cytosolic material, including portions of, or whole organelles. Once formed, the autophagosomes fuse with the lysosome, where the degradation process takes place, via lysosomal enzymes (56). Macroautophagy is the best understood and the most studied type of autophagy (24), while CMA is emerging as a potentially relevant process involved the development and progression of metabolic diseases. Both macroautophagy and CMA will be the focus of the remainder of this review.

1.4 Macroautophagy

The term autophagy was coined by C. de Duve in 1963 (57), eight years after discovering the lysosome. Interestingly, macroautophagy was discovered in rodent models, but most of the research between the late 90's and the beginning of the new millennium was conducted in yeast, where the regulation of this process was described in detail, especially by Ohsumi and his research group (58, 59). Initially, the scope of macroautophagy's research was related to cell-death mechanisms and its relevance in oncogenesis. It was not until 2005 that macroautophagy's relevance broadened outside the cancer-related scope and began to be linked with diseases, including metabolic disturbances, such as fatty liver disease, as well as neurodegenerative diseases (59). While once considered to be a non-selective bulk degradation system, it is now acknowledged that macroautophagy is a highly selective process. This selectivity is acknowledged by a variety of terms which relate to the target for degradation, such as mitophagy (mitochondria), glycophagy (glycogen), lipophagy (lipids), ribophagy (ribosomes) and xenophagy (pathogens) (60).

1.4.1 The phases of macroautophagy

The process of macroautophagy is divided into the following five steps: (a) induction, (b) nucleation and expansion, (c) cargo selection, (d) fusion with the lysosome and (e) degradation and efflux (24). Among the stimuli that are widely known to activate autophagy are cell nutrient deprivation (61, 62), oxidative stress (63) and calcium imbalance (64). These stimuli result in acute posttranslational modifications of proteins involved in autophagy regulation, which are then followed by a change in the autophagy transcriptional program (24). Most of what it is known about macroautophagy regulation is derived from studies in yeast and rodent liver tissue (59).

1.4.1 (i) Induction

The formation of the phagophore, the autophagosome precursor, is the first step of autophagy induction (23) and it is initiated via the translocation and activation of the unc-51-like kinase 1 (ULK-1) complex, consisting of ULK-1, FIP200 (focal adhesion kinase family interacting protein of 200 kDa), autophagy-related protein (Atg) 13, and Atg1 (65). Upon autophagy induction, the ULK-1 complex translocates to the vicinity of the phagophore formation site and it activates via auto-phosphorylation (66), where the nucleation and phagophore expansion phases start (24). Firstly, the active ULK-1 complex activates the Beclin-1 complex, consisting of beclin-1, class III phosphatidylinositol 3-kinase (PI3K), vacuolar sorting protein 34 (Vsp 34) and 15 (Vsp 15), activating molecule in BECN1 regulated autophagy protein1 (AMBRA1), ultraviolet irradiation resistance-associated gene (UVRAG) and Atg14 (67), which promotes the generation of phosphatidylinositol-3 phosphate (PI3P) and is essential for phagophore expansion (23). (Figure 1.2).

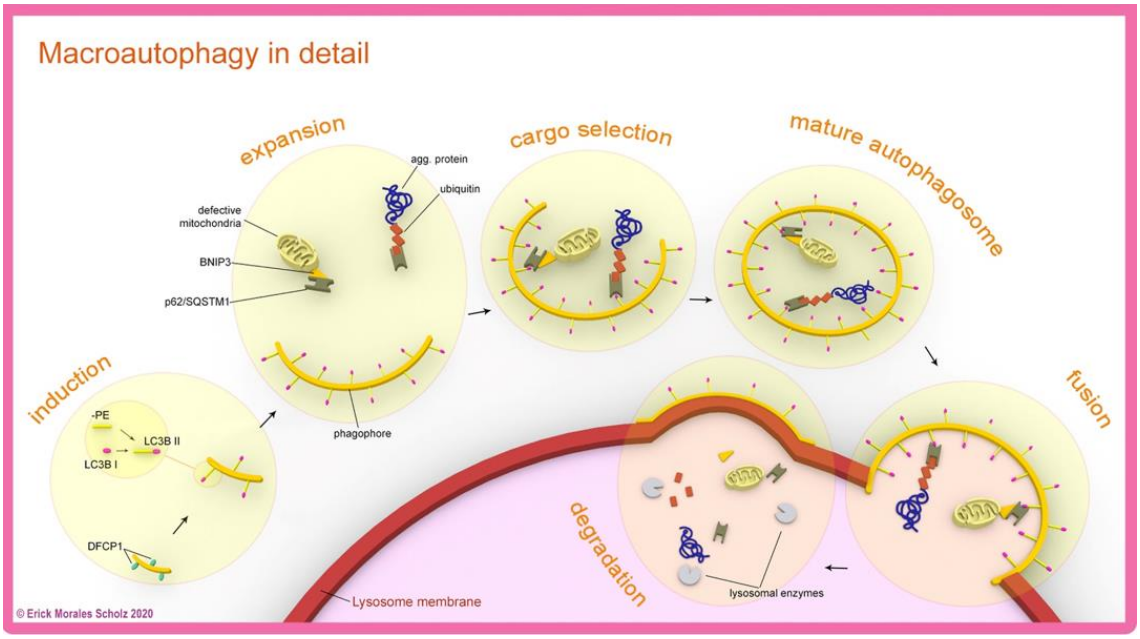

Figure 1.2. Macroautophagy in detail. Macroautophagy phases: i) induction; ii) expansion; iii) cargo selection; iv) mature autophagosome formation; v) fusion with the lysosome; vi) autophagosome content degradation. PE: phosphatidylethanolamine. See text for more details. Adapted from (5, 50-52) .Graphic design by Erick Morales Scholz.

1.4.1.(ii) Nucleation and expansion

The growing phagophore also requires membrane donors, the origins of which are still elusive, but potential sources could include the mitochondria, the ER, the plasma membrane, the nuclear envelope, (46), the Golgi apparatus, or even the cytosolic lipid droplets (68). A reliable cell marker of early phagophore formation is double FYVE domain-containing protein 1 (DFCP1 or FZYVE1) (69), a protein that binds to the phagophore membrane by recognizing PI3P (70) a step that is regulated by the beclin-1 complex. As the phagophore expands, microtubule-associated protein light chain 3B (LC3B) and GABA receptor-associated protein (GABARAP), are also recruited to its membrane (69, 71). This requires LC3B or GABARAP processing, which is carried out by two ubiquitin-like enzyme systems. In the case of LC3B, it is first converted from the pro-LC3B form to LC3B-I (23, 24). This is achieved by a cysteine protease, Atg4, which exposes the C-terminal glycine residue, after which LC3B-I undergoes lipidation and conversion to LC3B-II (72). LC3B-I, firstly interacts with Atg7 (LC3B-Atg7) and then with Atg3 (LC3B-Atg3), by forming thioester intermediates (72). Once LC3B-Atg3 is formed, it is converted to LC3B-II, by adding a phosphatidylethanolamine (PE) group, a process conducted by the Atg12-Atg5-Atg16L1 complex (73). LC3B-II is then incorporated into the autophagosomal membrane, where it can interact with different adaptor proteins (73). The abundance of LC3B-II correlates well with the number of autophagosomes, therefore is a well-used marker to determine autophagosome content (71, 74). Furthermore, typically LC3B-II and LC3B-I are expressed as a ratio, which provide information about LC3B-II conversion (74) (Figure 1.2).

1.4.1 (iii) Cargo selection

Macroautophagy's selectivity seems to rely on adaptor proteins, which recognize specific cytosolic targets for degradation. Examples of these proteins include p62/SQSTM1, tumour protein 53 induced nuclear protein 2 (TP53INP2) (33, 75) and BCL2/adenovirus E1B 119 kDa interacting protein 3 (BNIP3) (76, 77). Proteins like p62/SQSTM1 or TP53INP2 possess a ubiquitin-binding domain and an LC3B-interacting region (LIR), thereby serving as scaffold proteins between the ubiquitinated substrates and the autophagosome (78). However, BNIP3, an outer mitochondrial membrane protein, interacts directly with LC3B-II without the necessity of ubiquitin, due to its LIR (79).

Autophagy target recognition not only happens through ubiquitination of substrates, but also due to changes in some physiological properties, for example, mitochondrial membrane depolarization (24). In some cases, mitochondrial oxidative damage leads to depolarization of the outer membrane and this increases the PTEN-induced putative kinase 1 (PINK) or BNIP3 recruitment to the mitochondria (79). Increases in PINK recruit Parkin, an ubiquitin ligase, which targets these substrates for degradation through mitophagy (80) (Figure 1.2).

1.4.1 (iv) Fusion with the lysosome

Once the autophagosome is mature it then, fuses with the lysosome. The lysosomal membrane is coated with several proteins, in particular lysosome-associated membrane proteins 1 and 2 (LAMP-1 and LAMP-2), which assist in this fusion process (81). Furthermore, evidence in rodent models suggest that the lipid composition of both the autophagosomal and the lysosomal membrane determine the fusogenic activity between these two organelles (82). Interestingly, autophagosomes isolated from rodents fed a high-fat diet (HFD) showed a decreased ability to fuse with the lysosomes (82). These findings support the proposed pathological mechanism, where macroautophagy defects might be due to defects in lipid composition of the autophagosome/lysosomal membrane caused by excessive lipids coming from the diet (Figure 1.2).

1.4.1 (v) Degradation and efflux

The degradation of all autophagy targets takes place within the lysosome. Inside the lysosome, a variety of hydrolytic enzymes are present, these include sulfatases, glycosidases, peptidases, phosphatases, lipases and nucleases. These enzymes function optimally at a low pH which is regulated by the action of a V-ATPase located at the lysosomal membrane (83). Once the substrates are degraded by these enzymes, the end-products exit the lysosome thorough specific transporters depending on their chemical nature and can be re-used for metabolic processes (84-87). It is important to mention that adaptor proteins, such as p62/SQSTM1, not only select the cargo to be degraded, but they undergo degradation themselves, once the autophagosome is fused

with the lysosome. This feature makes p62/SQSTM1 a key marker for autophagosome degradation (74) (Figure 1.2).

1.5 Quantitative approaches to study autophagy *in vivo*

Autophagy is a highly dynamic process involving multiple steps which are constantly in states of flux, characteristics that present a challenge when assessing this process, particularly *in vivo*. The gold standard method of measuring autophagy are flux measurements, which involve the chemical inhibition of the fusion process between the autophagosome and the lysosome and/or the lysosomal function itself which will halt the degradation of the autophagosome. The subsequent assessment of classic autophagy markers, such as LC3B and p62/SQSTM1 (74). This approach has been well used particularly *in vitro* given the ease of applying chemical inhibitors. For example, an increase in both LC3B-II and p62/SQSTM1 would be expected in the presence of a chemical inhibitor if conditions result in an increase in autophagy flux (e.g. nutrient deprivation). However, this approach is not without its limitations. Since the lysosome is not exclusive to autophagy, lysosomal inhibition through chemical inhibitors may(88) interfere with other cellular processes and constitute a confounding factor during the analyses. Furthermore, chemical inhibitors used (e.g. leupeptin, chloroquine, Bafilomycin) are rarely specific to the lysosome and may have off-target effects. Importantly, this approach to assess autophagy flux cannot currently be performed in human experiments, at least *in vivo*, which somewhat limits the clinical translation of autophagy work. For consistency, the typical approach to assess autophagy responses in human tissues is to assess the protein abundance, via immunoblotting, as well as gene expression of key autophagy markers (e.g. LC3B and p62/SQSTM1). Such approaches are recommended as an alternative when assessing autophagy in the absence of flux measurements (74) and have been widely used in previous studies that assessed autophagy in human and animal tissues (6, 89-92).

1.6. Molecular regulation of macroautophagy

Macroautophagy is a highly complex cellular process and it is tightly regulated in the cell by both extracellular and intracellular metabolic cues. Modulation of macroautophagy

activity is biphasic (24). Acute changes in cellular metabolic status, for example due to nutrient deprivation, induce first a rapid response that increases autophagy flux. This is mediated by posttranslational modifications of key autophagy-regulating signalling proteins, such as AMPK, mTOR, ULK-1, among others. This typically occurs within minutes to hours after the initial stimulus (24). Secondly, more long-lasting effects occur as a consequence to changes in the expression of autophagy-related transcription factors and upregulation of the expression of autophagy genes. The latter response is governed by the activity of three master transcriptional regulators of macroautophagy: transcription factor EB (TFEB), tumor suppressor protein 53 (p53) and Forkhead box protein class O (FoXO) (93). These transcriptional regulators are controlled by nutrient availability, energy disturbances, as well as the levels of several growth factors (93).

1.6.1 (i) Post-translational modifications

The precise intracellular signalling processes that acutely regulate macroautophagy initiation are still not fully explained, however attention has focused around the activity of AMPK and mTOR. It is classically accepted that AMPK activation leads to autophagy induction, while active mTOR inhibits autophagy (94). Evidence suggests that under basal conditions, AMPK is constitutively active and it is the variations of mTOR activation that modulate AMPK activity and subsequent macroautophagy activation (95, 96). Nutrient deprivation is one of the most powerful and well-studied stimulators of autophagy activity (24, 97) and this is thought to be accomplished in part through the activation of AMPK, due to declines in mTOR activity (98). Interestingly, it seems that mTOR activity is one of the primary mechanisms by which macroautophagy is regulated, particularly in skeletal muscle *in vivo* (99-101). Lowered mTOR activity stimulates ULK-1 by an increase in its phosphorylation on serine 555 (p-ULK-1^{S555}) (94) and lowered phosphorylation of its inhibitory site at serine 757 (p-ULK-1^{S757}) (98), events that induce ULK-1 complex formation. The active ULK-1 complex stimulates Beclin-1 complex activation (94, 102-104), which is crucial for phagophore formation and expansion, since it is responsible for PI3P formation, a fundamental constituent of the phagophore membrane (94, 102-104). Exercise stimulates B-cell lymphoma 2 (Bcl-2) phosphorylation, which promotes its dissociation from Beclin-1 and stimulates autophagy (11). Additionally, AMPK activity increases during exercise (100, 105), which activates tuberous sclerosis complex 2 (TSC2). TSC2 activation inhibits mTOR by inhibiting its

upstream activating protein Rheb, ultimately leading to autophagy activation overall (98). Nutrient scarcity also activates TSC2 by decreasing Akt activity, a recognised TSC2 inhibitor (106) (Figure 1.2).

On the other hand, increases in nutrient availability inhibits macroautophagy in cells. The latter process is governed by active mTOR, which is one of the major inhibitors of autophagy (94, 106). Activation of mTOR can occur indirectly via the insulin-Akt pathway, which decreases TSC2 inhibition on mTOR (107), or directly due to amino acid (particularly leucine) and/or lipid increases, which act on mTOR independently of the insulin-Akt pathway (108, 109). Activation of mTOR, via phosphorylation on serine 2448 (p-mTOR^{S2448}), leads to the formation of the mTOR complex 1 (mTORC1), which inhibits autophagy (110, 111) through increases in p-ULK-1^{S757} (98). It is worth noting that both phosphorylated forms of ULK-1, as well as p-mTOR^{S2448}, expressed in relation to their total protein levels have been widely used to assess how autophagy is induced (69) (Figure 1.2).

1.6.1 (ii) Transcriptional program modifications

Longer term changes in macroautophagy activity occur as a consequence to changes in the expression of autophagy-related transcription factors, such as TFEB, p53 and FoXO3. TFEB regulation is dependent on subcellular localization. Under fed conditions, TFEB remains sequestered in the cytosol after being phosphorylated by mTOR. In response to fasting, mTOR activity decreases and TFEB is active and able to translocate to the nucleus to activate transcription of key macroautophagy genes (107, 112, 113), such as genes involved in autophagosome biogenesis (114, 115), as well as PGC1α and PPARα genes and proteins involved in fatty acid import into the cell and its metabolism (83). On the other hand, FoxO belongs to a family of transcription factors that integrate different upstream signals and orchestrate various cell processes, such as cell growth, glucose metabolism (116) and protein catabolism (117), thereby ensuring cell and tissue homeostasis. This family of transcription factors are inhibited by the Akt signalling pathway (116) and are therefore, sensitive to systemic nutritional status. Similar to TFEB, FoXO3's activity is regulated by subcellular localization. Akt phosphorylates FoXO3 and retains it in the cytosol, but during starvation or fasting this pathway is less active (117, 118), which allows FoXO3 to translocate to the nucleus and exert its function by binding to promoters of several autophagy genes, like BNIP3, a known mitophagy inductor (31).

Furthermore, p53, is well known for its tumour-suppressor activity, but has also been linked to macroautophagy regulation. Under stress conditions, such as starvation and/or physical exercise, it becomes active (119), and induces lipid catabolism (120-122) and couples it to macroautophagy activity (123), since it increases the expression of several autophagy proteins, such as autophagy-related protein (Atg) 7, ULK-1 (124), as well as TSC (125).

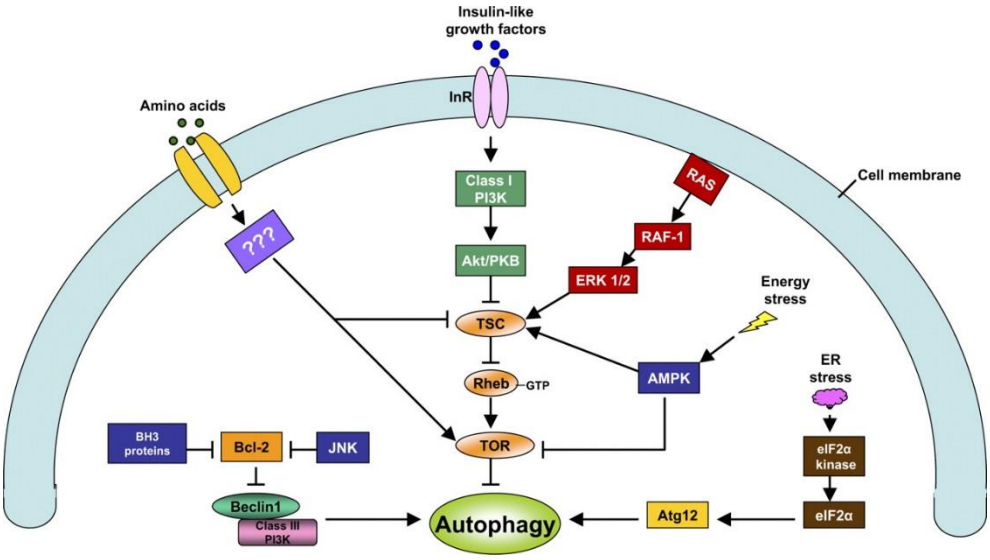

Figure 1.3. Acute molecular regulation of macroautophagy. After a meal, plasma insulin levels rise in response to increases in nutrients, like glucose and amino acids. Both insulin and amino acids are able to inhibit autophagy through mTOR activation. Insulin activates PI3K-Akt-pathway, which inhibits TSC, a known mTOR inhibitor, while amino acids can stimulate mTOR through an Akt-independent pathway, either directly or through TSC inhibition. On the other hand, AMPK, activated by energy stress cues, such as nutrient deprivation, activates autophagy, by activating TSC and inhibiting mTOR Taken from (126).

1.6.2. Nutritional regulation of autophagy

Under physiological conditions, insulin is produced and secreted into the bloodstream by the pancreas in response to increases in plasma nutrients, especially glucose and amino acids, following a meal (127). It exerts its function on its target tissues by binding to the insulin receptor located on the surface of the plasma membrane (21). The latter activates several insulin receptor substrates, in particular insulin receptor substrate-1 (IRS-1) through tyrosine-residue phosphorylation (128). Among the intracellular pathways that IRS-1 activates, the mitogen-activated protein kinase (MAPK) pathway, which exerts the long term transcriptional effects of insulin, and the phosphatidylinositol 3-kinase (PI3K) pathway require special attention (128). The latter activates Akt, which modulates the activity of various downstream signalling events and mediates insulin's acute metabolic effects. In terms of insulin's glucoregulatory function, insulin action promotes glucose uptake in most peripheral tissues, of which skeletal muscle is of primary importance, and inhibits hepatic glucose output (127, 128). Therefore, both skeletal muscle and the liver constitute the two most important tissues that normalise glycaemia after food ingestion to ensure glucose homeostasis (128). However, post-prandial rises in insulin, in combination with increased nutrient availability, primary amino acids, also exert metabolic effects beyond glucose regulation, including the regulation of protein and lipid metabolism. For example, insulin suppresses forkhead box protein class O-3 (FoXO3) (3, 128) and both a rise in insulin and amino acid availability activate mTOR, the main driver of protein synthesis (22). It is worth mentioning that under nutrient deprived conditions, insulin levels decrease and glucagon levels rise, which in combination lead to opposite metabolic effects to the previously described ones in both, the liver and skeletal muscle (129). Furthermore, it has been described that lysosomal location changes depending on the nutrient availability; in nutrient deprived conditions lysosomes tend to cluster around the cell's nucleus, which is believed to facilitate autophagosome-lysosome interactions, while during nutrient excess conditions, lysosomes are found to be located peripherally (130).

As highlighted previously in this section, similar pathways are important in regulating autophagy in response to fluctuations in nutrient and hormonal levels caused by fasting and re-feeding periods. As the liver and skeletal muscle are the two main insulin-responsive tissues regulating glucose and protein metabolism, the following sections will examine the evidence that nutrient availability determines autophagy activity in these tissues.

1.6.2 (i) Liver

The liver is one of the most metabolically active organs in the human body and macroautophagy has been broadly researched in this tissue (60). Under healthy conditions autophagy ensures sufficient energetic supply in the liver through three main mechanisms: 1) intracellular energy store breakdown; 2) efficient mitochondrial turnover; and 3) key metabolic enzyme regulation (34). An early study investigating autophagy in rat liver reported an increase in autophagy activity, assessed by an increase in the efflux of labelled amino acids from the lysosome, together with visual increase in lysosomal volume, after a period of starvation (4-6 h) (131). An elegant study reported that starvation (~8 h) in mice induced hepatic macroautophagy and specifically lipophagy. This was determined by a visual increase in the number of lipid droplets associated to autophagosomes via electron microscopy, and increased LC3B-II association to lipid droplets as determined by co-purification studies (29). Additionally, studies investigated macroautophagy in a mouse model, where Atg7, a key autophagy inductor, was specifically knocked out in the liver. Electron microscopy showed that this genetic manipulation impairs autophagosome formation during 24 h starvation and resulted in accumulation of aberrant mitochondria, protein aggregates and lipid droplets compared to control mice. Furthermore, immunoblotting demonstrated no changes in LC3B-II, despite increases in LC3B-I (132), implying a possible defect on autophagosome formation (i.e. macroautophagy induction) and/or on autophagosome degradation. The latter results suggest that a 24 h starvation period, normally induces liver macroautophagy, and that Atg7 is not only important in inducting this process, but also increasing the degradation rate at its latest stages. Additionally, evidence in perfused rodent livers showed that immediate amino acid withdrawal increased autophagosome content, followed by the appearance of the autolysosomes a few minutes later (61, 62). Furthermore, *in vivo* studies using perfused mouse livers have shown that 4-6 h fasting is sufficient to stimulate macroautophagy, determined by an increased lysosomal release of labelled amino acids, as well increased lysosomal volume (131) and after 8 h fasting there is a switch in the type of substrate targeted to degradation, from proteins to lipids (29).

On the other hand, feeding has the opposite effect on macroautophagy activity, as it constitutes a potent autophagy inhibitor. In fact, increases in amino acid availability, as well as rises in plasma insulin concentrations are likely to explain much of the macroautophagy supressing responses ton feeding. Additionally, leucine was found to

be the most effective amino acid to inhibit autophagy, which is in line with leucine's role as a strong stimulus of mTOR activity (108). A few studies have looked at the autophagy response in the transition from the fasted to the fed state in mice. However, the autophagy measurements were performed after a 24-48 h fasting period and 1-3 days of *ad libitum* refeeding (61, 62). Although these study designs are useful to study some aspects of macroautophagy behaviour, they do not resemble macroautophagy responses in a normal fasting-feeding scenario that occurs with normal feeding behaviour. Therefore, the acute liver responses in macroautophagy activity due to physiological changes in nutrient availability *in vivo* have not been thoroughly investigated and due to the nature of its regulation, need to be addressed in a more physiological setting.

1.6.2 (ii) Skeletal muscle

Skeletal muscle comprises around 40 % of body mass and it adapts very quickly to changes in contractile activity and nutrient availability (24). This tissue's subcellular organelles are continually modified and undergo constant turnover, which eliminates dysfunctional or damaged proteins/organelles and ensures optimal cell function (133). As in liver, macroautophagy in skeletal muscle ensures homeostasis (134, 135). Initially, the focus of macroautophagy studies in skeletal muscle was myopathies, since accumulation of unfolded protein aggregates and dysfunctional organelles correlated well with the level of macroautophagy impairment (136, 137). In fact, specific knockout models (Atg 5, Atg7) revealed the relevance of autophagy in skeletal muscle mass maintenance, since they presented aberrant mitochondria, higher oxidative stress and sarcomere disorganization and increased muscle wasting (138, 139). An important feature of autophagy is that to effectively maintain cellular homeostasis, there must be a balance in the level of its activity. Indeed, studies in rodent models that have shown that muscle wasting can result from either inhibition or activation of macroautophagy (140). Additionally, in humans an impairment of macroautophagy and an increase in lysosomal accumulation has been associated with congenital muscle-wasting diseases, such as Danon (141) or Pompe's desease (138). However, an exaggerated increase in macroautophagy activity have similar effects, such as X-linked myopathy with excessive autophagy (MEA) (134). Therefore, given the important role of macroautophagy in regulating substrate supply for protein synthesis and ATP production, the ability to

adequately regulate macroautophagy activity during periods of fasting and feeding is likely important to maintain cellular function. Furthermore, it has been observed that macroautophagy activity declines with age, which has been linked to age-related loss of muscle mass. However, upregulation of macroautophagy through calorie restriction seems to slow down the decline in metabolic function and maintains muscle mass with age and may extend lifespan (142, 143)

As in the liver, skeletal muscle macroautophagy is acutely regulated by changes in nutrient availability. Studies in rodent models have described a fasting-induced increase in macroautophagy as shown by decreases in p62/SQSTM1 protein levels and increases in LC3B-II/LC3B-I ratio (94, 144). *In vivo*, autophagy in skeletal muscle has been shown to increase after a 9.5 h fasting period in mice, as measured by an increase in markers of mitophagy (BNIP3 and Parkin protein levels), as well as LC3B-II/LC3B-I ratio. LC3B-II/LC3B-I ratio changes presented without variation in *Lc3b* gene expression (90), meaning that LC3B-II/LC3B-I ratio changes were due to increased lipidation of LC3B, which is indicative of macroautophagy induction. Interestingly, under basal conditions, rodent skeletal muscle shows differences in autophagy depending on the muscle fibre-type. The content of the autophagy machinery and basal autophagy flux in mice, assessed by increased LC3B-II/LC3B-I ratio and decreased p62/SQSTM1 levels, was found to be highest in primarily oxidative muscle (soleus) and lowest in muscle composed of primarily glycolytic fibres (white vastus lateralis) (145). Moreover, rat skeletal-muscle autophagy response to prolonged fasting (24 – 72 h) was also found to be fibre-type specific, since fast-twitch fibres undergo higher macroautophagy induction (146). Therefore, it may be important to consider these differences, while analysing autophagy responses. Importantly, human muscle fibre-type specific markers of macroautophagy have not been investigated.

Few studies have examined the impact of acute feeding on macroautophagy in human skeletal muscle. One study showed a suppression of macroautophagy, assessed by decreases in LC3B-II abundance and LC3B-II/LC3B-I ratio, in skeletal muscle following a 100 min-euglycemic-hyperinsulinemic clamp performed after an overnight fast (6). These findings indicate that rises in plasma insulin alone are sufficient to suppress macroautophagy. However, the use of the euglycaemic-hyperinsulinemic clamp constitutes a non-physiological approach, since glucose levels are strictly maintained at a constant level, while a state of hyperinsulinemia prevails for a period of 100 min (6).

Physiologically, there is a transient increase in plasma glucose and insulin that peak around 30-60 min after each meal and return to basal concentrations within a 2-3 h timeframe (147). To date, only one study has examined the macroautophagy responses in human skeletal muscle following a single meal. There was decrease in the LC3B-II/LC3B-I ratio in human skeletal muscle 30 min following the ingestion of a mixed meal (101). This corresponded to an increase in ULK-1^{S757}, which is downstream of mTOR and inhibits macroautophagy induction (101). It is worth mentioning that this study did not indicate how both LC3B protein isoforms behaved independently, which could have strengthened the conclusion about macroautophagy activity after feeding. Complete descriptions of the macroautophagy response to such acute physiologically relevant changes in nutrient and hormonal concentrations are lacking, even though it is widely assumed that this cellular process is sensitive to acute changes in nutrient availability.

1.7 Chaperone-mediated autophagy, regulation and relevance in disease states

Chaperone-mediated autophagy is an alternative form of autophagy that does not involve the formation of an autophagosome in order to target proteins to be delivered to the lysosome. Instead, the chaperone Hsc-70 forms a complex that recognizes an exposed KFERQ sequence or its homologues on the protein targets, forming a complex allowing the targeted material to be delivered directly to the lysosome (148). Hsc-70 starts unfolding the target protein while directing it to the lysosomal surface, where the complex enters the lysosomal lumen through lysosomal associated membrane protein-2A (LAMP2-A) (53-55). Substrate internalization is possible due to the formation of a translocation complex in the lysosomal membrane, comprised by multiple LAMP-2A however, the presence of Hsc-70 inside the lysosome is also required (149) (Figure 1.4).

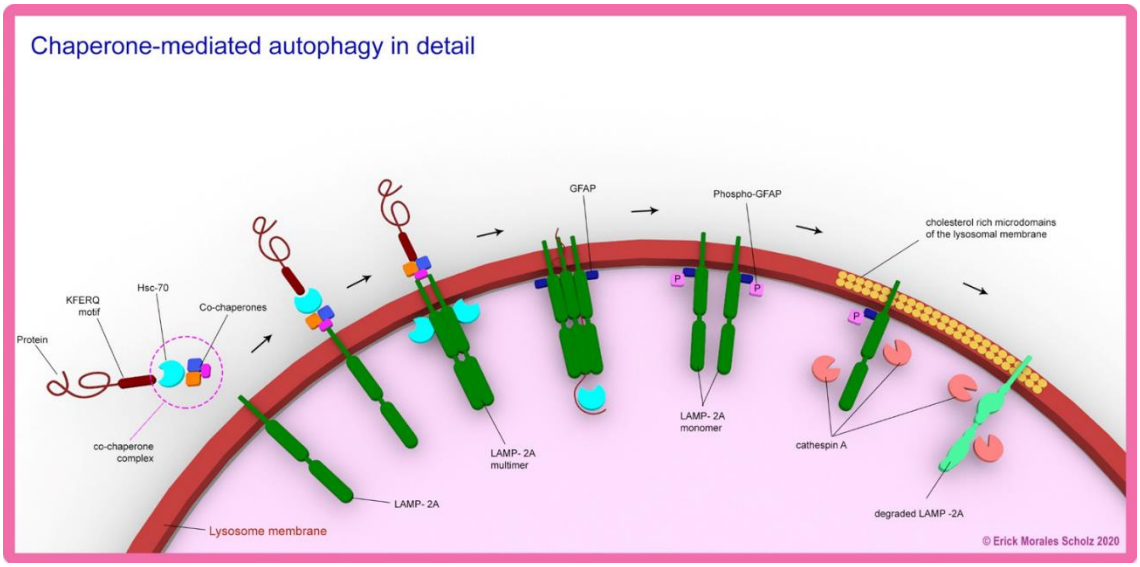

Figure 1.4. Chaperone-mediated autophagy in detail. Hsc-70 recognises the KFERQ motifs in proteins and translocates the targeted proteins to the lysosomal receptor LAMP2-A. The protein is translocated into the lysosome lumen through a channel formed by a LAMP-2A multimer, where degradation by lysosomal enzymes takes place. Once the target protein is translocated to the lysosome lumen it undergoes degradation by the lysosomal enzymes. The GFAP stabilizing the LAMP-2A monomer is phosphorylated and promotes the LAMP-2A multimer disassembly into monomers, which are introduced into lipid rich microdomains of the lysosome membrane to then undergo degradation. Adapted from (47-49). Graphic design by Erick Morales Scholz.

LAMP-2A abundance, as well as its translocation complex assembly and disassembly in the lysosome membrane has been recognised as the limiting step regulating CMA. Once in the lysosomal membrane, the LAMP-2A translocation complex is stabilized by the glial fibrillary acidic protein (GFAP), which prevents it from being disassembled by Hsc-70 (150). Stabilization by GFAP is only possible when this protein is not phosphorylated, therefore GFAP phosphorylation would indirectly promote LAMP-2A complex disassembly and hence, its degradation. GFAP phosphorylation is carried out by Akt, whose activity is regulated by the mammalian target of rapamycin complex 2 (mTORC2) and pleckstrin homology domain and leucine-rich repeat protein phosphatase 1 (PHLPP1) (151). mTORC2 inhibits CMA by activating Akt, while PHLPP1 stimulates CMA by inactivating Akt. Additionally, the membrane expression of this LAMP-2A depends on its degradation by cathepsin A (152) after being incorporated as a monomer into cholesterol rich microdomains of the lysosomal membrane (149, 153) (Figure 1.4).

A growing body of evidence has linked CMA to maintenance of cell homeostasis. CMA alterations have been implicated in a variety of conditions, such as Parkinson's disease, Huntington's disease, cancer and ageing. In both Parkinson's disease (154, 155) and Huntington's disease (156, 157), CMA impairments have been associated with exacerbated protein aggregation and worsening of the clinical symptoms. Moreover, an abnormal upregulation of CMA has been described to be a key factor guaranteeing cancer cell survival (158). In contrast, a decline in CMA activity has been associated with loss of hepatic homeostasis and function in aged-rodent models (159). Interestingly, studies inhibiting CMA in mouse livers have reported a rapid progression to NAFLD indicating the importance of CMA in metabolic homeostasis (34). However, the specific role of CMA in skeletal muscle has not yet been addressed.

Additionally, previous evidence has shown that in livers of rats, CMA was activated after 8 h of starvation, a response that peaked after 24 h of starvation. This was assessed by the progressive increase in Hsc-70 abundance in the lysosomal fraction, when compared to the cytosolic fraction, via immunoblotting (160). However, to date, CMA responses to feeding and fasting have not been addressed in skeletal muscle.

1.8 Insulin resistance and autophagy function

As mentioned previously in Section 1.1, over nutrition, among other factors, can lead to the development of insulin resistance. While the precise mechanisms responsible for the development of insulin resistance are unclear (2), the inhibition of the insulin signalling pathway underlie the impaired insulin responses in various tissues. The most common hypothesis focuses on the impact of ectopic accumulation of specific lipid species (e.g. diacylglycerol (DAG) and ceramides) that ultimately disrupt insulin signalling at the level of the (IRS-1) and/or Akt leading to a decrease in the downstream activation of the PI3K-Akt pathway. This disrupted insulin signalling transduction results in reduced insulin-mediated suppression of hepatic glucose production and reduced insulin-mediated glucose uptake by skeletal muscle. In combination, this leads to increases plasma glucose excursions after food ingestion and compensatory increases in insulin secretion (2) (Figure 1.5).

Additional metabolic dysfunctions have been described in insulin resistant conditions. mTOR hyperactivation in insulin resistant livers has been reported in obese mice, and has been attributed to either excess circulating amino acids and/or hyperinsulinemia (20). A resultant excessive downstream activation of the mTOR target, ribosomal protein S6 kinase of 70 kDa (p70S6K), has also been linked to inhibition of IRS-1 via abnormal serine-residue phosphorylation (20) (Fig.1.3). Furthermore, defective mTOR signalling in obese and insulin resistant conditions has more recently been linked to impaired regulation of anabolic pathways in skeletal muscle and impairments in rates of postprandial protein synthesis (161).

Since plasma glucose levels are tightly regulated by insulin's action on the liver and skeletal muscle, understanding the mechanisms and impact of insulin resistance in these tissues are pivotal to better comprehend the development and progression of insulin resistant conditions. As mentioned previously, there is clear overlap between autophagy and insulin signalling pathways and therefore, it is logical that autophagy could be dysregulated in insulin resistant conditions. The main focus of previous research efforts in this area has been the liver, due to the close relationship between insulin resistance and the development of NAFLD, the most common chronic liver disease, worldwide (2). However, given that skeletal muscle also has a vital role in maintaining metabolic health, further attention is warranted in this tissue.

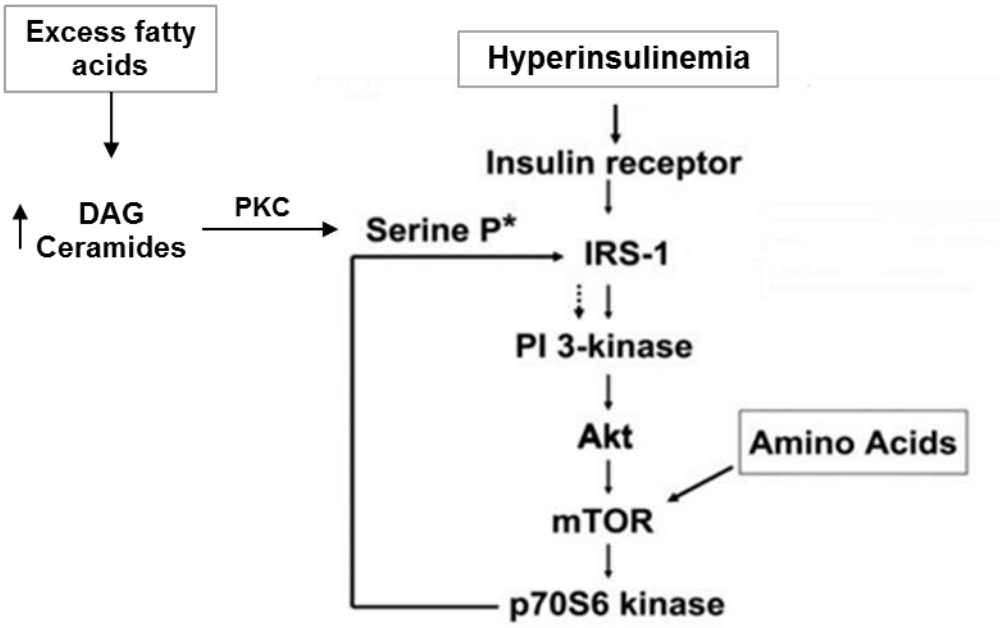

Figure 1.5. Insulin signalling pathway under physiological or insulin resistant conditions. Adapted image from (1, 20). Insulin binds to its membrane receptor and activates the PI3K/Akt pathway, which activates mTOR and p70S6 kinase. Under pathological conditions, hyperinsulinemia or excess amino acids hyper activate mTOR. The latter abnormally increases p70S6 activity, which in turn phosphorylates IRS-1 in serine residues, inhibiting its physiological function and contributing to insulin resistance development. Furthermore, excess fatty acids increase intracellular DAG and ceramides, which also inhibit IRS-1 through PKC activity.

1.8.1 Assessment of insulin resistance

The gold standard procedure to assess insulin resistance is the hyperinsulinemic-euglycaemic clamp. During this procedure a continuous infusion of insulin is maintained to achieve a desired insulin concentration. Additionally, plasma glucose is measured every 5 minutes and exogenous glucose is administered at a variable rate adjusted to maintain plasma glucose concentrations constant at fasting levels. Given that both plasma insulin and glucose are maintained at the same concentrations during the duration of the procedure, it measures insulin sensitivity under steady-state conditions (162). However, this technique presents disadvantages as well. It is highly invasive, laborious and exposes the organism to sustained hyperinsulinemia, often at supraphysiological concentrations, and is therefore considered a non-physiological approach (163). Given that autophagy activity is inhibited by insulin, this technique would alter autophagy measurements. Alternative techniques to assess insulin resistance have been used throughout this thesis.

Fasting plasma insulin is considered the most practical approach to assess insulin resistance and it involves a blood sample taken from a subject after an overnight fast, to avoid other confounding factors (164). However, a down side to these procedures is the inter-assay variability, which makes robust comparisons between results obtained using different assay kits difficult (163). Another method to assess insulin resistance is the use of the homeostasis model assessment (HOMA-IR), which is a mathematical model developed to include the interactions between fasting plasma insulin and glucose concentrations that has a strong correlation with the hyperinsulinemic-euglycaemic clamp (165). This method is particularly useful in the assessment of insulin resistance at a larger scale and in different populations, ranging from mild glucose intolerance to overt diabetes (166, 167). However, this approach does not allow a dynamic measure that looks at insulin responsiveness to changes in glucose availability and its applicability has been questioned in animal research, given the lack of data validation in most animal species (168). Additionally, the oral glucose tolerance test (OGTT) is commonly used to detect glucose intolerance as well as type 2 diabetes (169). It is widely used in the medical practice, as well as in animal research and it involves the oral administration of exogenous glucose and subsequent blood sampling to determine how fast it is cleared from the plasma. Furthermore, it resembles the natural glucose and insulin dynamics following ingestion of a meal more closely than with the hyperinsulinemic-euglycaemic clamp. However, it only provides information about glucose intolerance, but not insulin

resistance *per se* (163). Despite this fact, the interpretation of the OGTT results can be presented as areas under the curve for both insulin and glucose, which are useful tools to compare results between intervention time points and conclude about changes in insulin sensitivity (170).

Given the necessity of a more physiological approach to assess both insulin resistance and to study autophagy in response to changes in nutrient availability, fasting and dynamic measures of insulin resistance via an oral glucose/mixed meal tolerance tests were used in this thesis.

1.8.2 Hepatic autophagy dysfunction and metabolic disease

In diet-induced insulin resistant rodent models, hepatic autophagy was impaired, assessed by lower p62/SQSTM1 and higher LC3B-II protein levels (171, 172). These findings have been linked with increased hepatic triglyceride accumulation, a common NAFLD and liver insulin resistance manifestation (29, 172). These results stress the potential role that impaired insulin/mTOR signalling might have in this context. Supporting the evidence, other studies have shown that decreases in hepatic macroautophagy activity, assessed by increases in LC3B-II/LC3B-I ratio and p62/SQSTM1, correlate with increased ER stress and obesity levels (35, 173) and can also lead to decreases in liver glucose output in nutrient deprived conditions, all well known to be features present in insulin resistant conditions (174).

The link between macroautophagy and insulin sensitivity in the liver is further demonstrated by studies which have investigated insulin action in response to genetic manipulation of macroautophagy. In both cultured hepatocytes and mouse liver *in vivo,* macroautophagy inhibition, via the genetic suppression of the *Atg7* gene, results in lipid accumulation, increases in lipid droplet content, decreases in beta-oxidation rates and defective insulin action (29, 35). Furthermore, TFEB overexpression in the liver-induced autophagy and also protected against HFD induced liver steatosis (83, 175, 176) and the progression of fatty liver disease associated with insulin resistance (177). On the other hand, studies that have induced macroautophagy in fatty liver models, either pharmacologically or through aerobic exercise, have described an improvement in the liver's metabolic profile, such as decreases in the lipid content (178, 179), reduced ER stress and improved insulin signalling (180). Together, there is substantial evidence to recognize there is a link between disturbed macroautophagy regulation and insulin resistance-related features in the liver. However, although this link between impaired

insulin signalling and defective macroautophagy exists, no studies have characterized the macroautophagy response to the transition from a fasted to a fed state in insulin resistant conditions.

1.8.3 Skeletal muscle and metabolic disease

As far as skeletal muscle is concerned, animal models exposed chronically to a HFD, have increased lipid deposition, higher lipid metabolite concentration and also develop insulin resistance in skeletal muscle (2). Furthermore, mice fed a HFD also show signs of decreased basal macroautophagy, measured by increased LC3B-II and p62/SQSTM1, when compared to muscle from animals fed a normal chow diet (107). Interestingly, evidence has shown that genetically-induced mTOR hyperactivation, a common signalling disruption present in insulin resistant conditions (20), was sufficient to block macroautophagy activity, demonstrating mTOR's pivotal role in macroautophagy regulation in this tissue (99). There is also conflicting evidence regarding the possible role of macroautophagy in skeletal muscle. Specific skeletal muscle knockout of Atg7 seems to protect this tissue from diet-induced insulin resistance (181). Interestingly, a skeletal muscle-specific deletion of *Atg7* gene in mice resulted in protection from diet-induced obesity, insulin resistance, as well as increased fatty acid oxidation and browning in white adipose tissue, suggesting a role for Atg7 as a driver of metabolic tissue crosstalk (181). Whether these observations are due to pure macroautophagy defects or other disrupted pathways due to the broader functions of Atg7 remains to be established.

In humans, an increase in intramuscular lipid accumulation, a decrease in type I and an increase in type II fibres (182-184), as well as reductions in mitochondrial mass and function have been described in insulin resistant conditions (185, 186). Despite these well described observations, very few studies have explored skeletal muscle in the context of insulin resistance. *In vitro* studies, performed in cultured human myoblasts obtained from severely obese women showed that macroautophagy activity, measured by protein degradation rate of long-lived proteins in the presence of a proteasome inhibitor, was significantly decreased compared to controls (42).

While few studies have focused on basal macroautophagy, important macroautophagy defects may be apparent in response to feeding. For example, Beals et al. (161)

demonstrated that overweight/obese individuals exhibit elevated total and p-mTOR^{S2448} protein content in fasted conditions, and a failure to increase p-mTOR^{S2448} and protein fractional synthetic rate in response to feeding. Furthermore, insulin-stimulation acutely decreases macroautophagy (based on increased p62/SQSTM1 content) in skeletal muscle of insulin sensitive, but not insulin resistance obese individuals (187). However, the latter study was performed under an euglycaemic-hyperinsulinemic clamp conditions, a non-physiological setting as stated in section 1.4.2.(ii) (188). It is worth mentioning that although this method is useful to assess insulin sensitivity, it is a non-physiological scenario, which does not represent the transient increases in blood glucose and insulin levels that occur during the transition from the post-absorptive to the post-prandial period (188).

Taken together, macroautophagy activity and insulin action share common intracellular signalling pathways, therefore macroautophagy dysfunction in an insulin resistant context could be expected. Additionally, macroautophagy activity is dependent on both classic insulin signalling and mTOR pathways, which are disturbed in insulin resistant conditions. However, little is known about the macroautophagy response in the transition from the fasting to the post-prandial period and whether this response remains intact in insulin resistant conditions. Disturbances in these acute macroautophagy responses in the liver and skeletal muscle could result in long term accumulation of cellular macroautophagy targets, such as intramuscular lipid and damaged/dysfunctional mitochondria. As these are proposed to be mechanistically linked to the development and progression of insulin resistance, disturbances in macroautophagy could then result in a vicious cycle of deteriorating cellular metabolic function and worsening of tissue-specific and whole-body insulin resistance.

1.9 Aerobic exercise training

Aerobic exercise training has proven to exert numerous beneficial metabolic effects. An increase in skeletal muscle oxidative capacity and increases in insulin sensitivity are of immense clinical importance and likely contributes to the lower risk of diabetes development with exercise training (119, 189). Interestingly, acute skeletal muscle contraction/exercise has shown to induce macroautophagy activity in rodent models (11, 90, 134). Studies in mice have described acute aerobic exercise-induced increases in

macroautophagy, measured by an increase in LC3B-II/LC3B-I ratio, together with a decrease in p62/SQSTM1 levels (90). Moreover, macroautophagy activity increases were greater when exercise was performed in a fasted state (90). This indicates that although exercise and fasting share some overlap in macroautophagy activation pathway, as discussed in section 1.6.1 (i), the additive effect points towards activation of distinct signaling pathways. While these mechanisms are not fully explained, nutrient withdrawal, typical during a fasting period, results in reduced mTOR activity, whilst exercise stimulates increased AMPK activity.

However, contrary to the results in rodents, acute aerobic exercise performed in a fasted state in humans lowers LC3B-II/LC3B-I ratio indicative of reduced levels of autophagosomes (6, 101). There are conflicting interpretations of this data in the literature (6, 101). Some publications report this as an increase in autophagy due to increased clearance of autophagosome (101), whereas others interpret this data as a reduction in the induction of autophagy, due to a lower conversion of LC3B-I to LC3B-II (6).

Importantly, macroautophagy has also shown to be fundamental for skeletal muscle adaptation to exercise training. Mice with an impaired ability to induce macroautophagy in skeletal muscle through genetic knock-down of Atg6, do not display normal increases in mitochondrial proteins and capillary density in response to exercise training. Furthermore, they also fail to improve exercise performance and are not protected from HFD-induced insulin resistance (11, 145). Moreover, evidence suggests that training adaptations in rodents differ depending on muscle fibre-type, since endurance training apparently increased autophagy protein levels (LC3B, Atg8) in both oxidative and glycolytic muscle, yet increased basal autophagy ‘flux’ and mitophagy markers in the glycolytic muscle only (145).

There are limited studies investigating the effect of exercise training in humans. Two studies have shown that endurance training in young, lean insulin sensitive individuals increases LC3B-I protein levels without changes in LC3B-II content, resulting in decreases LC3B-II/LC3B-I ratio. This indicates an enhanced capacity for macroautophagy induction with no changes in the autophagosome content (6, 190). Moreover, limited evidence suggests that exercise training intensity does not play a role in the magnitude of macroautophagy activation in human skeletal muscle (190). Together, this evidence shows that both acute and chronic aerobic exercise may impact

macroautophagy activity and potentially in a muscle fibre-type specific manner. However, no studies have investigated muscle fibre-type specific adaptation in the macroautophagy machinery to exercise training.

1.11 Scope and outline of the thesis

Autophagy is acutely modulated by hormonal and nutrient fluctuations (i.e. fasting and feeding) and it is proposed that autophagy regulation is disrupted in important metabolic tissues under conditions of insulin resistance. Therefore, in Chapter 2 and Chapter 3, insulin resistant animal models were used to examine the autophagy responses in the liver and skeletal muscle in response to physiological changes in nutrient availability. In Chapter 2, autophagy responses in mice fed a high fat, high sucrose diet were investigated in both fasted conditions and in response to an oral glucose load. In Chapter 3, the effect of feeding status on macroautophagy markers in liver and skeletal muscle was examined in a mouse model of overt T2DM, the *db/db* mouse. To further investigate the effect of fasting and feeding on autophagy responses in human skeletal muscle, the experiments in Chapter 4 examined autophagy markers 30 min and 90 min following the ingestion of a mixed meal. Based on the findings of muscle fibre-type differences in autophagy proteins in mouse muscle presented in section 1.4.2 (ii), these assessments were made in whole muscle and in pooled type I and type IIa muscle fibres to explore muscle fibre-type specific autophagy responses to meal ingestion. Based on the rationale presented in section 1.7, stating that exercise training modulates autophagy responses, the aim of Chapter 5 was to investigate the effect of a 6-week aerobic exercise training intervention on muscle autophagy responses in both whole muscle and in pooled single fibres. Finally, the general discussion (Chapter 6) reviews the findings of each experimental chapter and places them in a broader context of the current literature. Strengths and limitations of the experimental chapters are also discussed and future research directions in the area of autophagy in the context of metabolic diseases, such as type 2 diabetes, are suggested. Upcoming research should aim to investigate the underlying mechanisms underpinning the differences described in the present thesis. This information will help us to gain a better understanding of macroautophagy's relevance in the context of metabolic disease with insight into potential therapeutic approaches.

Chapter 2

Differential hepatic and skeletal muscle macroautophagy responses in mice fed a high fat, high sucrose diet

2.1 Abstract

Autophagy involves the targeting and delivery of cellular components to the lysosome for degradation and is suggested to become dysfunctional in insulin resistant tissues. The aim of the present study was to investigate the effect of high fat diet-induced insulin resistance on autophagy markers in the liver and skeletal muscle of mice in the fasted state and following an oral glucose bolus.

Forty 8-week-old, male C57BL/6J mice were randomly divided into 2 groups (n=20 each) and were fed either a high fat, high sucrose (HFSD) or standard chow control (CON) diet for 16 weeks. At the end of the diet intervention mice received either water (sham) or glucose (50 mg) via oral gavage after a 5 h fast. Skeletal muscle and liver samples were collected 15 min post gavage and tissue lipid accumulation was assessed. Markers of autophagy activity, lysosome and lipid-droplet associated protein gene expression and protein content were measured.

Compared to CON, the HFSD intervention increased LC3B-II and p62/SQSTM1 abundance, which is indicative of elevated autophagosome content via reduced clearance. These changes coincided with inhibitory autophagy signalling through elevated p-mTOR ^{S2448} and p-ULK1^{S758} abundance. HFSD had no impact on autophagy markers in skeletal muscle. Glucose administration had no effect on autophagy markers or upstream signalling responses in either tissue regardless of diet.

Taken together, a HFSD intervention induces tissue-specific autophagy impairments, where hepatic autophagosome accumulation indicates reduced lysosomal clearance. In contrast, the absence of autophagy impairments in the muscle suggests a lower susceptibility of this tissue to autophagy dysfunction in the presence of diet-induced insulin resistance.

2.2 Introduction

Obesity is a worldwide epidemic and the development of obesity-related insulin resistance (IR) is central to many modern diseases, such as non-alcoholic fatty liver disease (NAFLD), type 2 diabetes and cardiovascular disease. Although the precise mechanisms linking obesity to the development of IR remain elusive, lipid accumulation and mitochondrial dysfunction have been implicated in the impairment of insulin action in both skeletal muscle and liver (191). Recently, impairments in cellular degradation via autophagy have been linked to the metabolic disturbances present in insulin resistant tissues.

Autophagy constitutes one of the major cell degradation systems and involves the targeting and delivery of cytosolic contents to the lysosome for degradation. Autophagy is classified according to the mode of content delivery to the lysosome. Macroautophagy involves the enclosure of cytosolic material by a double membrane structure called the phagophore (192). The autophagosome is formed upon closure of the phagophore, which then fuses with the lysosome where it is degraded by lysosomal enzymes. The formation of the ULK-1 complex is one of the first steps of autophagy induction (193), which triggers the formation and expansion of the phagophore (94, 102-104). Therefore, LC3B-II is considered a valid marker of autophagosome content (74). The targeted cargo is recognised by a family of proteins via post-translational modifications including ubiquitination. As p62/SQSTM1 tags ubiquitinated proteins and is also degraded by the lysosome, it constitutes a useful marker to monitor autophagy degradation (74). In contrast, chaperone-mediated autophagy (CMA) targets cytosolic proteins containing a specific KFERQ motif via the chaperone Hsc-70 (194). This protein complex then enters the lumen of the lysosome through a channel formed by a LAMP-2A multimer, which constitutes a CMA-specific receptor.

Both macroautophagy and CMA are acutely sensitive to energy availability. An increase in nutrient availability as reflected by elevated levels of insulin and amino acids can both independently inhibit initiation of phagophore nucleation, via activation of mTOR and downstream phosphorylation of ULK-1^{S758}, which inhibits ULK-1 complex formation (50, 195). In contrast, nutrient deficiency activates autophagy (35, 196). While the specific signalling mechanisms are not fully elucidated, evidence suggests that phagophore nucleation through the ULK-1 complex occurs via increased AMPK activity (94), which has been proposed to be inactivated by mTOR in response to feeding (95, 96).

Regardless of the mechanism, it is generally considered that autophagy activity will cycle with repeated feeding and fasting periods throughout the course of a day.

Ectopic lipid accumulation occurs concurrent with the development of insulin resistance and is also linked with mitochondrial dysfunction, oxidative stress and accumulation of unfolded proteins, which in turn causes endoplasmic reticulum (ER) stress (9). Given that autophagy targets include intracellular lipids (lipophagy), dysfunctional mitochondria (mitophagy), aggregated proteins and damaged ER (ER-phagy) (29, 52), autophagy has been linked to the development of tissue specific insulin resistance. Autophagy dysfunction occurs in the liver of genetic and dietary models of obesity (35) and liver specific autophagy inhibition results in hepatic steatosis, impaired insulin action and loss of glycaemic control (29, 35). Furthermore, autophagy restoration reverses hepatic steatosis and enhances insulin action in obesity models (35). However, few studies have investigated autophagy in the context of insulin resistance in skeletal muscle. Rodents fed a high fat diet to induce insulin resistance displayed modest reductions in markers of autophagy compared to chow-fed controls (11, 197). Therefore, further studies investigating autophagy defects in the liver and skeletal muscle in insulin resistant conditions are warranted.

Autophagy has been linked to the development of insulin resistance in the liver. The aim of the present study was to directly compare the impact of fully developed diet-induced insulin resistance on autophagy markers in both liver and skeletal muscle following 16 weeks of high fat, high sucrose feeding in mice. This diet duration is recognised to induce profound insulin resistance in both tissues (198). Given that autophagy is also acutely regulated by nutrient availability and its associated signalling pathways, we investigated autophagy in the fasted state and following an oral glucose bolus. We hypothesized that high fat feeding would impair autophagy in both liver and skeletal muscle in the fasted and postprandial state.

2.3 Methods

Animals and sample collection

Male C57BL/6J mice (n=40; Animal Resources Centre, Perth, Western Australia) were housed (5 per cage) and acclimatised to the facility for 4 weeks in an environmental controlled room on a 12 hour light/dark cycle with free access to water and standard chow diet (9% energy from fat, Barastoc Rat & Mouse, Ridley AgriProducts, Australia). At 8 weeks of age, mice were randomly allocated into two groups (n = 20 each) and either fed a standard chow control (CON; 9% energy from fat, Barastoc Rat & Mouse, Ridley AgriProducts, Australia, n=20) or a high fat, high sucrose diet (HFSD; 43% total energy from fat and 20% from sucrose; cat. no. SF04-001, Specialty Feeds, Australia, n=20) for sixteen weeks. One week prior to the conclusion of the diet intervention (15 weeks) all mice underwent an OGTT. Upon conclusion of the diet intervention, all mice were fasted for 5 hours, and then 10 mice from each group (CON and HFSD) were administered via oral gavage a bolus of glucose, consisting of 50 mg of glucose in a total water volume of 200 µl. The remaining mice from each group (CON and HFSD, n=10 per group) were administered via oral gavage an equivalent volume of water to the glucose treated mice. Venous blood was collected from the tail vein at baseline (0 min), 5 min and 15 min post gavage. Mice were euthanised by cervical dislocation 15 min after the oral gavage and quadriceps muscle, liver were collected and snap frozen in liquid nitrogen and stored at -80 °C until further analysis. Epididymal and inguinal fat were dissected and weighed to assess fat mass. The study was approved by the Monash University Animal Ethics Committee (Code: MARP-2012-046).

Analyses

Blood analysis

Plasma insulin was measured by ELISA (Millipore, St Louis, MO, USA) according to manufacturer's instructions and blood glucose was measured with a glucose meter (Accu-Check, Roche, NSW, Australia).

Tissue triglyceride content

Quadriceps muscle (40-50 mg) and liver (30-40 mg) from each animal were weighed and homogenised in 2.5 mL of chloroform:methanol (2:1) and 0.5 mL of pure chloroform was added to each sample and incubated for an hour before 1.5 ml of ddH_2O was added to each sample. The samples were shaken for 10 min and then centrifuged at 2000 rpm for 10 min. The lower chloroform phase was removed, and the remaining sample was left to evaporate. The resultant dried extract was dissolved in 250 µl of absolute ethanol.
The samples and respective standards were prepared and analysed in duplicate with the Triglycerides GPO-PAP kit (cat. no. 11730711 216, Roche Diagnostics GmbH, Mannheim, Germany) according to manufacturers' instructions.

Gene expression

Tissues from the water gavage animals were homogenized in TriZol reagent (Invitrogen, 1 ml per 75 mg of tissue each time) and RNA was extracted with RNeasy© Mini Kit (cat. no 74106, QIAGEN, Victoria, Australia) according to manufacturer's instructions.

Reverse transcription of total RNA to cDNA was performed using the Maxima H Minus First Strand cDNA Synthesis Kit (Thermo Fischer Scientific, Massachusetts, USA) according to manufacturer's instructions. The samples were incubated in the thermocycler according to the following protocol: 30 min at 50 °C, then 5 min at 85 °C and finally 5 min at 4 °C. Quantification of total cDNA was performed using the Quant-IT™ Oligreen™ ss DNA Assay kit (Thermo Fischer, Oregon, USA). After the cDNA samples were diluted (1:10 for skeletal muscle and 1:20 for liver) RT-PCR was performed (cat. No TCR0096, PikoReal 96, Thermo Fischer, Vanta, Finnland). Reactions were performed in a total volume of 10 µl containing: 1 µl cDNA, 9 µl Sybr Green master mix buffer (Quanti-Tect, Qiagen, Hilden). PCR conditions were 10 min at 95°C, then 40 cycles of 95°C for 30 s and 60°C for 60 s. The relative amounts of mRNAs were calculated using the relative quantification (CT) method using the PikoReal Software 2.1 (Thermo Scientific, Vantaa, Finnland) (199) and the results were normalized to total cDNA. The use of house-keeping reference genes, whose expression is assumed to remain the same between samples, has been widely used as a normalisation procedure when quantifying gene expression. However, housekeeping gene expression can vary between tissues and in response to the different experimental treatments (200). To overcome this variability, the use of validated internal controls for each experimental

condition has been strongly suggested (200). Alternatively, the normalisation of the data with each sample cDNA content has been validated as a more robust normalisation method (201). This method is based on the assumption that the overall RNA content remains unchanged across different experimental conditions and that cDNA levels would encompass the possible discrepancies that may arise during reverse transcription between the samples (201). Quantification of total cDNA levels for each sample is possible by using Oligreen, a dye that emits fluorescence once it binds to single stranded DNA, such as cDNA, but it does not bind to free nucleotides and/or short oligonucleotides (202). The following autophagy-related genes of interest were determined: *Plin2, Plin3, Lc3b, p62/Sqstm1* and *Gabarapl1* (Table 2.1).

Table 2.1. Names and sequences of primers for real-time PCR

Gene name	DNA Sequence (5' to 3')
Lc3b	*Forward: CATGAGCGAGTTGGTCAAGA*
	Reverse: TTGACTCAGAAGCCGAAGGT
Gabarapl1	*Forward: ATGTCATTCCACCCACCAGT*
	Reverse: TACCATTACCCCTCCTGCTG
p62/Sqstm1	*Forward: AAGAACGCGTGCTGATACCT*
	Reverse: GCACCAGTCTCTTCCTGGAG
Plin2	*Forward: GGAGTGGAAGAGAAGCATCG*
	Reverse: TGGCATGTAGTCTGGAGCTG
Plin3	*Forward: AAACAGGGTGTGGACCAGAG*
	Reverse: CTCCACCTGCTCTGGCTTAG

Immunoblotting

The abundance of autophagy markers (LC3B, GABARAPL1, p62/SQSTM1, Hsc-70, LAMP-2A), lipid droplet-associated proteins (PLIN2, PLIN3) and upstream signalling events (Akt, p-Akt$^{T308,\ Ser473}$, mTOR, p-mTOR^{Ser2448}, ULK-1, p-ULK-1^{Ser758}) were determined by immunoblotting.

Frozen liver and quadriceps samples were cryosectioned (~20 sections at 10 µm) at -20 °C (Leica CM1850 Cryostat, Nussloch GmbH, Germany) and placed into 50 µl of solubilizing buffer (0.125 M Tris-Cl [pH 6.8], 4 % [w/v] sodium dodecyl sulfate (SDS), 10 % glycerol, 4 M urea, 10% [v/v] mercapthoethanol, and 0.001% [v/v] bromophenol blue) (203) and left to denature for 1 h at room temperature. After one freeze-thaw cycle the samples were loaded onto a stain-free gel (4–15% Criterion™ TGX Stain-Free™ Protein Gel, 26 well, 15 µl, cat. no. 5678085, Bio-Rad, California, USA). A 4-point standard calibration curve consisting of a mix of every sample (1, 2, 4, 8 µl into a well), was also loaded on each gel to ensure that the amount of protein fell within the linear range of detection (203). Antibodies against Akt (cat. no. 9272S), p-Akt^{T308} (cat. no. 9275S), p-Akt^{S473} (cat.no. 9271S) mTOR (cat. no. 2972S), p-mTOR^{S2448} (cat. no. 2971S) and GABARAPL1 (cat. no. 13733S) were purchased from Cell Signalling (Massachusetts, USA). The following antibodies were also used: anti-LAMP-2A (cat. no. 51-2200, Thermo Fisher Scientific, Massachusetts, USA), anti-Hsc-70 (cat. no. SMC-151, StressMarq Biosciences, British Columbia, Canada), anti-p62/SQSTM1 (cat. no. ab56416, Abcam, Cambridge, UK), anti-PLIN2 (cat. no. 610102, PROGEN Biotechnik GmbH, Heidelberg, Germany), anti-PLIN3 (cat. no. NB110-40764, Novus Biologicals, Colorado, USA, anti-LC3B (cat. no. L7543, Sigma Aldrich, Missouri, USA). Both stain free gels and blotted membranes were imaged using the ChemiDoc XRS+ imaging system (cat. No. 1708265, Bio-Rad, California, USA) and analysed using the Image Lab™ software (Bio-Rad, California, USA). Protein density was expressed relative to its respective standard calibration curve and then normalised to the total protein loading, quantified on the pre-transfer stain free gel image (204). Data was expressed relative to the respective control (fasted CON).

Statistical analyses

An *a priori* power calculation was performed on data from previous evidence investigating differences in LC3B-II/LC3B-I ratio in mouse liver between a control chow fed group and a group of mice fed a high fat diet (HFD) (35, 171). This data indicates that the LC3B-II/LC3B-I ratio in the control groups was 1.0 ± 0.2 arbitrary units (mean ± SD), while the LC3B-II/LC3B-I ratio in the HFD group was 0.5 ± 0.1 arbitrary units (mean ± SD). This gives an effects size of 3.16, meaning the n = 4 in each group would give an expected power of 0.9. As there is no data on the effect of a high fat diet intervention on LC3B-II/LC3B-I ratio in mouse skeletal muscle, n=10 in each group was chosen to

ensure sufficient statistical power to assess changes in LC3B-II/LC3B-I ratio in skeletal muscle.

Data were analysed using a two-way ANOVA to explore effect of diet (HFSD versus CON) and acute feeding (glucose gavage versus water gavage) using GraphPad Prism version 8.0.0 for Windows (GraphPad Software, San Diego, California USA). Post hoc analyses using the Bonferroni correction were run in the case of significant interactions. Statistical significance was set at $P<0.05$. Data are presented as means or individual data ± standard deviation (SD).

2.4 Results

Metabolic Characteristics

Body mass progression and fat mass throughout the diet intervention period, as well as plasma glucose and insulin responses to the OGTT are presented in Figure 2.1. Body mass was significantly higher in the HFSD group after the first week and until completion of the diet intervention when compared to the CON group (Figure 2.1A, $P<0.0001$). Both epididymal and inguinal fat mass were also higher in the HFSD group (Figure 2.1B, $P<0.0001$). The HFSD groups displayed a significantly greater HOMA-IR compared to the CON groups (Figure 2.1F, $P<0.01$). During the OGTT at 15 weeks of the diet intervention, plasma glucose and insulin were significantly higher in the HFSD compared to CON (Figure 2.1 D, F; $P<0.0001$). The increases in plasma glucose and insulin observed in the HFSD groups were further supported by significant increases in both glucose (Figure 2.1E, $P<0.01$) and insulin AUC (Figure 2.1F, $P<0.01$) during the OGTT. Plasma insulin concentration peaked at 15 min, and was chosen as the most suitable timepoint to evaluate autophagy responses in both liver and skeletal muscle.

Hepatic triglyceride concentration was approximately 5-fold higher in the HFSD group compared to the control group (Figure 2.2A, $P<0.001$). This was mirrored by a significant increase in the lipid droplet associated proteins, PLIN2 and PLIN3, in the HFSD group (Figure 2.2 C, E $P<0.05$). Evidence suggests that PLINs, not only indicate the amount of lipid droplets in a cell, but they also control how the cell utilizes this metabolic substrate, since PLIN degradation leads to increases in fat oxidation (53). Similarly, muscle triglyceride content was approximately 3-fold higher in the HFSD compared to the CON mice (Figure 2.2B, $P<0.001$). However, PLIN2 levels were lower in the HFSD compared to the CON mice (Figure 2.2D $P<0.05$), while PLIN3 remained unchanged (Figure 2.2F, $P>0.05$). There was no difference between water or glucose gavage on either triglyceride content or PLIN protein abundance in liver or skeletal muscle ($P>0.05$).

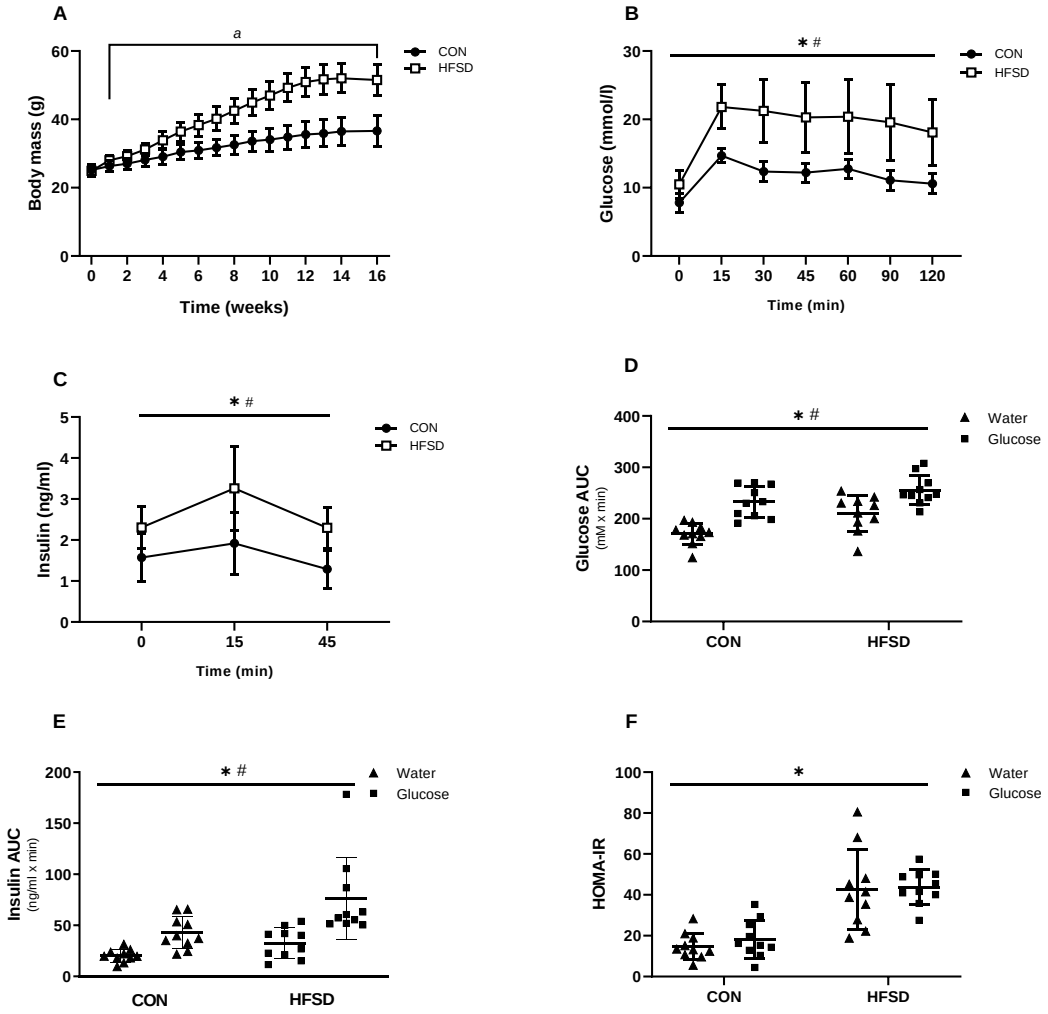

Figure 2.1. Body mass (A) throughout the course of the 16-week diet intervention in control (CON) and high fat, high sucrose diet (HFSD) group. Plasma glucose (B) and plasma insulin (C) levels during the oral glucose tolerance test after 15 weeks of the diet intervention. Glucose area under the curve (AUC) (D) and insulin AUC (E). HOMA-IR (F) before water or glucose gavage in control (CON) and high fat, high sucrose diet (HFSD). Values are presented as individual data and/or means ± SD * indicates main effect of diet (P<0.0001), # indicates main effect of time (P<0.05), ^{a} indicates interaction effect (time x diet treatment) between week 1 and 16 (P<0.0001).

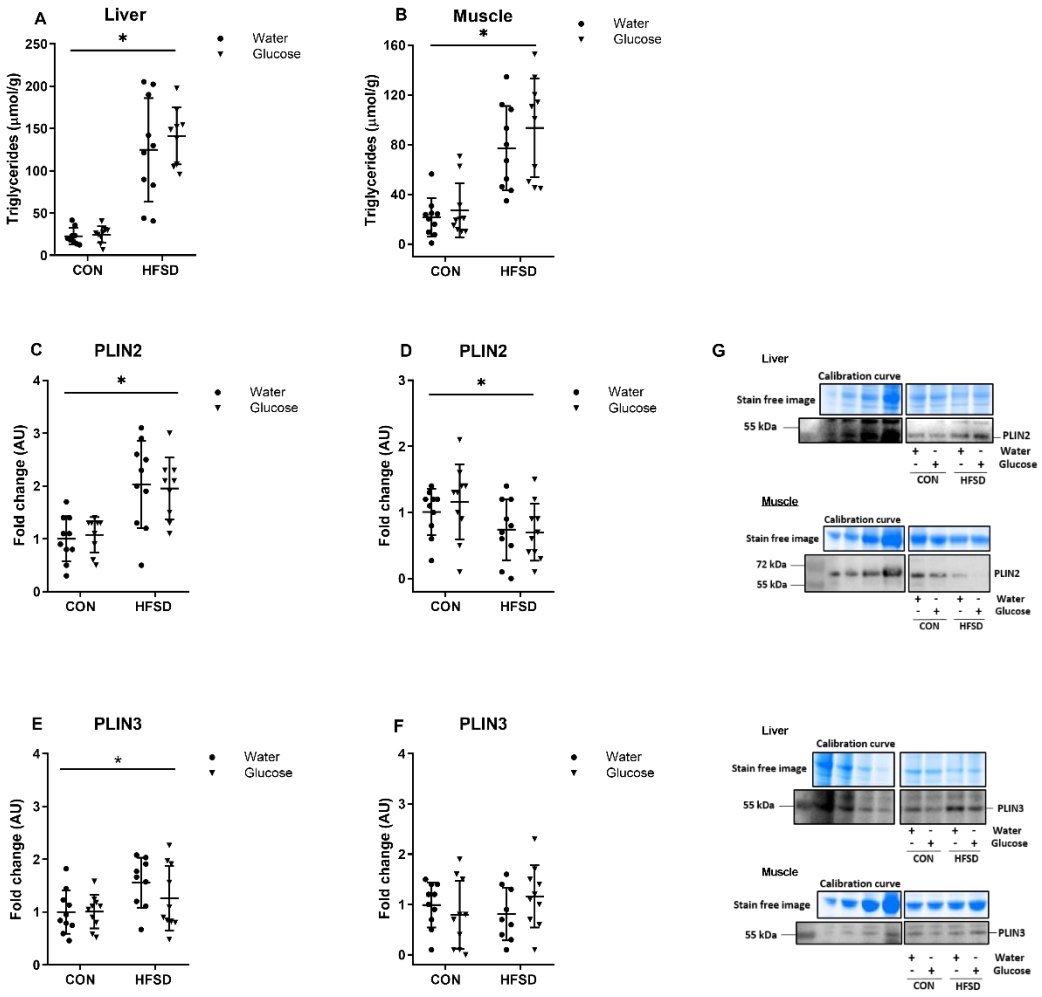

Figure 2.2. Tissue triglyceride content in the liver (A) and quadriceps muscle (B) of the CON and HFSD groups and abundance of Perilipin 2 and 3 (PLIN2, PLIN3) in the liver (C, E) and quadriceps muscle (D, F) of the CON and HFSD groups before and after oral gavage (Water vs glucose). Values are presented as individual data and means ± SD. AU indicates arbitrary units. Stain free images providing an example of total protein loading and corresponding representative blots are shown (G). * indicates main effect of diet ($P<0.05$). Representative blots for each protein were taken from the same membrane and accompanying stain free images were taken from the same gel. Standard curves are taken from the same gels/membrane with non-contiguous lanes indicated with spaces .

Hepatic Autophagy Responses to High Fat, High Sucrose Diet

A comparison of several autophagy markers in the liver of HFSD and CON mice 15 min following either glucose or water gavage are presented in Figure 2.3. LC3B-I remained unchanged by HFSD (Figure 2.3A), however there was a significantly greater abundance of LC3B-II in the HFSD group compared to the CON group (Figure 2.3B, $P<0.05$). This resulted in a greater LC3B-II/LC3B-I ratio in the HFSD group compared to CON (Figure 2.3C, $P<0.05$). There was no effect of acute glucose gavage on either LC3B forms or the LC3B-II/LC3B-I ratio in either diet condition. The abundance of GABARAPL1 isoforms and p62/SQSTM1 are shown in Figure 2.3 D-G. In a similar manner to LC3B, the lipidated form of GABARAPL1 (GABARAPL1-II) was higher in the HFSD group compared to CON (Figure 2.3E, $P<0.05$), with no changes in the non-lipidated isoform (GABARAPL1-I, figure 3D) or the GABARAPL1-II/GABARAPL1-I ratio (Figure 2.3F). The abundance of p62/SQSTM1 was significantly greater in the HFSD group compared to CON (Figure 2.3G). There was no effect of glucose gavage on the abundance of either p62/SQSTM1 or GABARAPL1.

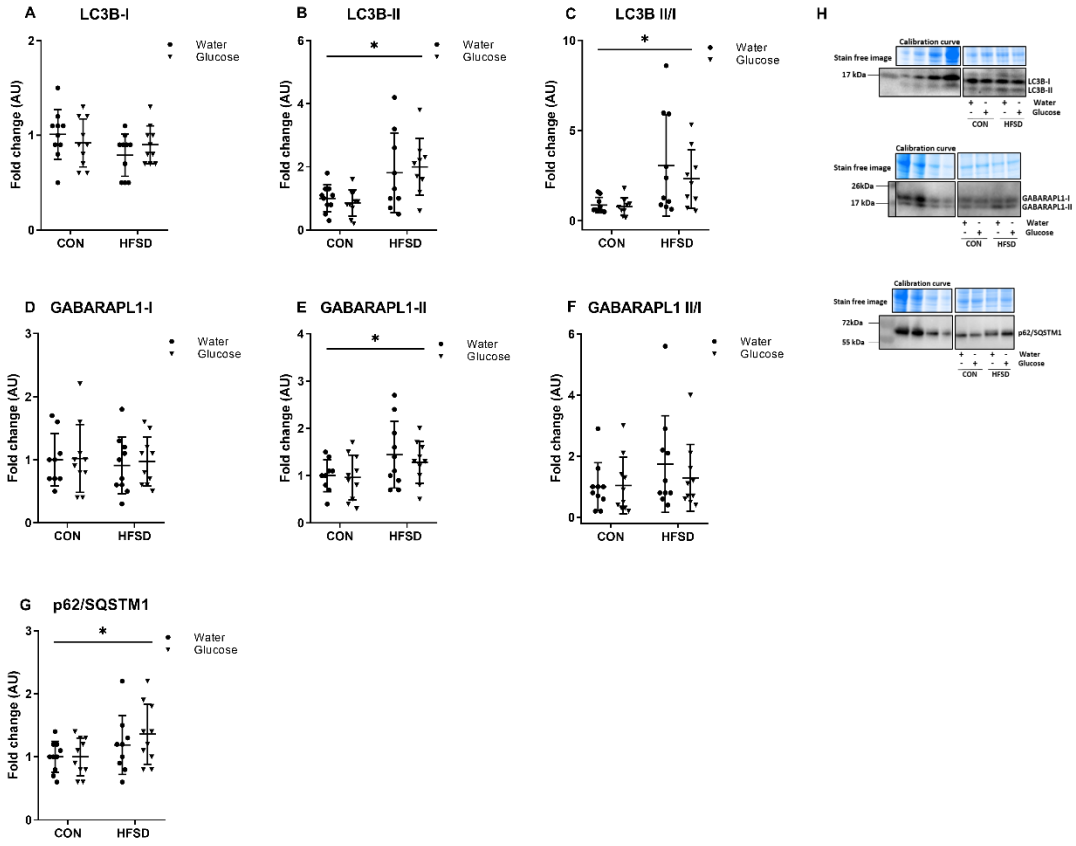

Figure 2.3. Autophagy markers in the liver of HFSD and CON mice. Abundance of LC3B-I (A), LC3B-II (B), LC3B-II/LC3B-I ratio (C), GABARAPL1-I (D), GABARAPL1-II (E), GABARAP-II/I ratio (F) and p62/SQSTM1 (G) 15 min following oral gavage with water or glucose in HFSD and CON diet intervention. Values are presented as individual data and means ± SD. AU indicates arbitrary units. Stain free images providing an example of total protein loading and corresponding representative blots are shown (H). * indicates main effect of diet ($P<0.05$). Representative blots for each protein were taken from the same membrane and accompanying stain free images were taken from the same gel. Standard curves are taken from the same gels/membrane with non-contiguous lanes indicated with spaces. .

Chaperone-mediated autophagy (CMA) markers were also investigated in the liver (Figure 2.4). There was an increase in LAMP-2A abundance in the HFSD groups (Figure 2.4A, $P<0.05$,) compared to the CON groups, without any concomitant changes in Hsc-70 (Figure 2. 4B, $P>0.05$). There was no effect of glucose gavage on the abundance of either LAMP-2A or Hsc-70.

Key upstream autophagy-related signalling responses in the liver are shown in Figure 2.5. The HFSD intervention did not have any effect on p-Akt^{T308} compared to the CON groups (Figure 2.5A). However, the HFSD group displayed increased p-Akt^{S473}, p-mTOR^{S2448} and its downstream target, the autophagy inhibitory site p-ULK-1^{S758} (Figure 2.5 B, D, F, $P<0.05$), without any changes in total Akt, mTOR or ULK-1 (Figure 2.5 C, E, G; $P>0.05$). There was no difference between glucose and water gavage on any of the measured upstream signalling responses.

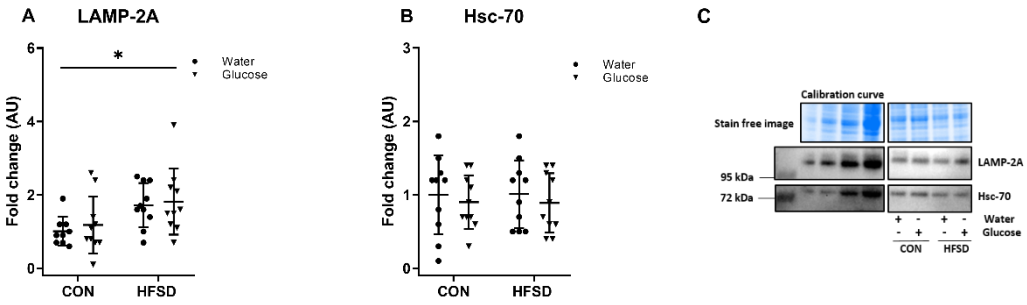

Figure 2.4. Abundance of CMA markers, LAMP-2A (A) and Hsc-70 (B) in the liver of HFSD and CON mice 15 min following oral gavage with water or glucose in response to HFSD and CON diet interventions. Values are presented as individual data and means ± SD. AU indicates arbitrary units. Stain free images providing an example of total protein loading and corresponding representative blots are shown (C). * indicates main effect of diet ($P<0.05$). Representative blots for each protein were taken from the same membrane and accompanying stain free images were taken from the same gel. Standard curves are taken from the same gels/membrane with non-contiguous lanes indicated with spaces. .

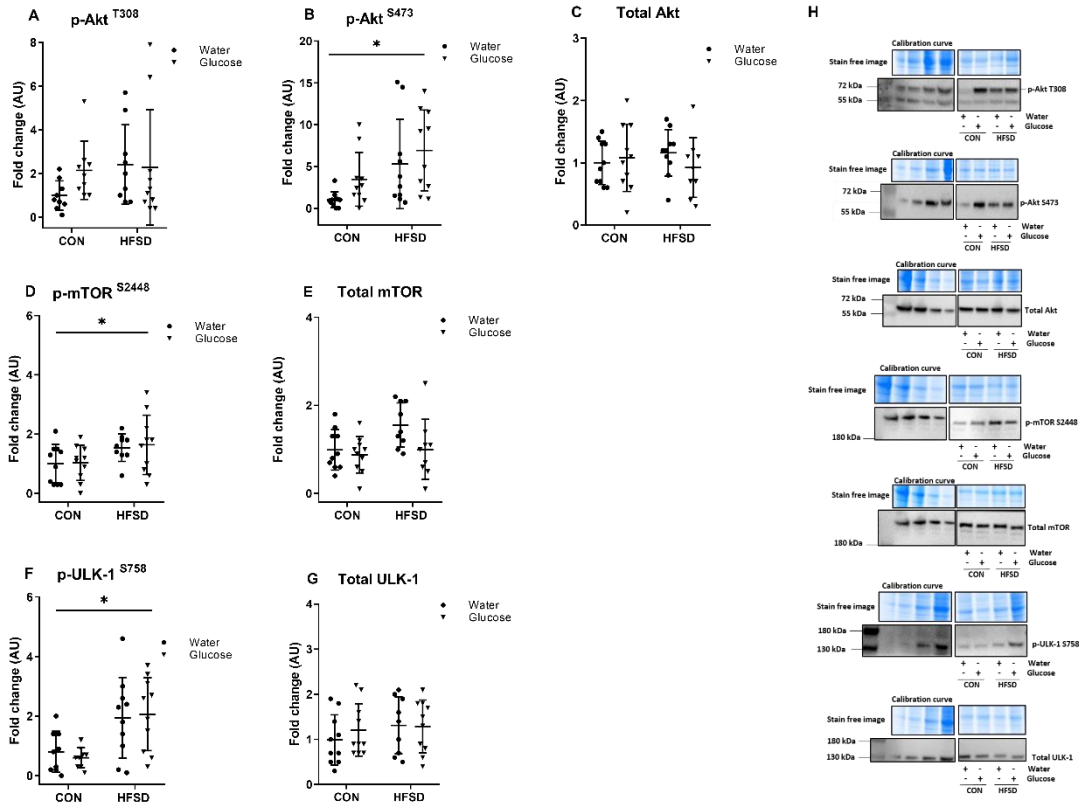

Figure 2.5. Abundance of signalling markers regulating autophagy in the liver of HFSD and CON mice. p-Akt^{T308}, p-Akt^{S473}, total Akt (A, B, C), p-mTOR^{S2448} and total mTOR (D, E) and p-ULK-1^{S758} and total ULK-1 (F, G) 15 min following oral gavage with water or glucose in HFSD and CON diet intervention. Values are presented as individual data and means ± SD. AU indicates arbitrary units. Stain free images providing an example of total protein loading and corresponding representative blots are shown (H). * indicates main effect of diet (P<0.05). Representative blots for each protein were taken from the same membrane and accompanying stain free images were taken from the same gel. Standard curves are taken from the same gels/membrane with non-contiguous lanes indicated with spaces. .

The liver gene expression analyses are summarized in Figure 2.6A. *Plin3* gene expression was higher in the HFSD groups ($P<0.05$) compared to the CON groups, however *Lc3b, Gabarapl1, p62/Sqstm1,* and *Plin2* gene expression levels were not different between the CON and HFSD interventions ($P>0.05$).

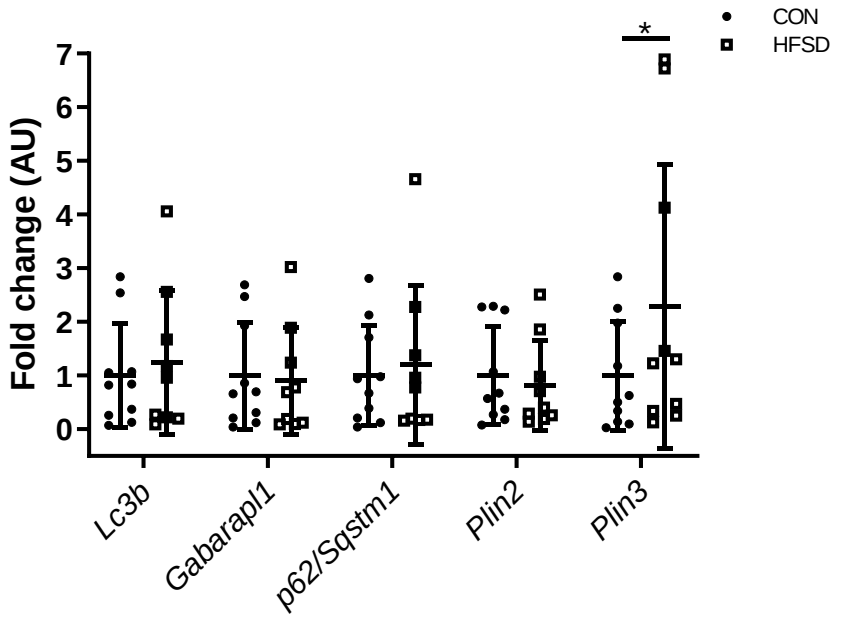

Figure 2.6. Gene expression levels of *Lc3b, Gabarapl1, p62/Sqstm1, Plin2, Plin3* in the liver in response to a 16-week high fat, high sugar diet (HFSD) or control (CON) intervention following 15 min following oral gavage with water. Values are presented as individual data and means ± SD. AU indicates arbitrary units. * indicates main effect of diet (P<0.05).

Skeletal Muscle Autophagy Responses to High Fat, High Sucrose Diet

Autophagy markers in mouse quadriceps muscle of HFSD and CON mice 15 min following either glucose or water gavage are presented in Figure 2.7. The 16-week HFSD intervention decreased total GABARAPL1 abundance (P<0.05), with no changes in either LC3B-I or LC3B-II abundance or the LC3B-II/LC3B-I ratio (Figure 2.7 A-D, P>0.05). Moreover, p62/SQSTM1 levels also remained unchanged between the HFSD and CON groups (Figure 2.7E, P>0.05). No acute effect of glucose gavage was observed in LC3B-I, LC3B-II, GABARAPL1 or p62/SQSTM1 in either of the groups (P>0.05).

Key upstream signalling events regulating autophagy in the muscle are shown in Figure2.8. The abundance of p-Akt^{T308} levels was decreased in the HFSD compared to the CON mice (Figure 2.8A, P<0.05) but was unaffected by the glucose bolus. On the other hand, diet had no effect on p-Akt^{S473} but there was an increase in p-Akt^{S473} 15 min post glucose load in both diet conditions (Figure 2.8B, P<0.05). There were no changes in total Akt abundance (Figure 2.8C, P>0.05) in response to either the diet intervention or glucose load (P>0.05). Neither the HFSD intervention nor the glucose load had an influence on p-mTOR^{S2448} or total mTOR abundance (Figure 2.8 D, E, P>0.05).

The abundance of CMA markers in quadriceps muscle are summarised in Figure 2.9. Neither the HFSD nor the acute glucose load had an influence on LAMP-2A or Hsc-70 protein abundance (Figure 2.9 A and B, P>0.05).

The muscle gene expression analyses are summarized in Figure 2.10. No changes in the mRNA quantities of *Lc3b, Gabarapl1, p62/Sqstm1, Plin2* and *Plin3* were observed between the HFSD and CON (P>0.05).

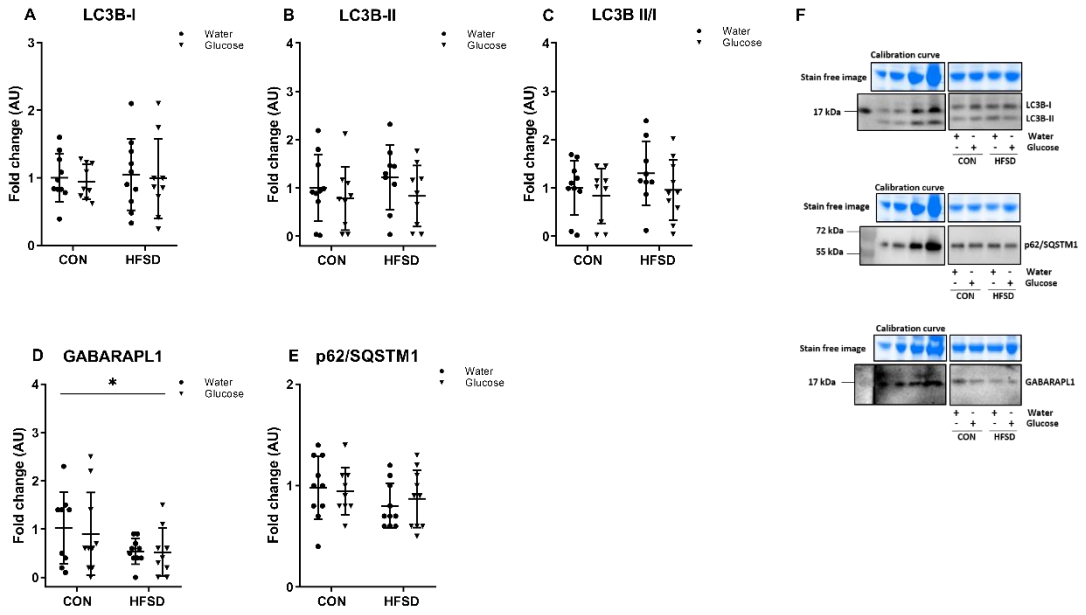

Figure 2.7. Protein abundance of autophagy markers in the quadriceps muscle of HFSD and CON mice. LC3B-I (A), LC3B-II (B), LC3B-II/LC3B-I ratio (C), GABARAP (D) and p62/SQSTM1 (E) abundance 15 min following oral gavage with water or glucose in HFSD and CON diet intervention. Values are presented as individual data and means ± SD. AU indicates arbitrary units. Stain free images providing an example of total protein loading and corresponding representative blots are shown (F). * indicates main effect of diet ($P<0.05$). Representative blots for each protein were taken from the same membrane and accompanying stain free images were taken from the same gel. Standard curves are taken from the same gels/membrane with non-contiguous lanes indicated with spaces. .

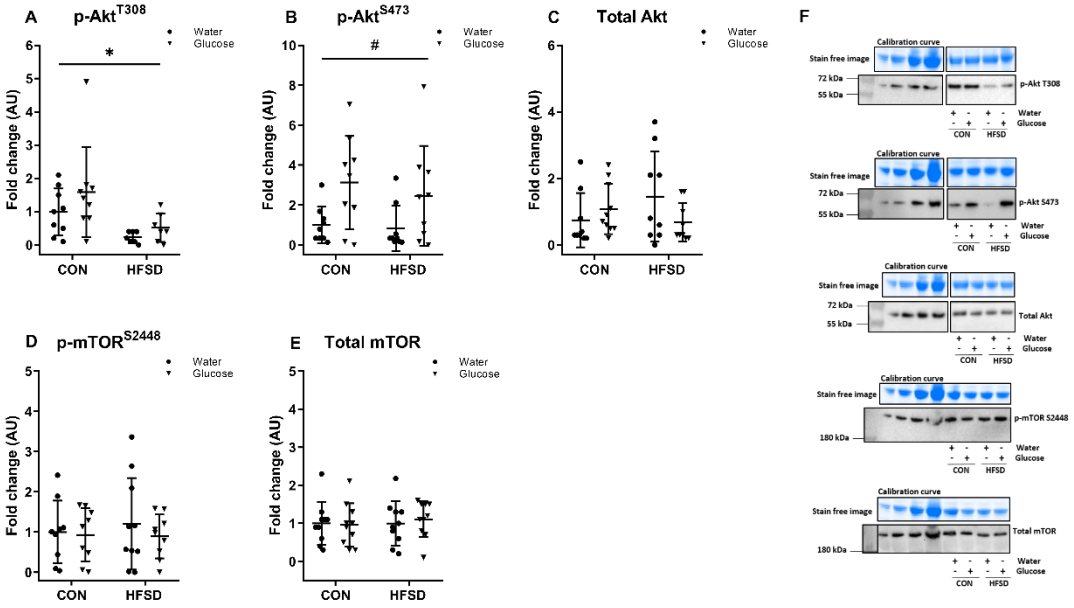

Figure 2.8. Protein abundance of signalling markers regulating autophagy in quadriceps muscle of HFSD and CON mice. p-Akt^{T308}, p-Akt^{S473} and total Akt (A, B, C), p-mTOR^{S2448} and total mTOR (D, E) 15 min following oral gavage with water or glucose) in HFSD and CON diet intervention. Values are presented as individual data and means ± SD. AU indicates arbitrary units. Stain free images providing an example of total protein loading and corresponding representative blots are shown (F). * indicates main effect of diet (P<0.05); # indicates main effect of acute feeding (P<0.05). Representative blots for each protein were taken from the same membrane and accompanying stain free images were taken from the same gel. Standard curves are taken from the same gels/membrane with non-contiguous lanes indicated with spaces. .

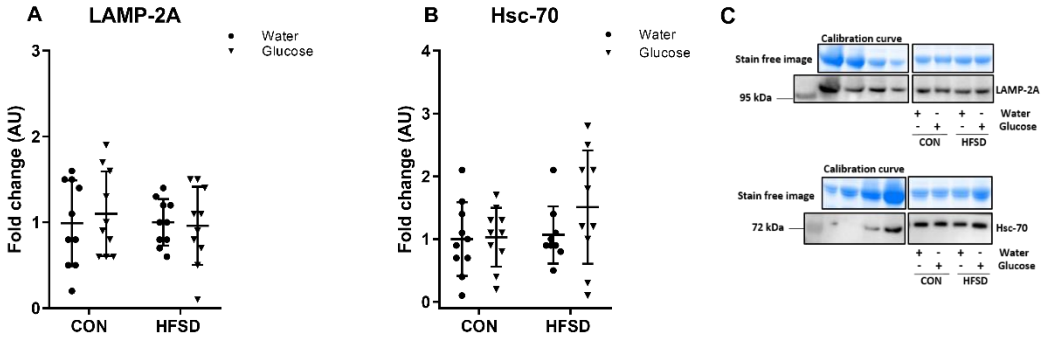

Figure 2.9. Protein abundance of CMA markers, LAMP2A (A) and Hsc-70 (B) in the quadriceps muscle of HFSD and CON mice 15 min following oral gavage with water or glucose in HFSD and CON diet interventions. Values are presented as individual data and means ± SD. AU indicates arbitrary units. Stain free images providing an example of total protein loading and corresponding representative blots are shown (C). Representative blots for each protein were taken from the same membrane and accompanying stain free images were taken from the same gel Standard curves are taken from the same gels/membrane with non-contiguous lanes indicated with spaces.
.

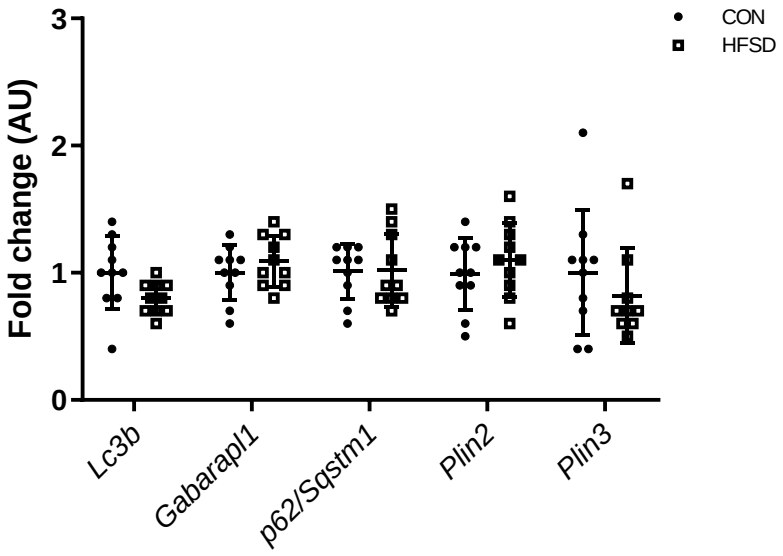

Figure 2.10. Gene expression levels of *Lc3b, Gabarapl1, p62/Sqstm1, Plin2, Plin3* in the quadriceps muscle of mice following HFSD and CON diet interventions. Values are presented as individual data and means ± SD. AU indicates arbitrary units.

2.5 Discussion

Autophagy is essential for maintaining cellular homeostasis and function through the targeted degradation of proteins and organelles. Autophagy is acutely regulated by nutrient availability via nutrient and hormone sensitive signalling pathways. Emerging evidence indicates that autophagy dysfunction is present in insulin resistant tissues and may contribute to the progression of metabolic disease (29, 35). The aim of this study was to investigate the effects of diet-induced insulin resistance on autophagy markers in liver and skeletal muscle in the fasted stated and following an acute glucose load. We found that HFSD resulted in marked changes in autophagy markers in the liver, characterised by accumulation of LC3B-II and p62/SQSTM1 which is indicative of a greater autophagosome content, likely due to lower autophagosome clearance (74). In contrast, autophagy markers in skeletal muscle were largely unaffected by HFSD. The glucose load administered following a 5 h did not impact autophagy markers in either liver or skeletal muscle.

The persistently elevated plasma glucose (Figure 2.1D) and insulin levels (Figure 2.1F) throughout the OGTT, as well as the 3-fold higher HOMA-IR index (Figure 2.1C) in the HFSD mice compared to the controls demonstrate that 16 weeks of HFSD induced whole body insulin resistance. Furthermore, as lipid accumulation is intimately linked with the onset of tissue specific insulin resistance (198), the marked lipid accumulation observed following 16 weeks of HFSD (Figure 2.2) supports the development of insulin resistance in both liver and skeletal muscle. Our results showed that 16 weeks of HFSD also resulted in ~2-fold increase in LC3B-II and GABARAPL1-II abundance in the liver (Figure 2.3). LC3B and GABARAPL1 belong to the mammalian family of Atg8-like proteins and are lipidated and subsequently incorporated to the autophagosome upon autophagy induction (74). As such, lipidated LC3B (LC3B-II) is a recognised marker for autophagosome content (74). As the autophagosome is in a state of constant flux between delivery to the lysosome and subsequent degradation, the increase in LC3B-II could be due to an increase in its lipidation or a reduction in its degradation in the lysosome. To gain further insight into LC3B-II accumulation, we further assessed additional autophagy markers at the level of gene and protein expression, as recommended in methodological guidelines for autophagy assessment (74). There were no differences between CON and HFSD groups in the gene expression of the autophagy markers of interest. This suggests that the increase in LC3B-II and GABARAPL1-II

content was not due to changes at the transcriptional level (Figure 2.6) and that there were no changes in autophagy initiation/induction. However, we did observe an increase in p62/SQSTM1 protein, a recognised marker of autophagosome clearance, in the HFSD group (74). As such, these data suggest that hepatic autophagosome accumulation with HFSD is due to reduced autophagosome clearance by the lysosome. This is partly in line with previous observations in mice fed a high fat diet for 8-16 weeks, where hepatic autophagy clearance was also found to be suppressed (35, 171).

We also examined the upstream signalling pathways regulating autophagy activity and found that the HFSD groups displayed a higher level of inhibitory autophagy signalling, based on increased p-mTOR^{S2448} and downstream increases in p-ULK-1^{S758} (Figure 2.5 C, E). Autophagy induction (i.e. formation of the phagophore) is stimulated by the formation of the ULK-1 complex, which is negatively regulated by increases in insulin and amino acids via p-mTOR ^{S2448} (50). The resultant association between the mTOR complex and the ULK-1 complex increases p-ULK-1^{S758}, which in turn, inhibits phagophore nucleation (50, 195). This results in lower conversion of LC3B-I to LC3B-II and reduced autophagy induction. The observed increase in hepatic p-mTOR^{S2448} in models of diet-induced obesity have been previously described (205-207). Hence, the increased inhibitory autophagy signalling observed in the HFSD mice supports our conclusion that increased LC3B-II abundance is due to defects in autophagosome degradation rather than upstream signalling events promoting LC3B lipidation and autophagosome formation. Other autophagy studies that have also shown defective autophagy clearance, determined by increases in LC3B-II and p62/SQSTM1 abundance, in genetically obese mice (*ob/ob)* (35), as well as in rat hepatocytes exposed to lipids (82). This may explain the lower autophagosome clearance following HFSD in the present study.

We observed an increase in abundance of LAMP-2A in the livers of HFSD mice, suggesting CMA upregulation through a higher CMA-lysosome capacity (Figure 2.4) (208). CMA has been linked to the regulation of metabolism via the targeted degradation of enzymes and structural proteins that regulate glucose and lipid metabolism and can influence lipid storage (34). The increased LAMP-2A protein levels observed here are in-line with the early increases in CMA activity observed in *in vitro* studies upon lipid loading (209), and in mice, either fed a high fat diet (210) or in a model of non-alcoholic steatohepatitis (211). Interestingly, previous studies have demonstrated an upregulation

of CMA in the presence of macroautophagy impairments (212, 213). Therefore, it is also possible that upregulation of CMA capacity in the liver following HFSD is a compensatory response to maintain proteostasis while macroautophagy is impaired.

In skeletal muscle, despite a three-fold increase in skeletal muscle lipid content (Figure 2.2B) we found no differences in the abundance of LC3B forms, total GABARAPL1 and p62/SQSTM1 between HFSD and control fed mice, which together indicate there were no differences in autophagosome content or degradation (Figure 2.7). Furthermore, there were no significant differences in the CMA markers (LAMP-2A or Hsc-70) between dietary groups. Previous evidence regarding the effects of HFD on autophagy markers in skeletal muscle are partly in line with our findings. Two independent studies have reported no differences in autophagosome content, shown by unchanged levels in LC3B-II, in skeletal muscle of mice following a 12-16 week high fat diet intervention (11, 197). However, in contrast to our findings, these studies reported significant increases in p62/SQSTM1 protein in the HFD groups. Interestingly, Campbell, *et.al* observed that p62/SQSTM1 increases occurred in predominantly oxidative muscle (soleus), but not in predominantly glycolytic muscle (plantaris) (197). These muscle-specific differences could explain our findings in quadriceps muscle, which is composed of a mixture of oxidative and glycolytic muscle fibres (214). Also, although we did observe some impairments in insulin signalling in skeletal muscle, shown by an overall reduction in p-Akt^{T308} (Figure 2.8A) after 16 weeks of HFSD diet, these were not translated into differences in p-Akt^{S473} or p-mTOR^{S2448} between groups. The absence of consistent autophagy-related signalling impairments could also explain why there were no differences in the autophagy markers in skeletal muscle measured in this study. Taken together, these results indicate that skeletal muscle is less susceptible to diet-induced obesity mediated autophagy impairments in comparison to the liver. In support of this finding, Ehrlicher and colleagues (215) demonstrated that diet-induced insulin resistance in mice did not affect autophagy markers in skeletal muscle under basal or hyperinsulinemic conditions. Furthermore, the abundance of autophagy markers were not different in skeletal muscle in humans with type 2 diabetes (187). However, severely insulin resistant, hyperglycaemic, long-standing, insulin-treated diabetic patients have been shown to have decreased expression of autophagy-related proteins (91). It is therefore plausible that autophagy modulation in skeletal muscle is dependent upon the severity of insulin resistance and the degree of hyperinsulinemia and/or hyperglycaemia.

The glucose gavage administered following a 5 h fast in the present study did not impact autophagy markers in either liver or skeletal muscle. Furthermore, acute glucose administration had little impact on upstream signalling pathways regulating autophagy induction in either tissue. Studies using hyperinsulinemic-euglycemic clamp and amino acid infusion in mice following a 24 h fast have shown that autophagy in the liver is mainly inhibited by amino acid availability, whilst insulin plays a key role in inhibiting autophagy in skeletal muscle (216). However, the significance of nutrient modulation of autophagy remains to be explored in shorter term fasting and refeeding conditions that more closely resemble habitual feeding behaviour (216). In the present study, although the ~2-fold increase in plasma glucose levels following glucose gavage increased plasma insulin concentrations in the HFSD group this did not impact autophagy marker abundance in either tissue. Therefore, it remains to be demonstrated whether transient and physiological nutrient and hormonal responses following the typical feeding patterns are sufficient to suppress autophagy.

2.6 Conclusions

The present study has shown that 16 weeks of HFSD that induces whole body insulin resistance does not influence autophagy marker abundance or upstream signalling events in skeletal muscle. On the contrary, exposure to a HFSD resulted in autophagosome accumulation in the liver, possibly through impairments in autophagosome clearance. We propose that hepatic autophagy impairments contribute to the development of liver insulin resistance through accumulation of autophagy targets linked with the development of metabolic dysfunction such as ectopic lipid accumulation and dysfunctional mitochondria. Further investigations are required to understand the tissue specific autophagy responses to typical feeding patterns that occur over the course of a day.

Chapter 3

Diabetic db/db mice display differential macroautophagy responses in liver and skeletal muscle

3.1 Abstract

Autophagy is an intracellular recycling process that is modulated by nutrient- and hormonal-mediated signaling pathways. As the metabolic responses to such stimuli are disturbed in type 2 diabetes, it is likely that autophagy impairments contribute to the development and progression of metabolic disease. The aim of the present study was to investigate the effects of overt diabetes on autophagy markers in the liver and skeletal muscle in the fed and the fasted state using *db/db* mice and db/+ controls.

Male C57BL/6J *db/db* (n=16) and control heterozygous mice (*db/*+, n=16) were fed a normal chow diet until 12 weeks of age. Blood samples, quadriceps muscle and liver were collected in the fed state or following a 4 h fast. The gene and protein expression of autophagy markers and the activation of key upstream signalling events were assessed.

In the muscle of *db/db* mice, both LCB3 forms and *Lc3b* gene were increased, along with lower p62/SQSTM1 indicating an upregulation of autophagosome turnover. These occurred alongside a reduction in total and phosphorylated mTOR. In contrast, in the liver of *db/db* mice, *Lc3b* gene, LC3B-I abundance and inhibitory signalling cues (i.e. p-Akt^{T308}, p-Akt^{S473}, p-mTOR^{S2448}) were lower, with no changes observed in LC3B-II and p62/SQSTM1 content, indicating a lower capacity for autophagosome formation, without changes in autophagosome content or autophagosome clearance. Feeding status did not alter autophagy markers in either *db/db* or *db/*+ mice.

Taken together, the present study shows divergent autophagy responses in liver and skeletal muscle from diabetic mice, where the upregulation in macroautophagy in skeletal muscle appears to be part of a broader upregulation of proteolytic activity that likely underlies muscle metabolic dysfunction in diabetes.

3.2 Introduction

Diabetes mellitus is the ninth major cause of death worldwide, of which type 2 diabetes (T2D) accounts for 90% of all cases (217). The rise in obesity over the last 30 years is considered to be the primary driver of the high global prevalence of T2D today. Obesity is closely associated with the development of whole-body insulin resistance, which is a key stage in the pathogenesis of T2D and a hallmark feature of the disease. In the liver, insulin resistance (IR) results in a failure of insulin to suppress hepatic glucose output, whilst in peripheral tissues, insulin resistance inhibits insulin-mediated glucose uptake, of which skeletal muscle is of major importance. The presence of whole-body insulin resistance is initially compensated by hyperinsulinemia, which can maintain adequate glucose homeostasis. However, with time, overt T2D ultimately develops with the failure of the insulin secretory response in pancreatic β-cells in combination with severe insulin resistance in the liver and peripheral tissues, resulting in loss of glycemic control and sustained hyperglycemia. Obesity-related lipid accumulation is central to the development of insulin resistance in both the liver and skeletal muscle. Non-alcoholic fatty liver disease (NAFLD) is present in the majority of T2D cases, and other liver diseases such as non-alcoholic steatohepatitis (NASH), cirrhosis hepatocellular carcinoma and liver failure are also prevalent. In skeletal muscle, lipid accumulation is acutely linked with the onset of skeletal muscle insulin resistance and mitochondrial dysfunction, impairments in protein metabolism and muscle weakness, which are all characteristics of skeletal muscle in T2D patients.

Autophagy is a conserved intracellular recycling process that constitutes a key mechanism that ensures optimal tissue function. It maintains cell quality control by degrading cell components such as dysfunctional mitochondria, lipids and aggregated proteins (74, 113, 218, 219). Autophagy is sensitive to nutrient and hormonal fluctuations with significant elevation in autophagy activity during fasting conditions and inhibition during raised insulin and amino-acids concentrations that occur during feeding (94, 95, 220). Given that tissue insulin resistance manifests with accumulation and dysfunction of classic autophagy targets, several research groups have investigated autophagy in models of metabolic disease. In cultured hepatocytes and mouse liver, autophagy inhibition results in lipid accumulation, decreases in β-oxidation rates and defective insulin action (29, 35), while inhibition of autophagy in skeletal muscle results in muscle wasting (99, 221, 222). Additionally, in diet induced IR rodent models, the presence of

NAFLD was associated with decreased autophagy, measured by higher LC3B-II and p62/SQSTM1 abundance (29, 171, 172). Furthermore, in Chapter 2 of this thesis, we found that autophagy impairments in the liver in response to a 16-week high fat, high sucrose diet manifested as disrupted autophagosome clearance. Further evidence that autophagy is relevant for tissue insulin resistance is that pharmacological autophagy induction in the liver of rodents protects against whole body diet-induced insulin resistance (83, 175, 176, 223).

Previously (Chapter 2) we used a validated diet-induced mouse model to study obesity-related insulin resistance, and demonstrated impairments in autophagy in the liver, but not in skeletal muscle. This indicates that autophagy may not be involved in the initial development of insulin resistance of skeletal muscle however, it is unclear whether autophagy impairments contribute to the deterioration in skeletal muscle metabolism and function with the development of overt T2D. In the present chapter, the impact of overt diabetes was studied using the *db/db* mouse model, which is created by inducing an autosomal recessive mutation in the leptin receptor (224). The mutation causes the animals to become hyperphagic, obese, hyperinsulinemic and hyperglycaemic (225) and the *db/db* mouse displays a natural history of T2D that parallels that of humans (226). Moreover, in Chapter 2, acute feeding was investigated through glucose administration via oral gavage, but it would be advantageous to describe the autophagy responses in a fed and a fasted state that more accurately reflects the changes in habitual food intake. Therefore, the aim of the present study was to investigate the effects of overt diabetes on autophagy markers in the liver and skeletal muscle in the fed and the fasted state using *db/db* mice and *db/+* controls. It was hypothesized that impairments in autophagy markers would be present in both liver and skeletal muscle in the *db/db* mice when compared to controls, and that the magnitude of the impairments in autophagy markers in *db/db* mice would display a blunted response in the fed state compared to fasting.

3.3 Methods

Animals

Male C57BL/6J *db/db* (n=16) and control heterozygous mice (*db/+*, n=16) were purchased from the Animal Resources Centre, Perth, Western Australia. At 4 weeks of age mice were housed (5 per cage) and acclimatised to the Deakin University animal facility in an environmentally controlled room on a 12/12 h light/dark cycle with free access to water and standard chow diet (9% energy from fat, Barastoc Rat and Mouse, Ridley AgriProducts, Australia). At 12 weeks of age, blood samples were taken (12 pm) from the tail vein of mice following either a 4 h fast (food retrieved at 8 am; n=8 *db/db*, n=8 *db/+*) or in the fed state (n=8 *db/db*, n=8 *db/+*) where mice had free access to the standard chow diet. A 4 h fast was chosen for this study in *db/db* mice, instead of a 5 h fast performed in C57BL6 mice in Chapter 2. This was based on previous experience in the laboratory, given that a longer fasting period is not well tolerated in the *db/db* mice. Immediately following blood sampling mice were culled by cervical dislocation and liver and quadriceps muscle were collected and frozen at -80◦C until further analyses. The present study was approved by the Deakin University Animal Ethics Committee (Code: G09-2012).

Analyses

Glucose homeostasis was assessed by measuring blood glucose levels via a glucometer (Accu-Check, Roche, NSW, Australia) using blood samples from the tail vein. The abundance of autophagy markers (LC3B, GABARAPL1, p62, Hsc-70, LAMP-1, LAMP-2A), lipid droplet-associated proteins (PLIN2, PLIN3, PLIN5) and upstream signaling events (total Akt, p-Akt$^{Thr308, Ser473}$, total mTOR, p-mTOR^{Ser2448}, total ULK-1, p-ULK-1$^{Ser758, Ser556}$) were determined by immunoblotting. Gene expression analyses were performed on *Lc3b, Gabarapl1, p62/Sqstm1 and Lamp1* by real time qPCR.

Immunoblotting

Frozen liver and quadriceps samples were prepared, loaded onto stain free gels, blotted and quantified as described in detail in Chapter 2. Antibodies against Akt, p-Akt^{S473}, mTOR, p-mTOR^{S2448}, GABARAPL1 p62/SQSTM1, ULK-1, p-ULK-1, LAMP-2A, LAMP1,

Hsc-70 anti-PLIN2, anti-LC3B were used to determine the abundance of these proteins (see details on Chapter 2). Data was expressed relative to the respective control (*db/+* 4 h fasted).

Gene expression analyses

RNA extraction and real-time PCR were conducted in both liver and quadriceps muscle from all animals as described in detail in Chapter 2. The following autophagy-related genes of interest were determined: Lc3b, Gabarapl1, p62/Sqstm1 and Lamp1 (Table 3.1).

Table 3.1. Names and sequences of primers for real-time PCR

Gene name	DNA Sequence (5' to 3')
Lc3b	*Forward: CATGAGCGAGTTGGTCAAGA*
	Reverse: TTGACTCAGAAGCCGAAGGT
Gabarapl1	*Forward: ATGTCATTCCACCCACCAGT*
	Reverse: TACCATTACCCCTCCTGCTG
p62/Sqstm1	*Forward: AAGAACGCGTGCTGATACCT*
	Reverse: GCACCAGTCTCTTCCTGGAG
LAMP1	*Forward: GATGAATGCCAGCTCTAGCC*
	Reverse: CTGGACCTGCACACTGAAGA

Statistical analyses

An *a priori* power calculation was performed on data from the Chapter 2 investigating LC3B-II/LC3B-I ratio changes in liver between control and mice fed a high fat, high sucrose diet. The data from Chapter 2 demonstrate that the LC3B-II/LC3B-I ratio in the control group was 1.0 ± 0.5 arbitrary units (mean ± SD), while the LC3B-II/LC3B-I ratio in the HFD group was 3.0 ± 1.5 arbitrary units (mean ± SD). This gives an effect size of 1.79, meaning that n = 8 in each group would give an expected power of 0.9. Given that the *db/db* mice are more insulin resistant, we would hypothesize that any change would be at least as large as in the HFSD group studied in Chapter 2.

A two-way ANOVA was used to analyse the data using GraphPad Prism version 8.0.0 for Windows (GraphPad Software, San Diego, California USA). The main effects of genotype (*db/+* versus *db/db*) and feeding state (4 h fasted versus fed) were examined. Post hoc analyses were run in the case of significant interactions using the Bonferroni correction. Statistical significance was set at $P<0.05$. Data are presented as individual data and means +/- standard deviation (SD).

3.4 Results

General characteristics

The general characteristics between the *db/db* mice and control *db/+* mice are shown in Table 3.2 The *db/db* mice had increased body mass and fat deposits (P<0.05) compared to the *db/+* mice. The diabetic condition of the *db/db* mice was confirmed by the presence of hyperglycemia, with plasma glucose concentrations approximately three-fold higher (P<0.05) compared to the *db/+* mice.

Table 3.2. General characteristics of *db/db* and *db/+* mice.

	db/+	***db/db***
	n=16	n=16
Body mass (g)	31.19 ± 1.97	39.69 ± 5.74*
Fat mass (g)		
- ***Mesenteric***	0.18 ± 0.06	0.55 ± 0.24 *
- ***Epididymal***	0.28 ± 0.09	1.26 ± 0.37*
- ***White adipose tissue***	0.15 ± 0.06	0.78 ± 0.32*
Fasting plasma glucose (mmol·l^{-1})	9.76 ± 1.88	27.56 ± 7.61*

Values are presented as means ± SD * indicates main effect of genotype (P<0.05)

Autophagy in the liver

The abundance of key autophagy markers in the liver of *db/+* and *db/db* mice in the fed and the 4-h fasted state is presented in Figure 3.1. Compared to the *db/+*, there was a significant decrease in the non-lipidated LC3B form, LC3B-I, in the *db/db* mice (Figure 3.1A, P<0.01). Despite the changes observed in LC3B-I, LC3B-II protein levels remained unchanged between genotypes (Figure 3.1B). This resulted in a significant elevation in the LC3-II/I ratio in the *db/db* mice (Figure 3.1C). Moreover, there were no significant differences in p62/SQSTM1 protein levels between genotypes (Figure 3.1D). There was a significant main effect of feeding status on LC3B-I, with a ~30% reduction observed in the *db/+* mice and a ~15% reduction in the *db/db* mice in the fed state compared to the 4 h fasted state. There was no effect of feeding status on LC3B-II, LC3B-II/LC3B-I ratio or p62/SQSTM1 abundance.

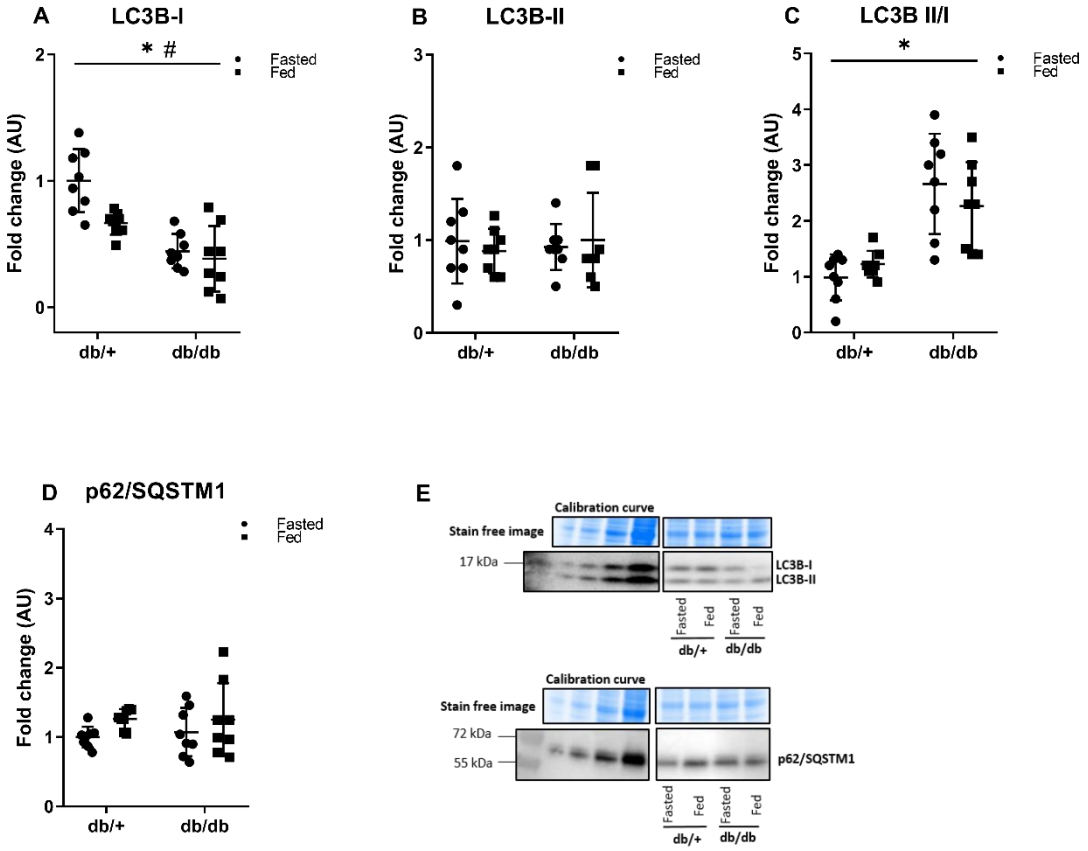

Figure 3.1. Autophagy markers in the liver of *db/+* and *db/db* mice in a fed and 4 h fasted state, including abundance of LC3B-I (A), LC3B-II (B) and LC3B-II/LC3B-I ratio (C), p62/SQSTM1 (D). Values are presented as individual data and mean ± SD. AU indicates arbitrary units. Stain free images provide an example of total protein loading and corresponding representative blots are shown (E). * indicates main effect of genotype (P<0.05); # indicates main effect of feeding status (P<0.05). Representative blots for each protein were taken from the same membrane and accompanying stain free images were taken from the same gel. Standard curves are taken from the same gels/membrane with non-contiguous lanes indicated with spaces. .

Key upstream signaling events responsible for regulating autophagy were further investigated in *db/db* and *db/+* mice (Figure 3.2 and 3.3). In the *db/db* mice, there were significant increases in both, p-Akt^{S473} and p-mTOR^{S2448} compared to *db/+* (Figure 3.2 B and D, $P<0.05$), although there was no difference in p-Akt^{T308} or total Akt between genotypes (Figure 3.2A, $P>0.05$). It is worth noting that there were 2 samples that displayed a large (40-80 fold) increase in p-Akt^{S473}. This variability was not seen in p-Akt^{T308} or total Akt ruling out that this was due to uneven protein loading. Additionally, the significant genotype differences in p-Akt^{S473} remains even if these samples were removed from the analyses. This variability is unexplained, but it may be due to biological variation. Furthermore, there were no downstream effects on ULK-1 signaling as there were no differences in either p-ULK-1^{S758}, p-ULK-1^{S556} or total ULK-1 abundance between *db/db* and *db/+* mice (Figure 3.3 A-C, $P>0.05$). There was no effect of feeding status on any signaling responses in either genotype (Figure 3.3, $P>0.05$). When corrected to their respective total proteins, no differences in any of the phosphorylated isoforms were observed (Figure 3.3 D and E, $P>0.05$).

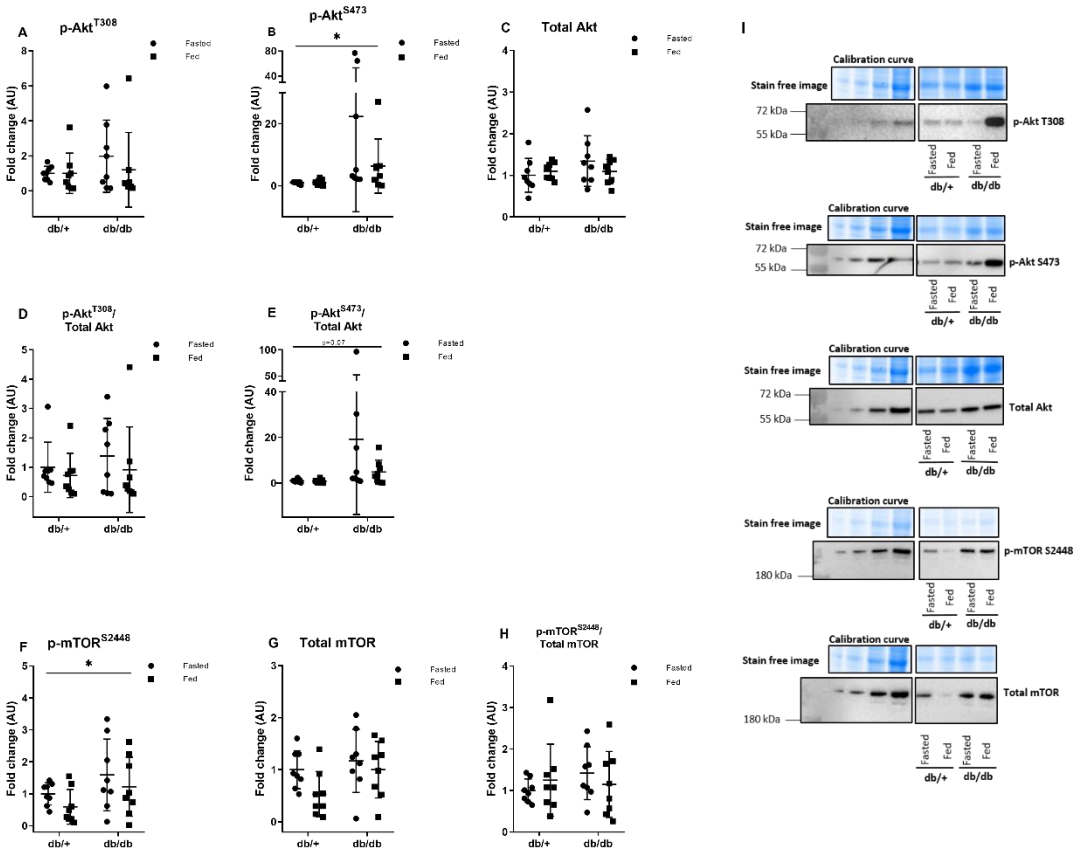

Figure 3.2. Abundance of signalling markers regulating autophagy in the liver of *db/+* and *db/db* mice in a fed and 4 h fasted state, including abundance of p-Akt^{T308}(A), p-Akt^{S473} (B), total Akt (C), corrected p-Akt^{T308} (D), corrected p-Akt^{S473} (E), p-mTOR ^{S2448} (F), total mTOR (G) and corrected p-mTOR ^{S2448} (H). Values are presented as individual data and mean ± SD. AU indicates arbitrary units. Stain free images provide an example of total protein loading and corresponding representative blots are shown (I). * indicates main effect of genotype (*P*<0.05); presented p-value indicates trend in main effect of genotype (P=0.07). Representative blots for each protein were taken from the same membrane and accompanying stain free images were taken from the same gel. Standard curves are taken from the same gels/membrane with non-contiguous lanes indicated with spaces. .

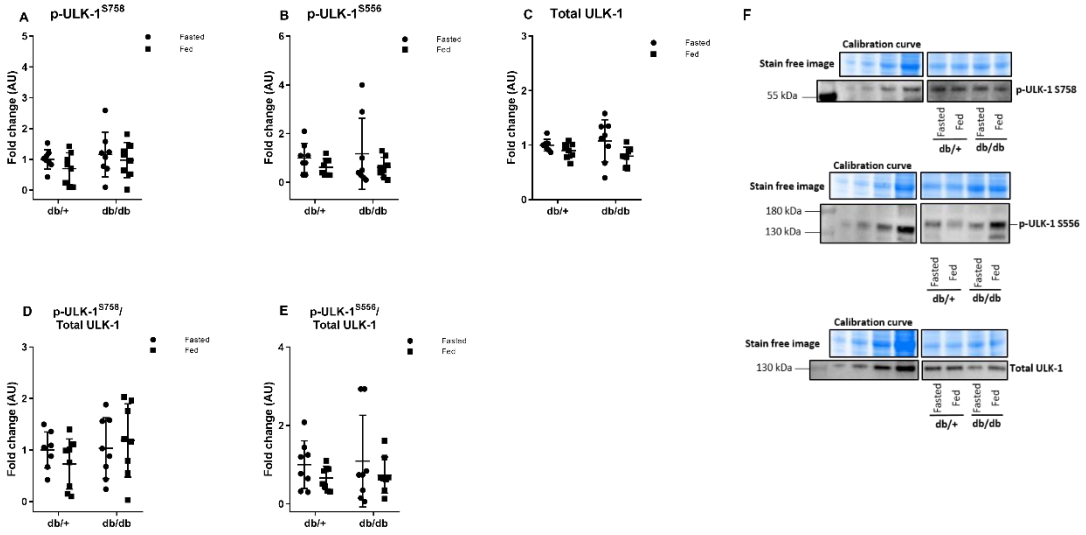

Figure 3.3. Abundance of signalling markers regulating autophagy in the liver of *db/+* and *db/db* mice in a fed and 4 h fasted state, including abundance of p-ULK-1 ^{S758} (A), p-ULK-1 ^{S556} (B), total ULK-1 (C), corrected p-ULK-1^{S758} (D) and corrected p-ULK-1^{S556} (E). Values are presented as individual data and mean ± SD. AU indicates arbitrary units. Stain free images provide an example of total protein loading and corresponding representative blots are shown (F). * indicates main effect of genotype (P<0.05). Representative blots for each protein were taken from the same membrane and accompanying stain free images were taken from the same gel. Standard curves are taken from the same gels/membrane with non-contiguous lanes indicated with spaces.
.

Lysosomal markers, as well as proteins involved in chaperone mediated autophagy (CMA) were also assessed in the liver (Figure 3.4). No differences were found in the CMA-specific receptor, LAMP-2A (Figure 3.4A, $P>0.05$) or the CMA-linked chaperone, Hsc-70, between genotypes (Figure 3.4B). However, there was a significant increase in liver LAMP1 (Figure 3.4C, $P<0.05$) and PLIN2 protein (Figure 3.4D, $P<0.05$) levels observed in the *db/db* mice. Feeding status did not influence LAMP1, LAMP-2A, Hsc-70 or PLIN2 abundance (Figure 3.4, $P>0.05$).

The expression of key autophagy genes was assessed and is shown in Figure 3.5. The *db/+* mice displayed significant higher expression of *Lc3b* ($P<0.05$), compared to the *db/db* mice. There were no other changes in the measured genes, *i.e. Gabarapl1, p62/Sqstm1* or *Lamp1* between genotypes. *Lc3b* gene expression was decreased with feeding (main effect of feeding status, $P<0.05$), which was primarily driven by reduced expression in the fed state in *db/+* mice. Feeding did not impact the gene expression of the other assessed genes.

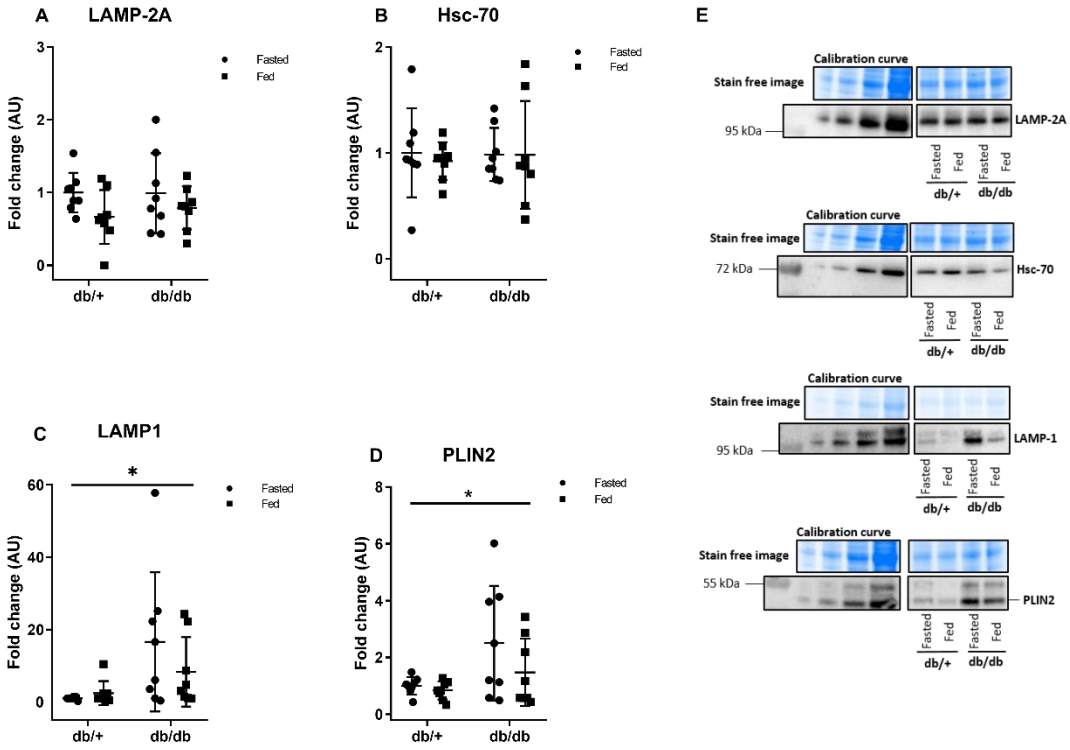

Figure 3.4. Chaperone-mediated autophagy (CMA), lysosomal and intracellular lipid markers in the liver of *db/+* and *db/db* mice in a fed and 4 h fasted state, including abundance of LAMP-2A (A), Hsc-70 (B) LAMP1 (C) and PLIN2 (D). Values are presented as individual data and mean ± SD. AU indicates arbitrary units. Stain free images provide an example of total protein loading and corresponding representative blots are shown (E). *indicates main effect of genotype (P<0.05). Representative blots for each protein were taken from the same membrane and accompanying stain free images were taken from the same gel. Standard curves are taken from the same gels/membrane with non-contiguous lanes indicated with spaces. .

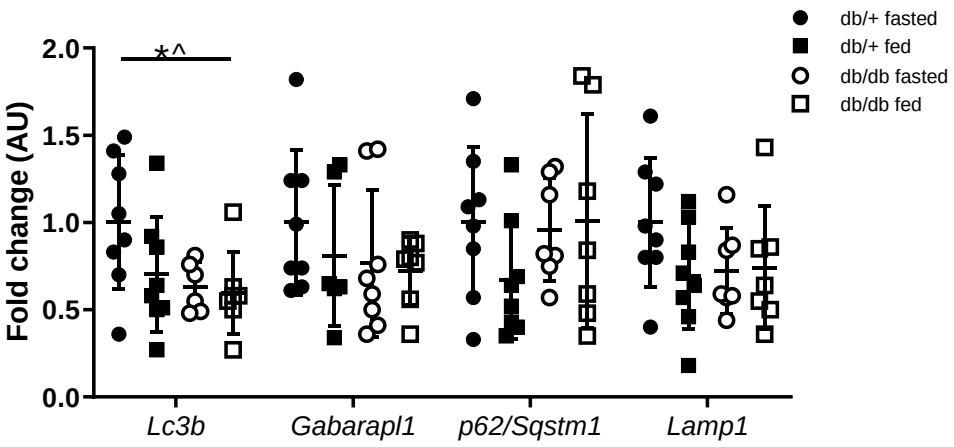

Figure 3.5. Gene expression levels of *Lc3b, Gabarapl1, p62/Sqstm1* and *Lamp1* in the liver of *db/+* and *db/db* mice in a fed and 4 h fasted state. Values are presented as individual data and mean ± SD. AU indicates arbitrary units. * indicates main effect of genotype (P<0.05); ^ indicates main effect of feeding status (P<0.05).

Autophagy in skeletal muscle

The abundance of autophagy markers in the quadriceps from *db/db* and control *db/+* mice in the 4 h fasted and fed state is summarised in Figure 3.6. LC3B-I protein levels were significantly higher in the muscle of *db/db* mice compared to the *db/+* mice (Figure 3.6A, $P<0.05$). These findings were translated into higher levels of the lipidated form of LC3B, LC3B-II, in the *db/db* mice (Figure 3.6B, $P<0.05$), while the LC3B-II/LC3B-I ratio was unchanged between genotypes (Figure 3.6C). Furthermore, a decrease in muscle GABARAPL1 (Figure 3.6D, $P<0.05$), as well as lower p62/SQSTM1 protein levels was observed (Figure 3.6E, $P<0.05$) in the *db/db* mice compared to the *db/+* mice. There was no effect of feeding status on the abundance of autophagy markers in either of the groups.

Key upstream signaling events regulating autophagy were assessed in the muscle of the *db/db* and the *db/+* mice, in both the 4 h fasted and fed state (Figure 3.7). Compared to the fasting state, there was a significant increase in p-Akt^{T308} in the fed state in the *db/+* mice, an effect which was completely absent in the *db/db* mice (Figure 3.7A, $P<0.05$). The same increase in p-Akt^{T308} in the *db/+* mouse only was observed when expressed relative to total Akt (Figure 3.7D, $P<0.05$). There was a main effect of feeding status on p-Akt^{S473} with greater abundance in the fed compared to the fasting state (Figure 3.7B, $P<0.05$). When expressed relative to total Akt, there was an additional effect of genotype, with greater p-Akt^{S473} observed in the *db/+* compared to the *db/db* mice (Figure 3.7E, $P<0.05$). There was a significant effect of genotype for both total mTOR and p-mTOR^{S2448}, which were both decreased in the *db/db* mice (Figure 3.7 F-G, $P<0.05$) compared to the *db/+* mice. In addition, p-mTOR^{S2448} was increased in the fed conditions, regardless of genotype (Figure 3.7F, $P<0.05$). There was no effect of genotype or feeding when p-mTOR^{S2448} was expressed relative to total mTOR (Figure 3.7H, $P>0.05$).

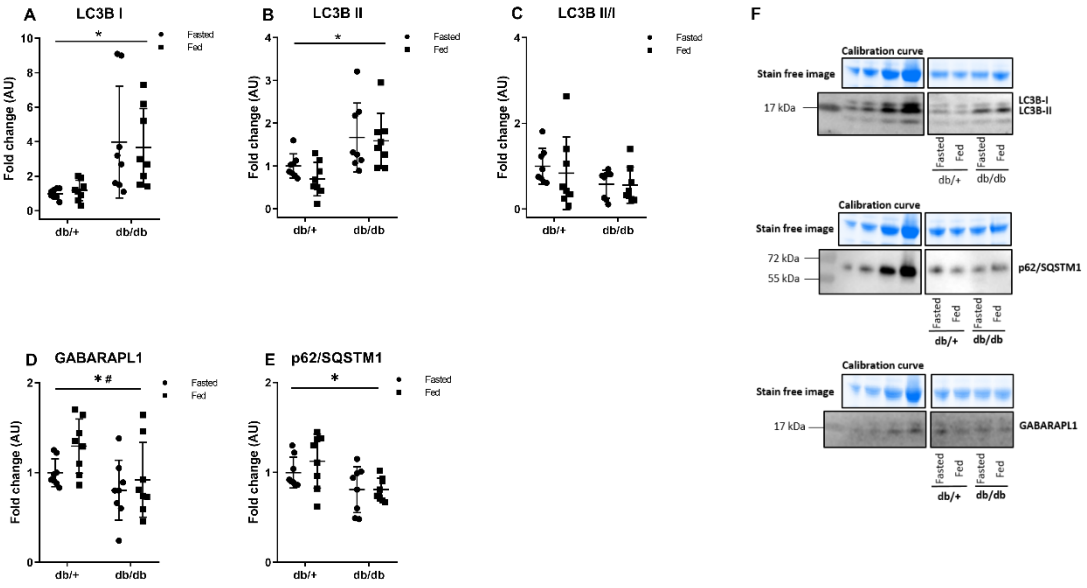

Figure 3.6. Autophagy markers in the quadriceps muscle of *db/+* and *db/db* mice in a fed and 4 h fasted state including abundance of LC3B-I (A), LC3B-II (B), LC3B-II/LC3B-I ratio (C), GABARAPL1 (D) and p62/SQSTM1 (E). Values are presented as individual data and mean ± SD. AU indicates arbitrary units. Stain free images provide an example of total protein loading and corresponding representative blots are shown (F). * indicates main effect of genotype (P<0.05); # indicates main effect of feeding status (P<0.05). Representative blots for each protein were taken from the same membrane and accompanying stain free images were taken from the same gel. Standard curves are taken from the same gels/membrane with non-contiguous lanes indicated with spaces.
.

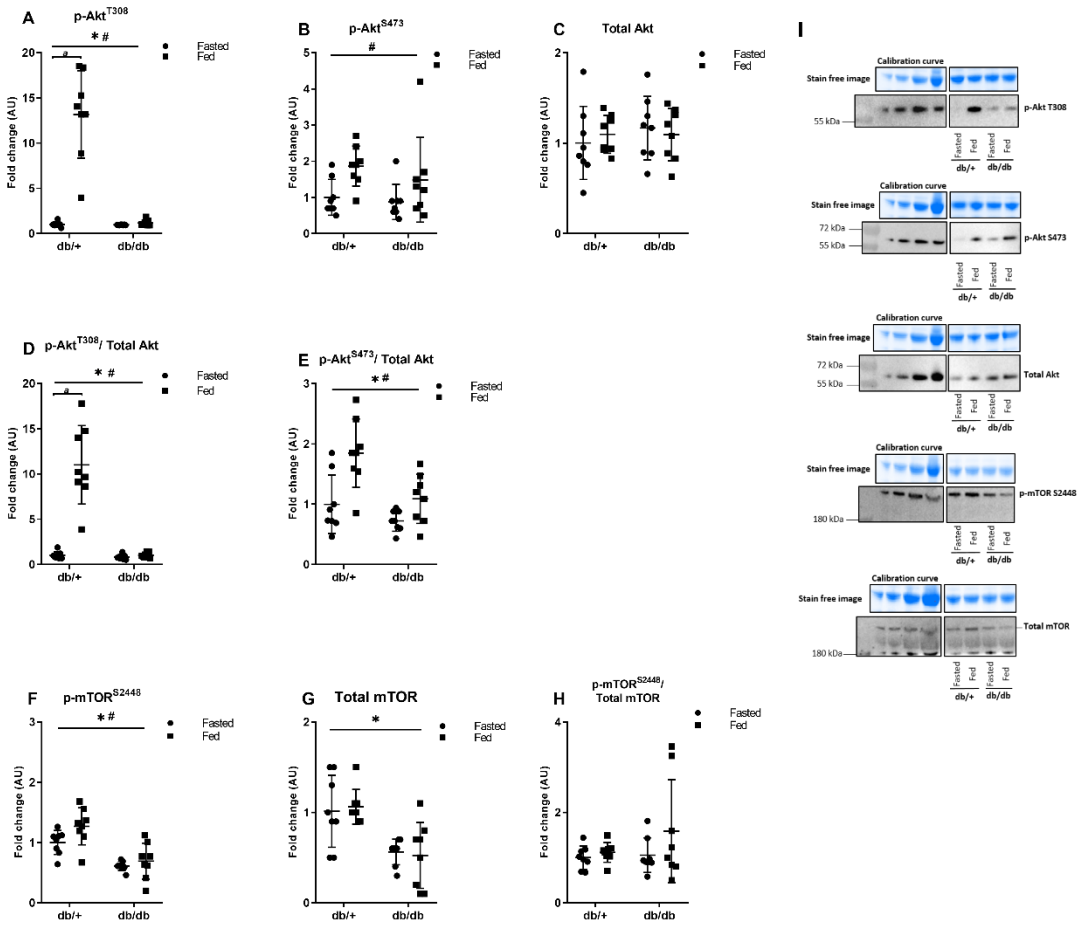

Figure 3.7. Abundance of signalling markers regulating autophagy in the quadriceps muscle of *db/+* and *db/db* mice in a fed and 4 h fasted state. p-Akt ^{T308}(A), p-Akt ^{S473} (B) total Akt (C), corrected p-Akt ^{T308}(D), corrected p-Akt ^{S473} (E), p-mTOR ^{S2448} (F) and total mTOR (G), p-mTOR ^{S2448} (H). Values are presented as individual data and mean ± SD. AU indicates arbitrary units. Stain free images provide an example of total protein loading and corresponding representative blots are shown (I). * indicates main effect of genotype (P<0.05); # indicates main effect of feeding status (P<0.05); ^{a} indicates P<0.05 between *db/+* fed vs *db/+* fasted. Representative blots for each protein were taken from the same membrane and accompanying stain free images were taken from the same gel. Standard curves are taken from the same gels/membrane with non-contiguous lanes indicated with spaces. .

The abundance of chaperone mediated autophagy (CMA) markers, the general lysosomal marker LAMP1, as well as PLIN2 in skeletal muscle is shown in Figure 3.8. The specific CMA receptor, LAMP-2A, was significantly decreased in the *db/db* compared to the *db/+* mice (Figure 3.8A, $P<0.05$), while the Hsc-70 abundance remained unchanged between genotypes (Figure 3.8B, $P>0.05$,). Furthermore, LAMP1 protein was higher in the *db/db* (Figure 3.8A, $P<0.05$) compared to the *db/+* mice. Feeding status had no effect on the abundance of the CMA markers or LAMP1 in either of the groups. There was also an increase in muscle PLIN2 levels in the *db/db* mice (Figure 3.8D, $P<0.05$,) compared to the *db/+* mice.

Gene expression levels of *Lc3b, p62/Sqstm1, Gabarapl1* and *Lamp1* were also assessed in the *db/db* and *db/+* mice (Figure 3.9). Both *Lc3b* and *p62/Sqstm1* genes were significantly increased in the *db/db* mice ($P<0.05$), while there were no changes in *Gabarapl1 n*or *Lamp1* expression levels between genotypes. Feeding status had no effect on the expression of any of the measured genes in either genotypes.

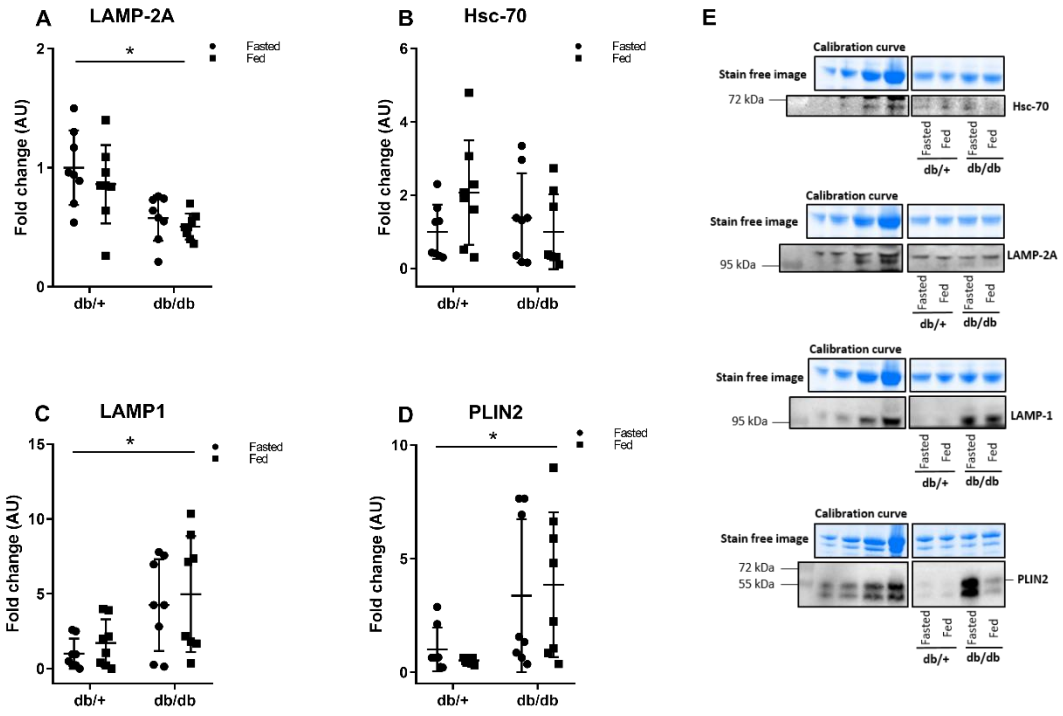

Figure 3.8. Chaperone-mediated autophagy (CMA) lysosomal and intracellular lipid markers in the quadriceps muscle of *db/+* and *db/db* mice in a fed and 4 h fasted state, including abundance of LAMP-2A (A), Hsc-70 (B) LAMP1 (C) and PLIN2 (D). Values are presented as individual data and mean ± SD. AU indicates arbitrary units. Stain free images provide an example of total protein loading and corresponding representative blots are shown (E). * indicates main effect of genotype (P<0.05). Representative blots for each protein were taken from the same membrane and accompanying stain free images were taken from the same gel. Standard curves are taken from the same gels/membrane with non-contiguous lanes indicated with spaces. .

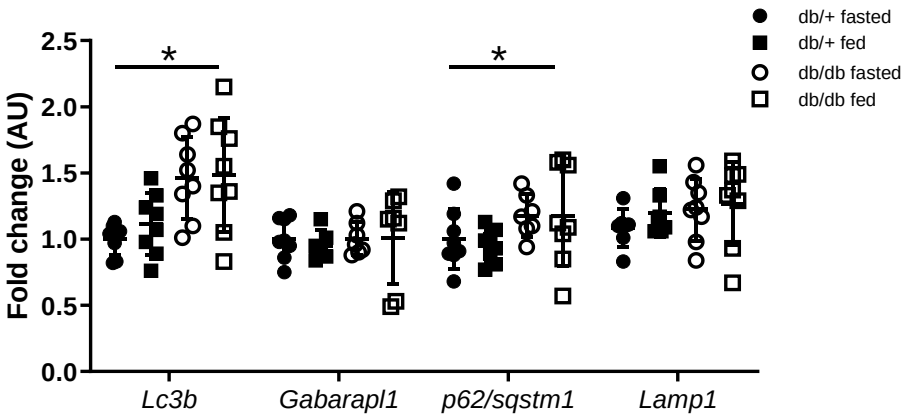

Figure 3.9. Gene expression levels of *Lc3b, Gabarapl1, p62/Sqstm1* and *Lamp1* in the quadriceps muscle of *db/+* and *db/db* mice in a fed and 4 h fasted state. Values are presented as individual data and mean ± SD. AU indicates arbitrary units. * indicates main effect of genotype ($P<0.05$).

3.5 Discussion

Autophagy is an intracellular recycling process that is modulated by nutrient- and hormonal-mediated signaling pathways. As the plasma insulin and amino acids concentrations and subsequent metabolic responses are disturbed in T2D, it has been hypothesized that autophagy impairments develop in liver and skeletal muscle which may contribute to the development and progression of the disease. In Chapter 2, diet-induced whole-body insulin resistance coincided with autophagy impairments in the liver, whereas autophagy markers in skeletal muscle were largely unaffected. Moreover, in Chapter 2 acute feeding was investigated through oral gavage, which allowed us to specifically control the delivery method (forced vs voluntary) and food composition (CHO vs mixed). However, this approach may not emulate the acute physiological responses that occur in response to habitual food intake. Therefore, the aim of the present study was to use the *db/db* mouse model to investigate the impact of overt type 2 diabetes on autophagy markers and upstream signaling responses in the liver and skeletal muscle in a fed state and following a 4 h fast. In skeletal muscle of diabetic mice, we found an increase in the abundance of both LC3B-I and LC3B-II occurred concurrent with an increase in *Lc3b* gene expression regardless of feeding status. Furthermore, decreases in p62/SQSTM1 were also observed in *db/db* mice, which is indicative of increased lysosomal clearance. Together, these findings strongly indicate an increase in autophagy activity in skeletal muscle of diabetic mice. Interestingly, these findings also occurred alongside a reduction in the rate limiting receptor for chaperone-mediated autophagy, LAMP2A. In contrast, LC3B-I protein abundance and gene expression were decreased in the liver of diabetic mice, indicating a reduction in autophagy capacity in this tissue. Taken together, these results demonstrate that overt type 2 diabetes results in marked, but divergent changes in autophagy markers in the liver and skeletal muscle.

Autophagy in skeletal muscle of *db/db* mice

In skeletal muscle, the increase in both LC3B-I and LC3B-II isoforms in the *db/db* mice compared to *db/+* mice (Figure 3.6 A and B) appears to be driven by upregulation of transcription, given that *Lc3b* gene expression was also higher in *db/db* mice (Figure 3.9). Additionally, these changes in LC3B occurred concurrent with decreases in the autophagosome clearance marker, p62/SQSTM1 (Figure 3.6E), and an increase in the

lysosome marker LAMP1 (Figure 3.8C). Together, these results, suggest that the muscle of diabetic mice had a broad upregulation of autophagosome turnover across transcription, autophagosome formation and autophagosome clearance in the lysosome.

Our findings in skeletal muscle are in line with previous studies that have used alternative diabetic rodent models. Increases in LC3B-II and LC3B puncta determined by immunofluorescence have been reported in muscle of streptozocin-induced diabetic rodent models (227), along with and reductions in the degradation marker p62/SQSTM1 (228), strongly indicating higher autophagy activity in skeletal muscle of diabetic rodents when compared to controls. However, contrary to our results, Tam, *et.al* found that skeletal muscle of *db/db* mice displayed significant decreases in LC3B-II/LC3B-I ratio, along with increases in in p62/SQSTM1, when compared the control group (229), suggesting autophagy suppression in skeletal muscle of diabetic mice. However, LC3B-II and LC3B-I abundance were not reported which makes direct comparisons with the current study difficult (229).

Although we do not have a measure of muscle mass in the current study, decreased muscle mass, as well as reduced muscle force are commonly reported diabetic complications in *db/db* mice (227, 229) and in humans with type 2 diabetes (230). In humans, it is thought that profound insulin resistance induces atrophy signalling in skeletal muscle. Typically in insulin resistant muscle from humans, the insulin-Akt pathway is impaired (231) leading to increased activity of FoxO transcription factors. This increases the transcription of genes involved in muscle atrophy, such as muscle RING finger 1 (MuRF1) and Atrogin-1 (232). In rodents, this muscle wasting phenotype occurs alongside elevated protein degradation and activity of the proteasome system, determined in *ex vivo* skeletal muscle by the rate of tyrosine release into the media and the proteasome chymotryptic-like activity (233). Given that autophagy plays a fundamental role in protein degradation, the increase in macroautophagy observed in our study suggests a broad upregulation of protein breakdown pathways in diabetic skeletal muscle. These findings contrast with the findings in Chapter 2, where diet-induced whole-body insulin resistance alone had no impact on muscle autophagy markers suggesting that the changes observed in this study are due to the diabetic condition, rather than obesity per se.

To explore the mechanisms behind the upregulation of macroautophagy, we investigated the upstream signaling events regulating autophagy gene expression. The transcription

factors forkhead box O3 (FoxO3) and transcription factor EB (TFEB) are considered master regulators of autophagy induction (83, 234). Upon activation, they upregulate the expression of key autophagy-related genes, including *Lc3b* (235), as well other genes encoding autophagy proteins, such as ATG7 (83, 236) which is critical to autophagy induction, given its role in mediating LC3B-I lipidation (237). While FoxO3 activity and its translocation to the nucleus is inhibited by Akt phosphorylation (238), TFEB translocation to the nucleus and therefore, its activity is inhibited by p-mTOR^{S2448} levels (107). We observed significantly reduced absolute abundance of p-mTOR^{S2448} in the muscle of *db/db* mice (Figure 3.7F), which could initiate increased autophagy gene transcription via promotion of TFEB nuclear translocation. Future work should investigate whether elevated nuclear translocation of TFEB or FoxO3 explains the differences in autophagy gene expression in *db/db* muscle compared to control mice.

It is relevant to note that the reduction in p-mTOR^{S2448} in the muscle of *db/db* mice was driven by reductions in total mTOR content (Figure 3.7H) as no differences were observed between *db/db* and *db/+* when p-mTOR was expressed as a ratio of total mTOR. It could be relevant to examine downstream markers of mTOR (e.g. p-p70s6K or p-4-EBP1) as a further assessment of mTORC1 activity. Nevertheless, an inverse relationship between mTOR abundance and autophagy activity has been reported previously. Findings by Hwang, et.al (239) in hippocampal CA1 neurons indicate that mTOR itself is an autophagy target, whereby the reduction in mTOR protein in response to global ischemia is prevented by autophagy inhibition. Future studies could explore whether the elevation in autophagy activity in diabetic muscle drives the observed reduction in total mTOR which could have important implications for understanding muscle atrophy in diabetic conditions.

Intriguingly, despite an apparent upregulation of macroautophagy, we found a decrease in the abundance of LAMP-2A in the muscle of diabetic mice (Figure 3.8A). As LAMP-2A is the rate limiting receptor of CMA (148, 240), these results indicate a reduction in CMA capacity in skeletal muscle of diabetic mice. CMA has been relatively well described in the liver, but very little is known about CMA in skeletal muscle and to our knowledge, this is the first time that CMA markers have been studied in skeletal muscle in the context of diabetes. In the liver, inhibition of CMA activity via reductions in LAMP-2A abundance occurs with ageing, due to the relocation of LAMP-2A to specific lipid microdomains in the lysosomal membrane that are targeted by cathepsin A (159).

Interestingly, an increase in markers of macroautophagy, lysosomal markers (34, 209) and the ubiquitin-proteasome system occur when CMA is inhibited in the liver via LAMP-2A knock-down. Studies in cultured cells have shown that the upregulation of other proteolytic systems is able to maintain proteostasis during CMA inhibition (212, 213). While this is the first report of altered CMA capacity in the muscle of a diabetic rodent model, numerous validated CMA target proteins, mainly glycolytic enzymes, such as Aldolase, Enolase, GAPDH, Pyruvate Kinase, are elevated in the muscle from patients with diabetes (241), and we show consistent elevations in protein abundance of the CMA target PLIN2 (Figure 3.8D). These results indicate that defective CMA may play a role in the metabolic and functional defects in skeletal muscle in *db/db* mice and requires further mechanistic follow-up investigations.

Autophagy in the liver of *db/db* mice

In contrast to the observations in skeletal muscle, *Lc3b* gene and LC3B-I protein levels in the liver were lower in the *db/db* mice compared to *db/+* mice which suggests inhibition of gene transcription and potentially, a lower capacity for autophagosome formation (Figure 3.1A). However, these changes did not translate into genotype differences in autophagosome content or autophagosome clearance, as shown by unchanged LC3B-II and p62/SQSTM1 content (Figure 3.1 B and D). These findings are distinctly different to the responses to high fat diet-induced insulin resistance described in Chapter 2 of this thesis, where autophagosome accumulation occurred due to apparent defects in lysosomal clearance. Interestingly, we found a significant increase in LAMP1 in the *db/db* mice indicating an increase in the lysosomal content (Figure 3.4C). Increased macroautophagy activity in the liver has been shown to decrease lysosomal populations (213). Whether the increases in LAMP1 protein levels in the liver of the *db/db* mice are a compensatory response to the decline in *Lc3b* gene transcription and lower autophagy capacity remains to be addressed.

To further understand the mechanisms behind the LC3B-I changes in the liver of the *db/db* mice we assessed key upstream signaling markers regulating autophagy. A higher abundance of p-Akt^{S473} and its downstream target, p-mTOR^{S2448} (Figure 3.2 B and F) were observed in the liver of the diabetic cohort which is likely a function of the hyperinsulinemia measured in these diabetic mice. Taken together, these results typically represent inhibitory cues to autophagy-related gene transcription via the suppression of ULK-1 activation (94), yet no differences were detected in the autophagy

inhibitory site p-ULK-1^{S758} (Figure 3.3A) (94). However, this may be explained by the lack of difference in we p-mTOR^{S2448} when expressed relative to total mTOR abundance (Figure 3.2H). Together, these findings suggest that diabetes downregulates autophagy capacity in the liver at the early stages of autophagy induction, by suppressing the transcription of autophagy-related encoding genes, although understanding the precise mechanisms requires further work.

These results are partly in line with Zhong, *et.al,* where they described significant increases in both inhibitory signals, p-Akt^{S473} and p-mTOR^{S2448}, in the liver of *db/db* diabetic mice compared to the control mice. However, they found significant decreases in LC3B-II/LC3B-I ratio, suggesting a decline in autophagy initiation (242, 243). Furthermore, they also reported decreases in autophagosome number in the diabetic group, evidenced by both immunofluorescence and TEM (242, 243). The two studies by Zhong, et al. only reported LC3B-II/LC3B-I ratio and not the abundance of both LC3B forms individually, so it is difficult to directly compare the data with the results in the present study (242, 243). Additionally, the differences between this study and the findings reported by Zhong and collaborators could partly arise due to differences in the mouse background strain on which the *db/db* model was developed (C57BL/6J vs C57BLKS/J). Zhong and collaborators used *db/db* mutant mice on the C57BLKS/J background and it has been reported that these mice, display severe hyperglycaemia and pancreatic islet atrophy. However, the same *db/db* mutation on the C57BL/6J background used in the current study, display mild diabetes with hyperglycaemia and pancreatic islet hypertrophy (Fontaine, 2016). These metabolic differences may explain the differences observed in autophagy markers between the two mouse models. Furthermore, in contrast to our methods, both studies conducted by Zhong, et al. the muscle samples were centrifuged and only the resulting supernatant was used to determine the abundance of the autophagy markers. It has been reported that protein yield can be significantly impacted by this method, given that a portion of the protein of interest can remain in the discarded pellet (204).

Collectively, these results indicate that although the early autophagy-stage markers seem to be blunted in the liver of diabetic mice (i.e. lower *Lc3b* gene and LC3B-I protein) this did not influence autophagosome content or clearance. It is possible that the reduced autophagy capacity could become apparent under further stress conditions, such as starvation, which is known to substantially upregulate autophagy activity. Under such

conditions of elevated autophagy flux, hepatocytes from the diabetic mice may display a lower ability to initiate autophagosome formation.

The diabetic mice did not display any differences in the measured CMA markers. There is evidence suggesting that CMA alterations occur along with the presence of macroautophagy clearance defects (212). Supporting the latter, in Chapter 2 impairments in macroautophagy clearances in the liver were accompanied with an upregulation in CMA markers. However, in the present study, there was no evidence of clearance impairments, therefore it is unlikely to expect any significant changes in CMA activity when compared to the control group.

Responses to refeeding

Rises in insulin and amino acids following feeding constitute major autophagy inhibitors (74) however, feeding status did not have an impact on any of the markers assessed in the liver (Figure 3.1). While plasma insulin and amino acid concentration were not specifically measured in these samples due to sample availability, the absence of a main effect of feeding on p-Akt^{S473} and p-mTOR^{S2448} indicate that the metabolic differences and subsequent downstream signalling responses between the 4 h fast and fed status were insufficient to elicit any significant changes in hepatic autophagy activity. It is possible that the 4 h fast is insufficient to adequately upregulate autophagy in the liver, considering differences have been reported when rodents underwent a 24 h starvation period (61, 62). In skeletal muscle, the fed *db/+* mice showed activation of insulin signaling in response to feeding, as shown by substantial increases in p-Akt^{T308} (Figure 3.7A), an effect that was significantly blunted in the *db/db* mice (244). However, the activation of the proximal insulin signaling pathway in the fed *db/+* fed mice did not translate into significant activation of the mTOR pathway when assessed through p-mTOR^{S2448}. Similar to the findings in the liver, the results in skeletal muscle indicate that a 4 h fast, nor a fed state had any impact on the abundance of autophagy markers (Figure 3.6). Previous studies have found increases in LC3B in skeletal muscle after fasting periods between 8 h-24 h of duration (90, 245), possibly indicating that a prolonged fasting period (i.e. longer than 4 h) also seems to be required to activate autophagy pathways in rodent skeletal muscle. Yet, little is known about the effect of physiological insulin fluctuations following food consumption, on autophagy markers. To date, this is the first study that has attempted to address this gap in knowledge in both liver and skeletal muscle in the context of diabetes.

3.6 Conclusions

The present study has shown that in a rodent model of diabetes the liver and skeletal muscle have divergent autophagy responses. The upregulation of skeletal muscle macroautophagy and lysosomal markers occur alongside reductions in phosphorylated and total mTOR protein. These findings appear to be part of a broader upregulation of proteolytic activity that likely underlies muscle metabolic dysfunction and muscle atrophy in diabetes. In contrast, there is a reduction in LC3B-I abundance in the liver of T2D mice that does not seem to impact autophagosome abundance or clearance, at least in the fed state and following a 4 h fast. Furthermore, the reduction in LAMP-2A content in skeletal muscle of diabetic mice warrants further investigation to understand its impact on CMA activity and subsequent metabolic outcomes.

Chapter 4

Muscle fibre-type specific autophagy responses following an overnight fast and mixed meal ingestion in human skeletal muscle

4.1 Abstract

Autophagy is an intracellular recycling process sensitive to acute changes in nutrient availability and fundamental in maintaining muscle protein homeostasis. The aim of the present study was to investigate the skeletal muscle fibre-type specific autophagy responses after an overnight fast and following ingestion of a mixed meal in humans.

Twelve overweight, physically inactive and apparently healthy young male volunteers underwent a 3h mixed meal tolerance test following an overnight fast. Blood samples were collected at baseline, 10, 20, 30, 60, 90, 120, 150 and 180 min post meal ingestion. Skeletal muscle biopsies were collected at baseline, 30 and 90 min post meal ingestion. Protein content and gene expression of key autophagy and lysosome markers, and upstream signalling responses were measured in whole muscle and pooled single fibres.

In the fasted state type I fibres displayed lower LC3B-I abundance, higher LC3B-II content, as well as higher LC3B-II/LC3B-I ratio compared to type IIa fibres, indicative of higher autophagy induction in type I fibres. These findings coincided with lower p-Akt^{S473}, but similar p-mTOR^{S2448} abundance, indicating lower inhibitory upstream signalling type I fibres after an overnight fast. Following the mixed meal ingestion there was a reduction in LC3B-II abundance in both whole muscle and both fibre types, indicative of autophagosome reduction with acute feeding. These findings were mirrored by an increase in inhibitory signalling (i.e. p-Akt^{S473} and p-mTOR^{S2448}), with no difference amongst fibre types.

These results demonstrate that autophagy is higher in type I muscle fibres in the fasted state. Autophagy in human skeletal muscle is acutely inhibited in both type I and type IIa fibres by activation of the nutrient and hormonal signalling pathways 90 minutes following the ingestion of a single meal.

4.2 Introduction

Skeletal muscle comprises around 40% of our body mass and features a high level of metabolic flexibility by adapting quickly in response to elevations in energy expenditure and changes in nutrient availability (24). Skeletal muscle proteins display high turnover rates through constantly eliminating dysfunctional intracellular organelles and proteins which provides metabolic substrates and ensures ongoing maintenance of cell function (133). In the fed state, a positive energy balance promotes anabolic processes i.e. protein synthesis, to elicit a positive net protein accumulation (246). In contrast, in the fasted state, a negative energy balance favours catabolic reactions, i.e. protein breakdown, to elicit net protein loss (247). Given that autophagy in skeletal muscle plays a fundamental role in regulating substrate availability for protein synthesis and ATP production, adequate autophagy regulation throughout the feeding and fasting periods is likely important in maintaining muscle homeostasis.

Evidence has shown that the nutrient and hormonal fluctuations that typically occur during periods of fasting and feeding, acutely regulate autophagy activity. Classically, rodent work has used prolonged fasting periods (24 h) to induce autophagy, demonstrated by decreases in LC3B-I abundance, as well as increases in LC3B-II abundance (132, 248) however, similar changes have also been reported with shorter fasting periods (~9.5 h) (90). Moreover, studies in human skeletal muscle from young and physically active males have shown a decrease in autophagy markers thought to be due to lower autophagy induction and reduced LC3B-I lipidation (i.e. lower LC3B-II and lower LC3B-II/LC3B-I ratio) following the ingestion of a mixed meal (101) or a 100 min-euglycemic-hyperinsulinemic clamp after an overnight fast (6). This inhibition of autophagy is likely to be due to independent effects of insulin and amino acids resulting in the activation of the insulin-Akt-mTOR signalling pathway. In turn, the activation of this pathway inhibits the formation of the ULK-1 complex that triggers autophagosome formation (94, 101). It is important to mention that most of the evidence regarding autophagy regulation by fasting and feeding has been conducted in response to prolonged fasting periods and through non-physiological approaches, such as the euglycemic-hyperinsulinemic clamp. The impact of the typical nutrient and hormonal fluctuations occurring with the daily feeding/fasting patterns on autophagy markers in human skeletal muscle is limited.

In rodents, higher autophagy protein expression and basal autophagy flux is higher in oxidative muscle, demonstrated by high LC3B-II/LC3B-I ratio and low p62/SQSTM1 abundance (145). Other studies have reported a greater induction of fasting-induced autophagy in glycolytic fibres (146). In human skeletal muscle, the activation of the insulin signalling cascade in response to a euglycaemic-hyperinsulinemic clamp appear to be similar between fibre types. However, the capacity of the mTOR pathway is reported to be elevated in type II fibres compared to type I fibres. (249, 250). To date all studies exploring autophagy in human skeletal muscle have investigated whole muscle, but none have investigated the muscle fibre-type specific responses.

The aim of the present study was to investigate the muscle fibre-type specific autophagy responses after an overnight fast and following ingestion of a mixed meal in humans by examining autophagy markers in whole muscle and in pooled single muscle fibres. We hypothesize that LC3B-II is higher in type I muscle fibres after an overnight fast, whereas acute feeding leads to decreases in LC3B-II abundance and LC3B-II/LC3B-I ratio in type I, but not in type IIa pooled fibres.

4.3 Methods

Twelve overweight, physically inactive and apparently healthy young men (aged 18-40 years, BMI 25-35 $kg \cdot m^{-2}$) were recruited into the study. Participants were recruited via social media, presentations, digital platforms, and flyers (Appendix 1). Participants' written and informed consent was obtained after an initial individual meeting where the study protocol and associated risks were discussed (Appendix 2). Ethics approval for this study was attained by the University's Human Research Ethics Committee (code: 2017-29).

In order to be included in the study, participants had to meet the following criteria (Table 4.1):

Table 4.1. Inclusion and exclusion criteria for the study

Inclusion criteria	Exclusion criteria
Age: 18 - 40 years	Age: < 18 or > 40 years
Sex: male	Sex: female
Body mass index (BMI): 25-35 $kg \cdot m^{-2}$	BMI < 20 $kg \cdot m^{-2}$or > 35 $kg \cdot m^{-2}$
Physically inactive*	Medical history of metabolic diseases (e.g. type 2 diabetes), active smoking, thyroid, renal, cardiovascular and/or psychiatric diseases.

* according to self-report daily activity descriptions

Pre-screening

Participants were asked to fill in a medical questionnaire (Appendix 3) to identify any contraindications to take part in the study and were screened to rule out the incidence of impaired fasting glucose and type 2 diabetes (T2DM) via a 2 h oral glucose tolerance test (OGTT), according to the following criteria: fasting plasma glucose ≤7.0 mmol/l (126 mg/dl) or 2 h-plasma glucose ≤ 11.1 mmol/l (200 mg/dl) (251). Participants were asked to arrive at the laboratory in the morning after a 10 h-overnight fast, where they were

asked to consume a 75 g oral glucose load (GlucoScan, Carbonated Glucose Draught, made for Daniels Making Healthcare Safer, Australia) and blood glucose levels were assessed via finger prick blood sample and glucometer (Accu-Check, Roche, NSW, and Australia) at baseline and 10, 20, 30, 60, 90 and 120 min post-ingestion.

Experiment

For those participants that were eligible for inclusion into the study following the OGTT, arrived in the laboratory on one morning (between 6-8 am) following a 10 h-overnight fast. Anthropometric data, such as height (m), body mass (kg) and BMI ($kg \cdot m^{-2}$) were assessed (Tanita BC-418 Pro Segmented Body Composition Analyzer, Shanghai, China). A cannula (20 gauge, cat.no. 5066, Optiva® I.V. Catheter Radiopaque, Smiths Medical Australasia, Suite 2.03, NSW, Australia) was inserted into an antecubital vein and two resting blood samples (5 ml) were taken 10 min apart after which a resting muscle biopsy was taken (see section skeletal muscle sample collection below). Upon completion of the muscle biopsy, the participants were given a standardized mixed meal (147), consisting of a 75 g glucose drink and an egg and cheese omelette (1 egg beaten and 70 g of shredded mozzarella cheese; total of 582 kcal: 313 kcal carbohydrates (78 g), 158 kcal fat (18 g) and 87 kcal protein (22 g). Participants were instructed to finish their meal in less than 10 min and to remain in a rested seated position for 180 min (3 h) with blood samples collected at 10, 20, 30, 60, 90, 120, 150 and 180 min post meal ingestion. After every blood collection the catheter was flushed with 1 ml sterile 0.9 % saline solution (Fresenius Kabi, NSW, Australia) to avoid blood clotting.

The blood collected at each time point was either placed in EDTA or lithium-heparin coated tubes. Following centrifugation at 4,000 rpm for 5 min at 4 °C, plasma was removed and stored at -20°C for later analyses. The plasma collected in the EDTA tubes was used to determine insulin, C-peptide and free fatty acids (FFA), while the plasma collected in the lithium heparin tubes was used to determine glucose (see plasma analyses below).

Muscle biopsies were collected from the *vastus lateralis* using a Bergström needle modified with suction (252). With the participant laying supine the skin area was anaesthetised with ~2-3 ml 1% xylocaine without adrenaline (AstraZeneca Pharmaceuticals, UK) under aseptic conditions. The biopsy needle was advanced into

the skeletal muscle through a 0.5 cm incision in the skin. Next, suction was applied, and skeletal muscle tissue was drawn (approximately 100-200 mg). The incision was then closed with Steri-Strips® (cat. no. R1546, 3M, Neuss, Germany) and covering with Tegaderm® and gauze (cat. no. R1546, 3M, Neuss, Germany) and a compression bandage was applied to avoid excessive bleeding (253). Upon biopsy collection, the muscle sample (~200 mg) was immediately frozen in liquid nitrogen and stored at – 80 °C until later processing and analyses (see 'Single muscle fibre isolation', 'Fibre typing of single muscle fibres', 'Immunoblotting' and 'Gene expression analyses' sections below).

Analyses

Plasma Analyses

Plasma insulin and C-peptide were measured by ELISA (Millipore, St Louis, MO, USA) and plasma free fatty acids were determined with a non-esterified fatty acid (NEFA-C) kit (Wake Pure Chemical Industries, Ltd., Osaka, Japan), all according to manufacturers' instructions.

Plasma glucose concentrations were determined via a glucose oxidase assay. A total of 10µl of each glucose standard (0, 1.25, 2.5, 5, 10 and 12.5 mmol/L) and sample was pipetted, in duplicate, into a 96-well plate. 250µl of glucose assay buffer [250µL 0.12M phosphate buffer (pH 7.0), 2µL/mL 250mg 4-aminoantipyrine/mL phosphate buffer (no phenol), 1µL/mL 5.78mg peroxidase (277U/mg)/mL phosphate buffer (no phenol) and 5µL/mL 20mg glucose oxidase (100U/mg)/mL phosphate buffer (no phenol)] was then added to each well. The plate was covered and then incubated for 25 minutes at 37°C, before being read in a spectrophotometer (xMark™ Microplate Spectrophotometer, Bio-Rad, California, USA) at a 490nm wavelength.

Single muscle fibre isolation

Approximately 10 mg of frozen muscle sample was transferred into a new 2 ml microtube and the lid was pierced prior to freeze-drying (Alpha 2-4 LD plus, Martin Christ Gefriertrocknungsanlagen GmbH, Osteröde am Harz, Germany). The samples were placed in the freeze dryer at -80 °C for at least 30 min, before starting the 48-h drying

process (pressure= 0.0016 mbar). Upon completion of the freeze-drying process, the samples were transferred into an air-tight container with desiccant and stored at -80 °C until further analyses. Single muscle fibres (25-30 fibres per time point) were isolated with fine tweezers (cat.no F6521, Merck KGaA, Darmstadt, Germany) under a stereoscopic microscope (SMZ745T, Nikon, South Australia, Australia) (see figure 4.1). Each fibre was individually stored in 10 µl of solubilizing buffer (see details on Chapter 2) and vortexed at room temperature every 15 min for one hour. Samples were then stored at -80 °C until further analyses.

Fibre typing of single muscle fibres

Skeletal muscle fibre type was assessed through dot blotting as recently described (254). After activating polyvinylidene fluoride (PVDF) membranes in a 95 % methanol solution for 5 min, 1 µl of each sample was loaded onto membranes and left to dry. Membranes were then blocked with 5 % skim milk in tris-buffered saline Tween 20 (TBST) (0.05% Tween-20, 50 mM Tris, 150 mM NaCl, pH 7.6) for an hour at room temperature after which they were incubated with myosin heavy chain IIa primary antibody (1 in 200, MHC IIa, clone A4.74, Developmental Studies Hybridoma Bank [DSHB]) for 1h at room temperature. Subsequently, membranes were rinsed with TBST and then were incubated with horseradish peroxidase (HRP)-conjugated goat anti-mouse IgG (1 in 20,000, cat. no. 31430, Thermo Fischer Scientific) for 1 h at room temperature. Chemiluminescent images were detected with the Chemidoc XRS+ imaging system (Bio-Rad, California, USA) following exposure to Clarity© chemiluminescent reagent (Bio-Rad, California, USA). The membranes were imaged (see image 4.2) using Image Lab™ software (Bio-Rad, California, USA). The membranes were then stripped for 10 min (Restore™ PLUS Western blot Stripping Buffer, cat. no. 46430, Thermo Scientific, Massachusetts, USA) and were incubated with MHC I primary antibody (1 in 200, clone A4.80, DSBH) for 1h at room temperature and subsequently incubated with HRP-conjugated goat anti-mouse IgM secondary antibody (1 in 20,000 cat.no. sc-2064, Santa Cruz Biotechnology, Texas, USA) and imaged as described above.

Muscle fibre type was classified based upon the presence of a single MHC isoform and single fibres were pooled together according to their fibre type (either MHC I or MHC IIa; MCHIIx was not probed) (Figure 4.2). Fibres that stained for both MHC isoforms were

considered hybrid and the ones not stained by either MHCI or MHCIIa were assumed to be type IIx. Neither hybrid nor type IIx fibres were used for the analyses.

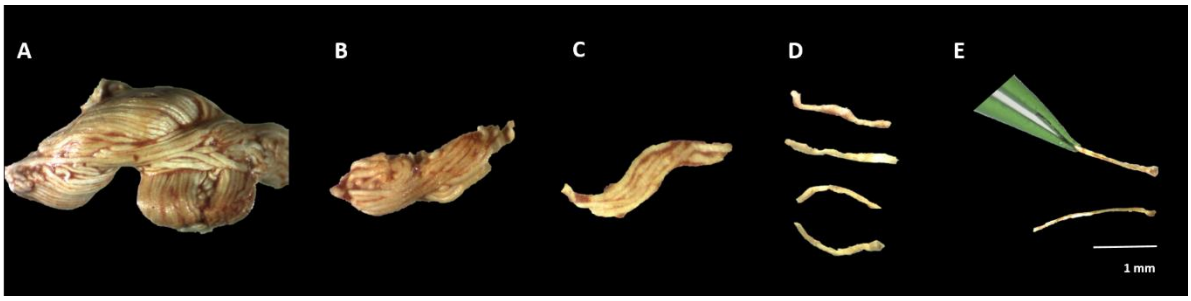

Figure 4.1. Muscle single fibre isolation. (A) Freeze-dried whole muscle sample (B, C). Further separation into smaller portions of whole muscle. (D, E) Isolated single fibres ready to be transferred in solubilizing buffer.

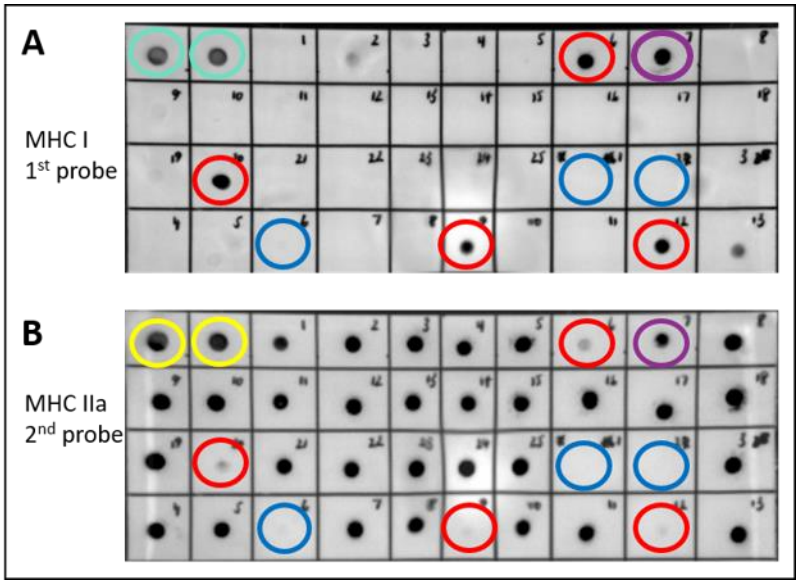

Figure 4.2. Fibre typing using the dot blotting technique. Based on MHC isoform expression (A. MHC I; B. MHC IIa), single fibres were characterised as type I (red circles) or type IIa (no circles). Some dot/samples remained negative after the two probes (blue circles, assumed to be type IIx fibres), while one sample was positive for both probes (purple circles; assumed to be hybrid) and classified as a hybrid single fibre. Green and yellow circles indicate the positive controls (whole-muscle crude homogenates).

Immunoblotting

Whole muscle samples were cryo-sectioned at -20 °C, placed into 50 µl of solubilizing buffer and left to denature for 1 h at room temperature as described in detail in Chapter 2. Both whole muscle and pooled single fibre samples were loaded onto a stain-free gel after one freeze-thaw cycle. A 4-point standard calibration curve consisting of a mix of every sample (0.8, 1.6, 3.2, 6.4 µl into a well), was also loaded on each gel to ensure that the amount of protein fell within the linear range of detection (203). The following primary antibodies were used to assess autophagy activity and associated signaling responses in whole muscle: anti-Akt (cat. no. 9272S), anti-p-Akt (S473; cat. no. 9271S), anti-mTOR (cat. no. 2972S), anti-p-mTOR (S2448; cat. no. 2971S) all purchased from Cell Signaling (Massachusetts, USA), as well as anti-LAMP-2A (cat. no. 51-2200, Thermo Fisher Scientific, Massachusetts, USA), anti-LAMP2 (cat.no. AP1824d, Abgent, California, USA), anti-Hsc70 (cat. no. SMC-151, StressMarq Biosciences, British Columbia, Canada), anti-LAMP1 (cat. no. 1D4B, Developmental Studies Hybridoma Bank, Iowa, USA), anti-p62/SQSTM1 (cat. no. ab56416), anti-OXPHOS Human WB antibody cocktail (cat. no. ab110411) both purchased from Abcam (Cambridge, UK) and anti-LC3B (cat. no. L7543, Sigma Aldrich, Missouri, USA). To assess autophagy activity in single fibres, primary antibodies targeting LC3B, p62/SQSTM1, p-mTOR^{S2448}, total mTOR, p-Akt^{S473} and total Akt were used (as above).

Gene expression analyses

Skeletal muscle RNA was extracted a described in Chapter 2. Whole muscle (10 mg) was homogenised in 1 ml of TriZol. Pre (0 min) and post meal (90 min) time points were used to determine the effect of the mixed meal ingestion on gene expression as described in Chapter 2. The following genes were analysed: *Lc3b, Gabarapl1, p62/Sqstm1, Lamp2a* and *Hsc-70* (Table 4.2).

Table 4.2. PCR primer sequence information

Gene name	DNA sequences (5' to 3')
Lc3b	*Forward*: CAGAGAGTCCCTGGTTCCTG *Reverse:* GAGGGACAACCCTAACACGA
Gabarapl1	*Forward:* GGAGGGGTAATGGTGGAGTT *Reverse:* TGATGTGCCTCCTACCTTCC
p62/Sqstm1	*Forward:* CTGTATTGGGAAAGGGCTCA *Reverse:* GGGGGTCCAAAGACTTCAAT
Hsc-70	*Forward:* GGAGGTGGCACTTTTGATGT *Reverse:* AGCAGTACGGAGGCGTCTTA
Lamp2a	*Forward:* GGTTAATGGCTCCGTTTTCA *Reverse:* TGTTCTCGTCCAGCAGACAC

Statistical analyses

An *a priori* power calculation was performed on data from previous evidence investigating LC3B-II/LC3B-I ratio changes in human skeletal muscle before and after the ingestion of a meal (101). This data indicates the LC3B-II/LC3B-I ratio in the fasted state was 1.0 ± 0.5 arbitrary units (mean ± SD), while the LC3B-II/LC3B-I ratio in the fed state was 0.5 ± 0.3 arbitrary units (mean ± SD). This gives an effects size of 1.14, meaning that a total of n = 11 would give an expected power of 0.9. There is no existing data on the effect of a meal on autophagy markers in human single muscle fibres. Therefore, n=12 was chosen for the current study.

All data were expressed as individual data and means ± SD. A one-way repeated measures ANOVA was performed to identify differences between time points in plasma responses, as well as in whole muscle. A paired t-test was performed to determine baseline differences between muscle fibre types. A two-way repeated measures ANOVA was performed to identify significant main effects of muscle fibre types and time in response to feeding. When significant interactions were detected, further post-hoc analyses were conducted using the Bonferroni correction. $P<0.05$ was considered as statistically significant.

4.4 Results

Mixed meal tolerance test

Twelve young males (age: 25 ± 6 years; height: 1.82 ± 0.07 m; body mass: 97.43 ± 11.65 kg; BMI: 29.42 ± 2.52 $kg \cdot m^{-2}$; fasting plasma glucose: 5.4 ± 0.78 mmol/l; fasting plasma insulin: 9.9 ± 6.0 µIU/l) completed the present study. Plasma concentrations of glucose, insulin C-peptide and FFA over a 3 h-mixed meal tolerance test are shown in Figure 4.3. Plasma glucose peaked 30 min post meal ingestion and was higher at 20 min and 30 min post meal ingestion when compared to baseline measurements (Figure 4.3A, $P<0.05$). Plasma free-fatty acids were significantly lower than baseline values from 60 min post meal ingestion onwards (Figure 4.3C, $P<0.05$). Plasma insulin and C-peptide were higher compared to baseline values at every time point (Figure 4.3 B and D, $P<0.05$) and both peaked 60 min post meal ingestion.

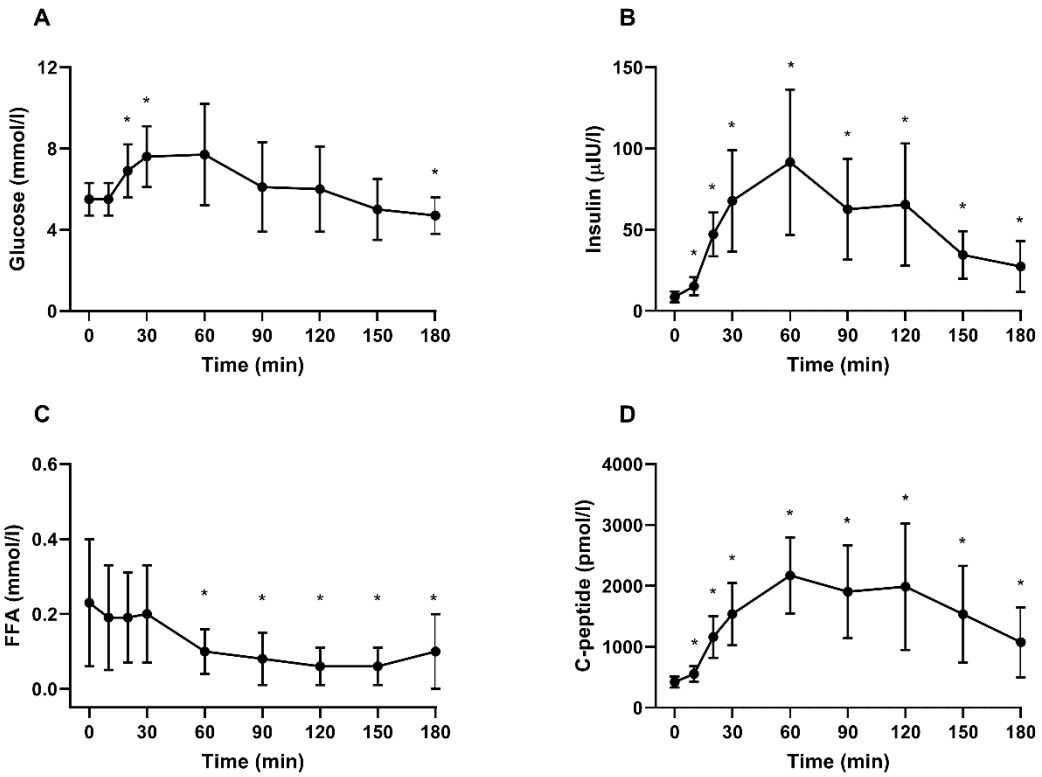

Figure 4.3. Plasma glucose (A), insulin (B), free fatty acids (FFA) (C) and C-peptide (D) during a 3 h-mixed meal tolerance test (n=12). Values are presented as means ± SD. * indicates *P*<0.05 compared to 0 min.

Autophagy in skeletal muscle

Fasting measurements on the autophagy markers in pooled single fibres are summarised in Figure 4.4. LC3B-I abundance was significantly lower in type I fibres (Figure 4.4A, $P<0.05$), LC3B-II protein content was higher when compared to type IIa fibres (Figure 4.4B, $P<0.05$). Additionally, LC3B-II/LC3B-I ratio was increased in type I fibres (Figure 4.4C, $P<0.05$) whereas the abundance of p62/SQSTM1 was not different between type I and type IIa pooled fibres at baseline (Figure 4.4 D-F, $P>0.05$).

Additionally, fasting markers of the insulin-Akt-mTOR pathway in single pooled fibres are summarised in Figure 4.5. Total Akt and absolute p-Akt^{S473} abundance were not different between fibre types (Figure 4.5 A and B, $P>0.05$) however, p-Akt^{S473} was significantly lower in type I fibres when expressed relative to total Akt content (Figure 4.5 C, $P<0.05$). No differences between fibre types were found in total mTOR, p-mTOR^{S2448} abundance or when p-mTOR^{S2448} was expressed relative to total mTOR content (Figure 4.5 D-F, $P>0.05$).

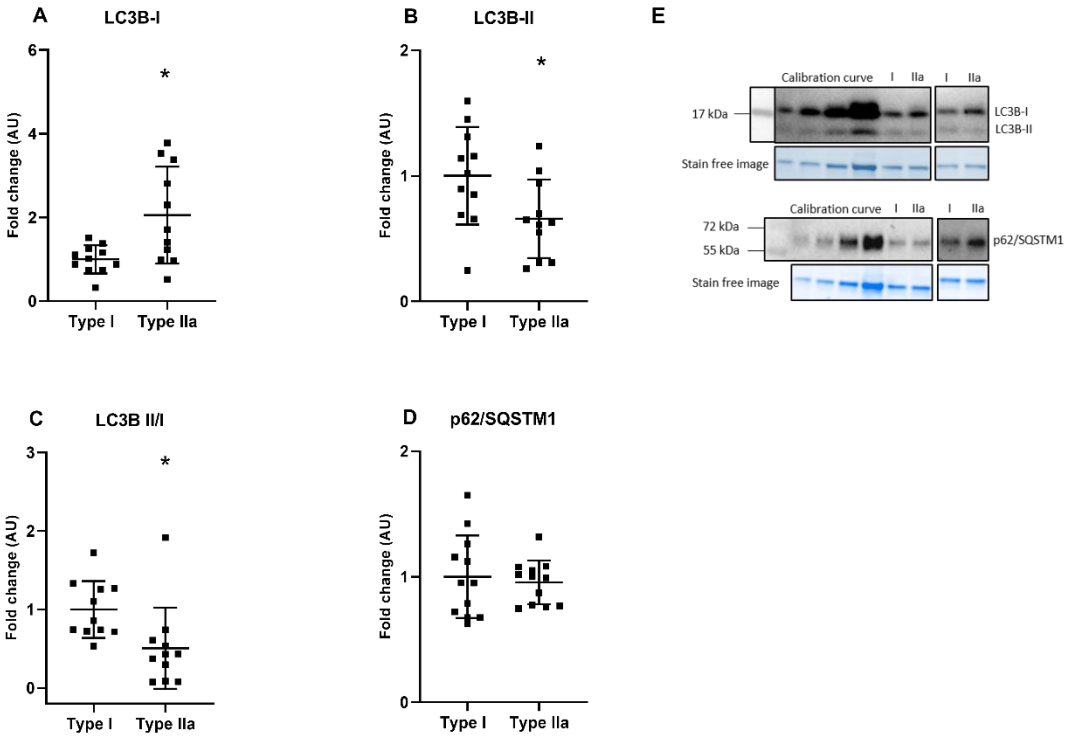

Figure 4.4. Macroautophagy markers in human skeletal muscle (*vastus lateralis)* at baseline (0 min) between type I and type IIa pooled single fibres (n=12) including LC3B-I (A), LC3B-II (B), LC3B-II/LC3B-I ratio (C), p62/SQSTM1 (D). Values are presented as individual data and means ± SD. AU indicates arbitrary units. Stain free images providing an example of total protein loading and corresponding representative blots are shown (E). * indicates *P*<0.05 vs type I fibres. Representative blots for each protein were taken from the same membrane and accompanying stain free images were taken from the same gel. Non-contiguous portions of the same blots, with the same exposure time are separated with spaces.

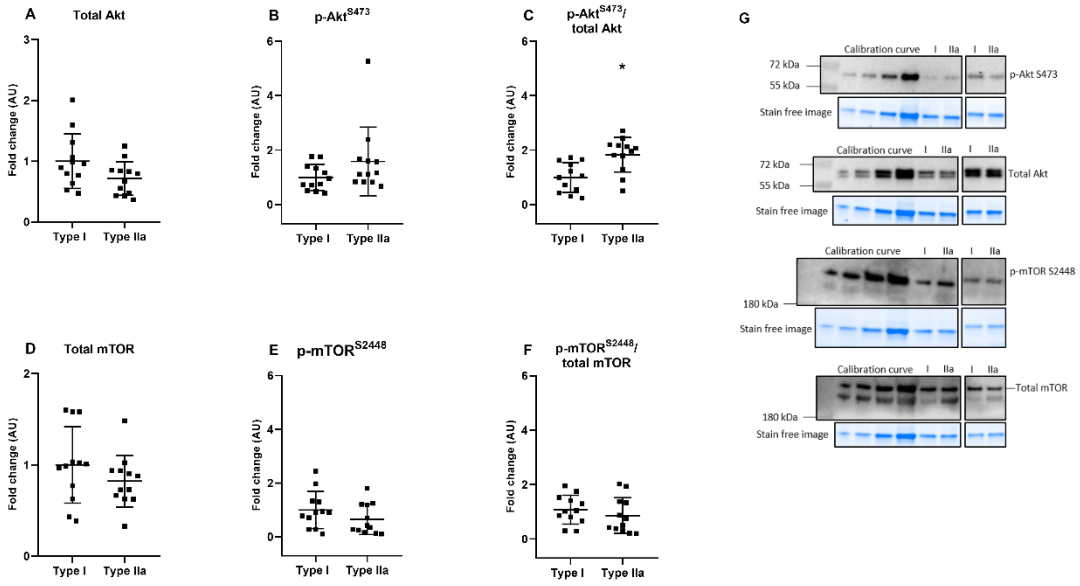

Figure 4.5. Abundance of signaling markers regulating autophagy in human skeletal muscle *(vastus lateralis)* at baseline (0 min), between type I and type IIa pooled single fibres (n=12) including total Akt (A), p-Akt^{S473} (B), p-Akt^{S473} relative to total Akt (C), total mTOR (D), p-mTOR^{S2448} (E), and p-mTOR^{S2448} relative to total mTOR (F). Values are presented as individual data and means ± SD. AU indicates arbitrary units. Stain free images providing an example of total protein loading and corresponding representative blots are shown (G). * indicates *P*<0.05 vs type I fibres. Representative blots for each protein were taken from the same membrane and accompanying stain free images were taken from the same gel. Non-contiguous portions of the same blots, with the same exposure time are separated with spaces.

The abundance of macroautophagy markers in response to the ingestion of a mixed meal is summarised in Figure 4.6. When macroautophagy markers were assessed in whole muscle, no main effects of feeding in the abundance of non-lipidated form of LC3B, LC3B-I, were observed (Figure 4.6A, $P>0.05$). However, LC3B-II abundance was significantly reduced at 90 min compared to baseline and 30 min values (Figure 4.6C, $P<0.05$). Furthermore, feeding did not have an impact LC3B-II/LC3B-I ratio (Figure 4.6E, $P>0.05$) or p62/SQSTM1 protein abundance (Figure 4.6G, $P>0.05$) in whole muscle. In pooled single fibres, the ingestion of a mixed meal did not impact the abundance of LC3B-I (Figure 4.6B, $P>0.05$), however, there was a main effect of fibre type, with LC3B-I abundance significantly lower in type I fibres compared to type IIa fibres (Figure 4.6B, $P<0.05$). In contrast, there was a main effect of meal ingestion with a reduction in LC3B-II abundance following feeding, (Figure 4.6D, $P<0.05$). There was a tendency for a main effect of muscle fibre type on LC3B-II which failed to reach statistical significance ($P = 0.09$). Additionally, there was a main effect of fibre type on the LC3B-II/LC3B-I ratio, ($P>0.05$) with lower values in type IIa fibres, as well as a main effect of feeding ($P<0.05$) with a reduction in the ratio following feeding (Figure 4.6F). Similar to the results in whole muscle, there was no main effects of either meal ingestion or fibre type on p62/SQSTM1 abundance in pooled single fibres (Figure 4.6H, $P>0.05$).

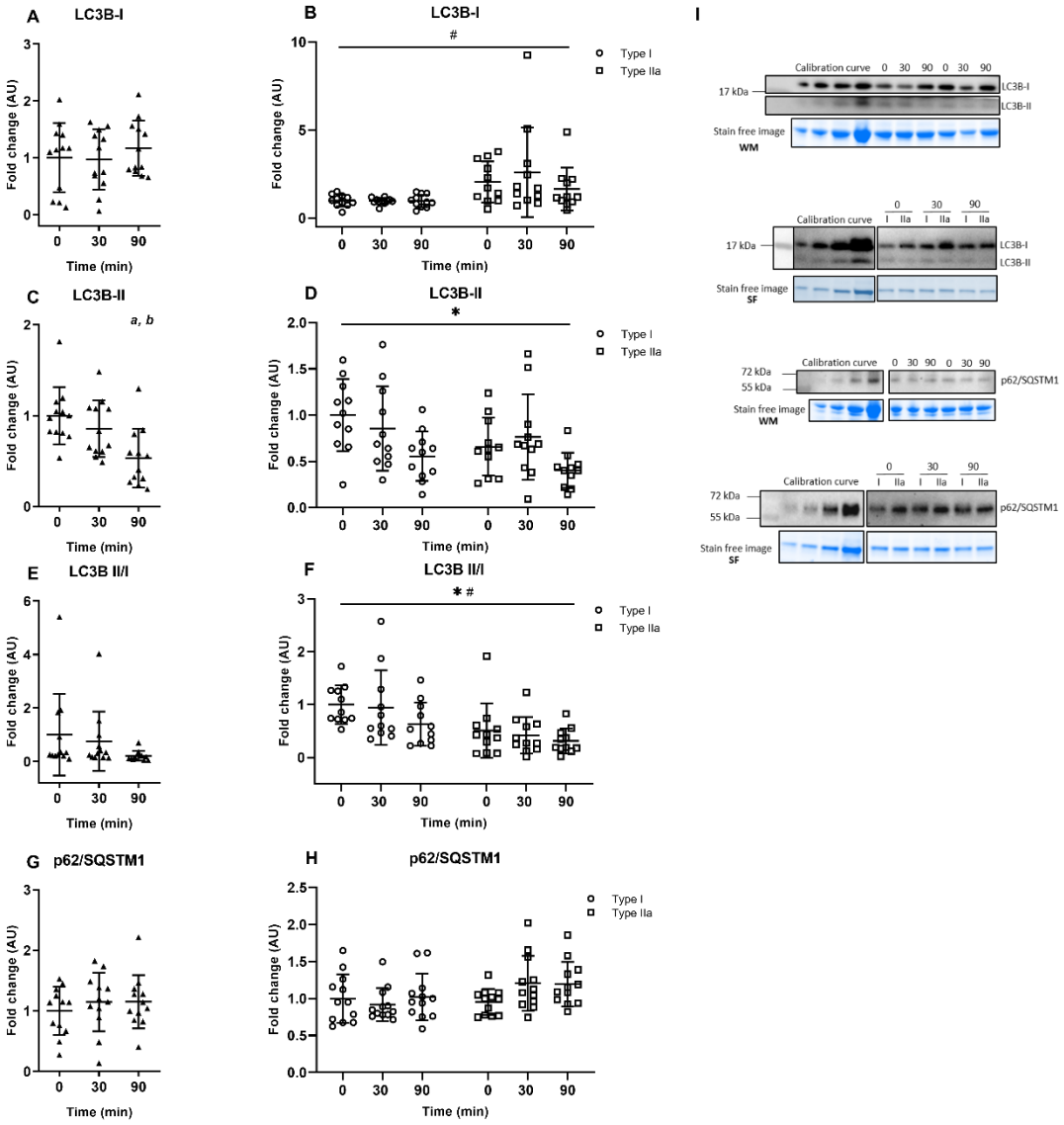

Figure 4.6. Macroautophagy markers in human skeletal muscle (*vastus lateralis)* at baseline (0 min), 30 min and 90 min after a mixed meal ingestion (n=12). Abundance of LC3B-I (A), LC3B-II (C), LC3B-II/LC3B-I ratio (E) and p62/SQSTM1 (G) in whole muscle. Abundance of LC3B-I (B) and LC3B-II (D), LC3B-II/LC3B-I ratio (F) and p62/SQSTM1 (H) in type I and type IIa muscle fibres. Values are presented as individual data and means ± SD. AU indicates arbitrary units. Stain free images providing an example of total protein loading and corresponding representative blots are shown (I). * indicates main effect of feeding (P<0.05); # indicates main effect of fibre type (P<0.05); [a] indicates P<0.05 vs 30 min; [b] indicates P<0.05 vs 0 min. WM: whole muscle; SF: pooled single fibres. Representative blots for each protein were taken from the same membrane and accompanying stain free images were taken from the same gel. Non-contiguous portions of the same blots, with the same exposure time are separated with spaces.

Given that macroautophagy is regulated by the insulin-Akt-mTOR pathway, we investigated key markers of this pathway in whole muscle and pooled single fibres (Figure 4.7 and 5.8). In whole muscle, the abundance of p-Akt^{S473} was higher 30 min after the ingestion of a mixed meal (Figure 4.7A, P<0.05), with no impact on the abundance of total Akt (Figure 4.7C, P>0.05). Abundance of p-Akt^{S473} at 30 min also remained higher compared to baseline values when corrected to total Akt protein content (Figure 4.7F, P<0.05). When assessed in pooled single fibres, p-Akt^{S473} increased with the mixed meal ingestion (Figure 4.7B, P<0.05), regardless of fibre type, while feeding status did not impact Akt total protein abundance (Figures 4.7E, P>0.05). However, total Akt abundance was higher in type I fibres, regardless of feeding status (Figure 4.7D; P<0.05). When p-Akt^{S473} was corrected to its respective total protein abundance the main effect of feeding described in whole muscle was replicated (Figure 4.7F, P<0.05). Furthermore, a higher abundance of p-Akt^{S473} relative to total Akt was found in type IIa fibres when compared to type I fibres (Figures 4.7F, P<0.05).

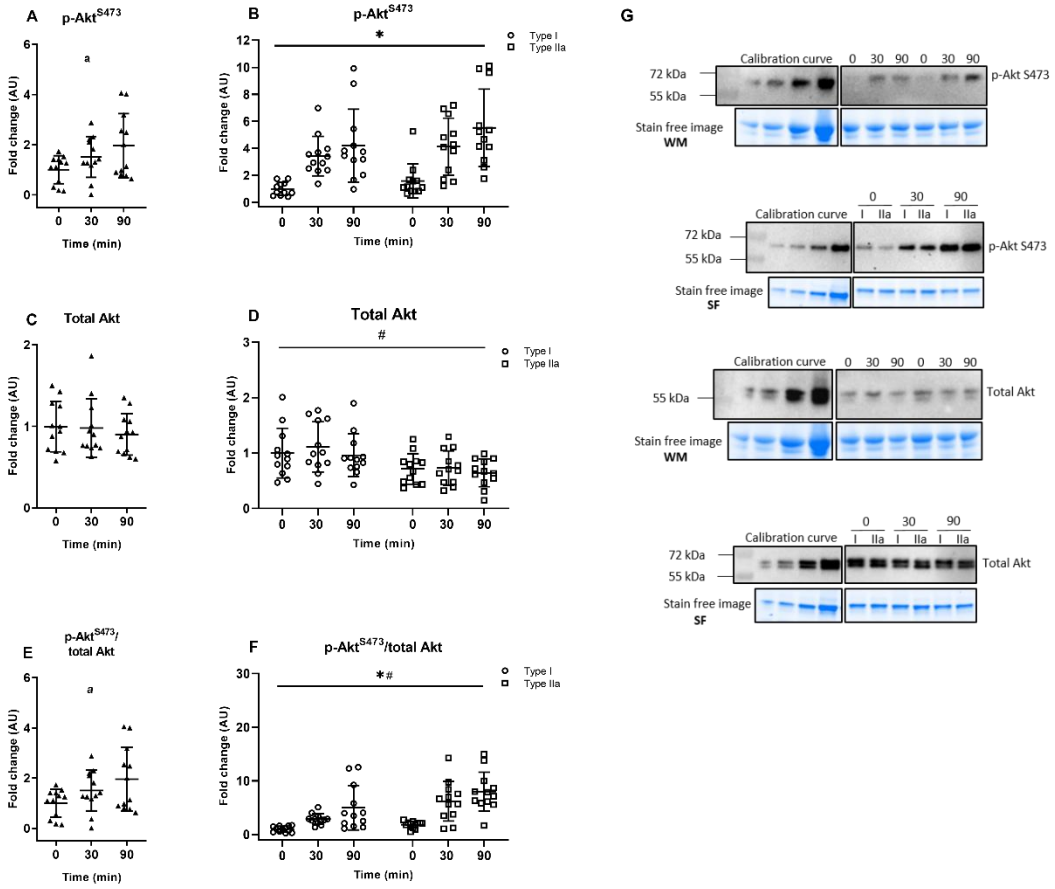

Figure 4.7. Abundance of signalling markers regulating autophagy in human skeletal muscle *(vastus lateralis)* at baseline (0 min), 30 min and 90 min after a mixed meal ingestion (n=12) including p-Akt^{S473}(A), total Akt (C), p-Akt^{S473} relative to total Akt (E) in whole muscle and p-Akt^{S473}(B), total Akt (D), p-Akt^{S473} relative to total Akt (F) in type I and type IIa pooled single fibres. Values are presented as individual data and means ± SD. AU indicates arbitrary units. Stain free images providing an example of total protein loading and corresponding representative blots are shown (G). * indicates main effect of mixed meal (P<0.05). * indicates main effect of feeding (P<0.05); # indicates main effect of fibre type (P<0.05); [a] indicates P<0.05 vs 0 min. WM: whole muscle; SF: pooled single fibres. Representative blots for each protein were taken from the same membrane and accompanying stain free images were taken from the same gel. Non-contiguous portions of the same blots, with the same exposure time are separated with spaces.

In whole muscle, p-mTOR^{S2448} abundance was higher 90 min after a mixed meal ingestion when compared to baseline and the 30 min time points (Figure 4.8A, *P*<0.05), with no significant changes in total mTOR protein (Figure 4.8B, *P*>0.05). The abundance of p-mTOR^{S2448} also displayed a tendency to increase when corrected to total mTOR content which bordered statistical significance (Figure 4.8C, P=0.06). When assessed in pooled single fibres, p-mTOR^{S2448} increased with the mixed meal ingestion (Figure 4.8B, *P*<0.05), regardless of fibre type, and feeding status did not impact mTOR total protein abundance (4.8D, *P*>0.05). Although not statistically significant, total mTOR content tended to be higher in type I fibres, regardless of feeding status (Figure 4.8D, P=0.07). The main effect of feeding was also observed when p-mTOR^{S2448} was corrected for its respective total protein abundance (Figure 4.8F, *P*<0.05).

We also investigated key CMA and general lysosomal content markers in whole muscle (Figure 4.9). The ingestion of a mixed meal did not influence the abundance of the CMA markers, LAMP-2A or Hsc-70 (Figure 4.9 A and B, *P*>0.05). No changes were observed in either LAMP2 or LAMP1 abundance (Figure 4.9 C and D, *P*>0.05).

The expression levels of key autophagy genes at baseline and 90 min post meal ingestions was also assessed and the results are summarised in figure 4.10. Feeding had no impact on *Lc3b, Gabarapl1, p62/Sqstm1, Lamp2a* or *Hsc-70* genes (*P*>0.05) when compared to baseline levels.

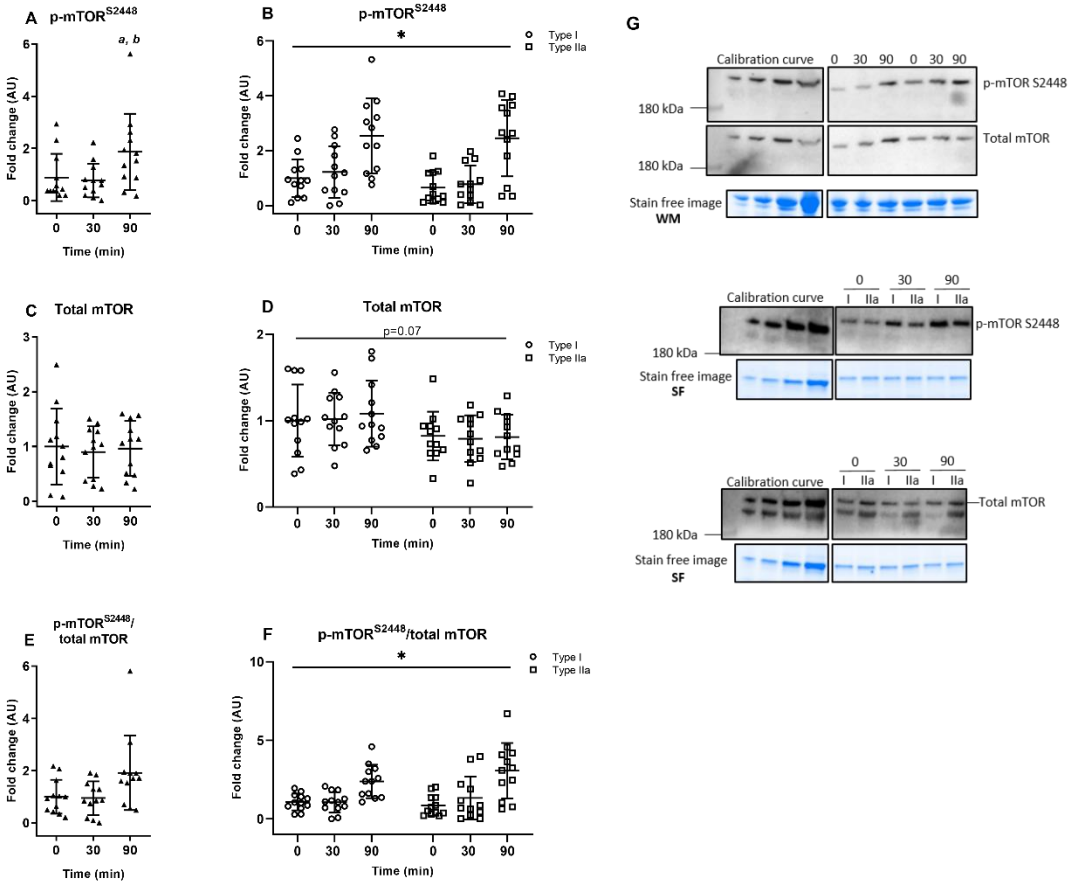

Figure 4.8. Abundance of signalling markers regulating autophagy in human skeletal muscle *(vastus lateralis)* at baseline (0 min), 30 min and 90 min after a mixed meal ingestion (n=12), including p-mTOR^{S2448} (A), total mTOR (C) and p-mTOR^{S2448} relative to total mTOR (E) in whole muscle and p-mTOR^{S2448} (B), total mTOR (D) and p-mTOR^{S2448} relative to total mTOR (F) in type I and type IIa pooled single fibres. Values are presented as individual data and means ± SD. AU indicates arbitrary units. Stain free images providing an example of total protein loading and corresponding representative blots are shown (G). * indicates main effect of mixed meal (P<0.05). * indicates main effect of feeding (P<0.05); [a] indicates P<0.05 vs 0 min; [b] indicates P<0.05 vs 30 min. WM: whole muscle; SF: pooled single fibres. Representative blots for each protein were taken from the same membrane and accompanying stain free images were taken from the same gel. Non-contiguous portions of the same blots, with the same exposure time are separated with spaces..

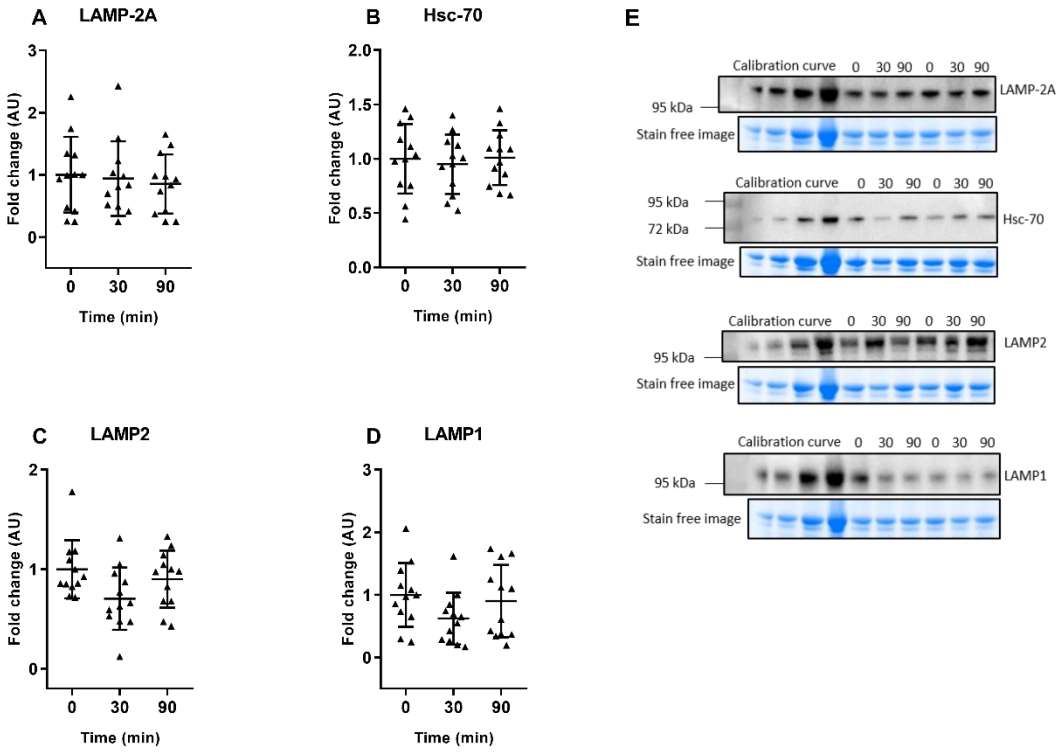

Figure 4.9. Chaperone-mediated autophagy and lysosomal content marker abundance in human skeletal muscle (*vastus lateralis)* at baseline (0 min), 30 min and 90 min after a mixed meal ingestion (n=12). LAMP-2A (A), Hsc-70 (B), LAMP2 (C) and LAMP1 (D) in whole muscle. Values are presented as individual data and means ± SD. AU indicates arbitrary units. Stain free images providing an example of total protein loading and corresponding representative blots are shown (E).

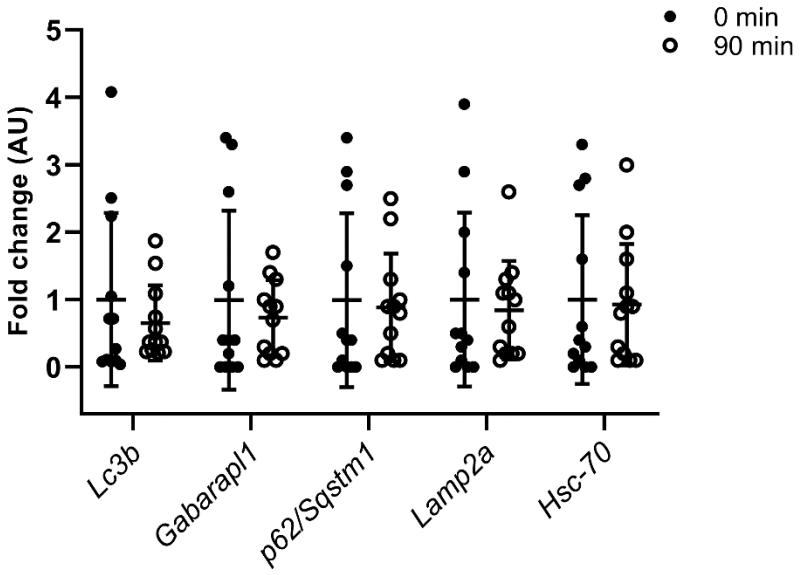

Figure 4.10. Gene expression levels of *Lc3b*, *Gabarapl1* and *p62/Sqstm1, Lamp2a, Hsc-70* in human skeletal muscle (*vastus lateralis)* at baseline (0 min) and 90 min after a mixed meal ingestion (n=12). Values are presented as individual data and means ± SD. AU indicates arbitrary units.

4.5 Discussion

Autophagy is a conserved intracellular process that is key in maintaining cellular homeostasis. It is acutely regulated by nutrient availability via the insulin-Akt-mTOR pathway, where insulin and amino acids independently inhibit autophagy induction. Evidence around the effects of the acute nutrient and hormonal fluctuations due to feeding on autophagy markers in human skeletal muscle is limited. Furthermore, although studies in rodents indicate there are muscle fibre-type differences in autophagy under basal conditions and in response to nutrient availability this has not been examined in human skeletal muscle. Therefore, the aim of this study was to investigate the impact of a mixed meal on key markers of autophagy in whole muscle and pooled single fibres. We found that after an overnight fast, LC3B-I abundance was substantially higher in type IIa fibres, whereas LC3B-II was higher in type I fibres, indicative of greater basal autophagy activity in type I muscle fibres. Despite these differences, ingestion of a mixed meal decreased LC3B-II abundance (Figure 4.5C), indicative of a decline in autophagosome content, in both type I and type IIa muscle fibres. These changes are likely driven by similar activation of upstream inhibitory Akt-mTOR signalling pathways (Figure 4.6 and 4.7).

An important and novel aspect of the current study is the muscle fibre-type specific analysis of key autophagy markers. Following an overnight (~10 h) fast, the abundance of LC3B-I was higher in type IIa fibres (Figure 4.5B), whereas LC3B-II was higher in type I fibres (Figure 4.5D), resulting in higher LC3B-II/LC3B-I ratio in type I muscle fibres (Figure 4.5F). As the abundance of the lysosome degradation marker p62/SQSTM1 was not different between fibre types (Figure 4.5H), these data indicate that the higher abundance of LC3B-II in type I muscle fibres, was due to greater autophagy induction and conversion of LC3B-I into LC3B-II. Our results align with a previous study in mice, where a higher LC3B-II abundance and higher LC3B-II/LC3B-I ratio was found in primarily oxidative muscle (i.e. soleus) when compared to predominantly glycolytic (i.e. plantaris) muscle (145). Although it should be noted that higher autophagy induction, based on higher LC3B-II abundance, has been described in rat plantaris muscle, a primarily glycolytic muscle, in response to prolonged fasting (between 48-72 h) (146).

The mechanisms underlying these fibre type differences in autophagy induction in the fasted state are not immediately clear. There were no fibre type differences in the abundance of upstream signalling proteins in the basal state (Akt, mTOR) (Figure 4.4 E

and F), however, there was a ~2-fold lower phosphorylation of Akt^{S473} in type I fibres (Figure 4.5C), but this did not translate into differences in p-mTOR^{S2448} between fibre types. However, previous work has demonstrated that despite there being no differences in mTOR content between fibres types, type II human muscle fibres have increased abundance of mTOR downstream targets, S6K1 and eEF2. This has been suggested as indicative of a higher capacity in the mTOR pathway with potential impact on mTOR-related processes e.g. protein synthesis, autophagy (250). It would be informative to explore fibre-type specific expression of other autophagy proteins and key signalling proteins regulating autophagy induction to determine whether the entire autophagy machinery and regulatory signalling pathways is expressed or activated in a fibre-type specific manner. Unfortunately, we have been unable to get adequate western blots to examine ULK-1 in human skeletal muscle and the fibre-type specific analysis of other autophagy proteins (e.g. Atg6, Atg7, Atg9, Atg13, BECN1, FoXO3, TFEB) was outside the scope of this thesis. There has also been speculation that greater autophagy induction in type I muscle fibres is reflective of a greater mitochondrial abundance and therefore higher requirement for mitophagy. Indeed, Lira et al (2013) found greater expression of the mitophagy protein BNIP3 in oxidative compared to glycolytic mouse muscle (145). While further work is required to explain the muscle fibre-type differences in autophagy shown here, these findings could be important when interpreting studies examining autophagy in muscle from populations where fibre type shifts occur (e.g. exercise training, ageing, sedentary populations, type 2 diabetes). For example, evidence suggests that the loss of type I muscle fibres observed in diabetic patients is linked to the development and worsening of the existing metabolic derangements (255), whereas long term exercise training promotes fibre type switching with a greater type I fibre phenotype. Therefore, a fibre type specific approach allows the measurement of autophagy markers which could otherwise be driven by fibre type shifts when assessed at the whole muscle level (42).

Given the significant differences in autophagy markers in fasting conditions, it was also relevant to investigate muscle fibre-type specific changes in these markers in response to feeding. In whole muscle and in pooled single muscle fibres, ingestion of a mixed meal significantly reduced LC3B-II protein content with ~50% reductions in LC3B-II occurring 90 min post-meal (Figure 4.5D), suggesting a reduction in autophagosome content. The decline in LC3B-II abundance with feeding is in line with the only other human study to examine the acute impact of feeding on autophagy in human muscle (101) and is in

agreement with animal studies that have shown substantial reductions in LC3B-II abundance in the fed versus fasted state (90). The reduction in LC3B-II abundance with feeding along with no changes in *Lc3b* gene expression (Figure 4.9) or p62/SQSTM1 protein abundance (Figure 4.5H) is likely explained by inhibition of autophagy induction and therefore reduced LC3B lipidation. In contrast, acute feeding did not have an impact on CMA markers or general lysosomal markers in whole muscle (Figure 4.8). The abundance of these markers was not quantified in pooled single muscle fibres. This is the first study investigating CMA markers in response to acute feeding and further research is warranted to describe its role in acute feeding.

Meal ingestion strongly activated the upstream signalling pathway that inhibits autophagy induction as demonstrated by marked increase in p-Akt^{S473} and p-mTOR^{S2448}, which are known to be activated by increases in both amino acid availability and rises in plasma insulin concentrations (95, 220). mTOR is a well described inhibitor of autophagy induction due its downstream inhibition of ULK-1, an event that blocks phagophore formation and expansion, preventing the formation of the autophagosome (94, 102-104).

Intriguingly, despite the differences observed in autophagy markers in the fasted condition, the reduction in LC3B-II abundance and therefore autophagosome content with acute feeding occurred to a similar extent in both type I and type IIa pooled fibres (Figure 4.5D), along with no changes observed in LC3B-I abundance in any of the fibre types (Figure 4.5B). This appears to reflect the fact that the activation of the Akt-mTOR pathway occurred to a similar extent in both type I and type IIa muscle fibres. Similar results have been reported previously, where both type I and type II fibres displayed a similar activation of Akt and its downstream targets, (249).

In this study, the time course of the autophagy responses to feeding was examined by taking biopsies at 30 min and 90 min post-meal ingestion. These time points were chosen to capture the early rise in insulin that occurs within the first 30 min and subsequent peaks in insulin concentrations that typically occur between 30 and 90 min post ingestion (147). Furthermore, evidence has shown that plasma and muscle amino acid concentrations peak 90 min following the ingestion of whey protein and decrease rapidly and that such rises subsequently increased mTOR activation, indirectly assessed by the activation of p70S6K1, a recognised mTOR downstream target. (256). Therefore, 90 min post meal appears to be a suitable time to capture the impact of mTOR activation in skeletal muscle following a meal ingestion. These results showed that the reductions in

LC3B-II abundance in whole muscle and pooled single fibres (Figure 4.5C) occurs at a similar time point as the phosphorylation and activation of mTOR (Figure 4.7A), which would be expected given its role in inhibition of autophagy induction. Muscle biopsy collection was restricted to 90 min post-meal in the present study therefore, it is not possible to know whether this represents the peak suppression of autophagy.

The response to feeding that we have shown here demonstrates that autophagy in human skeletal muscle does indeed cycle between activation and inhibition with normal cycles of fasting and feeding. Due to ethical reasons, it was not suitable to have a non-feeding control group. However, the observed responses in plasma insulin and glucose after the ingestion of a standardized breakfast clearly differ from baseline measurements and there was clear activation of nutrient signalling pathways in skeletal muscle (p-Akt, p-mTOR). Furthermore, the autophagy responses align with those described previously, therefore we can conclude with some confidence that there was a feeding effect upon autophagy. These findings add strength to the prevailing theory that autophagy activation during periods of fasting elevate the breakdown of proteins to ensure protein turnover and perhaps to liberate metabolic fuels. Whereas the inhibition of autophagy in the fed state is likely necessary to enable an anabolic state where new proteins are synthesized. Adequate regulation of this autophagy cycle is necessary as aberrant elevated or inhibited autophagy in muscle has been linked to negative outcomes such as muscle atrophy and metabolic dysfunction (136, 139). As we have shown that autophagy in skeletal muscle from diabetic mice is altered (Chapter 3), further studies in humans are required to determine whether the autophagy responses to fasting and feeding are also impaired in conditions of metabolic disease.

4.6 Conclusions

The results from the present chapter demonstrate a fibre-type differential response in autophagy in human skeletal muscle under overnight fasted conditions. These findings highlight the importance of considering muscle fibre type composition when investigating autophagy in human skeletal muscle in other scenarios, such as exercise, ageing, as well as chronic disease states, where fibre type composition may be altered. Further studies are warranted to investigate the mechanisms underlying the observed fibre type differences in macroautophagy. Furthermore, these results confirm that autophagy in

human skeletal muscle is acutely regulated by the nutrient and hormonal changes that occur in the transition from an overnight fast to the ingestion of a mixed meal, a response which is similar in type I and type IIa fibres.

Chapter 5

Muscle fibre-type specific changes in autophagy markers following a 6-week endurance training intervention in overweight males

5.1 Abstract

Autophagy is an intracellular recycling process that is important for maintaining cellular quality control and may mediate muscle adaptations to exercise. However, little is known about the effect of aerobic exercise training on autophagy markers in human skeletal muscle. The aim of this study was to investigate the impact of a six-week aerobic exercise intervention in overweight males on autophagy responses in whole muscle and pooled single fibres.

Ten young, physically inactive, overweight males (age 25±6 years, BMI 29.4±3 $kg \cdot m^{-2}$) with normal glucose tolerance completed a 6-week exercise intervention involving two moderate intensity and one high intensity interval exercise session per week. Muscle biopsies and mixed meal tolerance tests were completed before and after the intervention. Autophagy markers were analysed in whole muscle and pooled type I and type IIa single fibres using immunoblotting.

Despite increases in muscle oxidative capacity, macroautophagy marker protein abundance and gene expression levels were unchanged when assessed in whole muscle after the exercise intervention. However, there was an increase in LC3B-I in both type I and type IIa pooled fibres with exercise training, along with significant decrease in the autophagosome-content marker, LC3B-II, and LC3B-II/LC3B-I ratio in type I fibres. Interestingly, the key receptor for chaperone-mediated autophagy (CMA), LAMP-2A, was also significantly decreased with endurance training, regardless of fibre type. Taken together, these results suggest distinct muscle fibre-type dependent autophagy adaptations to endurance training, with reductions in autophagosome content in type I fibres only.

5.2 Introduction

The metabolic adaptations in response to aerobic exercise training have been widely characterised. Repetitive contractile activity in human skeletal muscle over a period of 6 weeks increases oxidative capacity due to increased mitochondrial content (257, 258) and greater capillary density (259, 260). Furthermore, higher oxidative muscle capacity contributes to a shift in substrate utilization, with a reduced dependence on carbohydrate and an increase in lipid oxidation rates (261, 262) and also an enhancement in insulin sensitivity (263). These skeletal muscle adaptations to exercise training are driven by the accumulation of relatively short-lived (~3-12 h) periods of transcriptional upregulation and protein synthesis rates (264), which eventually lead to an increase in the protein content when measured across repeated exercise bouts over weeks of training (265).

Recently, autophagy has emerged as a potential mechanism that may explain skeletal muscle adaptations to endurance training since protein and organelle turnover are fundamental to ensure higher protein synthesis, but also to maintain protein quality and function (266, 267). There is plenty of evidence that acute exercise modulates autophagy marker abundance in skeletal muscle. Several studies in mouse skeletal muscle have reported increases in both LC3B-I and LC3B-II forms immediately following treadmill exercise, suggesting autophagy activation (268, 269). In contrast, studies in human skeletal muscle have reported decreases in LC3B-II abundance, with no changes in LC3B-I content following an acute exercise bout (6, 92, 101).

Furthermore, intact autophagy function seems to be fundamental in mediating exercise training adaptations in skeletal muscle. In mice autophagy inhibition (i.e. through the inhibition of autophagosome formation or autophagy activation) blunted whole-body and muscle specific improvements in oxidative capacity, as well as glucose tolerance, with exercise training (11, 145). Additionally, exercise training in mice has shown to upregulate autophagy machinery proteins and autophagy flux, assessed by LC3B-II/LC3B-I ratio and p62/SQSTM1 abundance (145). The mechanisms behind these changes appear be due to increases in PCG1-α protein, which has been suggested to be positively modulated by TFEB protein expression (270). Furthermore, the lysosomal marker cathepsin D, was increased in a model of chronic contractile activity (CCA) (271) and the activity of this lysosomal enzyme was also found to be enhanced in skeletal muscle of exercised rats (272). Together this suggests an increased degradation capacity following endurance training. Evidence around the effect of exercise training on

autophagy markers in human skeletal muscle is limited. Endurance training has shown to increase LC3B-I abundance with no changes in LC3B-II, nor p62/SQSTM1 abundance in whole muscle (6, 190).

Skeletal muscle has been traditionally analysed as a whole, despite the knowledge that it is comprised of two main fibre types, which are functionally and metabolically distinct. Type I fibres display higher mitochondrial content, intramuscular lipids, along with higher oxidative capacity. Whereas type IIa fibres have a greater glycogen storage and greater glycolytic capacity (273, 274). Importantly, previous rodent studies (145) and the findings of Chapter 4 of this thesis demonstrated a greater autophagosome content in oxidative (i.e. type I) muscle fibres. Additionally, evidence in mice suggests that the changes observed in autophagy markers with exercise training are fibre-type specific. For example, autophagy machinery proteins (i.e. total LC3B and Atg6) were increased in both soleus (oxidative) and plantaris (mixed muscle) whereas autophagy flux, mitophagy and mitochondrial proteins were only increased in the mixed plantaris muscle (145). It is possible then, that increases in autophagy induction are linked to increased oxidative capacity. On the other hand, a study in rats reported that increases in autophagy induction, determined by increases in LC3B-II/LC3B-I ratio and LC3B-positive puncta, with long-term habitual exercise positively correlated with an increased proportion of oxidative muscle fibres (i.e. shift from type IIx to type IIa) (275). No studies have examined the muscle fibre-type specific responses to exercise training in human skeletal muscle.

Therefore, the aim of the present chapter was to investigate the muscle fibre-type specific responses in autophagy markers and related signalling proteins to 6 weeks of endurance-type exercise training in males. We hypothesized that endurance training will increase autophagy protein expression across type I and type IIa muscle fibres, while markers of autophagy flux will be specific to type IIa fibres.

5.3 Methods

Participants and ethical approval

Ten overweight, physically inactive and apparently healthy young men (aged 18-40 years, BMI 25-35 $kg \cdot m^{-2}$, physically inactive, see table 5.1) were recruited into the study. Participants were recruited via social media, presentations, digital platforms, and flyers (Appendix 1). Participants' written and informed consent was obtained after an initial individual meeting where the study protocol and associated risks were discussed (Appendix 2). Ethics approval for this study was attained by the University's Human Research Ethics Committee (code: 2017-29). From a total of 12 participants recruited 2 dropped out during the exercise training period, due to loss of interest.

In order to be included in the study, participants had to meet the following criteria:

Table 5.1. Inclusion and exclusion criteria for the study

Inclusion criteria	Exclusion criteria
Age: 18 - 40 years	18 > age > 40 years
Sex: male	Sex: female
Body mass index (BMI): 25-35 $kg \cdot m^{-2}$	BMI < 20 $kg \cdot m^{-2}$; BMI > 35 $kg \cdot m^{-2}$
Physically inactive*	Medical history of metabolic diseases (e.g. type 2 Diabetes), active smoking, thyroid, renal, cardiovascular and/or, psychiatric diseases, articular or skeletal muscle limitations that either alter metabolism and/or inhibit physical activity.

* according to self-report daily activity descriptions

Pre-screening

Participants were screened to rule out the incidence of diabetes via a 2 h oral glucose tolerance test (OGTT; fasting plasma glucose ≥7.0 mmol/l (126 mg/dl) or 2 h plasma glucose ≥ 11.1 mmol/l (200 mg/dl) (251). Participants were asked to arrive at the

laboratory after a 10 h-overnight fast, where they were asked to consume a 75 g oral glucose load and blood glucose levels were assessed via finger prick blood sample and glucometer at baseline and 10, 20, 30, 60, 90 and 120 min post-ingestion.

Pre-training assessment

For the first visit (visit 1), participants were asked to arrive in the morning after a 4 h fast and fill in a medical questionnaire to identify any contraindications to exercise (Appendix 3). Anthropometric data, such as height (m), body mass (kg), BMI ($kg \cdot m^{-2}$) and body composition determined by bio-electrical impedance were assessed. Bio-electrical impedance estimates body composition indirectly by measuring the body's electrical resistance, therefore variations in the hydration status have consistently been reported to significantly alter the results (i.e. dehydration increases the body's electrical resistance underestimating the measurement) (276, 277). Therefore, in order to obtain consistent body composition results, all participants were asked to comply with the following requirements; wake up at least 3 h prior; fast for a minimum of 3 h; refrain from vigorous exercise for a minimum of 12 h; empty bladder and bowels; refrain from alcohol consumption for a minimum of 12 h; and not drink or eat excessively in the 24 h prior to assessment (278).

Upon completion of the resting measurements the participants underwent an incremental exercise test on a cycle ergometer (Excalibur Sport, Lode B.V; Groningen, The Netherlands) to volitional exhaustion to determine peak aerobic capacity ($VO_{2\ peak}$). Exercise started at 30 W and increased resistance of 1 W every 4 s (15 W/min increases) until fatigue (279). Oxygen consumption (VO_2), carbon dioxide production (VCO_2), along with the respiratory exchange rate (RER) were monitored throughout by indirect calorimetry (Moxus, AEI Technologies). Heart rate (A300 [wrist worn watch] and H7 [chest strap], Polar Electro; Kempele, Finland) was simultaneously monitored throughout the test. The termination criteria were participant's volitional exhaustion or when 2 of the following were achieved: a) VO_2 levelling off despite increase in workload; b) RER > 1.1); c) within 85% of age-predicted maximum heart rate (according to the following formula: 206.9-0.67-age (y)) (280).

The following visit (visit 2) took place a minimum of 72 h after visit 1. Similar to Chapter 4, participants arrived in the laboratory in the morning following a 10 h-overnight fast. A

cannula was inserted into an antecubital vein and two resting blood samples were taken 10 min apart. The participants were given a standardized mixed meal after which blood samples were collected at 10, 20, 30, 60, 90, 150 and 180 min. Muscle biopsies were performed at rest pre and post exercise training intervention

Muscle biopsies were collected from the *vastus lateralis* using a Bergström needle modified with suction as described in detail in Chapter 4. With the participant laying supine, the skin area was anaesthetised under aseptic conditions. The biopsy needle was advanced into the skeletal muscle through a 0.5 cm incision in the skin and skeletal muscle tissue was drawn (approximately 100-200 mg). The incision was closed, and a compression bandage was applied to avoid excessive bleeding. Upon biopsy collection, the muscle sample (~200 mg) was immediately frozen in liquid nitrogen and stored at –80 °C until later processing and analyses.

Aerobic exercise training

Exercise sessions began at least 1 week after visit 2. Participants completed 3 exercise sessions per week on a cycle ergometer for a total of six weeks, which included 2 sessions of moderate intensity continuous exercise and one session of high intensity interval training (HIIT). Heart rate (A300 watch and H7 chest strap, Polar Electro; Kempele, Finland) and rating of perceived exertion (RPE) were recorded throughout each exercise bout. Evidence has shown that a period of six weeks of moderate exercise training increases insulin sensitivity in healthy, obese and insulin resistant subjects (263, 281), and it is sufficient to induce muscle adaptations to training, such as increased capillary density (259, 260) and mitochondrial content (257, 258). All training sessions began and ended with a 5 min warm up and cool down phases at 30% of their peak power output (W_{peak}), determined on the incremental exercise test. The length of continuous moderate intensity exercise bout was 60 min in duration (including warm up and cool down phases) and performed at 50 % of their W_{peak} (~60 % VO_{2max}). The high intensity interval training sessions incorporated 4 x 4 min bouts of exercise at an intensity of 70% W_{peak} (282) interspersed with 3 min of active recovery at 30% W_{peak}. The first three exercise training sessions within the first week of training (2 moderate sessions and 1 HITT session) were considered a familiarization period after which the training goal intensities were set. The two endurance familiarization sessions carried out during the first week of training were 40 min in duration, with the first 20 min at 50 % of W_{peak},

while the final 20 min were at 40 % of W_{peak}. The HIIT familiarization session was carried out in between the two endurance sessions and consisted of at least two intervals at 70% W_{peak}, and the intensity of the last two intervals was dropped to 60% W_{peak} if during the second interval two of the following three conditions were fulfilled: a) HR was above 95% of HRmax, b) RPE between 18-20, c) the participant had difficulty maintaining the cadence above 60 rpm. After which, a workload of 70% W_{peak} was completed for all HIT sessions for the remaining 5 weeks. After three weeks of training, the participants underwent a second incremental exercise test in order to reassess $VO_{2\ max}$ and W_{peak} and training intensity was adjusted accordingly. Attendance was recorded and training compliance was 97% ± 4%.

Post-training assessment

Upon completion of the exercise intervention, participants underwent the same procedures as previously described for the pre-training measurements (visit 1 and 2). A third VO_{2max} was completed within 48 h of the last training session to assess changes in maximal aerobic capacity. In order to guarantee no prevailing effect of the previous exercise session and to ensure that only the chronic responses to exercise training were evaluated, the mixed meal tolerance test and muscle sample collection took place at 48-72 h after the last exercise session.

Physical Activity and Energy Intake

Prior to the start of the first training session, each participant was asked to wear an accelerometer (model GT3X, Actigraph, Florida, USA) for eight consecutive days to monitor their physical activity levels and to complete a 3-day food diary to assess their energy intake. These assessments were repeated during the final training week period to ensure similar physical activity levels and food intake before and after the training intervention.

Analyses

Plasma analyses

Plasma insulin and C-peptide were measured by ELISA and plasma free fatty acids were determined with a non-esterified fatty acid (NEFA-C) kit and plasma glucose concentrations were determined via a glucose oxidase assay (see details on Chapter 4). Calculation of area under the curve (AUC) for C-peptide, insulin, glucose and FFA was performed by trapezoidal approximation (170) as follow:

$$AUC = 10 * \left[\left(\frac{Y_{0\,min}+Y_{10\,min}}{2}\right) + \left(\frac{Y_{10\,min}+Y_{20\,min}}{2}\right) + \left(\frac{Y_{20\,min}+Y_{30\,min}}{2}\right)\right] + 30 * \left[\left(\frac{Y_{30\,min}+Y_{60\,min}}{2}\right) + \left(\frac{Y_{60\,min}+Y_{90\,min}}{2}\right) + \left(\frac{Y_{90\,min}+Y_{120\,min}}{2}\right) + \left(\frac{Y_{120\,min}+Y_{150\,min}}{2}\right) + \left(\frac{Y_{150\,min}+Y_{180\,min}}{2}\right)\right]$$

Y_x: plasma concentration (C-peptide, insulin, glucose or FFA) at a determined time point.

Single muscle fibre isolation

Single muscle fibres were isolated as described in Chapter 4. Approximately 10 mg of muscle sample was freeze-dried, and the samples were transferred into an air-tight container with desiccant and stored at -80 °C until further analyses. Single muscle fibres were isolated with fine tweezers under a stereoscopic microscope as detailed in Chapter 4 (see figure 4.1). Each fibre was placed in 10 µl of solubilizing buffer (see details on Chapter 2) and vortexed at room temperature prior to storage at -80 °C until further analyses.

Fibre typing of single muscle fibres

Skeletal muscle fibre type of each muscle fibre was assessed through dot blotting as described in Chapter 4. Muscle fibre type was classified based upon the presence of a single MHC isoform (MHC I or MHC IIa) and single fibres were pooled together according to their fibre type (see Figure 4.2).

Immunoblotting

Whole muscle and pooled single fibres (pre- and post-training) were analysed by immunoblotting as described in Chapter 4. The following primary antibodies were used to assess autophagy activity and associated signalling responses in whole muscle: anti-Akt (cat. no. 9272S), anti-p-Akt (S473; cat. no. 92712S), anti-p-Akt (T308; cat. no. 9275S and S473; cat. no. 9271S), anti-p-mTOR (S2448; cat. no. 2971S) all purchased from Cell Signaling (Massachusetts, USA), as well as anti-LAMP-2A (cat. no. 51-2200, Thermo Fisher Scientific, Massachusetts, USA), anti-LAMP2 (cat.no. AP1824d, Abgent, California, USA), anti-Hsc70 (cat. no. SMC-151, StressMarq Biosciences, British Columbia, Canada), anti-LAMP1 (cat. no. 1D4B, Developmental Studies Hybridoma Bank, Iowa, USA), anti-p62/SQSTM1 (cat. no. ab56416 purchased from Abcam (Cambridge, UK) and anti-LC3B (cat. no. L7543, Sigma Aldrich, Missouri, USA). To assess autophagy activity in single fibres, primary antibodies targeting LC3B, p62/SQSTM1, LAMP-2A and Hsc-70 were used (as above).

Gene expression analyses

Skeletal muscle RNA was extracted a described in Chapter 2. Whole muscle (10 mg) was homogenised in 1 ml of TriZol. Baseline and 90 min-post meal ingestion time points were used to determine the effect of acute feeding on gene expression as described in Chapter 2. The following genes were analysed: *Lc3b, Gabarapl1, p62/Sqstm1, Lamp-2a, Hsc-70* (see Table 4.2 for primer sequences).

Statistical analyses

An *a priori* power calculation was performed on data from previous evidence investigating LC3B-I and LC3B-II/LC3B-I ratio changes in human skeletal muscle before and after a period of aerobic exercise training (6). This data indicates the LC3B-II/LC3B-I ratio before training was 1.0 ± 0.3 arbitrary units (mean ± SD), while the LC3B-II/LC3B-I ratio after the training intervention was 0.5 ± 0.3 arbitrary units (mean ± SD). This gives an effects size of 2.0 for LC3B-II/LC3B-II ratio, meaning that a total of n = 8 would give an expected power of >0.90. There is no existing data on the effect of exercise training on autophagy markers in human single muscle fibres. Therefore a conservative estimate

of n=10 was chosen for the current study to ensure sufficient statistical power and to account for participant drop-out.

All data were expressed as individual data and means ± SD. Paired t-tests were used to determine measurement differences before and after the exercise intervention for physiological outcomes and protein abundance in whole muscle. A two-way repeated measures ANOVA was performed to identify main effects of muscle fibre type and training. In the case of a significant interaction, post-hoc analyses were conducted using the Bonferroni correction. $P<0.05$ was considered as statistically significant.

5.4 Results

Participant Characteristics

The participant's characteristics are described in table 5.2. Total body mass, lean body mass, BMI, daily calorie intake, as well as estimated daily physical activity levels were not influenced by the aerobic exercise intervention. As expected, maximal aerobic capacity and peak power output were both increased by ~14% after six weeks of exercise training (P<0.05).

Mixed meal tolerance test

We investigated the plasma concentrations of glucose, insulin, C-peptide and FFA over a 3-h mixed meal tolerance test before and after the six-week exercise training intervention (Figure 5.1). Fasting plasma values for glucose, insulin, C-peptide and FFA were within the normal ranges (Table 5.1) and the aerobic exercise intervention did not impact the fasting plasma concentrations of any of the variables assessed (Figure 5.1 A, C, E, G, P>0.05). Furthermore, there was no effect of training in any of the plasma variables in response to a mixed meal tolerance test (Figure 5.1 A, C, E, G, P>0.05). Furthermore, exercise training did not affect the AUC for plasma glucose, insulin or FFA responses (Figure 5.1 B, D, H, P>0.05). The plasma C-peptide AUC was significantly higher after the exercise intervention (Figure 5.1F, P<0.05).

Table 5.2. Participant characteristics before and after a six-week aerobic exercise intervention

	Pre-training	3 weeks	Post-training
Age (years)	25 ± 6	–	–
Height (m)	1.83 ± 0.08	–	–
Body mass (kg)	98.19 ± 12.70	–	97.32 ± 11.79
Lean body mass (kg)	72.45 ± 6.93	–	74.47 ± 6.12
Lean body mass (% TBM)	74.18 ± 4.64	–	74.83 ± 4.28
BMI ($kg \cdot m^{-2}$)	29.39 ± 2.78	–	29.19 ± 2.82
Calorie intake ($kJ \cdot day^{-1}$)	10821 ± 937	–	10538 ± 1327
Physical activity levels ($min \cdot day^{-1}$)	46 ± 10	–	49 ± 12
$VO_{2\ peak}$ ($ml \cdot kg^{-1} \cdot min^{-1}$)	35.55 ± 5.77	38.03 ± 4.80	41.39 ± 4.64*
$VO_{2\ peak}$ ($l \cdot min^{-1}$)	3.53 ± 0.84	3.74 ± 0.65	4.02 ± 0.60*
W_{peak} (W)	275 ± 52	295 ± 41	313 ± 34*
Fasting plasma concentrations			
Glucose ($mmol \cdot l^{-1}$)	5.5 ± 0.8	–	5.4 ± 0.7
Insulin ($\mu IU \cdot l^{-1}$)	8.5 ± 3.6	–	8.8 ± 4.0
C-peptide ($pmol \cdot l^{-1}$)	415.2 ± 80.7	–	475.5 ± 170.9
FFA ($mmol \cdot l^{-1}$)	0.17 ± 0.1	–	0.22 ± 0.1

TBM: total body mass; BMI: body mass index; VO_2: oxygen consumption; W_{peak}: peak power output; FFA: free-fatty acids. *indicates *P<0.05* vs pre-training values (main exercise effect).

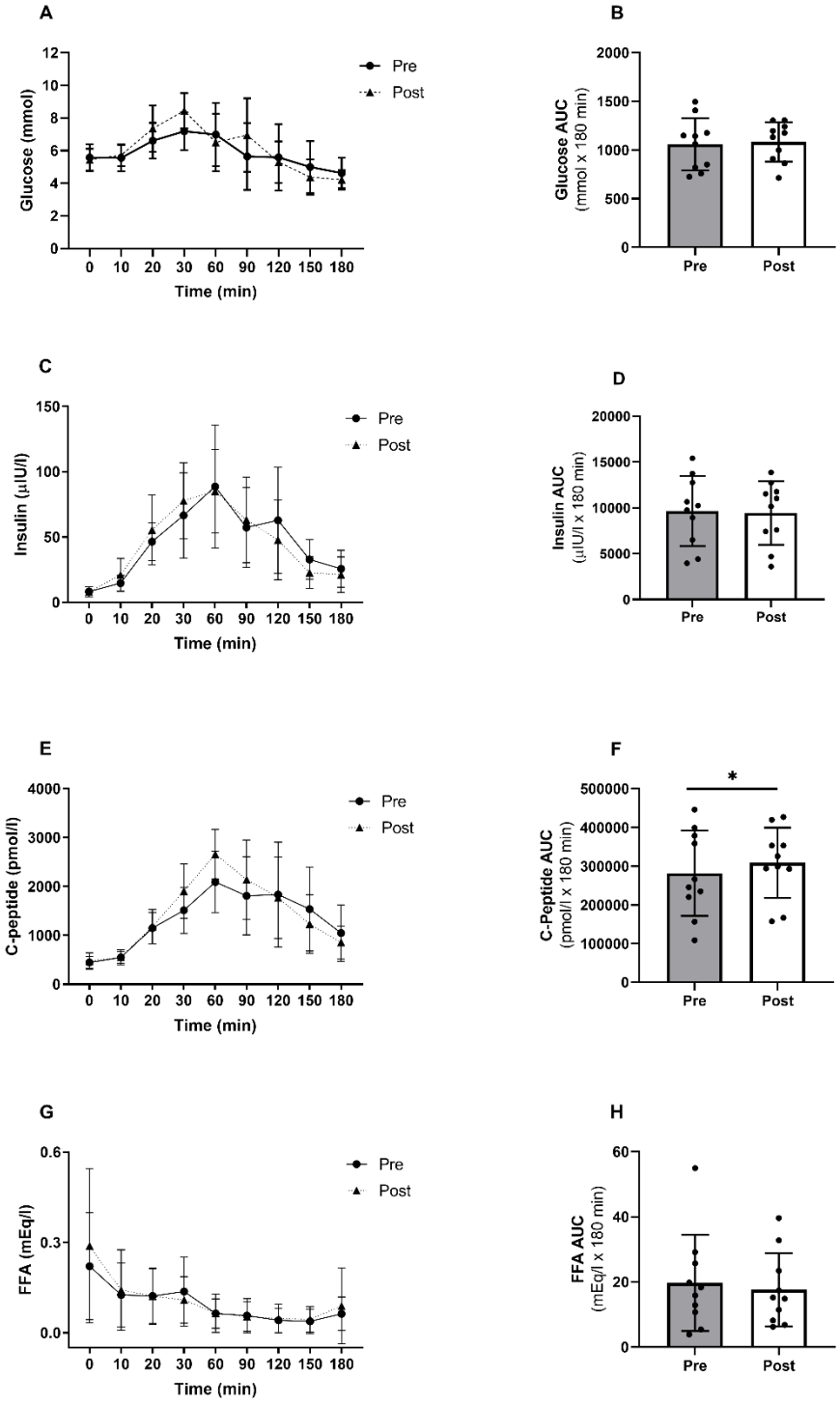

Figure 5.1. Plasma concentrations and area under the curve of glucose (A, B), insulin (C, D), C-peptide (E, F), and FFA (G, H) in response to a mixed meal tolerance test before and after a six-week aerobic exercise intervention (n=10). Values are presented as individual data and means ± SD. AU indicates arbitrary units. * indicates main effect of aerobic exercise training (*P<0.05*).

Skeletal muscle

The increase in $VO_{2\ peak}$ in response to training was complemented by an increase in skeletal muscle oxidative capacity, indirectly shown by greater levels of the mitochondrial electron transport chain complexes III, IV and V post-training (Figure 5.2, *P<0.*05).

The effects of exercise training on macroautophagy markers in whole muscle and in pooled single fibres are shown in Figure 5.3. Due to technical difficulties, it was only possible to analyse a subset of samples (n=6) for p62/SQSTM1 in pooled single muscle fibres. There was no effect of exercise training on LC3B-I, LC3B-II or the LC3B-II/LC3B-I ratio detected in whole muscle (Figure 5.3 A, C, E, *P*>0.05). Furthermore, there was no difference in p62/SQSTM1 in response to exercise training (Figure 5.3G, *P*>0.05). However, when macroautophagy markers were assessed in pooled single muscle fibres, there was a greater abundance of LC3B-I post-training (Fig 5.3B, main effect of training, *P*<0.05). Furthermore, there was a significant interaction and a significant reduction in LC3B-II and LC3B-II/LC3B-I ratio in type I pooled fibres with exercise training (Figure 5.3 D and F, *P*<0.05), with no changes in type IIa fibres. No changes were observed in p62/SQSTM1 abundance (Figure 5.3H, *P*>0.05).

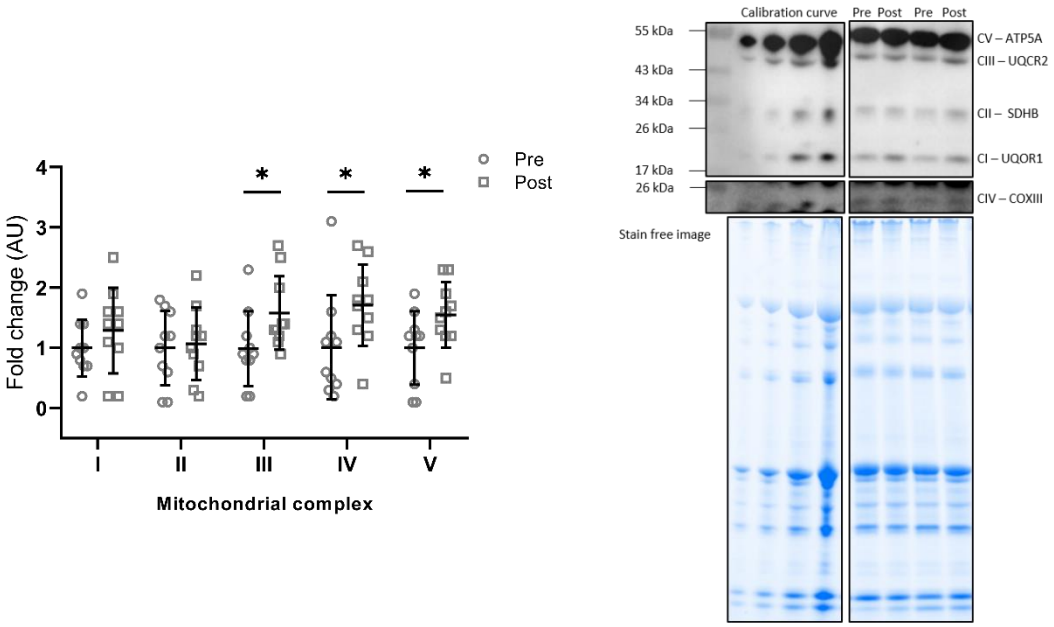

Figure 5.2. Mitochondrial electron transport chain complex protein abundance in human skeletal muscle (*vastus lateralis)* before and after a six-week aerobic exercise intervention (n=10). Values are presented as individual data and means ± SD. AU indicates arbitrary units; ATP5A: ATP synthase F1 subunit alpha; UQCR2: cytochrome b-c1 complex subunit 2; SDBH: succinate dehydrogenase, UQOR1: NADH dehydrogenase; COXIII: cytochrome c oxidase. Stain free images providing an example of total protein loading and corresponding representative blots are shown. Membrane was overexposed in order to visualize CIV (COXIII) bands. * indicates main effect of aerobic exercise training (*P<0.05*). Representative blots for each protein were taken from the same membrane and accompanying stain free images were taken from the same gel. Non-contiguous portions of the same blots, with the same exposure time are separated with spaces.

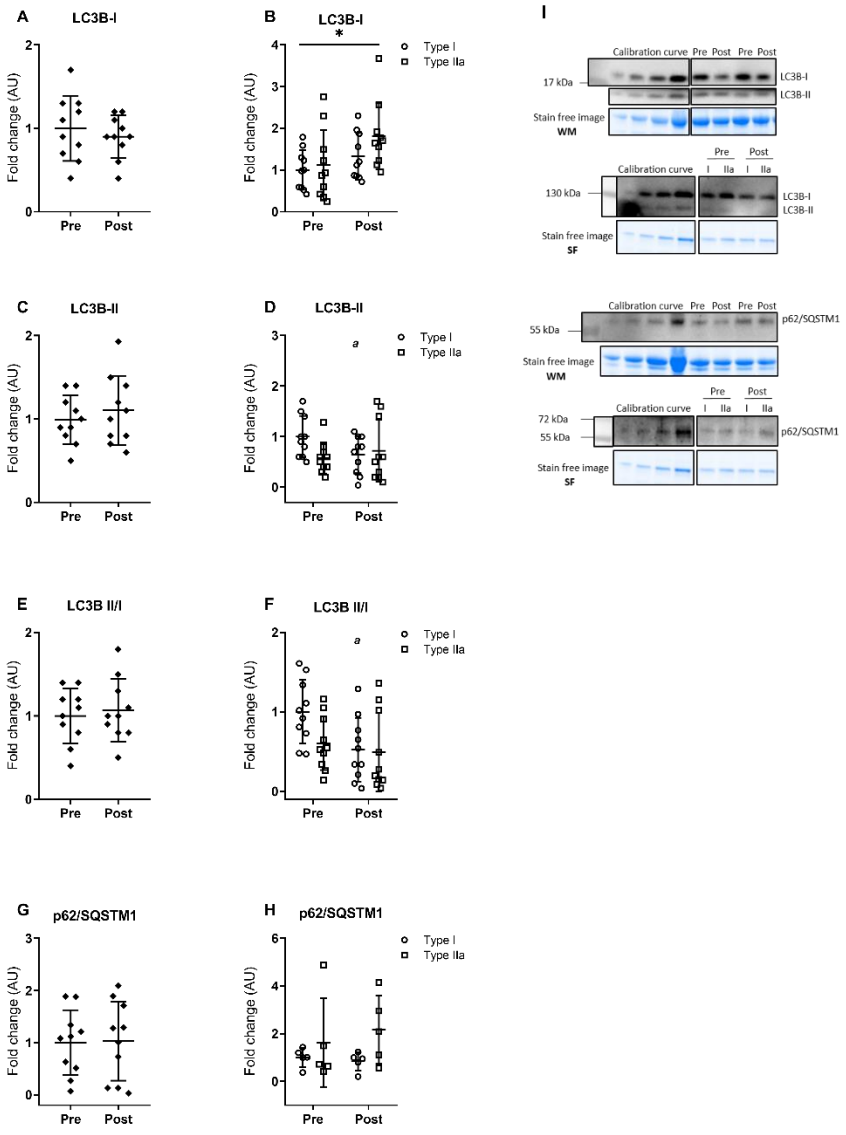

Figure 5.3. Macroautophagy markers in human skeletal muscle (*vastus lateralis)* before and after a six-week aerobic exercise intervention (n=10) in whole muscle (left hand panel) and type I and type IIa muscle fibres (right hand panel), including abundance of LC3B-I (A,B), LC3B-II (C,D) and p62/SQSTM1 (n=6; G,H). Values are presented as individual data and means ± SD. AU indicates arbitrary units. Stain free images providing an example of total protein loading and corresponding representative blots are shown (I). * indicates main effect of aerobic exercise training (*P<0.05*). [a] indicates *P*<0.05 type I post vs type I pre. WM: whole muscle; SF: pooled single fibres. Representative blots for each protein were taken from the same membrane and accompanying stain free images were taken from the same gel. Non-contiguous portions of the same blots, with the same exposure time are separated with spaces. .

The abundance of key proteins mediating chaperone-mediated autophagy (CMA) and general lysosomal markers are shown in Figure 5.4. When assessed in whole muscle, the abundance of the key CMA receptor, LAMP-2A, was significantly lower after the exercise intervention (Figure 5.4A, *P<0.05*). This finding was confirmed in pooled single muscle fibres, where there was a reduction in LAMP-2A abundance that occurred independent of fibre type (Figure 5.4B, main effect of training, *P<0.05*,). Exercise training did not influence Hsc-70 protein abundance when assessed in whole muscle (Figure 5.4C). However, when assessed in pooled single muscle fibres, Hsc-70 abundance was higher after the exercise training intervention (Figure 5.4D, main effect of training, *P<0.05*). Also, Hsc-70 protein content was increased post-training specifically in type IIa muscle fibres (Figure 5.4D, *P<0.05*). There were no changes in the lysosomal content markers, LAMP2 and LAMP1, with endurance training (Figure 5.4 E and F).

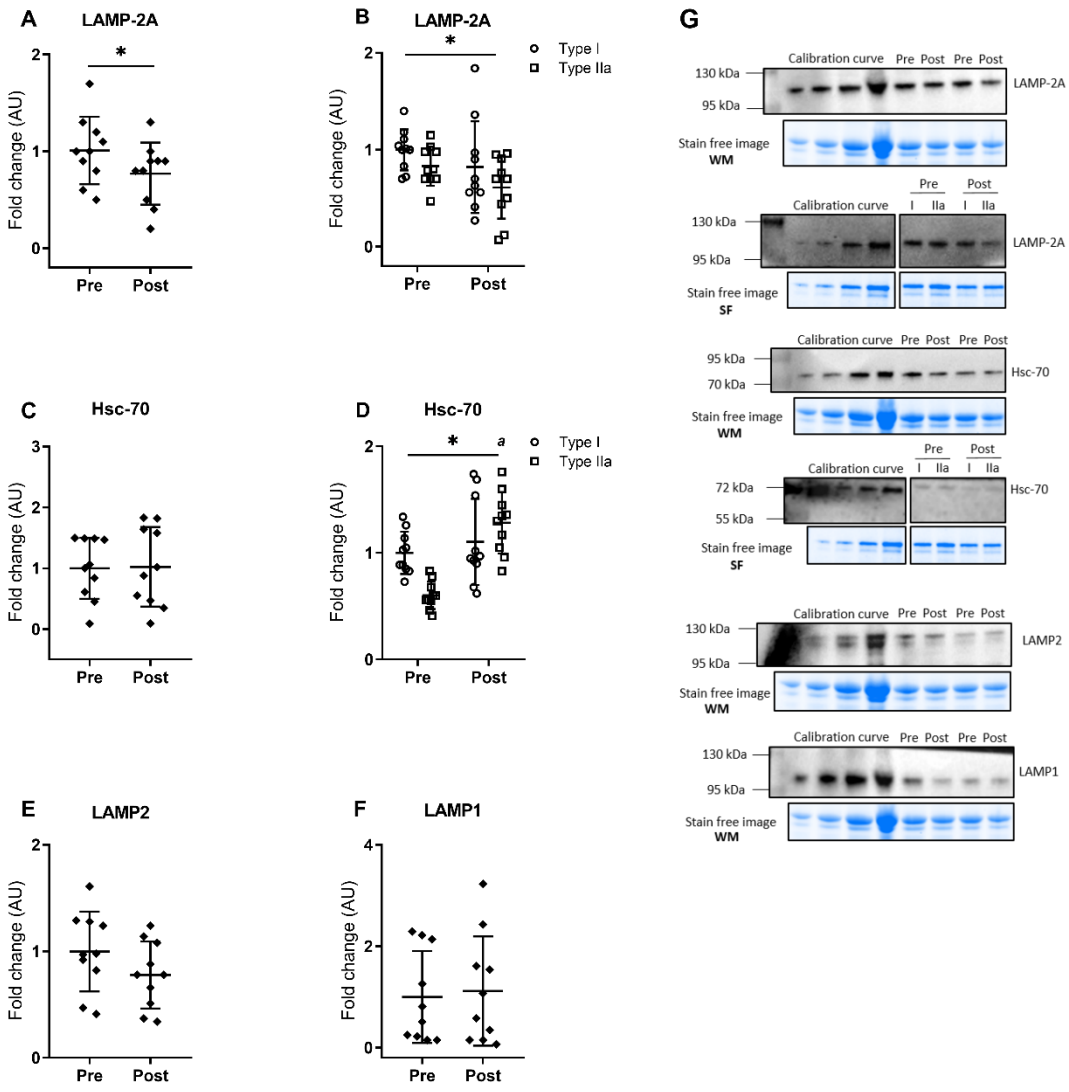

Figure 5.4. Chaperone-mediated autophagy and lysosomal content marker abundance in human skeletal muscle (*vastus lateralis)* before and after a six-week aerobic exercise intervention (n=10). LAMP-2A in whole muscle (A) and type I and type IIa fibres (B). Hsc-70 in whole muscle (C) and type I and type IIa fibres (D). LAMP2 (E) and LAMP1 (F) in whole muscle. Values are presented as individual data and means ± SD. AU indicates arbitrary units. Stain free images providing an example of total protein loading and corresponding representative blots are shown. * indicates main effect of aerobic exercise training (P<0.05); [a] indicates P<0.05 type IIa post vs type IIa pre. ** A three point calibration curve was used to quantify the band intensities from Hsc-70 in single fibres and LAMP2 in whole muscle, due to background difficulties with the first point of the calibration curve. All the sample band intensities fell within this three-point calibration curve. WM: whole muscle; SF: pooled single fibres. Representative blots for each protein were taken from the same membrane and accompanying stain free images were taken from the same gel. Non-contiguous portions of the same blots, with the same exposure time are separated with spaces. .

Key upstream signaling events regulating autophagy were assessed in the overnight fasted state before and after training and are shown in figure 5.5. The abundance of both p-Akt^{S473} and p-Akt^{T308}, remained unchanged with the exercise intervention (Figure 5.5 A and B, *P<0.05*), despite a significant increase in total Akt protein content observed post exercise training (Figure 5.5C, *P*<0.05). When expressed relative to total Akt abundance, no effects of exercise training were observed for both phospho-Akt isoforms (Figure 5.5 D and E, *P*>0.05). Furthermore, abundance of p-mTOR^{S2448} and total mTOR were both increased after the exercise intervention (Figure 5.5 F and G, *P<0.05*). However, there was no change in p-mTOR^{S2448} when expressed relative to total mTOR (Figure 5.5 H, *P*>0.05).

The gene expression profile of key autophagy proteins is shown in Figure 5.6. The exercise training intervention did not impact the expression levels of *Lc3b, Gabarapl1, p62/Sqstm1, Lamp2a* nor *Hsc-70,* when compared to baseline measurements.

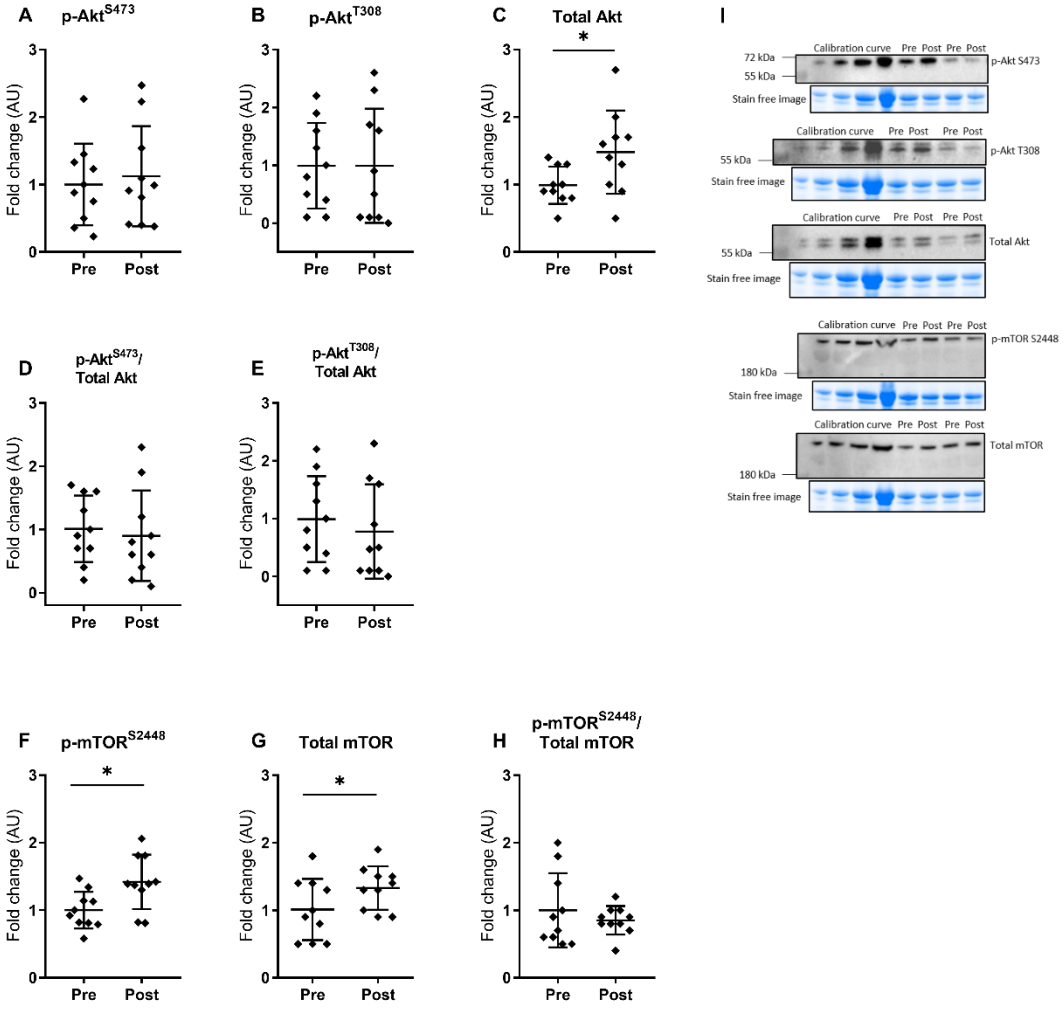

Figure 5.5. Abundance of signalling markers regulating autophagy in human skeletal muscle (*vastus lateralis)* before and after a six-week aerobic exercise intervention (n=10), including p-Akt^{S473}(A), p-Akt^{T308} (B), total Akt (C),corrected p-Akt^{S473}(D), corrected p-Akt^{T308}(E), p-mTOR^{S2448} (F), total mTOR (G), corrected p-mTOR^{S2448} (H) in whole muscle. Values are presented as individual data and means ± SD. AU indicates arbitrary units. Stain free images providing an example of total protein loading and corresponding representative blots are shown (I). * indicates main effect of aerobic exercise training (*P<0.05*). Representative blots for each protein were taken from the same membrane and accompanying stain free images were taken from the same gel. Non-contiguous portions of the same blots, with the same exposure time are separated with spaces. .

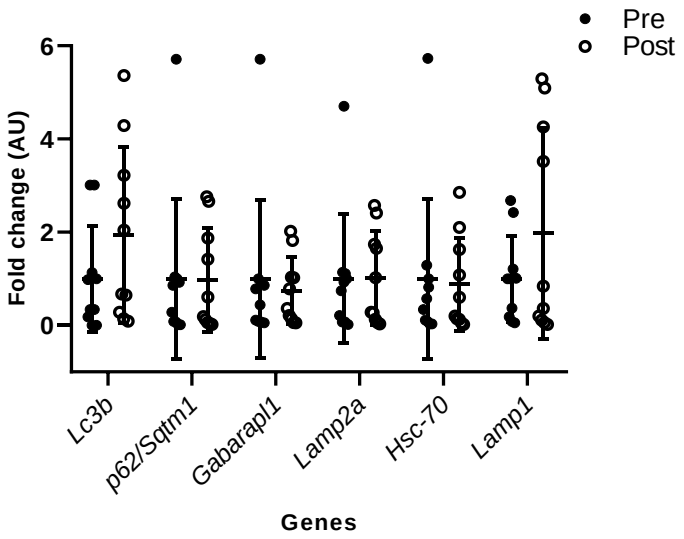

Figure 5.6. Gene expression levels of *Lc3b*, *Gabarapl1* and *p62/Sqstm1, Lamp2a, Hsc-70, Lamp1,* in human skeletal muscle (*vastus lateralis)* before and after a six-week aerobic exercise intervention (n=10). Values are presented as individual data and means ± SD. AU indicates arbitrary units.

5.5 Discussion

Autophagy is an intracellular recycling process that is important for maintaining cellular quality control and metabolic homeostasis and mediates adaptations to exercise (273, 274). Regular aerobic-type exercise stimulates metabolic adaptations in skeletal muscle that enhance whole-body aerobic capacity and improve metabolic health (283, 284). However, little is known about the effect of aerobic exercise training on autophagy markers in humans, particularly from a muscle fibre-type specific perspective. The aim of this study was to investigate the impact of a six-week aerobic exercise intervention in overweight males on autophagy responses in whole muscle and pooled single fibres. Despite the increases in muscle oxidative capacity, the exercise training intervention did not have an impact on macroautophagy marker protein abundance (Figure 5.2) or gene expression levels (Figure 5.6) when assessed in whole muscle. However, when analysed in pooled single muscle fibres, there was an increase in LC3B-I in both fibre types and a significant decrease in the autophagosome-content marker, LC3B-II, and LC3B-II/LC3B-I ratio in type I fibres after the exercise intervention (Figure 5.3). Interestingly, LAMP-2A, a key receptor for chaperone-mediated autophagy (CMA), was also significantly decreased in both fibre types with endurance training (Figure 5.4).

The exercise intervention employed in the current study was clearly successful in inducing whole-body and skeletal muscle specific adaptations demonstrated by the increased $VO_{2\ peak}$ (Table 5.2) and the greater abundance of mitochondrial respiratory complexes (Figure 5.2). The assessment of mitochondrial respiratory complex proteins was not carried out in single muscle fibres due to low sample availability, yet the data in whole muscle is sufficient to demonstrate the efficacy of the exercise training intervention. To our knowledge, this is the first study that has investigated the impact of endurance exercise training on fibre-type specific autophagy responses. Interestingly, when assessed in pooled single fibres LC3B-I abundance was increase post-training in both type I and type IIa muscle fibres (Figure 5.3). These data are in line with the few studies that have investigated the impact of exercise training in lean, physically active humans in whole muscle homogenates (6, 190). These studies also show significant increases in LC3B-occurred along with no changes p62/SQSTM1 abundance in whole muscle with endurance training (6, 190).

The data from the present study show that LC3B-II and LC3B-II/LC3B-I ratio is unchanged when assessed in whole muscle. This is again in line with whole muscle

analysis following 8 weeks of both sprint interval and moderate intensity exercise (190). However, a type I muscle fibre specific reduction in LC3B-II and LC3B-II/LC3B-I ratio with endurance training was detected in the present study (Figure 5.3). These findings indicate that subtle changes in fibre-type specific autophagy markers following exercise training might be overlooked when only whole muscle is analysed. In skeletal muscle in mice, endurance exercise training was initially shown to broadly upregulate autophagy and mitophagy protein expression (i.e. LC3B, BNIP3 and Parkin) and that increased muscle oxidative capacity was linked with increased autophagy induction (as assessed by an increase in LC3B-II/LC3B-I ratio) (145). Evidence in human whole muscle shows that endurance training promotes mitophagy, based on higher abundance of mitophagy specific markers, such as BNIP3 and Parkin (190, 266) and that these changes occur along with the reported increases in LC3B-I (190). Since an increase in LC3B-II and in LC3B-II/LC3B-I ratio has been typically associated with an increase in autophagy activity (74), the reduction in LC3B-II and LC3B-II/LC3B-I ratio specific to type I fibres observed with endurance training in this study, and without changes in p62/SQSTM1 abundance, is somewhat surprising. However, reductions in mitophagy flux occur as an adaptation to chronic contractile activity (CCA) in aged muscle, possibly as result of better organelle quality and less reliance on mitochondrial turnover (285). Although the participants in the current study had normal glucose tolerance, they were overweight (BMI ~30 $kg \cdot m^{-2}$), which is closely linked with mitochondrial dysfunction in muscle and metabolic inflexibility and is a well-established risk factor for the development of insulin resistance (286). Although speculative, it is possible that the reduced LC3B-II and LC3B-II/LC3B-I following training in the present study, reflects reduced autophagy 'flux' alongside enhanced muscle or mitochondrial 'quality'. We were unable to determine Parkin and BNIP3 abundance in the muscle samples in this study due to the presence of multiple non-specific bands. Although LC3B-I, LC3B-II and p62/SQSTM1 could be considered surrogate markers of mitophagy (287), the quantification of BNIP3 and Parkin alongside measures of mitochondrial function would be required to further explain the autophagy responses to endurance training seen in this study in more detail.

A notable observation in the present study is the discordant results in both LC3B forms assessed in whole muscle and in pooled single muscle fibres. This is somewhat surprising given that autophagy responses with feeding reported in Chapter 4 were largely aligned between single fibre and whole muscle measurements. It is unlikely that muscle fibre type shifts occurred in this study, given previous work has shown no

changes in muscle fibre type composition with 6 weeks of training (288). However, further analysis of fibre type using immunohistochemistry is required to confirm this. It may be relevant that skeletal muscle is not a homogenous tissue, and contains other cell types, such as intermuscular adipocytes. These adipocytes are more frequent in sedentary and obese individuals (289, 290) and can interfere with lipid-related assessments in homogenates prepared from skeletal muscle biopsies (291, 292). As autophagy is present in adipocytes (293), it is possible that contamination from other cell types influences autophagy protein assessments in muscle homogenates, particularly in the overweight individuals studied here. Single fibre isolation will remove any potential contamination from non-muscle tissue, which may underlie the differences between pooled single fibres and whole muscle in LC3B-I. Further work is required to determine whether this is indeed the case and could be confirmed with probing of adipocyte-specific proteins to check for adipocyte contamination (e.g. Perilipin 1).

Similar to the findings discussed in Chapter 4, LC3B-II abundance and LC3B-II/LC3B-I ratio was ~ 50 % higher in type I fibres compared to type IIa fibres (Figure 5.3). However, these differences were no longer observed after training. The participants in this study mostly exercised at a moderate intensity throughout the 6-week period, which is typically recognized to recruit mainly type I fibres (294). It appears that the absence of fibre-type differences post training is due to exercise training adaptations present in type I fibres, given the nature and intensity of the training.

When looking at upstream signaling pathways regulating autophagy, we found increased total Akt and mTOR abundance post training, with no increase in their respective phosphorylated forms when expressed relative to total protein abundance (Figure 5.4). These findings align with previous evidence, where endurance exercise increases total Akt (295-297) as well as mTOR content (298), without any changes in the phosphorylated forms in both diabetic and non-diabetic populations. It has been suggested that such increases in total protein content are part of the mechanisms responsible for the increases in insulin sensitivity in skeletal muscle observed with training (297). Therefore, the present findings could be reflecting increased muscle specific insulin sensitivity post training which is not detected in whole body assessments applied in this study.

Intriguingly, LAMP-2A, rate limiting receptor for CMA, was decreased after exercise training as assessed in both whole muscle and in pooled type I and type IIa fibres,

suggesting that endurance exercise training decreases CMA capacity (Figure 5.4). Evidence suggests that oxidative stress is a potent stimulus for CMA activation (299, 300) and exercise training is known to increase anti-oxidant enzymes, such as superoxide dismutase (SOD) (301). Future studies are warranted to elucidate whether the decreases in LAMP-2A observed in the present study are associated with a higher antioxidant capacity in skeletal muscle. Furthermore, it has been reported that LAMP-2A is degraded when it associates to cathepsin A (152) and once incorporated into lipid microdomains of the lysosomal membrane (149, 153) however, how exercise training may impact these processes remains to be addressed. To date, no other studies have looked at skeletal muscle proteins involved in CMA in response to endurance training. Hsc-70 levels were found to be increased after the exercise intervention, changes which were mainly driven by the increases in Hsc-70 abundance in type IIa fibres, indicating a fibre-type specific adaptation to training in type IIa fibres. Further studies are necessary to elucidate the meaning of these responses but indicate that the CMA pathway is modulated by endurance training.

Basal plasma glucose and insulin levels were within normal ranges (251), suggesting no evident baseline alterations in glucose homeostasis, despite being an overweight population. Also, the lack of changes in plasma glucose and insulin with endurance training (Figure 5.1) suggest no improvements in glucose tolerance. This is in agreement with previous evidence indicating that the majority of exercise benefits on glucose homeostasis are related to acute effects of the last exercise bout that are typically seen within 24 h of exercise (302). A strength of the current study is that the mixed meal tolerance test was completed >48-72 h after the last exercise bout to ensure that the results were not impacted by the prevailing effect of acute exercise. Interestingly, the observed increases in C-peptide AUC as a result of exercise training apparently reflect an enhancement in β-cell responsiveness to glucose or other nutrients and increased insulin secretion. However, the absence of changes in plasma insulin suggest greater hepatic insulin clearance post-training (Figure 5.1).This finding is particularly interesting given that impairments in insulin clearance appear to be an important early event contributing to the development of hyperinsulinemia in young individuals with normal glucose tolerance (303). Although not well studied, enhanced insulin extraction may be another adaptation that contributes to the metabolic benefits of regular exercise (12). A limitation of this study was the absence of a control group (healthy weight males), which limits the conclusions that can be made about how exercise specifically impacts

autophagy inan overweight group. Further studies are warranted to elucidate whether these responses differ from a healthy weight population.

5.6 Conclusions

The results from the present study demonstrate that a 6-week endurance training intervention increased LC3B-I across both fibre types, whereas type I fibre-specific decreases are observed in LC3B-II and LC3B-II/LC3B-I ratio in overweight males. These results demonstrate that exercise training increases the expression of proteins involved in the autophagy machinery, but suggests fibre-type specific adaptations in autophagy flux and autophagosome content. This work again highlights the utility of considering muscle fibre type specific responses when studying autophagy in human skeletal muscle. Additional studies are warranted to further elucidate the role of skeletal muscle CMA in exercise training and the potential implications in muscle and metabolic health.

Chapter 6

General discussion

6.1 Introduction

Autophagy constitutes one of the major cell degradation systems and involves the targeting and delivery of cytosolic contents to the lysosome for degradation (24). Primarily *in vitro* and animal experiments using prolonged fasting conditions have shown that autophagy is sensitive to hormonal and nutrient variations, whereby insulin and amino acids independently inhibit autophagy induction (50, 195), while autophagy is activated when nutrient availability and insulin concentrations decline (35, 196). While it is generally considered that autophagy activity will cycle with repeated feeding and fasting periods throughout the course of a day, little is known about the autophagy responses that occur with habitual patterns of feeding and fasting, particularly in human skeletal muscle.

Given that autophagy is regulated by the insulin and nutrient sensitive signalling pathways and these are disrupted in insulin resistant conditions, autophagy is proposed to be impaired in states of insulin resistance. Furthermore, tissues from insulin resistant hosts typically display accumulation of dysfunctional mitochondria, lipids and aggregated unfolded proteins, which constitute common autophagy targets (9, 29, 52). While a number of studies have indicated hepatic autophagy impairments in animal models of insulin resistance, few studies have explored skeletal muscle.

Exercise has been widely recognised as one of the first lines of treatment against obesity and insulin resistance, by increasing lipid turnover and enhancing insulin sensitivity. In addition, it has been well characterised as a potent autophagy inducer. This activation of autophagy with exercise appears to be a relevant process ensuring muscle homeostasis and also mediating adaptations to endurance training. Moreover, evidence mostly arising from rodent studies, has indicated differential autophagy responses in basal conditions and after endurance training in the different muscle fibre types. However, little is known about the effect of aerobic exercise training on autophagy markers in human skeletal muscle, particularly from a muscle fibre-type specific perspective.

Therefore, the main aims for the present thesis were i) to compare the autophagy response to feeding in liver and skeletal muscle in animal models of insulin resistance and overt T2D, ii) to describe the muscle fibre-type specific autophagy responses in human skeletal muscle in the fasted state and in response to acute feeding, and iii)

explore the muscle fibre type specific autophagy responses in humans following a 6-week aerobic exercise training intervention.

6.2 Autophagy in conditions of metabolic disease

The aim of Chapter 2 was to determine the impact of a HFSD intervention on autophagy markers in the liver and skeletal muscle of mice in a fasted state and following an oral glucose load. The presence of autophagosome clearance defects in the liver of diet-induced insulin resistant mice along with no changes observed in skeletal muscle autophagy markers was observed. The findings in liver are in line with previous studies (35, 171) and suggest that the hepatic autophagy disruptions may contribute to the development of hepatic insulin resistance. However, despite the presence of whole-body insulin resistance, the absence of changes in autophagy markers in skeletal muscle suggests that the initial stages of insulin resistance in this tissue are unrelated to autophagy. This finding is in-line with evidence showing no differences in autophagy-related proteins in human skeletal muscle of a T2DM group, when compared to an obese or lean group (187). However, it is important to note that significant decreases in muscle autophagy markers in a T2DM group, featuring long standing (~17 years) severely insulin resistant individuals (91) suggests that autophagy modulation in skeletal muscle could be dependent upon the severity of insulin resistance, hyperglycaemia and hyperinsulinemia.

In Chapter 3 the impact of overt T2DM on autophagy markers in liver and skeletal muscle in the fed and fasted state was investigated using the *db/db* mouse model. Similar to the findings in Chapter 2, overt diabetes exerts a differential impact on autophagy markers in liver and skeletal muscle. However, hepatic autophagy impairments, this time at the initial stages (i.e. transcription), along with an upregulation of macroautophagy markers in skeletal muscle were observed. The differences reported in the liver in comparison to Chapter 2 (autophagosome clearance vs autophagy initiation impairments) could be attributable to differences in the rodent models that were used (i.e. diet vs genetically induced obesity). Indeed, a study comparing both mouse models reported that although liver fat accumulation was present in both HFD and *db/db* mice, the livers from *db/db* mice displayed liver metabolic inflexibility, assessed by the complete inability to switch between fuel substrates, suggesting poor mitochondrial adaptations to hepatic lipid

accumulation, a derangement that was not found in the livers of HFD mice (304). It is possible that these differences in hepatic metabolic derangements could be differentially impacting autophagy activity.

Additionally, the decreases in LAMP-2A observed in the skeletal muscle of diabetic mice suggest a decline in CMA activity. This could be a compensatory response to the upregulation in macroautophagy, a phenomenon that has been reported previously in the liver (212, 213). The relevance of CMA in skeletal muscle metabolism and the development of metabolic disease requires further study. Collectively, the findings in Chapter 2 and Chapter 3 suggest that autophagy activity in liver is disrupted in conditions spanning whole body insulin resistance and overt diabetes, while autophagy disruptions within skeletal muscle only occur in overt diabetes and appears to be dependent on the severity of insulin resistance, hyperglycaemia and hyperinsulinemia.

6.3 Autophagy responses to fasting and feeding

Across chapters 2-4, autophagy responses in different states of nutrient availability were examined. In Chapter 2, there was no differences in autophagy markers between the fasted state and 15 min following an oral glucose load in either liver or skeletal muscle. The fact that the oral glucose load had little effect on the assessed upstream signalling markers suggests that the small increases in insulin (~2-fold) with glucose gavage in mice is insufficient to modulate autophagy. Therefore, although the glucose oral gavage enables close examination of glucose homeostasis, it may not resemble the changes in nutrient availability through habitual feeding behaviour in mice.

To examine the autophagy responses in the liver and skeletal muscle following more typical feeding patterns, Chapter 3 examined the autophagy responses in these tissues in the 4 h fasted and fed state. The findings in both liver and skeletal muscle suggest that feeding status had no impact on the abundance of autophagy markers. The absence of insulin measures due to lack of sample availability comprises a limitation to this study as it is difficult to assess the feeding responses in the animals and draw strong conclusions regarding the downstream signalling events. Nevertheless, despite increases in p-Akt^{S473} and p-mTOR^{S2448} in response to feeding in muscle, it is somewhat surprising that there was no impact on autophagy in this tissue. Rather the lack of effect

on autophagy responses in either tissues in both the fasted and fed state may be explained by the relatively short fasting period (4 h), which may be insufficient to induce autophagy.

In Chapter 4, the effect of acute feeding on skeletal muscle autophagy responses in humans was investigated. Furthermore, this chapter provides the first data on the fibre-type specific responses of autophagy markers in human skeletal muscle. Type I fibres displayed greater LC3B-II and lower LC3B-I content in the fasted state indicative of higher autophagy induction, however, these differences were not explained by variations in the assessed upstream signalling markers (p-Akt^{S473} and p-mTOR^{S2448}), which align with previous studies in mice (145). Additionally, the fibre-type basal differences in autophagy markers described in this chapter highlight the importance of looking at skeletal muscle in a fibre-type specific manner, particularly in populations that exhibit muscle fibre type shifts, such as the elderly, type 2 diabetics, and sedentary individuals (305, 306).

Moreover, a decrease in autophagosome content, assessed by LC3B-II abundance, was observed 90 min following ingestion of a mixed meal. This effect was similar in type I and type IIa fibres and reflected the increases in the upstream inhibitory signalling cues (p-Akt^{S473} and p-mTOR^{S2448}) in both fibre types. These findings align with previous work that showed no fibre-type specific differences in insulin-mediated Akt activation in human skeletal muscle (249). This data also suggests that the mechanisms behind the basal differences in autophagy markers are independent of differences in the insulin-Akt-mTOR signalling pathway.

6.4 Autophagy responses in skeletal muscle to 6 weeks of endurance training

In Chapter 5, the effects of aerobic exercise training on muscle fibre-type specific autophagy responses were investigated. Despite no differences observed in macroautophagy markers following endurance training when assessed in whole muscle, when assessed in pooled single fibres, there was an increase in LC3B-I in both fibre types, along with a significant decrease in the autophagosome-content marker, LC3B-II, and LC3B-II/LC3B-I ratio in type I fibres after the exercise intervention. These findings confirm that potential differences in autophagy markers may be overlooked when whole muscle is examined. Furthermore, given that the changes in autophagosome content (as

assessed by LC3B-II) were limited to type I fibres, it is possible that these reported changes mirror specific exercise training adaptations, as a result of targeted muscle fibre recruitment (294). The reduction in LC3B-II in type I fibres following endurance training are in contrast with the observations made in rodent models, which questions the translatability between rodent and human skeletal muscle autophagy responses to exercise. The observed decrease in LC3B-II could indicate improved muscle quality and function in this overweight population in response to aerobic exercise training and a lower requirement for autophagy induction (285). Additionally, the decreases observed in LAMP-2A abundance in both type I and type IIa muscle fibres require further study to unravel the role of CMA in skeletal muscle following endurance training.

6.5 Strengths and limitations

To study autophagy, we used immunoblotting as our principal technique to determine protein abundance of autophagy markers. Some important strategies previously described to influence the quality and nature of the results were taken into consideration (203, 204). Firstly, as sample enrichment through centrifugation can lead to loss of the protein of interest (204), the samples were not spun prior to loading them onto the electrophoresis gel ensuring assessment of the entire protein pool. This could be particularly important when the proteins of interest are distributed across different intracellular locations. For example, the cytosolic LC3B-I is incorporated into the phagophore membrane when lipidated (196) and part of the p62/SQSTM1 pool has been reported in various tissue fractions (307). Secondly, total protein was imaged using stain-free technology and used as a loading control. This is a superior approach as it eliminates the potential bias that could occur if the housekeeping protein is affected by any of the interventions (204). Thirdly, protein abundance was determined after confirming that the intensities were within a linear range of detection by using a 4-point standard calibration curve. This approach will avoid potential errors in quantitation when the proteins of interest are outside the linear range of detection. This superior approach provides us with ample confidence that the reported results are highly quantitative and therefore a true reflection of the changes occurring in the different tissues that were analysed.

Current limitations of the immunoblotting technique

As mentioned in Section 1.4, autophagy assessments often rely on the measurement of key autophagy protein content through immunoblotting. In the majority of the studies described in this literature review, these protein assessments have been performed in tissues that have undergone considerable centrifugation (e.g. ~20 min at 10,000 g/13,000 rpm) (6, 92, 145, 190, 242, 243, 245). This is a commonly adopted process that is performed in the belief that removing insoluble materials results in 'cleaner' immunoblots when assessing the protein of interest.

However, it has been reported that protein yield can be significantly impacted by considerable centrifugation, given that a portion of the protein of interest can remain in the discarded pellet (203, 204). This process may impact assessment of key autophagy markers as LC3B has been described to be present in the nuclear fraction and is distributed across cytosolic and membrane fractions depending upon the lipidation of the protein (144). Furthermore, p62/SQSTM1, the described marker of lysosome degradation is also distributed across nuclear, membrane and cytosolic fractions of skeletal muscle (307, 308). Therefore, it is feasible that portions of these proteins could be lost through any enrichment of the sample through centrifugation. Assessment of the entire protein pool would therefore be preferable. Throughout the four experimental chapters of this thesis this was achieved by not centrifuging any of the samples and therefore loading the entire sample onto the electrophoresis gel. Moreover, quantitative biochemical measurements typically implement the use of a calibration curve that notes the higher and lower limits of detection. However, assessment of autophagy proteins via immunoblotting in the previous studies described in Chapter 1 have not incorporated this. Nonetheless, it is possible to include such an approach by loading increasing volumes of a mixed sample of tissue homogenate to establish a 4-point calibration curve on every electrophoresis gel, which was done consistently on every electrophoresis gel that was run to present the data throughout all chapters in this document. This ensures the proteins measured lie in the linear range of detection and ensure the assessments of proteins of interest are truly quantitative (204).Including both of these approaches (i.e. no sample centrifugation and the addition of a calibration curve on every gel) provides us with confidence in the data that we obtained.

Throughout the four experimental chapters of this thesis, the role of autophagy was assessed via the abundance of well recognised autophagy markers (i.e. LC3B forms and

p62/SQSTM1), as well as gene expression analyses. This approach has been recommended in the assessment of autophagy in the absence of flux measurements (74) and has been a common approach when assessing autophagy changes in human and animal tissue (6, 90, 101, 309). However, LC3B and p62/SQSTM1, comprise broad markers of this process making it challenging to assess specific types of autophagy in detail (e.g. mitophagy, lipophagy, glycophagy, etc.). While a number of markers are described for mitophagy, validated markers are not available for the other forms of autophagy in the tissues of interest in this thesis. Identifying specific markers for specific autophagy processes will be important for future research to advance the area.

Autophagy is a highly dynamic process simultaneously involving the synthesis of new autophagosomes and their clearance in the lysosome. Therefore, determining the abundance of the autophagy markers at specific time points only provides a 'snapshot in time' of the entire process, limiting the conclusions that can be drawn the dynamics of autophagy (310). A more comprehensive panorama of how the different intervention could affect autophagy responses can be obtained by inhibiting specific steps involved in the autophagy process and therefore being able to measure differences in autophagy flux. Indeed, flux studies are considered the gold standard to monitor changes in this cellular process (74). However, while this remains the gold standard, this approach is not without its disadvantages. Firstly, lysosomes carry out numerous functions within the cell, which are not limited to autophagy only (88), therefore, inhibition of lysosome function could potentially interfere with other parallel intracellular processes. Secondly, such interventions cannot be carried out in human tissues, and therefore the clinical translation of animal studies into humans remains a critical missing step in autophagy research.

Furthermore, conflicting evidence between rodent and human reports regarding p62/SQSTM1 abundance variation following specific interventions has raised the question whether p62/SQSTM1 constitutes a reliable marker of autophagosome degradation in humans. Studies in rodents have consistently demonstrated reductions in the abundance of this protein in conditions of increased autophagy flux (11, 90). However, studies investigating a similar scenario in human tissues have failed to detect changes in p62/SQSTM1 abundance (6, 92). Such discrepancies amongst species suggest that p62/SQSTM1 might not be as dynamically regulated in human tissues and therefore it may not constitute a suitable and reliable marker for autophagosome

degradation (6). This poses an important challenge when assessing autophagosome degradation in human tissues *in vivo*, given that flux studies cannot be performed and to date no other marker of autophagosome degradation is available. Hence, the conclusions on autophagy responses in human tissues are limited.

Throughout the four experimental chapters, p-mTOR^{S2448} was used as an indirect measurement of mTORC1 activity to infer the state of autophagy inhibition. This phosphorylation site has long been considered important for mTOR activation (311, 312) This approach was chosen as a complementary analysis to inform on potential upstream signalling pathways mediating autophagy activity. However, recent evidence has reported that p-mTOR^{S2448} may not be a reliable marker for mTORC1 activation and that the phosphorylation status of other downstream targets, such as p70S6K and/or 4E-BP, may be preferable (313). Future studies, should aim to look at these downstream targets to provide a more comprehensive assessment of mTORC1 activity.

A strength of this thesis is that human skeletal muscle was not only analysed as a whole, but pooled type I and type IIa fibres were analysed for autophagy markers in Chapter 4 and 5. A fibre-type specific approach adds specificity to the results, given the different metabolic and functional features that type I and type IIa fibres exhibit (273, 274). However, it should be noted that due to sample limitations, the autophagy responses were not measured in all muscle fibre types (e.g. type IIx or hybrid fibres), which presents a limitation to the study. Furthermore, as this technique requires dissection of single fibres from the biopsy, it provides confidence that the results are not confounded by differences in autophagy activity from other cells that may be present in the whole muscle sample (291, 292).

Another strength of this thesis is that both macroautophagy and CMA marker abundance were consistently assessed throughout the four experimental chapters. However, the conclusions regarding the role of CMA in the different scenarios are limited based on the assessment of LAMP-2A and Hsc70 abundance only. Although the lysosomal LAMP-2A is the rate limiting enzyme for CMA, only the lysosomes containing Hsc-70 in their lumen are active for CMA (314). Indeed, Hsc-70 abundance was assessed, however this protein is not exclusively found in the lysosome, in fact, only a small amount of this protein is found inside this organelle (314). Therefore, although changes in LAMP-2A abundance may be indicative of changes in this pathway, further work is warranted to

examine the function of CMA in skeletal muscle and in human tissues in response to metabolic disease and exercise.

6.6 Future research directions

Based on the findings presented in this thesis, together with the limitations discussed previously it would be important to further investigate the role of autophagy in different circumstances and implementing some additional approaches. Currently, autophagy flux cannot be measured in human tissues using the same approaches implemented in animal models. Currently, quantification and analysis of LC3B-I, LC3B-II and p62/SQSTM1 protein content are the most common methods to assess autophagy in tissues. However, p62/SQSTM1 protein content can be affected independently of changes in autophagy flux (i.e. transcription changes (315) or the use of different specific adaptor proteins (316)), but also increases in LC3B-II protein could be missed, due to its rapid degradation under certain conditions, such as stress (317). However, recent evidence has documented the availability of a suitable new antibody against the phosphorylated form of Atg16L1 on serine 278 (p-Atg16L1^{S278}), a crucial protein responsible for stimulating the formation of the new phagophore and future autophagosome. Therefore, it provides accurate information about newly forming autophagosomes and autophagy rates and induction (318). It would be important to include these analyses in future studies to have more information on autophagy induction and the initial processes. Furthermore, the specific targets to be degraded via autophagy in skeletal muscle are unknown. Evidence, especially from studies conducted in the liver, have reported that intact lipophagy is essential to maintain hepatic metabolic homeostasis. Moreover, it is also known that degradation of lipid droplets (LD) occurs once PLIN2, known as the LD gatekeeper, is degraded via CMA. It would be interesting to investigate the relevance of lipophagy in skeletal muscle homeostasis by manipulating PLIN2 protein expression in skeletal muscle (overexpression or knockdown mouse models vs control), exposing these animals to a period of high-fat diet or exercise training, and assessing lipid droplet content through immunofluorescence, parallel to the general autophagy markers, LC3B and p62/SQSTM1. Furthermore, it would be interesting to perform co-localisation studies between autophagosomes and LDs, which would provide a better understanding around the nature, relevance and dynamics of these interactions in the context of health and disease.

The typical autophagy marker response to feeding in a glucose tolerant, male population was described in Chapter 4. Given that autophagy is regulated by the insulin-Akt-mTOR pathway, which is disrupted in insulin resistant and diabetic conditions, the question remains whether the autophagy feeding response is present in those metabolic disease. Additional studies focusing on the autophagy responses in pre-diabetic and overt diabetic individuals would further contribute to the evidence regarding the relevance of autophagy in human skeletal muscle homeostasis and its contribution to metabolic disease. Moreover, given the descriptive nature of the results presented, it would also be interesting to evaluate in detail the signalling responses (e.g. ULK-1 signalling responses) regulating autophagy amongst different populations (insulin sensitive vs insulin resistant vs diabetic) or between interventions (pre-vs post exercise intervention). Full description of the upstream signalling responses and potential disturbances would provide a solid foundation to investigate and develop potential pharmacological targets. Furthermore, the suppression of autophagy markers with feeding was seen at 90 min post meal ingestions, however it would be interesting to examine the duration of autophagy suppression after ingestion of a single mixed meal. This information would be relevant to understand how long is required between meals in order to activate autophagy throughout a day with normal feeding patterns. Such knowledge could potentially unravel yet another mechanism behind the metabolic benefits of dietary approaches, such as intermittent fasting.

Finally, growing evidence, especially in the liver, suggests that CMA might also play and important role in maintaining cell homeostasis. For example, inhibition of CMA via LAMP2A knock-down increases hepatic lipid storage and shifts metabolism towards carbohydrate oxidation (319). Currently no studies have explored the role of this pathway in skeletal muscle. This could be investigated by using a LAMP-2A knockdown approach and assessing the impact on muscle metabolism, lipid storage and the content of CMA substrates. Another way to investigate CMA further would be to isolate CMA-competent lysosomes containing both LAMP-2A and Hsc70 from skeletal muscle, which have either received a lysosomal inhibitor (e.g. leupeptin) or a control. Isolated lysosomes could then be analysed for their content to identify potential CMA substrates in muscle. A similar approach could also be used in models of metabolic disease (e.g. high fat fed mice, *db/db* mice) to explore the impact of insulin resistance on CMA capacity. Such approaches will help characterise the specific metabolic role of CMA in skeletal muscle and its contribution to metabolic disease.

6.7 Final Conclusions

The findings from this thesis have demonstrated that autophagy is a highly dynamic process which is disrupted in the context of metabolic disease, such as pre-diabetes and diabetes. However, the nature of these disruptions is dependent upon the stage of disease development and the specific tissues investigated. Understanding the contribution of these autophagy impairments to disease development and/or progression in further detail would help guide the development of pharmaceutical targets that can modulate autophagy and potentially improve metabolic health. Although the use of animal models is clearly advantageous in a variety of scenarios, autophagy responses between animal models and humans are not always aligned, therefore caution should be taken when comparing results across species. Moreover, conducting studies in human tissue are key for confirmation, as well as reliable clinical translation of the results obtained in cellular and animal models. Finally, muscle fibre-type specific analysis is required to provide a comprehensive understanding of the autophagy and metabolic responses in skeletal muscle. This approach may be particularly relevant when investigating populations known to exhibit shifts in muscle fibre type, such as aged, insulin resistant and endurance trained individuals.

This thesis provides novel insights into the autophagy responses in animal models of metabolic disease and in response to feeding and exercise in human skeletal muscle. This provides an important contribution to growing knowledge of autophagy and its role in metabolism. Improved understanding of autophagy regulation and its response to nutritional and exercise signals will guide the development and refinement of lifestyle and pharmaceutical treatments aiming to reduce the burden of metabolic disease associated with growing rates of obesity and an ageing population.

References

1. Morino K, Petersen KF, Shulman GI. Molecular Mechanisms of Insulin Resistance in Humans and Their Potential Links With Mitochondrial Dysfunction. Diabetes. 2006;55(Supplement 2):S9-S15.
2. Samuel VT, Shulman GI. Mechanisms for insulin resistance: common threads and missing links. Cell. 2012;148(5):852-71.
3. Codogno P, Meijer AJ. Autophagy: a potential link between obesity and insulin resistance. Cell metabolism. 2010;11(6):449-51.
4. Behrends C, Sowa ME, Gygi SP, Harper JW. Network organization of the human autophagy system. Nature. 2010;466(7302):68-76.
5. Boya P, Reggiori F, Codogno P. Emerging regulation and functions of autophagy. Nature cell biology. 2013;15(7):713-20.
6. Fritzen AM, Madsen AB, Kleinert M, Treebak JT, Lundsgaard AM, Jensen TE, et al. Regulation of autophagy in human skeletal muscle: effects of exercise, exercise training and insulin stimulation. The Journal of physiology. 2016;594(3):745-61.
7. Gallagher LE, Williamson LE, Chan EY. Advances in Autophagy Regulatory Mechanisms. Cells. 2016;5(2).
8. Kim KH, Lee MS. Autophagy as a crosstalk mediator of metabolic organs in regulation of energy metabolism. Rev Endocr Metab Disord. 2014;15(1):11-20.
9. Namkoong S, Cho CS, Semple I, Lee JH. Autophagy Dysregulation and Obesity-Associated Pathologies. Mol Cells. 2018;41(1):3-10.
10. Ruegsegger GN, Creo AL, Cortes TM, Dasari S, Nair KS. Altered mitochondrial function in insulin-deficient and insulin-resistant states. The Journal of clinical investigation. 2018;128(9):3671-81.
11. He C, Bassik MC, Moresi V, Sun K, Wei Y, Zou Z, et al. Exercise-induced BCL2-regulated autophagy is required for muscle glucose homeostasis. Nature. 2012;481(7382):511-5.
12. Hari A, Fealy CE, Kirwan JP. Short-Term Exercise Improves Hepatic Insulin Extraction in Individuals with Nonalcoholic Fatty Liver Disease. Diabetes. 2018;67(Supplement 1):1870-P.
13. Edwards CM, Cusi K. Prediabetes: A Worldwide Epidemic. Endocrinol Metab Clin North Am. 2016;45(4):751-64.
14. Tabák AG, Jokela M, Akbaraly TN, Brunner EJ, Kivimäki M, Witte DR. Trajectories of glycaemia, insulin sensitivity, and insulin secretion before diagnosis of type 2 diabetes: an analysis from the Whitehall II study. The Lancet. 2009;373(9682):2215-21.
15. Cavan D. IDF_Atlas 2015_UK. 2015.
16. Tabák AG, Herder C, Rathmann W, Brunner EJ, Kivimäki M. Prediabetes: a high-risk state for diabetes development. The Lancet. 2012;379(9833):2279-90.
17. Cefalu WTB, George; Blonde, Lawrence. Standards of medical care in diabetes. Diabetes care. 2016;39 Suppl 1:S1-S112.
18. World Health O. Global report on diabetes. Geneva: World Health Organization; 2016 2016.
19. Welfare AIoHa. Australia's health 2018. Australia's health series no 16 AUS 221 Canberra: AIHW. 2018.
20. Draznin B. Molecular mechanisms of insulin resistance: serine phosphorylation of insulin receptor substrate-1 and increased expression of p85alpha: the two sides of a coin. Diabetes. 2006;55(8):2392-7.
21. Kahn CR. The molecular mechanism of insulin action. Annual review of Medicine. 1985;36:429-51.

22. Dennis MD, Baum JI, Kimball SR, Jefferson LS. Mechanisms involved in the coordinate regulation of mTORC1 by insulin and amino acids. The Journal of biological chemistry. 2011;286(10):8287-96.
23. Cohen-Kaplan V, Livneh I, Avni N, Cohen-Rosenzweig C, Ciechanover A. The ubiquitin-proteasome system and autophagy: Coordinated and independent activities. Int J Biochem Cell Biol. 2016;79:403-18.
24. Vainshtein A, Grumati P, Sandri M, Bonaldo P. Skeletal muscle, autophagy, and physical activity: the menage a trois of metabolic regulation in health and disease. J Mol Med (Berl). 2014;92(2):127-37.
25. Gonzalez CD, Lee M-S, Marchetti P, Pietropaolo M, Towns R, Vaccaro MI, et al. The emerging role of autophagy in the pathophysiology of diabetes mellitus. Autophagy. 2014;7(1):2-11.
26. Scheen AJ. From obesity to diabetes: why, when and who? Acta clinica Belgica. 2000;55(1):9-15.
27. Kawahito S, Kitahata H, Oshita S. Problems associated with glucose toxicity: role of hyperglycemia-induced oxidative stress. World journal of gastroenterology. 2009;15(33):4137-42.
28. Unger RH. Lipotoxicity in the pathogenesis of obesity-dependent NIDDM. Genetic and clinical implications. Diabetes. 1995;44(8):863-70.
29. Singh R, Kaushik S, Wang Y, Xiang Y, Novak I, Komatsu M, et al. Autophagy regulates lipid metabolism. Nature. 2009;458(7242):1131-5.
30. Wang K. Molecular mechanism of hepatic steatosis: pathophysiological role of autophagy. Expert Rev Mol Med. 2016;18:e14.
31. Zhang J, Ney PA. Role of BNIP3 and NIX in cell death, autophagy, and mitophagy. Cell death and differentiation. 2009;16(7):939-46.
32. Zhande R, Mitchell JJ, Wu J, Sun XJ. Molecular Mechanism of Insulin-Induced Degradation of Insulin Receptor Substrate 1. Molecular and Cellular Biology. 2002;22(4):1016-26.
33. Sala D, Ivanova S, Plana N, Ribas V, Duran J, Bach D, et al. Autophagy-regulating TP53INP2 mediates muscle wasting and is repressed in diabetes. The Journal of clinical investigation. 2014;124(5):1914-27.
34. Schneider JL, Suh Y, Cuervo AM. Deficient chaperone-mediated autophagy in liver leads to metabolic dysregulation. Cell metabolism. 2014;20(3):417-32.
35. Yang L, Li P, Fu S, Calay ES, Hotamisligil GS. Defective hepatic autophagy in obesity promotes ER stress and causes insulin resistance. Cell metabolism. 2010;11(6):467-78.
36. Zhou L, Zhang J, Fang Q, Liu M, Liu X, Jia W, et al. Autophagy-mediated insulin receptor down-regulation contributes to endoplasmic reticulum stress-induced insulin resistance. Mol Pharmacol. 2009;76(3):596-603.
37. Cienchanover A. The ubiquitin-proteosome proteolytic pathway. Cell Adhesion and Communication. 1994;79:13-21.
38. Ikeda F, Dikic I. Atypical ubiquitin chains: new molecular signals. 'Protein Modifications: Beyond the Usual Suspects' review series. EMBO Rep. 2008;9(6):536-42.
39. Kirisako T, Kamei K, Murata S, Kato M, Fukumoto H, Kanie M, et al. A ubiquitin ligase complex assembles linear polyubiquitin chains. The European Molecular Biology Organization Journal. 2006;25:4877-87.
40. Gallastegui N, Groll M. The 26S proteasome: assembly and function of a destructive machine. Trends Biochem Sci. 2010;35(11):634-42.

41. Gamerdinger M, Carra S, Behl C. Emerging roles of molecular chaperones and co-chaperones in selective autophagy: focus on BAG proteins. J Mol Med (Berl). 2011;89(12):1175-82.
42. Bollinger LM, Powell JJ, Houmard JA, Witczak CA, Brault JJ. Skeletal muscle myotubes in severe obesity exhibit altered ubiquitin-proteasome and autophagic/lysosomal proteolytic flux. Obesity (Silver Spring). 2015;23(6):1185-93.
43. Fuertes G, Martin de Llano JJ, Villarroya A, Rivett AJ, Knecht E. Changes in the proteolytic activities of proteasomes and lysosomes in human fibroblasts produced by serum sithdrawal, amino-acid deprivation and confluent conditions. Biochemical Journal. 2003;375:75-85.
44. Zhao J, Brault JJ, Schild A, Cao P, Sandri M, Schiaffino S, et al. FoxO3 coordinately activates protein degradation by the autophagic/lysosomal and proteasomal pathways in atrophying muscle cells. Cell metabolism. 2007;6(6):472-83.
45. Berthet J, Berthet L, Appelmans F, De Duve C. Tissue fractionation studies. 2. The nature of the linkage between acid phosphatase and mitochondria in rat-liver tissue. Biochemical Journal. 1953;50(2):182-9.
46. Vainshtein A, Hood DA. The regulation of autophagy during exercise in skeletal muscle. Journal of applied physiology (Bethesda, Md : 1985). 2016;120(6):664-73.
47. Cuervo AM. Chaperone-mediated autophagy: Dice's 'wild' idea about lysosomal selectivity. Nature Reviews Molecular Cell Biology. 2011;12(8):535-41.
48. Cuervo AM, Wong E. Chaperone-mediated autophagy: roles in disease and aging. Cell Res. 2014;24(1):92-104.
49. Kaushik S, Bandyopadhyay U, Sridhar S, Kiffin R, Martinez-Vicente M, Kon M, et al. Chaperone-mediated autophagy at a glance. Journal of cell science. 2011;124(Pt 4):495-9.
50. Parzych KR, Klionsky DJ. An overview of autophagy: morphology, mechanism, and regulation. Antioxidants & redox signaling. 2014;20(3):460-73.
51. Kaur J, Debnath J. Autophagy at the crossroads of catabolism and anabolism. Nature reviews Molecular cell biology. 2015;16(8):461-72.
52. Singh R, Cuervo AM. Autophagy in the cellular energetic balance. Cell metabolism. 2011;13(5):495-504.
53. Schweiger M, Zechner R. Breaking the Barrier--Chaperone-Mediated Autophagy of Perilipins Regulates the Lipolytic Degradation of Fat. Cell metabolism. 2015;22(1):60-1.
54. Tasset I, Cuervo AM. Role of chaperone-mediated autophagy in metabolism. The FEBS journal. 2016;283(13):2403-13.
55. Ulbricht A, Gehlert S, Leciejewski B, Schiffer T, Bloch W, Hohfeld J. Induction and adaptation of chaperone-assisted selective autophagy CASA in response to resistance exercise in human skeletal muscle. Autophagy. 2015;11(3):538-46.
56. Wang C, Klionsky DJ. The molecular mechanism of autophagy. Molecular Medicine 2003;9(3/4):65-76.
57. De Duve C. The lysosome. Sci Am. 1963;208:64-72.
58. Mizushima N, Yoshimori T, Ohsumi Y. The role of Atg proteins in autophagosome formation. Annu Rev Cell Dev Biol. 2011;27:107-32.
59. Ohsumi Y. Historical landmarks of autophagy research. Cell Res. 2014;24(1):9-23.
60. Rocchi A, He C. Emerging roles of autophagy in metabolism and metabolic disorders. Front Biol (Beijing). 2015;10(2):154-64.
61. Hutson N, Mortimore GE. Suppression of cytoplasmic protein uptake by lysosome as the mechanism of protein regain in livers of starved-refed mice. The Journal of biological chemistry. 1962;257(16):9548-54.

62. Pfeifer U. Inhibition by insulin of the physiological autophagic breakdown of cell organelles. Acta Biol Med Ger. 1977;36(11-12):1691-4.
63. Kiffin R, Bandyopadhyay U, Cuervo AM. Oxidative stress and autophagy. Antioxidants and redox signaling. 2006;8(1 & 2).
64. Chen X, Li LJ, Zheng XY, Shen HQ, Shang SQ. Isolation of autophagosome subpopulations after induction of autophagy by calcium. Biochem Cell Biol. 2015;93(3):180-4.
65. Zachari M, Ganley IG. The mammalian ULK1 complex and autophagy initiation. Essays in biochemistry. 2017;61(6):585-96.
66. Turco E, Fracchiolla D, Martens S. Recruitment and Activation of the ULK1/Atg1 Kinase Complex in Selective Autophagy. Journal of molecular biology. 2019.
67. Itakura E, Kishi C, Inoue K, Mizushima N. Beclin 1 forms two distinct phosphatidylinositol 3-kinase complexes with mammalian Atg14 and UVRAG. Molecular biology of the cell. 2008;19(12):5360-72.
68. Wang CW. Lipid droplets, lipophagy, and beyond. Biochimica et biophysica acta. 2016;1861(8 Pt B):793-805.
69. Mizushima N, Yoshimori T, Levine B. Methods in mammalian autophagy research. Cell. 2010;140(3):313-26.
70. Tooze SA, Yoshimori T. The origin of the autophagosomal membrane. Nature cell biology. 2010;12(9):831-5.
71. Mizushima N, Yoshimori T. How to Interpret LC3 Immunoblotting. Autophagy. 2014;3(6):542-5.
72. Ichimura Y, Kirisako T, Takao T, Satomi Y, Shimonishi Y, Ishihara N, et al. A ubiquitin-like system mediates protein lipidation. Nature. 2000;408(6811):488-92.
73. Fujita N, Itoh T, Omori H, Fukuda M, Noda T, Yoshimori T. The Atg16L complex specifies the site of LC3 lipidation for membrane biogenesis in autophagy. Molecular biology of the cell. 2008;19(5):2092-100.
74. Klionsky DJ, Abdelmohsen K, Abe A, Abedin MJ, Abeliovich H, Acevedo Arozena A, et al. Guidelines for the use and interpretation of assays for monitoring autophagy (3rd edition). Autophagy. 2016;12(1):1-222.
75. Nowak J, Archange C, Tardivel-Lacombe J, Pontarotti P, Pebusque MJ, Vaccaro MI, et al. The TP53INP2 protein is required for autophagy in mammalian cells. Molecular biology of the cell. 2009;20(3):870-81.
76. Pankiv S, Clausen TH, Lamark T, Brech A, Bruun JA, Outzen H, et al. p62/SQSTM1 binds directly to Atg8/LC3 to facilitate degradation of ubiquitinated protein aggregates by autophagy. The Journal of biological chemistry. 2007;282(33):24131-45.
77. Shaid S, Brandts CH, Serve H, Dikic I. Ubiquitination and selective autophagy. Cell death and differentiation. 2013;20(1):21-30.
78. Liu L, Feng D, Chen G, Chen M, Zheng Q, Song P, et al. Mitochondrial outer-membrane protein FUNDC1 mediates hypoxia-induced mitophagy in mammalian cells. Nature cell biology. 2012;14(2):177-85.
79. Kubli DA, Gustafsson AB. Mitochondria and mitophagy: the yin and yang of cell death control. Circulation research. 2012;111(9):1208-21.
80. Twig G, Elorza A, Molina AJ, Mohamed H, Wikstrom JD, Walzer G, et al. Fission and selective fusion govern mitochondrial segregation and elimination by autophagy. The EMBO journal. 2008;27(2):433-46.
81. Huynh KK, Eskelinen EL, Scott CC, Malevanets A, Saftig P, Grinstein S. LAMP proteins are required for fusion of lysosomes with phagosomes. The EMBO journal. 2007;26(2):313-24.

82. Koga H, Kaushik S, Cuervo AM. Altered lipid content inhibits autophagic vesicular fusion. The FASEB Journal. 2010;24(8):3052-65.
83. Settembre C, De Cegli R, Mansueto G, Saha PK, Vetrini F, Visvikis O, et al. TFEB controls cellular lipid metabolism through a starvation-induced autoregulatory loop. Nature cell biology. 2013;15(6):647-58.
84. Munson MJ, Allen GF, Toth R, Campbell DG, Lucocq JM, Ganley IG. mTOR activates the VPS34-UVRAG complex to regulate autolysosomal tubulation and cell survival. The EMBO journal. 2015;34(17):2272-90.
85. Mony VK, Benjamin S, O'Rourke EJ. A lysosome-centered view of nutrient homeostasis. Autophagy. 2016;12(4):619-31.
86. Liu B, Du H, Rutkowski R, Gartner A, Wang X. LAAT-1 is the lysosomal lysine/arginine transporter that maintains amino acid homeostasis. Science (New York, NY). 2012;337(6092):351-4.
87. Town M, Jean G, Cherqui S, Attard M, Forestier L, Whitmore SA, et al. A novel gene encoding an integral membrane protein is mutated in nephropathic cystinosis. Nat Genet. 1998;18(4):319-24.
88. Luzio JP, Pryor PR, Bright NA. Lysosomes: fusion and function. Nature reviews Molecular cell biology. 2007;8(8):622-32.
89. Jamart C, Benoit N, Raymackers JM, Kim HJ, Kim CK, Francaux M. Autophagy-related and autophagy-regulatory genes are induced in human muscle after ultraendurance exercise. European journal of applied physiology. 2012;112(8):3173-7.
90. Jamart C, Naslain D, Gilson H, Francaux M. Higher activation of autophagy in skeletal muscle of mice during endurance exercise in the fasted state. American journal of physiology Endocrinology and metabolism. 2013;305(8):E964-74.
91. Moller AB, Kampmann U, Hedegaard J, Thorsen K, Nordentoft I, Vendelbo MH, et al. Altered gene expression and repressed markers of autophagy in skeletal muscle of insulin resistant patients with type 2 diabetes. Scientific reports. 2017;7:43775.
92. Moller AB, Vendelbo MH, Christensen B, Clasen BF, Bak AM, Jorgensen JO, et al. Physical exercise increases autophagic signaling through ULK1 in human skeletal muscle. Journal of applied physiology (Bethesda, Md : 1985). 2015;118(8):971-9.
93. Pietrocola F, Izzo V, Niso-Santano M, Vacchelli E, Galluzzi L, Maiuri MC, et al. Regulation of autophagy by stress-responsive transcription factors. Semin Cancer Biol. 2013;23(5):310-22.
94. Kim J, Kundu M, Viollet B, Guan KL. AMPK and mTOR regulate autophagy through direct phosphorylation of Ulk1. Nature cell biology. 2011;13(2):132-41.
95. Hosokawa N, Hara T, Kaizuka T, Kishi C, Takamura A, Miura Y, et al. Nutrient-dependent mTORC1 association with the ULK1-Atg13-FIP200 complex required for autophagy. Molecular biology of the cell. 2009;20(7):1981-91.
96. Jung CH, Jun CB, Ro SH, Kim YM, Otto NM, Cao J, et al. ULK-Atg13-FIP200 complexes mediate mTOR signaling to the autophagy machinery. Molecular biology of the cell. 2009;20(7):1992-2003.
97. Vendelbo MH, Moller AB, Christensen B, Nellemann B, Clasen BF, Nair KS, et al. Fasting increases human skeletal muscle net phenylalanine release and this is associated with decreased mTOR signaling. PloS one. 2014;9(7):e102031.
98. Settembre C, Ballabio A. Lysosome: regulator of lipid degradation pathways. Trends Cell Biol. 2014;24(12):743-50.

99. Castets P, Lin S, Rion N, Di Fulvio S, Romanino K, Guridi M, et al. Sustained activation of mTORC1 in skeletal muscle inhibits constitutive and starvation-induced autophagy and causes a severe, late-onset myopathy. Cell metabolism. 2013;17(5):731-44.
100. Miyazaki M, McCarthy JJ, Fedele MJ, Esser KA. Early activation of mTORC1 signalling in response to mechanical overload is independent of phosphoinositide 3-kinase/Akt signalling. The Journal of physiology. 2011;589(Pt 7):1831-46.
101. Schwalm C, Jamart C, Benoit N, Naslain D, Premont C, Prevet J, et al. Activation of autophagy in human skeletal muscle is dependent on exercise intensity and AMPK activation. FASEB journal : official publication of the Federation of American Societies for Experimental Biology. 2015;29(8):3515-26.
102. Egan DF, Shackelford DB, Mihaylova MM, Gelino S, Kohnz RA, Mair W, et al. Phosphorylation of ULK1 (hATG1) by AMP-activated protein kinase connects energy sensing to mitophagy. Science (New York, NY). 2011;331(6016):456-61.
103. Nazio F, Strappazzon F, Antonioli M, Bielli P, Cianfanelli V, Bordi M, et al. mTOR inhibits autophagy by controlling ULK1 ubiquitylation, self-association and function through AMBRA1 and TRAF6. Nature cell biology. 2013;15(4):406-16.
104. Russell RC, Tian Y, Yuan H, Park HW, Chang YY, Kim J, et al. ULK1 induces autophagy by phosphorylating Beclin-1 and activating VPS34 lipid kinase. Nature cell biology. 2013;15(7):741-50.
105. Jacobs BL, You JS, Frey JW, Goodman CA, Gundermann DM, Hornberger TA. Eccentric contractions increase the phosphorylation of tuberous sclerosis complex-2 (TSC2) and alter the targeting of TSC2 and the mechanistic target of rapamycin to the lysosome. The Journal of physiology. 2013;591(18):4611-20.
106. Inoki K, Zhu T, Guan KL. TSC2 mediates cellular energy response to control cell growth and survival. Cell. 2003;115(5):577-90.
107. Roczniak-Ferguson A, Petit CS, Froehlich F, Qian S, Ky J, Angarola B, et al. The transcription factor TFEB links mTORC1 signaling to transcriptional control of lysosome homeostasis. Sci Signal. 2012;5(228):ra42.
108. Poso AR, Surmacz CA, Mortimore GE. Inhibition of intracellular protein degradation by ethanol in perfused rat liver. The Biochemical journal. 1987;242(2):459-64.
109. Kwon B, Querfurth HW. Palmitate activates mTOR/p70S6K through AMPK inhibition and hypophosphorylation of raptor in skeletal muscle cells: Reversal by oleate is similar to metformin. Biochimie. 2015;118:141-50.
110. Sengupta S, Peterson TR, Laplante M, Oh S, Sabatini DM. mTORC1 controls fasting-induced ketogenesis and its modulation by ageing. Nature. 2010;468(7327):1100-4.
111. Sancak Y, Peterson TR, Shaul YD, Lindquist RA, Thoreen CC, Bar-Peled L, et al. The Rag GTPases bind raptor and mediate amino acid signaling to mTORC1. Science (New York, NY). 2008;320(5882):1496-501.
112. Martina JA, Chen Y, Gucek M, Puertollano R. MTORC1 functions as a transcriptional regulator of autophagy by preventing nuclear transport of TFEB. Autophagy. 2012;8(6):903-14.
113. Martina JA, Diab HI, Lishu L, Jeong AL, Patange S, Raben N, et al. The nutrient-responsive transcription factor TFE3 promotes autophagy, lysosomal biogenesis, and clearance of cellular debris. Sci Signal. 2014;7(309):ra9.
114. Palmieri M, Impey S, Kang H, di Ronza A, Pelz C, Sardiello M, et al. Characterization of the CLEAR network reveals an integrated control of cellular clearance pathways. Human molecular genetics. 2011;20(19):3852-66.
115. Settembre C, Di Malta C, Polito VA, Garcia Arencibia M, Vetrini F, Erdin S, et al. TFEB links autophagy to lysosomal biogenesis. Science (New York, NY). 2011;332(6036):1429-33.

116. Carter ME, Brunet A. FOXO transcription factors. Current biology : CB. 2007;17(4):R113-4.
117. Eijkelenboom A, Burgering BM. FOXOs: signalling integrators for homeostasis maintenance. Nature reviews Molecular cell biology. 2013;14(2):83-97.
118. Barthel A, Schmoll D, Unterman TG. FoxO proteins in insulin action and metabolism. Trends Endocrinol Metab. 2005;16(4):183-9.
119. Saleem A, Hood DA. Acute exercise induces tumour suppressor protein p53 translocation to the mitochondria and promotes a p53-Tfam-mitochondrial DNA complex in skeletal muscle. The Journal of physiology. 2013;591(14):3625-36.
120. Goldstein I, Rotter V. Regulation of lipid metabolism by p53 - fighting two villains with one sword. Trends Endocrinol Metab. 2012;23(11):567-75.
121. Finck BN, Gropler MC, Chen Z, Leone TC, Croce MA, Harris TE, et al. Lipin 1 is an inducible amplifier of the hepatic PGC-1alpha/PPARalpha regulatory pathway. Cell metabolism. 2006;4(3):199-210.
122. Peterson TR, Sengupta SS, Harris TE, Carmack AE, Kang SA, Balderas E, et al. mTOR complex 1 regulates lipin 1 localization to control the SREBP pathway. Cell. 2011;146(3):408-20.
123. Park EJ, Lee AY, Chang SH, Yu KN, Kim JH, Cho MH. Role of p53 in the cellular response following oleic acid accumulation in Chang liver cells. Toxicol Lett. 2014;224(1):114-20.
124. Kenzelmann Broz D, Spano Mello S, Bieging KT, Jiang D, Dusek RL, Brady CA, et al. Global genomic profiling reveals an extensive p53-regulated autophagy program contributing to key p53 responses. Genes Dev. 2013;27(9):1016-31.
125. Stambolic V, MacPherson D, Sas D, Lin Y, Snow B, Jang Y, et al. Regulation of PTEN transcription by p53. Molecular cell. 2001;8(2):317-25.
126. Periyasamy-Thandavan S, Jiang M, Schoenlein P, Dong Z. Autophagy: molecular machinery, regulation, and implications for renal pathophysiology. American journal of physiology Renal physiology. 2009;297(2):F244-56.
127. Taniguchi CM, Emanuelli B, Kahn CR. Critical nodes in signalling pathways: insights into insulin action. Nature reviews Molecular cell biology. 2006;7(2):85-96.
128. Newsholme EA, Dimitriadis G. <newsholme2001 physiological effects of insulin.pdf>. Experimental and Clinical Endocrinology and Diabetes. 2001;109(Suppl 2):S122-S34.
129. Ashford TP, Porter KR. Cytoplasmic components in hepatic cell lysosomes. The Journal of cell biology. 1962;12:198-202.
130. Korolchuk VI, Saiki S, Lichtenberg M, Siddiqi FH, Roberts EA, Imarisio S, et al. Lysosomal positioning coordinates cellular nutrient responses. Nature cell biology. 2011;13(4):453-60.
131. Mortimore GE, Lardeux BR, Adams CE. Regulation of microautophagy and basal protein turnover in rat liver. Effects of short-term starvation. The Journal of biological chemistry. 1988;263(5):2506-12.
132. Komatsu M, Waguri S, Ueno T, Iwata J, Murata S, Tanida I, et al. Impairment of starvation-induced and constitutive autophagy in Atg7-deficient mice. The Journal of cell biology. 2005;169(3):425-34.
133. Sandri M. Autophagy in skeletal muscle. FEBS Lett. 2010;584(7):1411-6.
134. Grumati P, Coletto L, Sandri M, Bonaldo P. Autophagy induction rescues muscular dystrophy. Autophagy. 2011;7(4):426-8.
135. O'Leary MF, Vainshtein A, Carter HN, Zhang Y, Hood DA. Denervation-induced mitochondrial dysfunction and autophagy in skeletal muscle of apoptosis-deficient animals. American journal of physiology Cell physiology. 2012;303(4):C447-54.

136. Grumati P, Coletto L, Sabatelli P, Cescon M, Angelin A, Bertaggia E, et al. Autophagy is defective in collagen VI muscular dystrophies, and its reactivation rescues myofiber degeneration. Nature medicine. 2010;16(11):1313-20.
137. Nogalska A, D'Agostino C, Terracciano C, Engel WK, Askanas V. Impaired autophagy in sporadic inclusion-body myositis and in endoplasmic reticulum stress-provoked cultured human muscle fibers. Am J Pathol. 2010;177(3):1377-87.
138. Dowling JJ, Moore SA, Kalimo H, Minassian BA. X-linked myopathy with excessive autophagy: a failure of self-eating. Acta Neuropathol. 2015;129(3):383-90.
139. Masiero E, Agatea L, Mammucari C, Blaauw B, Loro E, Komatsu M, et al. Autophagy is required to maintain muscle mass. Cell metabolism. 2009;10(6):507-15.
140. Neel BA, Lin Y, Pessin JE. Skeletal muscle autophagy: a new metabolic regulator. Trends Endocrinol Metab. 2013;24(12):635-43.
141. Rowland TJ, Sweet ME, Mestroni L, Taylor MR. Danon disease - dysregulation of autophagy in a multisystem disorder with cardiomyopathy. Journal of cell science. 2016;129(11):2135-43.
142. Kitaoka Y, Nakazato K, Ogasawara R. Combined effects of resistance training and calorie restriction on mitochondrial fusion and fission proteins in rat skeletal muscle. Journal of applied physiology (Bethesda, Md : 1985). 2016;121(3):806-10.
143. Wohlgemuth SE, Seo AY, Marzetti E, Lees HA, Leeuwenburgh C. Skeletal muscle autophagy and apoptosis during aging: effects of calorie restriction and life-long exercise. Experimental gerontology. 2010;45(2):138-48.
144. Huang R, Liu W. Identifying an essential role of nuclear LC3 for autophagy. Autophagy. 2015;11(5):852-3.
145. Lira VA, Okutsu M, Zhang M, Greene NP, Laker RC, Breen DS, et al. Autophagy is required for exercise training-induced skeletal muscle adaptation and improvement of physical performance. FASEB journal : official publication of the Federation of American Societies for Experimental Biology. 2013;27(10):4184-93.
146. Ogata T, Oishi Y, Higuchi M, Muraoka I. Fasting-related autophagic response in slow- and fast-twitch skeletal muscle. Biochemical and biophysical research communications. 2010;394(1):136-40.
147. Hayashi T, Boyko EJ, Sato KK, McNeely MJ, Leonetti DL, Kahn SE, et al. Patterns of insulin concentration during the OGTT predict the risk of type 2 diabetes in Japanese Americans. Diabetes care. 2013;36(5):1229-35.
148. Cuervo AM, Dice JF. A receptor for the selective uptake and degradation of proteins by lysosomes. Science (New York, NY). 1996;273(5274):501-3.
149. Bandyopadhyay U, Kaushik S, Varticovski L, Cuervo AM. The chaperone-mediated autophagy receptor organizes in dynamic protein complexes at the lysosomal membrane. Mol Cell Biol. 2008;28(18):5747-63.
150. Bandyopadhyay U, Sridhar S, Kaushik S, Kiffin R, Cuervo AM. Identification of regulators of chaperone-mediated autophagy. Molecular cell. 2010;39(4):535-47.
151. Arias E, Koga H, Diaz A, Mocholi E, Patel B, Cuervo AM. Lysosomal mTORC2/PHLPP1/Akt Regulate Chaperone-Mediated Autophagy. Molecular cell. 2015;59(2):270-84.
152. Cuervo AM, Mann L, Bonten EJ, d'Azzo A, Dice JF. Cathepsin A regulates chaperone-mediated autophagy through cleavage of the lysosomal receptor. The EMBO journal. 2003;22(1):47-59.
153. Kaushik S, Massey AC, Cuervo AM. Lysosome membrane lipid microdomains: novel regulators of chaperone-mediated autophagy. The EMBO journal. 2006;25(17):3921-33.

154. Cuervo AM, Stefanis L, Fredenburg R, Lansbury PT, Sulzer D. Impaired degradation of mutant alpha-synuclein by chaperone-mediated autophagy. Science (New York, NY). 2004;305(5688):1292-5.
155. Xilouri M, Brekk OR, Landeck N, Pitychoutis PM, Papasilekas T, Papadopoulou-Daifoti Z, et al. Boosting chaperone-mediated autophagy in vivo mitigates alpha-synuclein-induced neurodegeneration. Brain : a journal of neurology. 2013;136(Pt 7):2130-46.
156. Chen S, Ferrone FA, Wetzel R. Huntington's disease age-of-onset linked to polyglutamine aggregation nucleation. Proceedings of the National Academy of Sciences of the United States of America. 2002;99(18):11884-9.
157. Martinez-Vicente M, Talloczy Z, Wong E, Tang G, Koga H, Kaushik S, et al. Cargo recognition failure is responsible for inefficient autophagy in Huntington's disease. Nature neuroscience. 2010;13(5):567-76.
158. Kon M, Kiffin R, Koga H, Chapochnick J, Macian F, Varticovski L, et al. Chaperone-mediated autophagy is required for tumor growth. Science translational medicine. 2011;3(109):109ra17.
159. Schneider JL, Villarroya J, Diaz-Carretero A, Patel B, Urbanska AM, Thi MM, et al. Loss of hepatic chaperone-mediated autophagy accelerates proteostasis failure in aging. Aging cell. 2015;14(2):249-64.
160. Cuervo AM, Knecht E, Terlecky SR, Dice JF. Activation of a selective pathway of lysosomal proteolysis in rat liver by prolonged starvation. The American journal of physiology. 1995;269(5 Pt 1):C1200-8.
161. Beals JW, Sukiennik RA, Nallabelli J, Emmons RS, van Vliet S, Young JR, et al. Anabolic sensitivity of postprandial muscle protein synthesis to the ingestion of a protein-dense food is reduced in overweight and obese young adults. The American journal of clinical nutrition. 2016;104(4):1014-22.
162. DeFronzo RA, Tobin JD, Andres R. Glucose clamp technique: a method for quantifying insulin secretion and resistance. The American journal of physiology. 1979;237(3):E214-23.
163. Singh B, Saxena A. Surrogate markers of insulin resistance: A review. World J Diabetes. 2010;1(2):36-47.
164. Thomas GN, Critchley JA, Tomlinson B, Anderson PJ, Lee ZS, Chan JC. Obesity, independent of insulin resistance, is a major determinant of blood pressure in normoglycemic Hong Kong Chinese. Metabolism: clinical and experimental. 2000;49(12):1523-8.
165. Antunes LC, Elkfury JL, Jornada MN, Foletto KC, Bertoluci MC. Validation of HOMA-IR in a model of insulin-resistance induced by a high-fat diet in Wistar rats. Archives of endocrinology and metabolism. 2016;60(2):138-42.
166. Haffner SM, Gonzalez C, Miettinen H, Kennedy E, Stern MP. A Prospective Analysis of the HOMA Model: The Mexico City Diabetes Study. Diabetes care. 1996;19(10):1138.
167. Katsuki A, Sumida Y, Gabazza EC, Murashima S, Furuta M, Araki-Sasaki R, et al. Homeostasis Model Assessment Is a Reliable Indicator of Insulin Resistance During Follow-up of Patients With Type 2 Diabetes. Diabetes care. 2001;24(2):362.
168. Wallace TM, Levy JC, Matthews DR. Use and Abuse of HOMA Modeling. Diabetes care. 2004;27(6):1487.
169. Diagnosis and classification of diabetes mellitus. Diabetes care. 2014;37 Suppl 1:S81-90.
170. Le Floch JP, Escuyer P, Baudin E, Baudon D, Perlemuter L. Blood glucose area under the curve. Methodological aspects. Diabetes care. 1990;13(2):172-5.
171. Liu HY, Han J, Cao SY, Hong T, Zhuo D, Shi J, et al. Hepatic autophagy is suppressed in the presence of insulin resistance and hyperinsulinemia: inhibition of FoxO1-dependent

expression of key autophagy genes by insulin. The Journal of biological chemistry. 2009;284(45):31484-92.
172. Zhang Q, Li Y, Liang T, Lu X, Zhang C, Liu X, et al. ER stress and autophagy dysfunction contribute to fatty liver in diabetic mice. International journal of biological sciences. 2015;11(5):559-68.
173. Gonzalez-Rodriguez A, Mayoral R, Agra N, Valdecantos MP, Pardo V, Miquilena-Colina ME, et al. Impaired autophagic flux is associated with increased endoplasmic reticulum stress during the development of NAFLD. Cell death & disease. 2014;5:e1179.
174. Ezaki J, Matsumoto N, Takeda-Ezaki M, Komatsu M, Takahashi K, Hiraoka Y, et al. Liver autophagy contributes to the maintenance of blood glucose and amino acid levels. Autophagy. 2014;7(7):727-36.
175. O'Rourke EJ, Ruvkun G. MXL-3 and HLH-30 transcriptionally link lipolysis and autophagy to nutrient availability. Nature cell biology. 2013;15(6):668-76.
176. Tsunemi T, Ashe TD, Morrison BE, Soriano KR, Au J, Roque RA, et al. PGC-1alpha rescues Huntington's disease proteotoxicity by preventing oxidative stress and promoting TFEB function. Science translational medicine. 2012;4(142):142ra97.
177. Mei S, Ni HM, Manley S, Bockus A, Kassel KM, Luyendyk JP, et al. Differential roles of unsaturated and saturated fatty acids on autophagy and apoptosis in hepatocytes. J Pharmacol Exp Ther. 2011;339(2):487-98.
178. Alex S, Boss A, Heerschap A, Kersten S. Exercise training improves liver steatosis in mice. Nutr Metab (Lond). 2015;12:29.
179. Guo Q, Shi Q, Li H, Liu J, Wu S, Sun H, et al. Glycolipid Metabolism Disorder in the Liver of Obese Mice Is Improved by TUDCA via the Restoration of Defective Hepatic Autophagy. Int J Endocrinol. 2015;2015:687938.
180. Wang H, Sun RQ, Zeng XY, Zhou X, Li S, Jo E, et al. Restoration of autophagy alleviates hepatic ER stress and impaired insulin signalling transduction in high fructose-fed male mice. Endocrinology. 2015;156(1):169-81.
181. Kim KH, Jeong YT, Oh H, Kim SH, Cho JM, Kim YN, et al. Autophagy deficiency leads to protection from obesity and insulin resistance by inducing Fgf21 as a mitokine. Nature medicine. 2013;19(1):83-92.
182. Kelley DE, He J, Menshikova EV, Ritov VB. Dysfunction of mitochondria in human skeletal muscle in type 2 diabetes. Diabetes. 2002;51(10):2944-50.
183. Lillioja S, Young AA, Culter CL, Ivy JL, Abbott WG, Zawadzki JK, et al. Skeletal muscle capillary density and fiber type are possible determinants of in vivo insulin resistance in man. The Journal of clinical investigation. 1987;80(2):415-24.
184. Mogensen M, Sahlin K, Fernstrom M, Glintborg D, Vind BF, Beck-Nielsen H, et al. Mitochondrial respiration is decreased in skeletal muscle of patients with type 2 diabetes. Diabetes. 2007;56(6):1592-9.
185. Marin P, Andersson B, Krotkiewski M, Bjorntorp P. Muscle fiber composition and capillary density in women and men with NIDDM. Diabetes care. 1994;17(5):382-6.
186. Tanner CJ, Barakat HA, Dohm GL, Pories WJ, MacDonald KG, Cunningham PR, et al. Muscle fiber type is associated with obesity and weight loss. American journal of physiology Endocrinology and metabolism. 2002;282(6):E1191-6.
187. Kruse R, Vind BF, Petersson SJ, Kristensen JM, Hojlund K. Markers of autophagy are adapted to hyperglycaemia in skeletal muscle in type 2 diabetes. Diabetologia. 2015;58(9):2087-95.

188. Cersosimo E, Solis-Herrera C, Trautmann ME, Malloy J, Triplitt CL. Assessment of pancreatic beta-cell function: review of methods and clinical applications. Current diabetes reviews. 2014;10:2-42.
189. McGarrah RW, Slentz CA, Kraus WE. The Effect of Vigorous- Versus Moderate-Intensity Aerobic Exercise on Insulin Action. Curr Cardiol Rep. 2016;18(12):117.
190. Brandt N, Gunnarsson TP, Bangsbo J, Pilegaard H. Exercise and exercise training-induced increase in autophagy markers in human skeletal muscle. Physiological reports. 2018;6(7):e13651.
191. Petersen MC, Shulman GI. Mechanisms of Insulin Action and Insulin Resistance. Physiological reviews. 2018;98(4):2133-223.
192. Moulis M, Vindis C. Autophagy in Metabolic Age-Related Human Diseases. Cells. 2018;7(10).
193. Hara T, Takamura A, Kishi C, Iemura S, Natsume T, Guan JL, et al. FIP200, a ULK-interacting protein, is required for autophagosome formation in mammalian cells. The Journal of cell biology. 2008;181(3):497-510.
194. Kaushik S, Cuervo AM. The coming of age of chaperone-mediated autophagy. Nature reviews Molecular cell biology. 2018;19(6):365-81.
195. Sarparanta J, Garcia-Macia M, Singh R. Autophagy and Mitochondria in Obesity and Type 2 Diabetes. Current diabetes reviews. 2017;13(4):352-69.
196. Shibata M, Yoshimura K, Furuya N, Koike M, Ueno T, Komatsu M, et al. The MAP1-LC3 conjugation system is involved in lipid droplet formation. Biochemical and biophysical research communications. 2009;382(2):419-23.
197. Campbell TL, Mitchell AS, McMillan EM, Bloemberg D, Pavlov D, Messa I, et al. High-fat feeding does not induce an autophagic or apoptotic phenotype in female rat skeletal muscle. Exp Biol Med (Maywood). 2015;240(5):657-68.
198. Turner N, Kowalski GM, Leslie SJ, Risis S, Yang C, Lee-Young RS, et al. Distinct patterns of tissue-specific lipid accumulation during the induction of insulin resistance in mice by high-fat feeding. Diabetologia. 2013;56(7):1638-48.
199. Camera DM, West DW, Burd NA, Phillips SM, Garnham AP, Hawley JA, et al. Low muscle glycogen concentration does not suppress the anabolic response to resistance exercise. Journal of applied physiology (Bethesda, Md : 1985). 2012;113(2):206-14.
200. Vandesompele J, De Preter K, Pattyn F, Poppe B, Van Roy N, De Paepe A, et al. Accurate normalization of real-time quantitative RT-PCR data by geometric averaging of multiple internal control genes. Genome Biology. 2002;3(7):research0034.1.
201. Rhinn H, Scherman D, Escriou V. One-step quantification of single-stranded DNA in the presence of RNA using Oligreen in a real-time polymerase chain reaction thermocycler. Analytical biochemistry. 2008;372(1):116-8.
202. Reyderman L, Stavchansky S. Determination of single-stranded oligodeoxynucleotides by capillary gel electrophoresis with laser induced fluorescence and on column derivatization. Journal of chromatography A. 1996;755(2):271-80.
203. Mollica JP, Oakhill JS, Lamb GD, Murphy RM. Are genuine changes in protein expression being overlooked? Reassessing Western blotting. Analytical biochemistry. 2009;386(2):270-5.
204. Murphy RM, Lamb GD. Important considerations for protein analyses using antibody based techniques: down-sizing Western blotting up-sizes outcomes. The Journal of physiology. 2013;591(23):5823-31.

205. Khamzina L, Veilleux A, Bergeron S, Marette A. Increased activation of the mammalian target of rapamycin pathway in liver and skeletal muscle of obese rats: possible involvement in obesity-linked insulin resistance. Endocrinology. 2005;146(3):1473-81.
206. Korsheninnikova E, van der Zon GC, Voshol PJ, Janssen GM, Havekes LM, Grefhorst A, et al. Sustained activation of the mammalian target of rapamycin nutrient sensing pathway is associated with hepatic insulin resistance, but not with steatosis, in mice. Diabetologia. 2006;49(12):3049-57.
207. Ueno M, Carvalheira JB, Tambascia RC, Bezerra RM, Amaral ME, Carneiro EM, et al. Regulation of insulin signalling by hyperinsulinaemia: role of IRS-1/2 serine phosphorylation and the mTOR/p70 S6K pathway. Diabetologia. 2005;48(3):506-18.
208. Cuervo AM, Dice JF. Regulation of lamp2a levels in the lysosomal membrane. Traffic (Copenhagen, Denmark). 2000;1(7):570-83.
209. Kaushik S, Cuervo AM. Degradation of lipid droplet-associated proteins by chaperone-mediated autophagy facilitates lipolysis. Nature cell biology. 2015;17(6):759-70.
210. Rodriguez-Navarro JA, Kaushik S, Koga H, Dall'Armi C, Shui G, Wenk MR, et al. Inhibitory effect of dietary lipids on chaperone-mediated autophagy. Proceedings of the National Academy of Sciences of the United States of America. 2012;109(12):E705-14.
211. Das S, Seth RK, Kumar A, Kadiiska MB, Michelotti G, Diehl AM, et al. Purinergic receptor X7 is a key modulator of metabolic oxidative stress-mediated autophagy and inflammation in experimental nonalcoholic steatohepatitis. Am J Physiol Gastrointest Liver Physiol. 2013;305(12):G950-63.
212. Chava S, Lee C, Aydin Y, Chandra PK, Dash A, Chedid M, et al. Chaperone-mediated autophagy compensates for impaired macroautophagy in the cirrhotic liver to promote hepatocellular carcinoma. Oncotarget. 2017;8(25):40019-36.
213. Kaushik S, Massey AC, Mizushima N, Cuervo AM. Constitutive activation of chaperone-mediated autophagy in cells with impaired macroautophagy. Molecular biology of the cell. 2008;19(5):2179-92.
214. Yamada E, Bastie CC, Koga H, Wang Y, Cuervo AM, Pessin JE. Mouse skeletal muscle fiber-type-specific macroautophagy and muscle wasting are regulated by a Fyn/STAT3/Vps34 signaling pathway. Cell reports. 2012;1(5):557-69.
215. Ehrlicher SE, Stierwalt HD, Newsom SA, Robinson MM. Skeletal muscle autophagy remains responsive to hyperinsulinemia and hyperglycemia at higher plasma insulin concentrations in insulin-resistant mice. Physiological reports. 2018;6(14):e13810.
216. Naito T, Kuma A, Mizushima N. Differential contribution of insulin and amino acids to the mTORC1-autophagy pathway in the liver and muscle. The Journal of biological chemistry. 2013;288(29):21074-81.
217. Zheng Y, Ley SH, Hu FB. Global aetiology and epidemiology of type 2 diabetes mellitus and its complications. Nature reviews Endocrinology. 2018;14(2):88-98.
218. Lim YM, Lim H, Hur KY, Quan W, Lee HY, Cheon H, et al. Systemic autophagy insufficiency compromises adaptation to metabolic stress and facilitates progression from obesity to diabetes. Nature communications. 2014;5:4934.
219. Lo Verso F, Carnio S, Vainshtein A, Sandri M. Autophagy is not required to sustain exercise and PRKAA1/AMPK activity but is important to prevent mitochondrial damage during physical activity. Autophagy. 2014;10(11):1883-94.
220. Howell JJ, Manning BD. mTOR couples cellular nutrient sensing to organismal metabolic homeostasis. Trends Endocrinol Metab. 2011;22(3):94-102.

221. Bentzinger CF, Romanino K, Cloëtta D, Lin S, Mascarenhas JB, Oliveri F, et al. Skeletal Muscle-Specific Ablation of raptor, but Not of rictor, Causes Metabolic Changes and Results in Muscle Dystrophy. Cell metabolism. 2008;8(5):411-24.
222. Risson V, Mazelin L, Roceri M, Sanchez H, Moncollin V, Corneloup C, et al. Muscle inactivation of mTOR causes metabolic and dystrophin defects leading to severe myopathy. The Journal of cell biology. 2009;187(6):859-74.
223. Harada D, Seino Y. Growth Hormone and Bone. In: Klein GL, editor. Bone Drugs in Pediatrics: Efficacy and Challenges. Boston, MA: Springer US; 2014. p. 117-34.
224. Chen H, Charlat O, Tartaglia LA, Woolf EA, Weng X, Ellis SJ, et al. Evidence that the diabetes gene encodes the leptin receptor: identification of a mutation in the leptin receptor gene in db/db mice. Cell. 1996;84(3):491-5.
225. King AJ. The use of animal models in diabetes research. British journal of pharmacology. 2012;166(3):877-94.
226. Cefalu WT. Animal models of type 2 diabetes: clinical presentation and pathophysiological relevance to the human condition. ILAR journal. 2006;47(3):186-98.
227. O'Neill BT, Bhardwaj G, Penniman CM, Krumpoch MT, Suarez Beltran PA, Klaus K, et al. FoxO Transcription Factors Are Critical Regulators of Diabetes-Related Muscle Atrophy. Diabetes. 2019;68(3):556-70.
228. Yang B, Sun J, Yuan Y, Sun Z. Effects of atorvastatin on autophagy in skeletal muscles of diabetic rats. Journal of diabetes investigation. 2018;9(4):753-61.
229. Tam BT, Pei XM, Yung BY, Yip SP, Chan LW, Wong CS, et al. Unacylated ghrelin restores insulin and autophagic signaling in skeletal muscle of diabetic mice. Pflugers Archiv : European journal of physiology. 2015;467(12):2555-69.
230. Perry BD, Caldow MK, Brennan-Speranza TC, Sbaraglia M, Jerums G, Garnham A, et al. Muscle atrophy in patients with Type 2 Diabetes Mellitus: roles of inflammatory pathways, physical activity and exercise. Exercise immunology review. 2016;22:94-109.
231. Krook A, Roth RA, Jiang XJ, Zierath JR, Wallberg-Henriksson H. Insulin-Stimulated Akt Kinase Activity Is Reduced in Skeletal Muscle From NIDDM Subjects. Diabetes. 1998;47(8):1281.
232. Glass DJ. Signalling pathways that mediate skeletal muscle hypertrophy and atrophy. Nature cell biology. 2003;5(2):87-90.
233. Wang X, Hu Z, Hu J, Du J, Mitch WE. Insulin resistance accelerates muscle protein degradation: Activation of the ubiquitin-proteasome pathway by defects in muscle cell signaling. Endocrinology. 2006;147(9):4160-8.
234. Milan G, Romanello V, Pescatore F, Armani A, Paik JH, Frasson L, et al. Regulation of autophagy and the ubiquitin-proteasome system by the FoxO transcriptional network during muscle atrophy. Nature communications. 2015;6:6670.
235. Mammucari C, Milan G, Romanello V, Masiero E, Rudolf R, Del Piccolo P, et al. FoxO3 controls autophagy in skeletal muscle in vivo. Cell metabolism. 2007;6(6):458-71.
236. Settembre C, Zoncu R, Medina DL, Vetrini F, Erdin S, Erdin S, et al. A lysosome-to-nucleus signalling mechanism senses and regulates the lysosome via mTOR and TFEB. The EMBO journal. 2012;31(5):1095-108.
237. Arakawa S, Honda S, Yamaguchi H, Shimizu S. Molecular mechanisms and physiological roles of Atg5/Atg7-independent alternative autophagy. Proceedings of the Japan Academy Series B, Physical and biological sciences. 2017;93(6):378-85.
238. Medema RH, Kops GJ, Bos JL, Burgering BM. AFX-like Forkhead transcription factors mediate cell-cycle regulation by Ras and PKB through p27kip1. Nature. 2000;404(6779):782-7.

239. Hwang JY, Gertner M, Pontarelli F, Court-Vazquez B, Bennett MV, Ofengeim D, et al. Global ischemia induces lysosomal-mediated degradation of mTOR and activation of autophagy in hippocampal neurons destined to die. Cell death and differentiation. 2017;24(2):317-29.
240. Cuervo AM, Dice JF. Unique properties of lamp2a compared to other lamp2 isoforms. Journal of cell science. 2000;113 Pt 24:4441-50.
241. Kruse R, Hojlund K. Proteomic study of skeletal muscle in obesity and type 2 diabetes: progress and potential. Expert review of proteomics. 2018;15(10):817-28.
242. Zhong J, Gong W, Chen J, Qing Y, Wu S, Li H, et al. Micheliolide alleviates hepatic steatosis in db/db mice by inhibiting inflammation and promoting autophagy via PPAR-gamma-mediated NF-small ka, CyrillicB and AMPK/mTOR signaling. Int Immunopharmacol. 2018;59:197-208.
243. Zhong J, Gong W, Lu L, Chen J, Lu Z, Li H, et al. Irbesartan ameliorates hyperlipidemia and liver steatosis in type 2 diabetic db/db mice via stimulating PPAR-gamma, AMPK/Akt/mTOR signaling and autophagy. Int Immunopharmacol. 2017;42:176-84.
244. Guo S. Insulin signaling, resistance, and the metabolic syndrome: insights from mouse models into disease mechanisms. J Endocrinol. 2014;220(2):T1-T23.
245. Fritzen AM, Frosig C, Jeppesen J, Jensen TE, Lundsgaard AM, Serup AK, et al. Role of AMPK in regulation of LC3 lipidation as a marker of autophagy in skeletal muscle. Cell Signal. 2016;28(6):663-74.
246. Tipton KD, Hamilton DL, Gallagher IJ. Assessing the Role of Muscle Protein Breakdown in Response to Nutrition and Exercise in Humans. Sports medicine (Auckland, NZ). 2018;48(Suppl 1):53-64.
247. Carbone JW, McClung JP, Pasiakos SM. Skeletal muscle responses to negative energy balance: effects of dietary protein. Advances in nutrition (Bethesda, Md). 2012;3(2):119-26.
248. Mizushima N, Yamamoto A, Matsui M, Yoshimori T, Ohsumi Y. In vivo analysis of autophagy in response to nutrient starvation using transgenic mice expressing a fluorescent autophagosome marker. Molecular biology of the cell. 2004;15(3):1101-11.
249. Albers PH, Pedersen AJ, Birk JB, Kristensen DE, Vind BF, Baba O, et al. Human muscle fiber type-specific insulin signaling: impact of obesity and type 2 diabetes. Diabetes. 2015;64(2):485-97.
250. Edman S, Soderlund K, Moberg M, Apro W, Blomstrand E. mTORC1 Signaling in Individual Human Muscle Fibers Following Resistance Exercise in Combination With Intake of Essential Amino Acids. Frontiers in nutrition. 2019;6:96.
251. Colagiuri S, Davies D, Girgis S, R C. National Evidence Based Guideline for Case Detection and Diagnosis of Type 2 Diabetes Diabetes Australia and NHMRC. 2009.
252. Bergstrom J. Percutaneous needle biopsy of skeletal muscle in physiological and clinical research. Scandinavian journal of clinical and laboratory investigation. 1975;35(7):609-16.
253. Shanely RA, Zwetsloot KA, Triplett NT, Meaney MP, Farris GE, Nieman DC. Human skeletal muscle biopsy procedures using the modified Bergstrom technique. J Vis Exp. 2014(91):51812.
254. Christiansen D, MacInnis MJ, Zacharewicz E, Xu H, Frankish BP, Murphy RM. A fast, reliable and sample-sparing method to identify fibre types of single muscle fibres. Scientific reports. 2019;9(1):6473.
255. Simoneau JA, Colberg SR, Thaete FL, Kelley DE. Skeletal muscle glycolytic and oxidative enzyme capacities are determinants of insulin sensitivity and muscle composition in obese

women. FASEB journal : official publication of the Federation of American Societies for Experimental Biology. 1995;9(2):273-8.
256. Atherton PJ, Etheridge T, Watt PW, Wilkinson D, Selby A, Rankin D, et al. Muscle full effect after oral protein: time-dependent concordance and discordance between human muscle protein synthesis and mTORC1 signaling. The American journal of clinical nutrition. 2010;92(5):1080-8.
257. Howald H, Hoppeler H, Claassen H, Mathieu O, Straub R. Influences of endurance training on the ultrastructural composition of the different muscle fiber types in humans. Pflugers Archiv : European journal of physiology. 1985;403(4):369-76.
258. Essig DA. Contractile activity-induced mitochondrial biogenesis in skeletal muscle. Exercise and sport sciences reviews. 1996;24:289-319.
259. Carrow RE, Brown RE, Van Huss WD. Fiber sizes and capillary to fiber ratios in skeletal muscle of exercised rats. The Anatomical record. 1967;159(1):33-9.
260. Cotter M, Hudlicka O, Vrbova G. Growth of capillaries during long-term activity in skeletal muscle. Bibliotheca anatomica. 1973;11:395-8.
261. Holloszy JO, Coyle EF. Adaptations of skeletal muscle to endurance exercise and their metabolic consequences. Journal of applied physiology: respiratory, environmental and exercise physiology. 1984;56(4):831-8.
262. Talanian JL, Holloway GP, Snook LA, Heigenhauser GJ, Bonen A, Spriet LL. Exercise training increases sarcolemmal and mitochondrial fatty acid transport proteins in human skeletal muscle. American journal of physiology Endocrinology and metabolism. 2010;299(2):E180-8.
263. Perseghin G, Price TB, Petersen KF, Roden M, Cline GW, Gerow K, et al. Increased glucose transport-phosphorylation and muscle glycogen synthesis after exercise training in insulin-resistant subjects. The New England journal of medicine. 1996;335(18):1357-62.
264. Egan B, Zierath JR. Exercise metabolism and the molecular regulation of skeletal muscle adaptation. Cell metabolism. 2013;17(2):162-84.
265. Perry CG, Lally J, Holloway GP, Heigenhauser GJ, Bonen A, Spriet LL. Repeated transient mRNA bursts precede increases in transcriptional and mitochondrial proteins during training in human skeletal muscle. The Journal of physiology. 2010;588(Pt 23):4795-810.
266. Balan E, Schwalm C, Naslain D, Nielens H, Francaux M, Deldicque L. Regular Endurance Exercise Promotes Fission, Mitophagy, and Oxidative Phosphorylation in Human Skeletal Muscle Independently of Age. Frontiers in Physiology. 2019;10(1088).
267. Sanchez AM, Bernardi H, Py G, Candau RB. Autophagy is essential to support skeletal muscle plasticity in response to endurance exercise. American journal of physiology Regulatory, integrative and comparative physiology. 2014;307(8):R956-69.
268. Grumati P, Coletto L, Schiavinato A, Castagnaro S, Bertaggia E, Sandri M, et al. Physical exercise stimulates autophagy in normal skeletal muscles but is detrimental for collagen VI-deficient muscles. Autophagy. 2011;7(12):1415-23.
269. Vainshtein A, Tryon LD, Pauly M, Hood DA. Role of PGC-1alpha during acute exercise-induced autophagy and mitophagy in skeletal muscle. American journal of physiology Cell physiology. 2015;308(9):C710-9.
270. Erlich AT, Brownlee DM, Beyfuss K, Hood DA. Exercise induces TFEB expression and activity in skeletal muscle in a PGC-1alpha-dependent manner. American journal of physiology Cell physiology. 2018;314(1):C62-c72.
271. Parousis A, Carter HN, Tran C, Erlich AT, Mesbah Moosavi ZS, Pauly M, et al. Contractile activity attenuates autophagy suppression and reverses mitochondrial defects in skeletal muscle cells. Autophagy. 2018;14(11):1886-97.

272. Schott LH, Terjung RL. The influence of exercise on muscle lysosomal enzymes. European journal of applied physiology and occupational physiology. 1979;42(3):175-82.
273. Ferraro E, Giammarioli AM, Chiandotto S, Spoletini I, Rosano G. Exercise-induced skeletal muscle remodeling and metabolic adaptation: redox signaling and role of autophagy. Antioxidants & redox signaling. 2014;21(1):154-76.
274. Qaisar R, Bhaskaran S, Van Remmen H. Muscle fiber type diversification during exercise and regeneration. Free radical biology & medicine. 2016;98:56-67.
275. Tam BT, Pei XM, Yu AP, Sin TK, Leung KK, Au KK, et al. Autophagic adaptation is associated with exercise-induced fibre-type shifting in skeletal muscle. Acta physiologica (Oxford, England). 2015;214(2):221-36.
276. Saunders MJ, Blevins JE, Broeder CE. Effects of hydration changes on bioelectrical impedance in endurance trained individuals. Medicine and science in sports and exercise. 1998;30(6):885-92.
277. Ward LC. Bioelectrical impedance analysis for body composition assessment: reflections on accuracy, clinical utility, and standardisation. European journal of clinical nutrition. 2019;73(2):194-9.
278. Ferguson B. ACSM's Guidelines for Exercise Testing and Prescription 9th ed. Philadelphia, PA 19103: American College of Sports Medicine; 2014. 328 p.
279. Zuniga JM, Housh TJ, Camic CL, Bergstrom HC, Traylor DA, Schmidt RJ, et al. Metabolic parameters for ramp versus step incremental cycle ergometer tests. Applied physiology, nutrition, and metabolism = Physiologie appliquee, nutrition et metabolisme. 2012;37(6):1110-7.
280. Medicine ACoS, Riebe D, Ehrman JK, Liguori G, Magal M. ACSM's guidelines for exercise testing and prescription2018.
281. Kang HS, Gutin B, Barbeau P, Owens S, Lemmon CR, Allison J, et al. Physical training improves insulin resistance syndrome markers in obese adolescents. Medicine and science in sports and exercise. 2002;34(12):1920-7.
282. Buchheit M, Laursen PB. High-intensity interval training, solutions to the programming puzzle: Part I: cardiopulmonary emphasis. Sports medicine (Auckland, NZ). 2013;43(5):313-38.
283. Booth FW, Ruegsegger GN, Toedebusch RG, Yan Z. Endurance Exercise and the Regulation of Skeletal Muscle Metabolism. Progress in molecular biology and translational science. 2015;135:129-51.
284. Rivera-Brown AM, Frontera WR. Principles of exercise physiology: responses to acute exercise and long-term adaptations to training. PM & R : the journal of injury, function, and rehabilitation. 2012;4(11):797-804.
285. Carter HN, Kim Y, Erlich AT, Zarrin-Khat D, Hood DA. Autophagy and mitophagy flux in young and aged skeletal muscle following chronic contractile activity. The Journal of physiology. 2018;596(16):3567-84.
286. Kahn SE, Hull RL, Utzschneider KM. Mechanisms linking obesity to insulin resistance and type 2 diabetes. Nature. 2006;444(7121):840-6.
287. Gottlieb RA, Andres AM, Sin J, Taylor DP. Untangling autophagy measurements: all fluxed up. Circulation research. 2015;116(3):504-14.
288. Baumann H, Jäggi M, Soland F, Howald H, Schaub MC. Exercise training induces transitions of myosin isoform subunits within histochemically typed human muscle fibres. Pflügers Archiv. 1987;409(4):349-60.
289. Sachs S, Zarini S, Kahn DE, Harrison KA, Perreault L, Phang T, et al. Intermuscular adipose tissue directly modulates skeletal muscle insulin sensitivity in humans. American journal of physiology Endocrinology and metabolism. 2019;316(5):E866-e79.

290. Vettor R, Milan G, Franzin C, Sanna M, De Coppi P, Rizzuto R, et al. The origin of intermuscular adipose tissue and its pathophysiological implications. American journal of physiology Endocrinology and metabolism. 2009;297(5):E987-98.
291. Cai J, Pires KM, Ferhat M, Chaurasia B, Buffolo MA, Smalling R, et al. Autophagy Ablation in Adipocytes Induces Insulin Resistance and Reveals Roles for Lipid Peroxide and Nrf2 Signaling in Adipose-Liver Crosstalk. Cell reports. 2018;25(7):1708-17.e5.
292. Watt MJ, Heigenhauser GJ, Spriet LL. Intramuscular triacylglycerol utilization in human skeletal muscle during exercise: is there a controversy? Journal of applied physiology (Bethesda, Md : 1985). 2002;93(4):1185-95.
293. Kovsan J, Blüher M, Tarnovscki T, Klöting N, Kirshtein B, Madar L, et al. Altered Autophagy in Human Adipose Tissues in Obesity. The Journal of Clinical Endocrinology & Metabolism. 2011;96(2):E268-E77.
294. Barstow TJ, Jones AM, Nguyen PH, Casaburi R. Influence of muscle fibre type and fitness on the oxygen uptake/power output slope during incremental exercise in humans. Experimental physiology. 2000;85(1):109-16.
295. Christ-Roberts CY, Pratipanawatr T, Pratipanawatr W, Berria R, Belfort R, Kashyap S, et al. Exercise training increases glycogen synthase activity and GLUT4 expression but not insulin signaling in overweight nondiabetic and type 2 diabetic subjects. Metabolism: clinical and experimental. 2004;53(9):1233-42.
296. Frosig C, Rose AJ, Treebak JT, Kiens B, Richter EA, Wojtaszewski JF. Effects of endurance exercise training on insulin signaling in human skeletal muscle: interactions at the level of phosphatidylinositol 3-kinase, Akt, and AS160. Diabetes. 2007;56(8):2093-102.
297. Vind BF, Pehmøller C, Treebak JT, Birk JB, Hey-Mogensen M, Beck-Nielsen H, et al. Impaired insulin-induced site-specific phosphorylation of TBC1 domain family, member 4 (TBC1D4) in skeletal muscle of type 2 diabetes patients is restored by endurance exercise-training. 2011;54(1):157-67.
298. Kazior Z, Willis SJ, Moberg M, Apro W, Calbet JA, Holmberg HC, et al. Endurance Exercise Enhances the Effect of Strength Training on Muscle Fiber Size and Protein Expression of Akt and mTOR. PloS one. 2016;11(2):e0149082.
299. Bandyopadhyay U, Cuervo AM. Chaperone-mediated autophagy in aging and neurodegeneration: lessons from alpha-synuclein. Experimental gerontology. 2007;42(1-2):120-8.
300. Massey AC, Zhang C, Cuervo AM. Chaperone-mediated autophagy in aging and disease. Current topics in developmental biology. 2006;73:205-35.
301. Oh-ishi S, Kizaki T, Nagasawa J, Izawa T, Komabayashi T, Nagata N, et al. Effects of endurance training on superoxide dismutase activity, content and mRNA expression in rat muscle. Clinical and experimental pharmacology & physiology. 1997;24(5):326-32.
302. Morrison DJ, Kowalski GM, Grespan E, Mari A, Bruce CR, Wadley GD. Measurement of postprandial glucose fluxes in response to acute and chronic endurance exercise in healthy humans. American journal of physiology Endocrinology and metabolism. 2018;314(5):E503-e11.
303. Hamley S, Kloosterman D, Duthie T, Dalla Man C, Visentin R, Mason SA, et al. Mechanisms of hyperinsulinaemia in apparently healthy non-obese young adults: role of insulin secretion, clearance and action and associations with plasma amino acids. Diabetologia. 2019.
304. Burke SJ, Batdorf HM, Burk DH, Noland RC, Eder AE, Boulos MS, et al. db/db Mice Exhibit Features of Human Type 2 Diabetes That Are Not Present in Weight-Matched C57BL/6J Mice Fed a Western Diet. J Diabetes Res. 2017;2017:8503754.

305. Papa S. Mitochondrial oxidative phosphorylation changes in the life span. Molecular aspects and physiopathological implications. Biochimica et biophysica acta. 1996;1276(2):87-105.
306. Simoneau JA, Kelley DE. Altered glycolytic and oxidative capacities of skeletal muscle contribute to insulin resistance in NIDDM. Journal of applied physiology (Bethesda, Md : 1985). 1997;83(1):166-71.
307. Pankiv S, Lamark T, Bruun JA, Overvatn A, Bjorkoy G, Johansen T. Nucleocytoplasmic shuttling of p62/SQSTM1 and its role in recruitment of nuclear polyubiquitinated proteins to promyelocytic leukemia bodies. The Journal of biological chemistry. 2010;285(8):5941-53.
308. Sakuma K, Kinoshita M, Ito Y, Aizawa M, Aoi W, Yamaguchi A. p62/SQSTM1 but not LC3 is accumulated in sarcopenic muscle of mice. Journal of cachexia, sarcopenia and muscle. 2016;7(2):204-12.
309. Masschelein E, Van Thienen R, D'Hulst G, Hespel P, Thomis M, Deldicque L. Acute environmental hypoxia induces LC3 lipidation in a genotype-dependent manner. FASEB journal : official publication of the Federation of American Societies for Experimental Biology. 2014;28(2):1022-34.
310. Loos B, du Toit A, Hofmeyr JH. Defining and measuring autophagosome flux—concept and reality. Autophagy. 2014;10(11):2087-96.
311. Chiang GG, Abraham RT. Phosphorylation of mammalian target of rapamycin (mTOR) at Ser-2448 is mediated by p70S6 kinase. The Journal of biological chemistry. 2005;280(27):25485-90.
312. Reynolds THt, Bodine SC, Lawrence JC, Jr. Control of Ser2448 phosphorylation in the mammalian target of rapamycin by insulin and skeletal muscle load. The Journal of biological chemistry. 2002;277(20):17657-62.
313. Figueiredo VC, Markworth JF, Cameron-Smith D. Considerations on mTOR regulation at serine 2448: implications for muscle metabolism studies. Cellular and molecular life sciences : CMLS. 2017;74(14):2537-45.
314. Cuervo AM, Dice JF, Knecht E. A population of rat liver lysosomes responsible for the selective uptake and degradation of cytosolic proteins. The Journal of biological chemistry. 1997;272(9):5606-15.
315. Jiang X, Bao Y, Liu H, Kou X, Zhang Z, Sun F, et al. VPS34 stimulation of p62 phosphorylation for cancer progression. Oncogene. 2017;36(50):6850-62.
316. Shi J, Fung G, Deng H, Zhang J, Fiesel FC, Springer W, et al. NBR1 is dispensable for PARK2-mediated mitophagy regardless of the presence or absence of SQSTM1. Cell death & disease. 2015;6:e1943.
317. Kimura S, Fujita N, Noda T, Yoshimori T. Monitoring autophagy in mammalian cultured cells through the dynamics of LC3. Methods in enzymology. 2009;452:1-12.
318. Tian W, Alsaadi R, Guo Z, Kalinina A, Carrier M, Tremblay M-E, et al. An antibody for analysis of autophagy induction. Nature Methods. 2020;17(2):232-9.
319. Schneider JL, Cuervo AM. Liver autophagy: much more than just taking out the trash. Nat Rev Gastroenterol Hepatol. 2014;11(3):187-200.

Appendices

Appendix 1: Recruitment flyer

IPAN
INSTITUTE FOR PHYSICAL ACTIVITY AND NUTRITION

FREE EXERCISE TRAINING

PERSONALIZED FOR YOU!

YOUR schedule **YOUR** fitness levels

ARE YOU
(or someone you know)

- MALE
- aged 18-40 years
- interested in participating in a research study
- willing to undergo muscle biopsies
- overweight/obese (BMI 25-40 kg/m2)
- wanting to make a change? *

** must be willing to travel to Deakin University, Waurn Ponds*

CONTACT US!

BE PART OF INNOVATIVE RESEARCH!

GABY
gabriela.morales@deakin.edu.au
0423794621

BIANCA
btepper@deakin.edu.au
0401738816

Follow us on Facebook: @recyclediabetes

Institute for Physical Activity and Nutrition (IPAN), School of Exercise and Nutrition Sciences
Deakin University, 221 Burwood Highway, Burwood, VIC 3125
Tel 03 9244 6613 email ipan@deakin.edu.au www.deakin.edu.au/research/ipan
Deakin University CRICOS Provider Code: 00113B

DEAKIN UNIVERSITY

Appendix 2: Plain language statement and consent form

PLAIN LANGUAGE STATEMENT AND CONSENT FORM

TO:

Plain Language Statement

Date: 23 January 2017

Full Project Title: The effects of insulin resistance and exercise training on skeletal muscle autophagy

Principal Investigator: Dr Chris Shaw

Associate Researcher(s):
Dr Kirsten Howlett

Student Researcher:
Gabriela Morales-Scholz

This Plain Language Statement and Consent Form is 8 pages long. Please make sure you have all the pages.

1. Your Consent

You are invited to take part in this research project.

This Plain Language Statement contains detailed information about the research project. Its purpose is to explain to you as openly and clearly as possible all the procedures involved in this project before you decide whether or not to take part in it.

Please read this Plain Language Statement carefully. Feel free to ask questions about any information in the document. You may also wish to discuss the project with a relative or friend or your local health worker. Feel free to do this.

Once you understand what the project is about and if you agree to take part in it, you will be asked to sign the Consent Form. By signing the Consent Form, you indicate that you understand the information and that you give your consent to participate in the research project.

You will be given a copy of the Plain Language Statement and Consent Form to keep as a record.

2. Purpose and Background

Autophagy is a recycling process that takes place in almost all cells. It is responsible for removing defective components from the cell and providing the building blocks for producing new and functional proteins. Autophagy is responsive to the energy status of the body, as it is increased when energy availability is low (such as after a prolonged fast) and is blunted when energy availability is high, such as after eating a meal. The blunting effect with feeding is regulated by elevated insulin concentrations in the blood.

Recent studies have shown that switching autophagy on and off appropriately is important in maintaining muscle function. Disturbances in autophagy control may contribute to the muscle dysfunction that is involved in conditions of inactivity, weight gain and ageing. Interestingly, autophagy is also activated by exercise and is involved in how muscle adapts to exercise training and improves fitness. However, most of these research studies have been performed in cells and rodents, so our knowledge on autophagy in humans is limited.

The purpose of this project is to understand how autophagy activity in muscle responds to feeding in people with high and low sensitivity to insulin. We would like to invite you to participate in a research study in which we will examine autophagy activity in your muscle before and after 6 weeks of exercise training. This will help us to understand if insulin sensitivity changes the way muscle autophagy is regulated by food consumption and whether exercise has the ability to improve these acute responses.

The researchers will measure the following before and after 6 weeks of exercise training:

1. The content of proteins that indicate autophagy activity levels in your muscle
2. The changes to your blood sugar level following ingestion of a standard breakfast
3. Your aerobic fitness

You are invited to participate in this research project as you are within the required age range (18-40 years), have a BMI above 25 kg/m^2, and have no complicating medical issues that may affect the results.

3. Procedures

If you are interested, please read the following description of what is required to participate in this research and what we plan to do with your blood and muscle samples.

Pre-test Screening

We will first ask you to complete a medical questionnaire to determine your current health risks and determine what medication you are currently taking. This will help inform the researchers of your current health status.

If you are not suitable to participate in the study based on the information from your Pre-test Screening your medical information will be returned to you. If you are suitable for the study, we will invite you to participate in the trial and we will ask you to undergo a 2 hour oral glucose tolerance test, to determine the presence or absence of insulin resistance.

Dietary record: We will ask you to complete a dietary record for a 3 day period before you come in for visit 1 (detailed below) and three weeks after initiating the exercise training phase. This is to give us information on your typical dietary intake. It is important that you eat the food you normally consume during this time and record this on the form that we will give to you.

Physical activity record: we will ask you to wear an accelerometer before the training begins and at week 6 of the training (at least 7 days for a miminum of 10 h each day) to keep record of your level of physical activity outside the official training hours. An accelerometer is a device that is used around your waist that measures your movements throughout the day. It is important to know that this device should not be used if you are going to take part in any kind of watersports.

Participation in this project will involve:

Pre-visit screening: In your first visit to the Deakin University Research Laboratory (Building DD, Waurn Ponds campus) you will be asked to come in the morning after an overnight fast to undergo a 2 hour oral glucose tolerance test, where fingertip blood glucose will be measured before and during the followoing 2 hours after the ingestion of a sugary drink. This will determine the presence or absence of insulin resistance.

Visit 1 Aerobic fitness (VO_2max) test: In this visit to the Deakin University Research Laboratory (Building DD, Waurn Ponds campus), descriptive data such as height, weight and age will be collected. You will then complete a test of aerobic fitness called a maximum oxygen consumption (VO_2max) test on a bicycle ergometer. This test involves continuous, incremental cycling until exhaustion and lasts around 15 minutes. The test may be terminated earlier if you wish. You will exercise with a nosepeg on and have a mouthpiece in place. This allows us to collect and analyse the air you expire so that we can assess your aerobic fitness. However, you will be able to breathe freely at all times with the mouthpiece in place.

Visit 2 Muscle biopsy and blood sampling trial: You will be asked to refrain from vigorous exercise and from consumption of caffeine and alcohol in the 48 h prior to this visit. You will be asked to arrive at ~7am at the Deakin University Clinical Research Facility (Building DD, Waurn Ponds campus) after an overnight fast (eating no food from 9:30pm, including no breakfast). We will measure your height and then get you to stand on a set of scales whilst wearing your shirt and shorts (no shoes or socks), your body weight and blood pressure will be measured twice in resting conditions.
Biopsy procedure: A medical doctor (Dr Andrew Garnham or Dr Andrew Aldous) will give you an injection of local anaesthetic into the middle of the thigh. This local anaesthetic may sting slightly for a few seconds. After 10

minutes, when the local anaesthetic has numbed the area, the doctor will make a small cut for the biopsy through the skin above your thigh muscle. This cut will be 5mm long. Using a needle, the doctor will then take a small piece of muscle (about the size of a single “rice bubble”). This procedure is called a needle biopsy. **There are no pain sensors in the muscle; however pressure receptors will detect pressure as the needle is pushed in and may cause some localised pain and discomfort; similar to hitting your thigh on the corner of a table or a deep tissue massage**. The whole process of taking the sample lasts about 10 seconds. As soon as the small sample is collected, special sterile closures and a pressure bandage will be applied. This procedure will be repeated two more times 30 and 90 min after having had breakfast (see description below). The area where the biopsies were taken will be stiff for a day or so but you will be able to continue with your normal physical activity. A researcher will contact you the following day to check on your wellbeing.

Blood sampling: On reporting to the laboratory, we will place a small plastic tube (catheter) into a vein in your forearm using a needle and this will be used for blood sampling. We will then take two small blood sample (3 ml each). We will then ask you to have a breakfast that we will provide you. Throughout the next 3 hours, small blood samples will be obtained at regular intervals (8 x 3 ml in total). Each time a blood sample is collected the catheter will be flushed with a small amount of saline to stop the blood from clotting inside the catheter. This procedure is painless, except for the introduction of the catheter into the arm, which can cause slight discomfort. The total volume of blood taken during this procedure is approximately ten percent of the standard Red Cross donation volume.

You will be free to drink water and go to the toilet during these 3 hours. The entire time taken for visit 2 will be approximately 4 hours. A researcher will be present at all times to monitor your health and welfare. You will not be able to eat during this time, but we will provide you with a small meal as soon as it finishes. We will call you on the telephone the following day to enquire about your wellbeing.

Training: At least a week after visit 2, you will be asked to participate in a 6 week exercise training phase. You will be asked to come to the Deakin Waurn Ponds campus 3 times per week to perform a 50 min aerobic exercise session. Two of these sessions will be at a moderate intensity and one of them will consist of high intensity interval training (HIIT). All sessions will be supervised by a researcher and attendance will be recorded. Intensity adjustments based on your exercise heart rate might be made depending on how your physical fitness improves. You will be asked to undergo a second maximum oxygen consumption (VO_2max) test on a bicycle ergometer after completing the third week of training to reassess how your physical fitness condition has improved.

Post-training follow up: After the training phase has been completed we will ask you to undergo the same procedures described in visit 1 and 2.

4. Collection of Tissue Samples for Research Purposes
By consenting to take part in this study, you also consent to the collection, storage and use of tissue samples as specified below.

- Samples of blood will be taken from your arm vein and we will measure levels of nutrients such as glucose and also the levels of hormones regulating blood glucose (such as insulin).

- Samples of your thigh muscles will be taken by needle biopsy. This tissue will be used to measure proteins involved in muscle degradation processes and metabolism responsible for maintaining a healthy metabolic status. All of your samples will be assigned a code that is known only to the researcher. This code will be written on the small plastic containers to store your samples. All analysis will only use your code.

- All samples will be stored and analysed over the duration of the study. ***The samples and data collected in this study may be used by members of the research team for other purposes in the future; these purposes would be closely aligned with the original research project stated here. If we were to use the samples for other purposes which are unrelated to the current study we would contact you for your permission first.***

- No person other than the members of the research team will use your samples.

5. Possible Benefits
Understanding how autophagy activity levels change in response to feeding and exercise training will help us understand more about muscle metabolism and how it adapts to regular exercise to benefit our health. In the future, this may provide information to help clinical populations, such as people with diabetes.

6. Possible Risks
Possible risks, side effects and discomforts include having blood and skeletal muscle sampling. Taking blood from an arm vein involves the discomfort of having a needle and then a small flexible plastic catheter in the arm vein. This can be uncomfortable and may result in localised bruising. As you are young and have been found to be at low risk from cardiovascular disease, any risk from exercise, as for example, a cardiac event, is very small. However, it is possible that you will experience muscular discomfort and fatigue during and shortly after the VO_2 max test. However, these feelings will be short lived. If you experience extreme exhaustion, shortness of breath, dizziness and/or chest pain then we will terminate the test. The staff running the exercise tests are experiences exercise physiologists and are trained in first aid.

The bigger source of discomfort and risk are the needle biopsies. This process may cause localised discomfort. This normally passes quickly.

It is common to experience local soreness for 24-48 hours after the procedure, but this should not limit normal activity levels. Occasionally bruising, swelling or a small area of numbness may occur. The numbness may last for several weeks, although it should recover fully, and has no impact on muscle function. If there is slight swelling or tenderness, apply an ice pack for 10 minutes over a damp cloth. There is a risk of infection with the needle biopsy sampling procedure and blood sampling, however, this risk is minimised by having all procedures performed using sterile techniques. Over the last 15 years we have not had a single case of infection. We have performed over 5000 muscle biopsies in the last 15 years without major complication.

In the event of any ill-effects from the biopsy or blood samples (uncontrolled bleeding, severe pain, signs of infection) you should contact the researchers as soon as possible on the following phone number [Dr Shaw 0403825906 or Gabriela Morales 0423794621]. The researchers can contact the Physicians at any time if required.

7. Other Treatments Whilst on Study

It is important to tell the research staff about any treatments or medications you may be taking, including non-prescription medications, vitamins or herbal remedies and any changes to these during your participation in the study.

8. Privacy, Confidentiality and Disclosure of Information

Any information obtained in connection with this research project that can identify you will remain confidential and will only be used for the purpose of this research project. It will only be disclosed with your permission, except as required by law. If you give us your permission by signing the Consent Form, we plan to share the results of your medical questionnaire with the Medical Practitioner (Dr Andrew Garnham or Dr Andrew Aldous). The individual results will be coded and the code will be kept in a safe place, where it can only be accessed by the researchers, in case we need to contact you about your results. All other results from the study will be grouped.. The results of this research will be shared by the researchers as reports. Parts of these reports will also be prepared and published for scientific conferences and medical journals.

Furthermore, the information collected in connection with this research project could be used for other research purposes that are closely aligned with the current research project. The information will maintain its code, but this code will be kept safe at all times. If we were to use these samples for other purposes, all participants will be contacted, informed and will be asked to provide written permission before proceeding, and prior ethics approval will be sought.

9. Results of Project

Your results of the study and their interpretation will be forwarded to you on completion from Gabriela Morales-Scholz. Upon request, we can also send you a copy of the publication arising from this research.

10.Further Information or Any Problems
If you require further information or if you have any problems concerning this project (for example, any side effects), you can contact Gabriela Morales-Scholz, the principal researcher. Gabriela can contact the Physicians at any time if required. Gabriela will be available at any time on:

Work telephone: 03 5229 1686

Mobile: 0423794621

11.Complaints
If you have any complaints about any aspect of the project, the way it is being conducted or any questions about your rights as a research participant, then you may contact:

The Manager, Office of Research Integrity, Deakin University, 221 Burwood Highway, Burwood Victoria 3125, Telephone: 9251 7129, Facsimile: 9244 6581; research-ethics@deakin.edu.au.

Please quote project number **EC 2017-029**

12.Participation is Voluntary
Participation in any research project is voluntary. If you do not wish to take part you are not obliged to. If you decide to take part and later change your mind, you are free to withdraw from the project at any stage.

Your decision whether to take part or not to take part, or to take part and then withdraw, will not affect your routine treatment, your relationship with those treating you or your relationship with the School of Exercise and Nutrition Science, Deakin University.

If you have donated blood and tissue samples, you have the right to ask for these samples to be removed from all further analysis.

Before you make your decision, a member of the research team will be available so that you can ask any questions you have about the research project. You can ask for any information you want. Sign the Consent Form only after you have had a chance to ask your questions and have received satisfactory answers.

If you decide to withdraw from this project, please notify a member of the research team before you withdraw. This notice will allow that person or the research supervisor to inform you if there are any health risks or special requirements linked to withdrawing.

13.Reimbursement for your costs

You will not be paid for your participation in this trial. However, you will be provided with a meal for the visit to the laboratory that involves the blood sampling and muscle biopsy procedures.

14.Ethical Guidelines

This project will be carried out according to the *National Statement on Ethical Conduct in Human Research (2007)* produced by the National Health and Medical Research Council of Australia. This statement has been developed to protect the interests of people who agree to participate in human research studies.

The ethical aspects of this research project have been approved by the Human Research Ethics Committee of Deakin University.

15.Injury

In the event that you suffer an injury as a result of participating in this research project, hospital care and treatment will be provided by the public health service at no extra cost to you.

16.Termination of the Study

This research project may be stopped for a variety of reasons. These may include reasons such as: unacceptable side effects of the tissue sampling protocol.

PLAIN LANGUAGE STATEMENT AND CONSENT FORM

TO:

Consent Form

Date: 23 January 2017

Full Project Title: The effects of insulin resistance and exercise training on skeletal muscle autophagy

---

I have read and I understand the attached Plain Language Statement.

I freely agree to participate in this project according to the conditions in the Plain Language Statement.

I have been given a copy of the Plain Language Statement and Consent Form to keep.

The researcher has agreed not to reveal my identity and personal details, including where information about this project is published, or presented in any public form.

Participant's Name (printed)
……

Signature ……

Date ……

TO:

Consent Form for Tissue Sample Storage and Use

Date: 23 January 2017

Full Project Title: The effects of insulin resistance and exercise training on skeletal muscle autophagy

---

- I consent to the storage and use of blood and tissue samples taken from me for use in further closely aligned research as described in this Plain Language Statement by Dr. Chris Shaw.

Participant's name

(printed)……..…..

Signature Date

Name of Witness to Participant's signature
(printed)……..

Signature Date

Researcher's
name……...

Signature Date

Note: All parties signing the Consent Form must date their own signature.

Appendix 3: Medical questionnaire

DEAKIN UNIVERSITY AUSTRALIA

MEDICAL QUESTIONNAIRE

The effects of insulin resistance and exercise training on skeletal muscle autophagy

NAME:_____ **AGE:** _____ **DOB:**_ _____

WEIGHT (kg): _____ **HEIGHT (cm):** _____ **BP (mmHg):**_____ _____

TRAINING STATUS:
Are you currently undertaking any form of regular exercise?

_____
_____
_____

If yes, briefly describe the type (ie. running, soccer, swimming) and amount (ie. frequency, duration) of exercise you perform.

HEALTH STATUS:

1) Do you have high blood pressure? YES NO DON'T KNOW

If yes, please elaborate:_____

2) Do you smoke? YES NO

3) Do you or a member of your family have diabetes? YES NO DON'T KNOW

If yes, how long have you/ family member had diabetes?_____

4) Do you, or a member of your family, suffer from a bleeding disorder?

YES NO DON'T KNOW

5) Is there a family history of heart disease? YES NO DON'T KNOW

If yes, please elaborate: _____

6) Do you or a member of your family have high cholesterol? YES NO DON'T KNOW

If yes, please elaborate: _____

7) Are you overweight? YES NO DON'T KNOW

8) Do you have a heart murmur? YES NO DON'T KNOW

9) Are you asthmatic? YES NO DON'T KNOW

10) Do you have a current injury which may affect your ability to take part in the study? YES NO DON'T KNOW

If yes, please elaborate: _____

11) Do you have allergies (including to medications)? YES NO DON'T KNOW

If yes, please elaborate: _____

12) Are you currently on any medication? YES NO

If yes, what is the medication?:_____

13) Are you currently taking any aspirin? YES NO DON'T KNOW

14) Are you currently taking any herbal supplements? YES NO

If yes, what is the supplement?:_____

If you answer "yes" to any one of questions two to four it is necessary for you to be excluded from the study. If you answer "don't know" to question one, it will be necessary for us to test your blood pressure before a decision is made by our doctor concerning your involvement in the study. If you answer "yes" to any of questions five to twelve or "don't know" to questions three or four we will need to ask you for more details and then make a medical decision based on your specific circumstances.

I believe that the information I have provided is correct.

Name of Subject: _____ Signature of Subject: _____

Appendix 4: Accelerometer entry instructions and record sheet

How to Wear the ActiGraph Monitor

The ActiGraph is a small, lightweight activity monitor device that measures the intensity and amount of movement that you engage in. We **will not** be able to tell what kind of specific activity is happening. It is **extremely important** for our study that you wear the ActiGraph correctly. If it is not worn properly, you may be asked to wear it again. Please follow the instructions below. If you have any questions, please contact Gabriela Morales-Scholz (Email: gabriela.morales@deakin.edu.au Telephone: 0423794621).

The ActiGraph is worn on the right hip using the adjustable belt.

- Place the monitor so that the black cover is on top of the monitor and the smiley face sticker is smiling the right way for other people to look at.
- Please wear the monitor in the same position each day for **8 consecutive days.**
- You can wear the monitor over or under your clothes.
- Please wear the ActiGraph as much as possible. It is safe to wear whilst asleep, and during most sporting activities. If you take the monitor off for any reason, please complete the monitor record sheet on Page 2.
- **DO NOT WEAR THE MONITOR DURING WATER-BASED ACTIVITIES (e.g. showering, bathing, spa)**
- **DO NOT UNSCREW THE COVER.** There are no switches or counters; all of your movements are recorded automatically.

PLEASE REMEMBER THAT THIS EQUIPMENT IS VALUABLE AND EXPENSIVE TO REPLACE

Please return the ActiGraph monitor and the removal log to:

Gabriela Morales Scholz on _____

Red LED (Fault Indicator)

- **No Flashing (LED Off)** Normal operating condition or battery dead
- **2 Flashes** Low Battery (use ActiLife software to check for remaining battery life). The unit needs to be recharged.
- **3 Flashes** - Unexpected Battery Failure (Temporary battery power loss) or battery Level has fallen below 3.1V and the unit has entered Halt Mode

Green LED

- **No Flashing (LED Off)** Actively collecting data with "Flash Mode" disabled (recommended setting) or battery dead
- **1 Flash** - Delay before start mode (the LED always flashes prior to starting data collection) or actively taking data ("Flash Mode" enabled – not recommended)
- **2 Flashes** N/A
- **3 Flashes** - End of memory reached (device no longer collecting data) or battery died while unit was in delay before start mode (no data collected on device)

ActiGraph Record Sheet

Please complete the information requested below for each day of measurement (please use multiple rows as necessary)

Date	Time awake	Time arrive at work	Time left work	Time you went to sleep	Time & duration of monitor removal	Reason
e.g. 27/10	***6:15am***	***8:20am***	***5pm***	***10:15am***	***9pm – 30 minutes***	***Shower***

Appendix 5: Food diary entry record sheet

3-day food diary & physical activity recall

1. The following food diary is to be completed over 3 days prior to each laboratory visit. *An example day's completion is provided at the start of the booklet.*
If after reading these instruction you have further questions, contact Gabriela Morales on 0423794621 or gabriela.morales@deakin.edu.au

2. Sections for breakfast, morning tea, lunch, afternoon tea, dinner and additional food/drinks are provided each day for you to report your food/drink consumption.

3. In the "FOOD/DRINK" column, you should state the type of food/drink consumed. In the "DESCRIPTION AND PREPARATION" column, you should provide some information in relation to how the food/drink was prepared, the brand name of the food/drink (if relevant), and a description of the specific food/drink (e.g. type, flavour, and if fresh, frozen or canned). In the "AMOUNT" column, provide a brief description using common household measures (e.g. teaspoons, cups, approximate physical dimensions) of how much of the particular food/drink was consumed. Any additional information pertaining to what you ate, such as a recipe for a homemade food, should be included on the final page in "ADDITIONAL INFORMATION".

4. It is IMPORTANT that you accurately report what you have consumed. It is also important that you do not alter your normal diet during the recording period, such as for purposes of appearing healthier than usual or for ease of reporting.

5. Details about each food and beverage item you consume are crucial to us, so please include as many details as you can!
Describe the food as accurately as possible eg. milk - what kind (whole, 2%, non-fat); bread - (whole wheat, white, buttered).
The more details you include, the less likely you will be to receive a call from us later on to get those details.

6. *At the end of day 3*, please complete the attached physical activity questionnaire. This questionnaire relates to physical activity undertaken over the previous week.

DATE / / DAY OF WEEK

BREAKFAST		
FOOD/DRINK	*DESCRIPTION AND PREPARATION*	*AMOUNT*

MORNING TEA		
FOOD/DRINK	*DESCRIPTION AND PREPARATION*	*AMOUNT*

DATE / / DAY OF WEEK

LUNCH		
FOOD/DRINK	*DESCRIPTION AND PREPARATION*	*AMOUNT*

AFTERNOON TEA		
FOOD/DRINK	*DESCRIPTION AND PREPARATION*	*AMOUNT*

DATE / / DAY OF WEEK

DINNER		
FOOD/DRINK	*DESCRIPTION AND PREPARATION*	*AMOUNT*
ADDITIONAL FOODS/DRINKS		
FOOD/DRINK	*DESCRIPTION AND PREPARATION*	*AMOUNT*